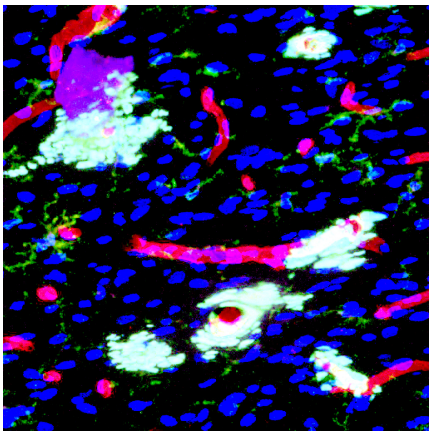


The Role of the Chemokine “CCL2” in Central Cardiovascular Control

Khalid Elsaafien, B.Sc. (Hons)

ORCI ID 0000-0001-9581-918X

A thesis submitted in total fulfilment of the requirements for the degree of

Doctor of Philosophy

November 2019

Faculty of Medicine, Dentistry and Health Sciences

The University of Melbourne

Florey Institute of Neuroscience and Mental Health

I dedicate this thesis to my parents Gamal and Salwa Elsaafien

and to my brothers Hassan and Abdul Elsaafien

Thank you for your continuous love and support

Abstract

Background: The cardiovascular system is under the constant control of a specialised neural network spanning a number of brain regions. This includes a distinct population of neurons found within the paraventricular nucleus (PVN) of the hypothalamus. Activation of these neurons increases sympathetic nerve activity to cardiovascular organs and raises blood pressure. The mechanisms driving increased activity in the network has not been fully elucidated. Recent evidence suggests that invasion of peripheral immune cells into key regions of the brain might play a role in this regard. The chemokine known as C-C- Ligand 2 (CCL2) is a key activator of peripheral immune cells in hypertension. Whether CCL2 facilitates the entry of immune cells into brain regions that are critical for blood pressure regulation is one of the fundamental questions that has not been addressed. Therefore, I hypothesised that CCL2 causes immune cells to invade specific brain regions to increase nerve activity and blood pressure. In this thesis, I established three main aims: firstly, to establish whether the chemokine CCL2 can activate and recruit peripheral immune cells to the PVN. Secondly, to establish whether immune cell invasion into the PVN leads to increased nerve activity to cardiovascular organs, resulting in elevated blood pressure. Finally, to understand the mechanisms by which CCL2 recruits immune cells into the PVN during the development of hypertension.

Methods: Rats were used in the studies. In the first study, CCL2 (71 nM; 50nL) was injected into the PVN of rats while blood pressure and renal sympathetic nerve activity were being recorded. In the second study, renal artery clipping was used to induce hypertension (mimicking renovascular hypertension). Rats were sacrificed at different time points, and brain

tissue was collected for post-mortem analysis. The third study involved infusion of a potent antagonist of CCL2 receptors (RS-102895; 70 μM) directly into the brain. Blood pressure was recorded using radiotelemetry transmitters implanted into the abdominal aorta. An osmotic minipump was implanted into lateral ventricles of the brain for the infusion of the CCL2 receptor antagonist (2.5 μl/hour). The antagonist was infused for a period of eight weeks, while blood pressure was continuously recorded via radiotelemetry in conscious, freely behaving, renovascular hypertensive rats.

Results: In the first study, I found that central injections of CCL2 activated and recruited peripheral circulating macrophages that infiltrated into the PVN. This invasion of macrophages into the brain increased sympathetic nerve activity to the kidney by 126±7%, leading to 10±1 mmHg increase in blood pressure. In the second study, CCL2 levels were increased in the plasma and the cerebrospinal fluid at the pre-hypertensive stage in the renovascular model of hypertension. Increased CCL2 caused the recruitment of macrophages into the PVN during the pre-hypertensive stage. This critical finding suggests the involvement of macrophage invasion into the PVN during the early stages of hypertension, possibly leading to blood pressure increases and the development of hypertension. These data are supported by the key finding of the third study, that macrophages are prevented from entering the PVN by antagonising CCL2 signalling mechanisms in the brain; leading to a decrease in blood pressure of 40±3 mmHg in renovascular hypertensive rats.

Conclusion: In conclusion, I found that the chemokine, CCL2, activates and recruits peripherally circulating immune cells to infiltrate the PVN, leading to increases in sympathetic nerve activity and blood pressure. This action, by CCL2, in the early pre-hypertensive stage of hypertension, might be a mechanism by which hypertension becomes established, *viz* by

activating and recruiting immune cells that infiltrate into the brain to activate key areas and neural networks critical for the moment-to-moment control of the cardiovascular system. Blocking the receptor via which CCL2 acts, decreases blood pressure. The findings reported here highlights the importance of this immune-brain pathway in the development of hypertension.

Declaration

I hereby declare that this thesis:

a) Comprises my original work, except where mentioned;

b) Acknowledges all other used materials within text;

c) Is less than 100,000 words in length, excluding tables, figures, bibliographies, and appendices; and

d) Adheres to the regulations set by the University of Melbourne for the degree of Doctor of Philosophy.

Name: Khalid Elsaafien…….

Date: March 2020……...

Preface

This thesis has not been or is being presented to any other university or institution towards another degree or qualification. None of the conducted research was commenced before enrolling as a PhD candidate at the University of Melbourne. Except where indicated, this text does not contain previously published material and is my own work. No work in this thesis was carried out in collaboration with external university or industrial laboratory groups.

The first chapter includes a modified version of a review article published by *Frontiers in Physiology*. The third chapter includes a version of an original research article in the progress of being submitted to *Circulation Research*. The fourth chapter includes a version of an original research article submitted to *Journal of the America College of Cardiology*. I am the first author of these articles and have contributed to more than 50% to its production, including planning, executing, data analysis, and writing. This is recognised in the completed "declaration for a thesis with publication" and the "co-author authorisation" forms that have been submitted with this thesis. The appendix section of this thesis includes published articles of which I have contributed to their production during my enrolment as a PhD candidate at the University of Melbourne. This includes a review article published by *Experimental Physiology* and an original research article published by *Cardiovascular Research.*

Intellectual feedback regarding study related questions, technical issues, study design, data analysis, and editing this thesis were mainly provided by my supervisor Dr Song Tieng Yao and my co-supervisor Prof Clive Newton May. Funding covering the expenses of these studies came from the National Health and Medical Research Council of Australia (GNT

1079680 to STY; GNT 1128108 to CMN and STY). The expenses of my PhD studies were covered by the Australian Government Research Training Program Scholarships, and the expenses of my travel were covered by the American Physiological Society and the Florey Institute of Neuroscience and Mental Health.

Acknowledgments

First and foremost, I would like to express my sincere acknowledgement of gratitude to both my supervisors, Dr Song Yao and Prof Clive May for their continuous support during my PhD candidature and related research, their patience, motivation, and immense knowledge. I am grateful to them for guiding and encouraging me to nurture my abilities and passion for research and writing of this thesis. Thank you for the time and effort you have invested in my work and for also providing opportunities to attend national and international conferences, allowing me to progress as a young investigator.

I would also like to acknowledge my mentor, Dr Willian Korim for the time and effort invested in guiding and supporting my abilities, to progress as a young researcher. My supervisors and colleagues at the Neurovascular Biology Laboratory have provided me with invaluable training and skill sets that I will require for my future endeavours. I could not have imagined having better advisors and mentors for my PhD study.

To the past and present members of the Neurovascular Biology Laboratory, Dr Yonis Abukar, Anthony Setiadi, Jasmine Sloan, Alicia Chan, and Skye Allan, thank you very much for always supporting me throughout my PhD, and for the unforgettable times and memories we shared together in the Lab.

Further recognition to my colleagues at the System Neurophysiology Division at the Florey Institute of Neuroscience and Mental Health, in particular Prof Robin McAllen, Prof Michael McKinley, Dr Stuart McDougall, Dr Rishi Dhingra, and Dr Yugeesh Lankadeva; for

always believing in me and for nurturing my passion for research. Thanks to my PhD committee, Prof Andrew Lawrence and Prof Andrew Allen, for their advice in the numerous progress meeting I had with them.

Thank you to the Advanced Microscopy Facility and the Melbourne Flow Cytometry Facility at the Florey Institute of Neuroscience and Mental Health for training, advice and assistance at the facility, and the Animal Facility personnel at the Florey Institute of Neuroscience and Mental Health for advice and help on animal welfare.

I would like to acknowledge the Commonwealth Government of Australia for providing a stipend that funded my PhD. Thanks to the Florey Institute of Neuroscience and Mental Health and to the American Physiological Society for presenting me with travel awards.

Last but not least, a big thank you goes to my family; my father Gamal, my mother Salwa, and my brothers Hassan and Abdul. To my friends, Andrew Butler and Hamza Habeeballah, thank you for supporting me throughout my PhD and my life in general.

I am exceptionally grateful for everyone's contribution towards making this thesis happen and I am excited to see what the future holds.

Publications

- **Elsaafien K,** Korim WS, Setiadi A, May CN & Yao ST. (2019). Chemoattraction and Recruitment of Activated Immune cells, Central Autonomic Control, and Blood Pressure Regulation. Frontiers in Physiology. doi: 10.3389/fphys.2019.00984.

- Korim WS*, **Elsaafien K***, Basser JR, Setiadi A, May CN & Yao ST. (2018). In renovascular hypertension, TNF-α type-1 receptors in the area postrema mediate increases in cardiac and renal sympathetic nerve activity and blood pressure. Cardiovascular Research. doi: 10.1093/CVR/CVY268.

- Setiadi A, Korim WS, **Elsaafien K**, & Yao ST. (2018). The role of blood-brain barrier in hypertension. Experimental Physiology. doi: 10.1113/EP086434.

CHAPTER	TITLE	STATUS
One	Chemoattraction and Recruitment of Activated Immune cells, Central Autonomic Control, and Blood Pressure Regulation	Published
Three	Chemoattraction of Immune Cells via CCL2-CCR2 Signalling into the Hypothalamic Paraventricular Nucleus Drives Sympathetic Nerve Activation and Causes Hypertension	In Progress
Four	Blockade of the C-C Motif Chemokine Receptor 2 in the Brain Attenuates Blood Pressure Increases in Renovascular Hypertension	Submitted

Conferences

YEAR	PRESENTATION	AUTHORS	TITLE	CONFERENCE
2019	**Featured Speaker**	**Elsaafien K**, Korim WS, May CN & Yao ST	The Chemoattraction of Immune Cells into the Hypothalamic Paraventricular Nucleus Elicits Sympathetically Mediated Blood Pressure Elevations in Hypertension	Experimental Biology; Orlando, USA
2019	Poster	**Elsaafien K**, Korim WS, May CN & Yao ST	The Chemoattraction of Immune Cells into the Hypothalamic Paraventricular Nucleus Elicits Sympathetically Mediated Blood Pressure Elevations in Hypertension	Experimental Biology; Orlando, USA
2019	Poster	Korim WS, **Elsaafien K**, Basser JR, Setiadi A, May CN & Yao ST	In Renovascular Hypertension, TNF-α Type-1 Receptors in the Area Postrema Mediate Increases in Cardiac and Renal Sympathetic Nerve Activity and Blood Pressure	Experimental Biology; Orlando, USA
2018	**Selected Speaker**	**Elsaafien K**, Korim WS, May CN & Yao ST	CCL2-CCR2 signalling in the hypothalamic paraventricular nucleus elicits sympathetically mediated blood pressure elevations through recruitment of immune cells in renovascular hypertension	Central Cardiorespiratory Control: Future Directions; Melbourne, Australia
2018	Poster	Korim WS, **Elsaafien K**, Basser	In Renovascular Hypertension, TNF-α Type-1 Receptors in	Central Cardiorespiratory

		JR, Setiadi A, May CN & Yao ST	the Area Postrema Mediate Increases in Cardiac and Renal Sympathetic Nerve Activity and Blood Pressure	Control: Future Directions; Melbourne, Australia
2018	**Selected Speaker**	**Elsaafien K**, Korim WS, May CN & Yao ST	CCL2-CCR2 signalling in the hypothalamic paraventricular nucleus elicits sympathetically mediated blood pressure elevations through recruitment of immune cells in renovascular hypertension	Australian Society for Medical Research; Melbourne, Australia
2018	**Selected Speaker**	**Elsaafien K**, Korim WS, May CN & Yao ST	CCL2-CCR2 signalling in the hypothalamic paraventricular nucleus elicits sympathetically mediated blood pressure elevations through recruitment of immune cells in renovascular hypertension	Experimental Biology; San Diego, USA
2018	Poster	**Elsaafien K**, Korim WS, May CN & Yao ST	CCL2-CCR2 signalling in the hypothalamic paraventricular nucleus elicits sympathetically mediated blood pressure elevations through recruitment of immune cells in renovascular hypertension	Experimental Biology; San Diego, USA
2017	**Selected Speaker**	**Elsaafien K**, Korim WS, May CN & Yao ST	The role of the chemoattractant CCL2 and leukocytes in neurogenic hypertension	Australasian Society for Neuroscience; Sydney, Australia
2017	Poster	**Elsaafien K**, Korim WS, May CN & Yao ST	CCL2-CCR2 signalling in the hypothalamic paraventricular nucleus elicits sympathetic-mediated blood pressure elevations through local monocytes and	Australasian Society for Neuroscience; Sydney, Australia

			lymphocytes recruitment	
2017	**Selected Speaker**	**Elsaafien K**, Korim WS, May CN & Yao ST	CCL2-CCR2 signalling in the hypothalamic paraventricular nucleus elicits sympathetic-mediated blood pressure elevations through local monocytes and lymphocytes recruitment	Central Cardiorespiratory Control: Future Directions; Sydney, Australia
2016	Poster	Korim WS, Basser JR, **Elsaafien K,** & Yao	TNF-α in the Area Postrema Elicits Sympathetic excitation to the hear in rats	Australasian Society for Neuroscience; Hobart, Australia
2016	Poster	Korim WS, Basser JR, **Elsaafien K,** & Yao	TNF-α in the Area Postrema Elicits Sympathetic excitation to the hear in rats	High Blood Pressure Research Council of Australia; Hobart, Australia
2016	**Selected Speaker**	**Elsaafien K**, Korim WS, May CN & Yao ST	Unravelling the cardiovascular role of the Chemokine "CCL2" in the Paraventricular Nucleus of the Hypothalamus	Central Cardiorespiratory Control: Future Directions; Melbourne, Australia
2015	**Selected Speaker**	**Elsaafien K**, May CN & Yao ST	Unravelling the cardiovascular role of the Chemokine "CCL2" in the Paraventricular Nucleus of the Hypothalamus	Central Cardiorespiratory Control: Future Directions; Sydney, Australia

Awards

YEAR	AWARD	AMOUNT	SOURCE
2019	International Early Career Physiologist Travel Award	1,000 USD	American Physiological Society
2019	Florey Postgraduate Travel Award	2,000 AUD	The Florey Institute of Neuroscience and Mental Health
2018	NCARnation Award	500 USD	American Physiological Society
2017	Australian Postgraduate Award	92,000 AUD	Australian Government Research Training Program Scholarships
2016	Melbourne Research Scholarship	26,888 AUD	The University of Melbourne
2015	Frances Elizabeth Thompson Trust Scholarship	5,000 AUD	The University of Melbourne

Table of Contents

Abstract I

Declaration IV

Preface V

Acknowledgments VII

Publications IX

Conferences X

Awards XIII

Table of Contents XIV

Figures XIX

Tables XXII

Abbreviations XXIII

1. General Introduction 1

1.1 Introduction to Hypertension 2

1.1.1 Peripheral Mechanisms of Hypertension 3

1.1.2 Central Mechanisms of Hypertension 4

1.1.3 Animal Models of hypertension 5

1.2 Central Cardiovascular Control 7

1.2.1 The Paraventricular Nucleus of the Hypothalamus (PVN) 9

1.2.2 The Rostral Ventrolateral Medulla (RVLM) 9

1.2.3 Circumventricular Organs (CVO) 10

1.2.4 Neurochemical Properties of the Cardiovascular Brain Centers 14

1.3 Inflammatory Mediators in Hypertension 18

1.3.1 Pro-inflammatory Cytokines in Hypertension 18

1.3.2 Immune Cells in Hypertension 19

1.3.3 Potential Role for CCL2? 22
1.4 Chemokines and Hypertension 24
1.4.1 What are Chemokines? 24
1.4.2 Chemokine (C-C motif) Ligand 2 (CCL2) 25
1.4.3 Expression of CCL2 and its Receptor CCR2 25
1.4.4 CCL2 in Hypertension 28
1.5 Proposed Role of CCL2 in Hypertension 32
1.6 Hypothesis and Aims 34
2. General Methods and Materials 42
2.1 Animals 43
2.1.1 Ethics Approval 43
2.1.2 Animal Strain and Housekeeping 43
2.2 Surgical Protocols 44
2.2.1 General 44
2.2.2 Rat Models of Hypertension 44
2.2.3 Femoral Cannulation 45
2.2.4 Telemetry Implantation 46
2.2.5 Renal Sympathetic Nerve Preparation 47
2.2.6 Cranial Surgery for Central Microinjections 49
2.2.7 PVN Microinjection 49
2.2.8 RVLM Microinjection 52
2.2.9 ICV Microinjection 54
2.2.10 Osmotic Minipump Implantation 54
2.2.11 Drugs 56
2.3 Tissue Collection 57
2.3.1 Cerebrospinal Fluid Sample Collection 57
2.3.2 Plasma Sample Collection 57
2.3.3 Transcardial Perfusion 57
2.3.4 Brain Collection Tissue 58
2.3.5 Heart and Kidney Collection 60

2.4 Immunohistochemical Studies 60
2.4.1 Immunofluorescence Labelling 60
2.4.2 Histological Analysis of Injection Sites 63
2.4.3 Photomicroscopy and Figure Preparation 64
2.4.4 Identifying Brain Regions 65
2.4.5 Validation of Immunohistochemistry 67
2.5 Biochemical Assays 70
2.5.1 Enzyme-Linked Immunosorbent Assay (ELISA) 70
2.5.2 Flow Cytometry 71
2.6 Experimental Protocols 77
2.6.1 Hypertensive Animal Experimental Series 77
2.6.2 Anaesthetized Animals Experimental Series 80
2.6.3 Conscious Animal Experimental Series 80
2.6.4 Tracer Study 81
2.6.5 Antagonizing CCR2 in Hypertensive Animal Experimental Series 81
2.7 Statistical Analysis 82
2.7.1 Physiological Responses Analysis 82
2.7.2 Immunohistochemical Analysis 84
3. Chemoattraction of Immune Cells via CCL2-CCR2 signalling into the Hypothalamic Paraventricular Nucleus Drives Sympathetic Nerve Activation and Causes Hypertension 88
3.1 Abstract 89
3.2 Introduction 90
3.3 Methods and Materials 92
3.4 Results 93
3.4.1 Immune Cell Profile in the PVN of a Primary Rat Model of Hypertension 93
3.4.2 Immune Cell Profile in the PVN of Renovascular Hypertensive Rats 95
3.4.3 Cardiovascular Effects of Exogenous Application of CCL2 into the PVN of Conscious and Anaesthetized Rats 99
3.4.4 Sympathetic Responses to Activation of CCL2-mediated Activation of CCR2 Receptors in the PVN 102
3.4.5 Location of CCR2 Receptors in the PVN 102

3.4.6 Cardiovascular Responses to PVN Injections of CCL2 After Blockade of Purinergic Transmission 103

3.4.7 Changes in the Profile of Immune Cells in Response to PVN Injections of CCL2 in Normotensive Rats 107

3.4.8 Anti-inflammatory Treatment Blocks the Sympathetic Responses to CCL2 Microinjection into the PVN 110

3.5 Discussion 112

3.6 Conclusion 117

3.7 Novelty and Significance 119

4. Blockade of the C-C Motif Chemokine Receptor Type 2 in the Brain Attenuates Blood Pressure Increases in Renovascular Hypertension 136

4.1 Abstract 137

4.2 Introduction 138

4.3 Methods and Materials 140

4.3.1 Experimental Protocol 140

4.3.2 Immunohistochemical Analysis 141

4.3.3 Enzyme-Linked Immunosorbent Assay (ELISA) 141

4.3.4 Fluorescence Activated Cell Sorting 142

4.3.5 Statistical Analysis 142

4.4 Results 143

4.4.1 Blockade of Brain CCR2 Receptors Inhibits the Increase in BP in Renovascular Hypertension 143

4.4.2 Blockade of Brain CCR2 Receptors Prevents the Increase in Plasma CCL2 in Renovascular Hypertension 146

4.4.3 Blockade of Brain CCR2 Receptors Prevents the Recruitment of Macrophages to the PVN of Renovascular Hypertensive Rats 148

4.4.4 Blockade of Brain CCR2 Receptors Reduces Microglia Activation in the PVN of Renovascular Hypertensive Rats 151

4.4.5 Blockade of Brain CCR2 Receptors Prevents Neuronal Activation in Autonomic Nuclei in Renovascular Hypertension 154

4.4.6 Cardiovascular Effects of the Injection of CCL2 into a Lateral Cerebral Ventricle in Normotensive Rats 157

4.5 Discussion 159

4.6 Perspectives 164

4.7 Novelty and Significance 166

5. General Discussion 173

5.1 Discussion 174

5.2 Caveats and Future Directions 178

5.3 Novelty and Clinical Significance 179

5.4 Conclusion 180

6. Bibliography 181

7. Appendices i

Figures

Figure 1.1: Regulatory mechanisms of blood pressure. 6

Figure 1.2: Cardiovascular centres of the brain that regulate the sympathetic input to cardiovascular organs. 8

Figure 1.3: Circumventricular organs (CVO) 12

Figure 1.4: CVOs communicating with peripherally circulating factors. 13

Figure 1.5: Levels of CCL2 in bone marrow, serum and CSF of SHR. 23

Figure 1.6: Expression of CCL2 and CCR2 receptors in brain cells 27

Figure 2.1: Baroreflex modulation of RSNA. 48

Figure 2.2: Validation of PVN microinjections 51

Figure 2.3: Validity of retrograde tracing using CTb. 53

Figure 2.4: Validity of intra-cerebroventricular (ICV) infusions. 55

Figure 2.5: Methodology used to identify different brain regions. 66

Figure 2.6: Distinguishing circulating macrophages from resident macrophages (microglia). 68

Figure 2.7: Validation of C-fos labelling 69

Figure 2.8: Viability of single cell suspension isolated from the PVN. 73

Figure 2.9: Validity of flow cytometry antibodies using a whole white blood sample 75

Figure 2.10: Validity of flow cytometry antibodies and positive events in the PVN 76

Figure 2.11: Body, heart, and kidney weights, and spectral analysis of the primary model of hypertension 78

Figure 2.12: Body, heart, and kidney weights, and the spectral analysis of the renovascular model of hypertension. 79

Figure 2.13: Morphology of resting and activated microglia. 86

Figure 2.14: Skeleton analysis for microglia. 87

Figure 3.1: Immune cells are activated and recruited to the paraventricular nucleus of the hypothalamus (PVN) in hypertension. 94

Figure 3.2: Recruitment and activation of immune cells by CCL2 precede blood pressure increases in hypertension. 98

Figure 3.3: CCL2 in the PVN produces a biphasic blood pressure response. 101

Figure 3.4: CCL2 evokes sympathetic mediated responses in BP. 106

Figure 3.5: CCL2 recruits immune cells that infiltrate into the PVN 109

Figure 3.6: Infiltration of immune cells into the PVN mediates and maintains the second phase of the CCL2 response. 111

Figure 3.7: The Chemoattraction of immune cells by CCL2 into the PVN induces neuroinflammation and sustained BP increases in hypertension 118

Supplementary Figure 3.1: Correlations between PVN immune cells and BP in the primary model of hypertension. 121

Supplementary Figure 3.2: Correlations between PVN immune cells, CCL2 levels and BP in the renovascular model of hypertension. 123

Supplementary Figure 3.3: Baseline controls of drugs microinjected into the PVN. 124

Supplementary Figure 3.4: L-glutamate PVN microinjection in anaesthetized and conscious rats. 125

Supplementary Figure 3.5: Validation of PVN microinjections. 126

Supplementary Figure 3.6: C-fos in the PVN and the RVLM following PVN microinjections with CCL2. 127

Supplementary Figure 3.7: Colocalization of CCR2 receptors with other cell types in the PVN. 129

Supplementary Figure 3.8: Validation of RVLM microinjections. 130

Supplementary Figure 3.9: Immune profile in PVN microinjected with saline. 131

Supplementary Figure 3.10: CCR2 expression in splenic and thymic immune cells 132

Supplementary Figure 3.11: C-fos activity in the PVN and the RVLM of the renovascular model of hypertension. 133

Supplementary Figure 3.12: Microglia activation in the PVN and the RVLM of the renovascular model of hypertension. 135

Figure 4.1: Central blockade of CCR2 receptors prevents blood pressure increases in renovascular hypertension. 145

Figure 4.2: Central blockade of CCR2 receptors prevents increases of plasma CCL2 in renovascular hypertension. 147

Figure 4.3: Central blockade of CCR2 receptors prevents macrophage recruitment to the PVN of renovascular hypertensive rats. 150

Figure 4.4: Central blockade of CCR2 receptors prevents microglia activation in the PVN of renovascular hypertensive rats 153

Figure 4.5: Central blockade of CCR2 receptors prevents neuronal activation in renovascular hypertension 156

Figure 4.6: Central administration of CCL2 recruits' macrophages to the PVN and increases blood pressure. 158

Figure 4.7: CCL2-CCR2 Signalling in the PVN causes Hypertension. 165

Supplementary Figure 4.1: Body weights and temperatures overtime in renovascular hypertensive. 168

Supplementary Figure 4.2: Validation of intra-cerebroventricular (ICV) infusions. 168

Supplementary Figure 4.3: Quantification of brain leukocytes through FACS gating. 169

Supplementary Figure 4.4: Experimental protocol of the present study. 170

Supplementary Figure 4.5: Kidney and heart weights of renovascular hypertensive rats. ... 171

Supplementary Figure 4.6: Identifying the different brain regions. 172

Tables

Table 1.1: Levels of inflammatory mediators in animal models of hypertension. 21

Table 2.1: List of all experimental drugs used in all series of experiments presented by this thesis. 56

Table 2.2: List of all primary antibodies used in all series of experiments presented by this thesis. 62

Abbreviations

2K1C	Two kidney- one clip
3v	Third ventricle
4v	Fourth ventricle
ACE	Angiotensin converting enzyme
aCSF	Artificial cerebrospinal fluid
Ambc	Compact part of the nucleus ambiguus
AMPA	α-amino-3-hydroxy-5-methyl-4-isoxazolepropionic acid
ANS	Autonomic nervous system
AP	Area Postrema
ARB	Angiotensin receptor blockers
Arc	Arcuate nucleus
AT_1R	Angiotensin type 1 receptor
ATP	Adenosine triphosphate
BBB	Blood brain barrier
BM	Bone marrow
BP	Blood pressure
CCL2	Chemokine (C-C motif) Ligand 2
CCR2	C-C Chemokine Receptor Type 2
CNS	Central nervous system
CSF	Cerebrospinal fluid
CTb	Cholera toxin subunit B
CVO	Circumventricular organs
CVS	Cardiovascular system
CX3CL1	C-X3-C motif chemokine ligand 1 or fractalkine
CXCL12	C-X3-C motif chemokine ligand 12
DBP	Diastolic blood pressure
EAE	Experimental autoimmune encephalitis
ec	External capsule
ELISA	Enzyme-linked immunosorbent assay

FACS	Fluorescence activated cell sorting
FDA	Food and drug administration
GABA	Gamma- aminobutyric acid
GFAP	Glial fibrillary acidic protein
Gr	Gracilis nucleus
HR	Heart rate
IL-1β	Interleukin-1β
IL-6	Interleukin-6
IL1R	Interleukin 1 receptor
IM	Inflammatory mediator
IML	Interomediolateral cell column of the spinal cord
LV	Lateral cerebroventricle
MAP	Mean arterial pressure
MBP	Mean blood pressure
MCP-1	Monocyte chemoattractant protein-1
NF-$_{\kappa}$B	Nuclear factor kappa-light-chain-enhancer of activated B cells
NH	Neurohypophysis
NMDA	N-methyl-D-aspartate
nNOS	Neuronal nitric oxide synthase
NTS	Nucleus of the solitary tract
OVLT	Vascular organ of lamina terminalis
PaDc	Dorsal cap of the PVN
PaPo	Medial PVN
PaV	Ventral PVN
PBS	Phosphate buffered saline
PFA	Paraformaldehyde
PI	Pineal
PRV	Pseudorabies virus
PVN	Paraventricular nucleus of the hypothalamus
RAS	Renin angiotensin system
RSNA	Renal sympathetic nerve activity
RVLM	Rostral ventrolateral medulla
RVMM	Rostral ventromedial medulla

SBP	Systolic blood pressure
SFO	Subfornical organ
SHR	Spontaneous hypertensive rats
SNA	Sympathetic nerve activity
SNS	Sympathetic nervous system
SPN	Sympathetic preganglionic neurons
SubP	Subpostremal area
TH	Tyrosine hydroxylase
TNF-α	Tumour necrosis factor-α
TNFR1	Tumour necrosis factor receptor 1
TPR	Total peripheral resistance
WKY	Wistar Kyoto

1. General Introduction

Remark: The following text is an extended version of the article published by *Frontiers in Physiology* on August 2019 (Elsaafien K et al. 2019). I have contributed to every aspect of its production. The full paper is attached to the end of this chapter.

1.1 Introduction to Hypertension

Hypertension is a cardiovascular disease, characterised by elevations in blood pressure (BP) (Heart Foundation, 2016). According to the most recent guidelines set by the American College of Cardiology and the American Heart Association; hypertension is defined as a systolic/diastolic BP of 130/90 mmHg or above (Whelton, Carey et al. 2018). In Australia, 32% of adult Australians suffer from hypertension (Heart Foundation, 2016), and the expenditure for treatment of hypertension is estimated to cost $7.6 billion per year, where hypertension is described as "the highest expenditure of any disease group in Australia" (Australian Institute of Health and Welfare, 2014). More than 69 antihypertensive drugs across 15 different classes are approved by the Food and Drug Administration (FDA) (Food and Drug Administration and the Department of Health and Human Services, 2011). Most of these drug classes have targets in the periphery; for example targeting components of the renin-angiotensin system (RAS), such as angiotensin converting enzyme inhibitors (ACE inhibitors) and angiotensin receptor blockers (ARBs) (Smith and Ashiya 2007). Despite this plethora of anti-hypertensive therapies; approximately 10-15% of the general hypertensive population have resistant hypertension; defined as uncontrollable BP in spite of the concurrent use of 3 or more anti-hypertensive agents of different classes (Persell 2011, Sim, Bhandari et al. 2013). As such, a better understanding of non-peripheral mechanisms that mediate hypertension is essential to improve current hypertensive therapies. Central mechanisms may be potential targets for anti-hypertensive therapies; as sympathetic nerve activity (SNA) elevation is a key component observed in hypertensive patients (Smith, Graham et al. 2004, Barretto, Santos et al. 2009).

1.1.1 Peripheral Mechanisms of Hypertension

Hypertension is a multifactorial chronic disease, where the aetiology is attributed to a range of factors. At its simplest, hypertension can be described as an imbalance in normal homeostasis. For many years the kidney and its associated hormones and peptides were believed to play an essential role in BP control and regulation (Guyton 1991). The "pressure natriuresis" hypothesis suggests the kidney's ability to excrete sodium, reducing bodily fluids, as a response to BP elevation to be crucial in controlling BP (Guyton 1991). Whereas hormones and peptides secreted by the kidney, such as angiotensin II and erythropoietin, are believed to play an important role in increasing BP. Early studies demonstrate the secretion of erythropoietin by the kidneys to cause vasoconstriction (Müller, Steffen et al. 1991, Suga, Kurihara et al. 1996). In addition, RAS and the excessive secretion of angiotensin II by the kidneys is involved in increasing BP (Francis, Goldsmith et al. 1984). Angiotensin II is a potent vasoconstrictor and mice lacking angiotensin type I receptor (AT_1R) are protected from developing hypertension, hence these receptors are targeted by anti-hypertensive drugs (Figure 1.1) (Crowley, Gurley et al. 2005, Crowley, Gurley et al. 2006). Furthermore, other peripheral factors contribute to the aetiology of hypertension and are targeted for anti-hypertensive therapies. These include dietary sodium intake (Meneton, Jeunemaitre et al. 2005), body-fluid volume (Machnik, Neuhofer et al. 2009), peripheral vascular resistance (Cowley Jr 1992), and many other contributing peripheral factors. These peripheral factors generally lead to end organ damage, as a complication of hypertension, which can exacerbate the disease. Increased cardiac hypertrophy and renal injury are reported as the main complications of hypertension (Elmarakby, Quigley et al. 2007, Matsuda, Umemoto et al. 2015). Finally, one of the main drivers in mediating hypertension is augmented sympathetic output (Smith, Graham et al. 2004), resulting in peripheral norepinephrine spill-over (Esler, Jennings et al. 1984, Rahn, Barenbrock et al. 1999). Therefore, activating adrenergic receptors on the heart and the

vasculature to increase heart rate (HR) and total peripheral resistance (TPR) (Freeman, Dewey et al. 2006); thus increasing BP.

1.1.2 Central Mechanisms of Hypertension

Increased sympathetic output is observed in many hypertensive patients. Recordings from muscle sympathetic nerves demonstrate sympathetic hyperactivity in patients with hypertension (Smith, Graham et al. 2002, Barretto, Santos et al. 2009). These findings suggest that brain mechanisms are involved in hypertension. To date, complex neural networks spanning a number of specialised brain structures are characterised as brain regions directly involved in the control and regulation of SNA (Schramm, Strack et al. 1993). Upon activation by either chemical of electrical stimulation, elevations in SNA and BP are observed (Guertzenstein and Silver 1974, Ross, Ruggiero et al. 1984, Guyenet, Haselton et al. 1988, Lawrence and Jarrott 1994). Thus, the over-excitation of specific subsets of neurons in the cardiovascular centres of the brain leads to aberrant elevations in SNA and contribute to the development of hypertension (Figure 1.1). In addition, glia plays an important role in regulating the excitability of these neurons. Microglia and astrocytes are known to influence excitatory neurotransmission (Pascual, Achour et al. 2012), and to play a role in sympatho-excitation (Gordon, Baimoukhametova et al. 2005, Gordon, Iremonger et al. 2009, Du, Jiang et al. 2015, Wu, Xu et al. 2017). Both microglia and astrocytes are active in the cardiovascular brain regions in experimental animal models of hypertension (Aiyar, Daines et al. 2001, Tomassoni, Avola et al. 2004, Shi, Diez-Freire et al. 2010, Shi, Raizada et al. 2010, Shen, Li et al. 2015). Furthermore, activating microglia or astrocyte results in establishing a pro-inflammatory state, elevating SNA and leading to the development of hypertension (Aiyar, Daines et al. 2001, Shi, Diez-Freire et al. 2010, Shi, Raizada et al. 2010, Shen, Li et al. 2015). The combination of neurotransmitter (excitability) and inflammatory imbalances (Jia, Kang et al. 2014), microglia

and astrocyte activation (Shi, Diez-Freire et al. 2010), lead to the over-excitation of neurons in the cardiovascular centres of the brain, resulting in detrimental SNA elevation leading to the development of hypertension.

1.1.3 Animal Models of hypertension

A number of animal models of hypertension have been developed ranging from models of primary (essential) to secondary hypertension. Spontaneously hypertensive rats (SHR) are a genetic model of hypertension (primary hypertension), where BP spontaneously increases at 5-6 weeks of age (Simms, Paton et al. 2008). On the other hand, the two kidneys – one clip (2K1C) or Goldblatt model is a model of secondary (renovascular) hypertension. In this model, hypertension is induced by the partial obstruction of one renal artery via a clip (Goldblatt, Lynch et al. 1934). The partial stenosis of the renal artery in this renovascular model of hypertension causes an immediate elevation in renin and angiotensin in the circulation (Martinez-Maldonado 1991). In this model sustained increases in BP occur during the third week and plateaus by the fifth week following clipping (Martinez-Maldonado 1991, Oliveira-Sales, Toward et al. 2014). Therefore, hypertension is fully established by 4-5 weeks after clipping the renal artery, mediated by not only the sustained release of renin and angiotensin in circulation but potentially other neural mechanisms.

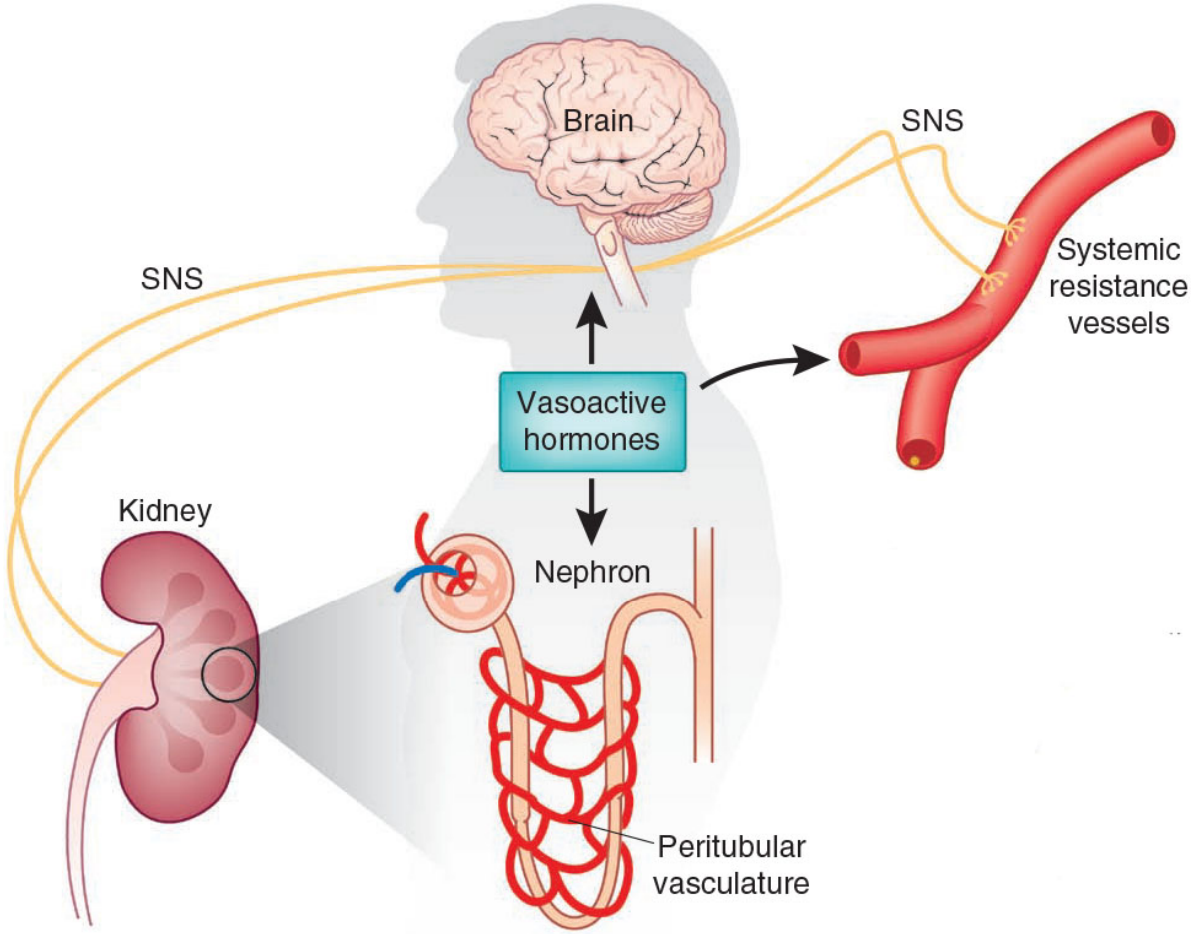
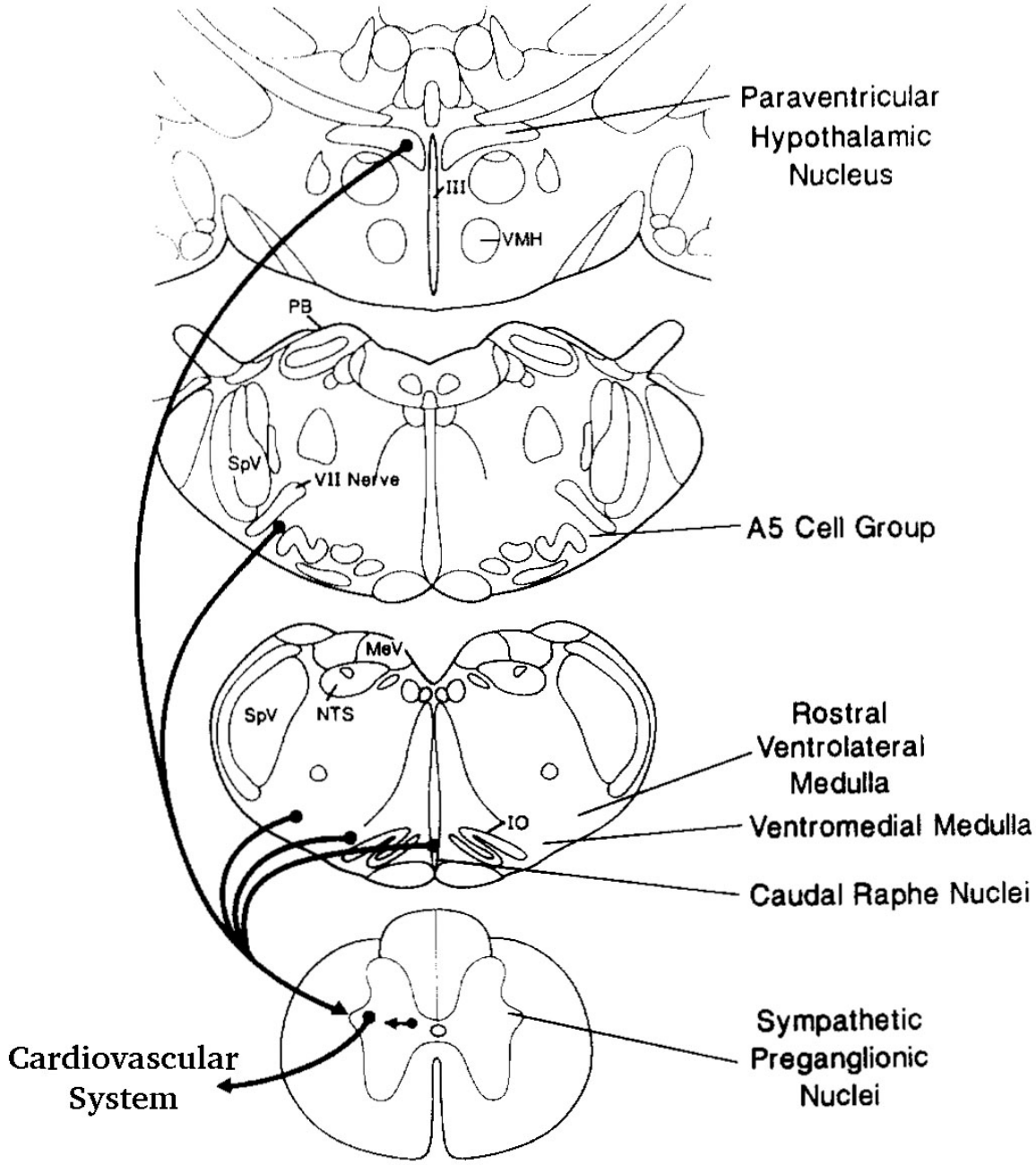


Figure 1.1: Regulatory mechanisms of blood pressure.

This schematic diagram depicts the regulatory mechanisms of blood pressure by both peripheral and central mechanisms. Vasoactive hormones such as Angiotensin II and erythropoietin are secreted by the kidney and act on the vasculature to induce vasoconstriction and increase blood pressure. Sympathetic activation that arises from the brain to the vasculature induces vasoconstriction and increases blood pressure. SNS; sympathetic nervous system, figure reproduced from (Coffman 2011).

1.2 Central Cardiovascular Control

The central nervous system (CNS) exerts constant control and regulation of arterial BP (Guyenet, Haselton et al. 1988, Dampney 1994). The sympathetic nervous system (SNS), which forms part of the autonomic nervous system (ANS), is utilised by central cardiovascular regions to control the cardiovascular system (CVS) (Pilowsky and Goodchild 2002, Freeman, Dewey et al. 2006). Sympathetic nerves, forming parts of SNS, originate from a distinct group of neurons located in the interomediolateral cell column (IML) of the spinal cord at the level of T1-L2 (Pilowsky and Goodchild 2002, Freeman, Dewey et al. 2006). In 1993, Larry Schramm and Arthur Loewy investigated the inputs to the IML from higher brain structures (Schramm, Strack et al. 1993). The group injected a pseudorabies virus (PRV), which has the ability to cross synapses, into the left adrenal glands of male rats, and after allowed the rats to recover, found that the PRV infected the IML at the level of T10-T13. Further analysis revealed that the virus also infected secondary neurons in five major brain structures, suggesting that those brain structures form the majority of the input to the IML and hence, play a role in regulating the sympathetic outflow via the IML. Those structures included the paraventricular hypothalamic nucleus (PVN), the A5 noradrenergic cell group, the rostral ventrolateral medulla (RVLM), the rostral ventromedial medulla (RVMM), and the caudal raphe nuclei (Fig 1.2) (Schramm, Strack et al. 1993). This study combined with others from the Loewy laboratory, unequivocally show these five brain region play a role in regulating the sympathetic outflow to the CVS (Strack, Sawyer et al. 1989, Strack, Sawyer et al. 1989). The main focus of this thesis will be on the PVN and the RVLM, as they are shown to be key areas targeted by inflammatory mediators in the different rodent models of hypertension (Kang, Zhang et al. 2014, Li, Qin et al. 2014, Song, Jia et al. 2014, Wang, Kang et al. 2018).



<u>Figure 1.2:</u> Cardiovascular centres of the brain that regulate the sympathetic input to cardiovascular organs.

The schematic diagram depicts the five major brain regions which project the sympathetic preganglionic neurons of the IML. Suggesting that these five main brain nuclei control and regulate the sympathetic outflow to the cardiovascular system. Figure reproduced from (Strack, Sawyer et al. 1989).

1.2.1 The Paraventricular Nucleus of the Hypothalamus (PVN)

The paraventricular nucleus of the hypothalamus (PVN) is a hypothalamic nucleus located in the diencephalon (Ettrup, Sorensen et al. 2010). It is a bilateral nucleus that appears as a distinct group of cells situated adjacent to the ventricular wall (third ventricle). It is a highly vascularised nucleus with an intact blood brain barrier (BBB) and is made up of two distinct types of neurons: lateral magnocellular and medial parvocellular neurons (Ettrup, Sorensen et al. 2010). Neurons from the parvocellular region project to autonomic nuclei in the brainstem (RVLM) and the spinal cord (IML), and are therefore capable of activating the SNS to regulate cardiovascular function (Yang and Coote 1998, Pyner and Coote 2000). These projections include, monosynaptic projections to each of the RVLM and the IML (Shafton, Ryan et al. 1998, Yang and Coote 1998, Pyner and Coote 2000, Hardy 2001), and a polysynaptic projection to both the RVLM and the IML (Badoer 2001). It is believed that 85% of these projections are glutamatergic (Strack, Sawyer et al. 1989, Strack, Sawyer et al. 1989). Moreover, blocking glutamatergic receptors in the PVN, reduces sympatho-excitation (Badoer, Ng et al. 2003). Whereas the other 15% of these projections are thought to be GABAergic (Bowman, Kumar et al. 2013), and the inhibition of GABAergic receptors in the PVN increases BP (Cruz and Machado 2009, Ramchandra, Hood et al. 2013).

1.2.2 The Rostral Ventrolateral Medulla (RVLM)

The rostral ventrolateral medulla (RVLM) is a bilateral nucleus located in the medulla oblongata of the brainstem. It is located ventral to the compact formation of the nucleus ambiguus and caudal to the facial nucleus (Guertzenstein and Silver 1974, Dampney 1994). The RVLM contains a population of neurons directly projecting to the sympathetic pre-ganglionic neurons (SPN) of the IML (Ross, Ruggiero et al. 1984, Dampney, Czachurski et al. 1987, Strack, Sawyer et al. 1989). These anatomical connections support the notion that the

RVLM plays in the maintenance of SNA and BP. Indeed, the bilateral destruction or inhibition of the RVLM produces profound reductions in BP (Guertzenstein and Silver 1974, Feldberg and Guertzenstein 1976). Furthermore, chemical and electrical stimulation of the RVLM elevates arterial BP and HR (Guertzenstein and Silver 1974, Ross, Ruggiero et al. 1984, Guyenet, Haselton et al. 1988). Neurons of the RVLM innervating SPN are excitatory catecholaminergic C1 neurons, that release glutamate to excite the SPN of the IML (Ross, Ruggiero et al. 1984, Dampney, Coleman et al. 2002, Pilowsky and Goodchild 2002). The excitation of these neurons through the local microinjection of glutamate induces elevations in BP in both anaesthetised (Dampney, Goodchild et al. 1985, McAllen 1986, McAllen and Dampney 1989) and in conscious animals (Bachelard, Gardiner et al. 1990).

1.2.3 Circumventricular Organs (CVO)

Historically, the BBB is a concept first described from the observation that the intravenous injection of dyes stained various organs except for the brain (Ehrlich 1885, Lewandowsky 1900, Goldman 1909). While the endothelium of the capillary walls in most non-neuronal tissue is permeable, in the nervous system the endothelium of capillaries restricts movement of molecules from blood to the brain (Katzman and Pappius 1973, Rapoport 1976, Bradbury 1979). However, the circumventricular organs (CVO) were later described as brain regions with fenestrated capillaries, high permeability and close vicinity to the ventricles (Weindl 1973). These regions are described as brain regions lacking an intact BBB and include autonomic areas such as; the subfronical organ (SFO), the vascular organ of the lamina terminalis (OVLT), and the area postrema (AP) (Fig. 1.3) (Weindl 1973). The lack of an intact BBB in CVOs allows communication between CVOs and the systemic circulation. Hence the CVOs can sense and respond to peripherally circulating factors. For example, systemic infusion of angiotensin II; activates the SFO, increasing SNA and BP, through SFO projections to the

PVN (Fig. 1.4) (Zucker, Schultz et al. 2004, Nunes and Braga 2011, Zubcevic, Santisteban et al. 2017).

1.2.3.1 The Area Postrema (AP)

The area postrema (AP) is located on the dorsal surface of the medulla and is a highly vascularised region lacking an intact BBB (Ettrup, Sorensen et al. 2010). It is a CVO containing neurons that are readily accessible to blood-borne factors found in the systemic circulation. Classically, the AP is well-known for inducing vomiting, as it contains chemo-sensors that trigger vomiting (Bonham and Jeske 1989). However, the connectivity of the AP to other cardiovascular regions of the brain suggests it also plays a role in autonomic regulation. The AP receives axonal projections from the parvocellular neurons of the PVN, and it also innervates the PVN via both monosynaptic and polysynaptic connections (van der Kooy and Koda 1983, Shapiro and Miselis 1985). In addition to the PVN, the AP has major inputs to the RVLM (Blessing, Hedger et al. 1987, Dampney, Czachurski et al. 1987), suggesting that the AP might also play an important role in BP regulation. Indeed, the surgical ablation of the AP in rats attenuates BP elevation and protects against the development of hypertension in the angiotensin II-mediated model of hypertension (Joy and Lowe 1970, Fink, Bruner et al. 1987). Furthermore, circulating angiotensin II increases fos protein expression in the AP and elevates BP, suggesting the activation of the AP to be involved in elevating BP (Ferrario, Barnes et al. 1987, Potts, Hirooka et al. 1999). In addition, the stimulation of the AP by the inflammatory mediator TNF-α excites the RVLM-projecting neurons of the AP leading to sustained increases in cardiac and renal sympathetic nerve activity and BP (Korim, Elsaafien et al. 2018).

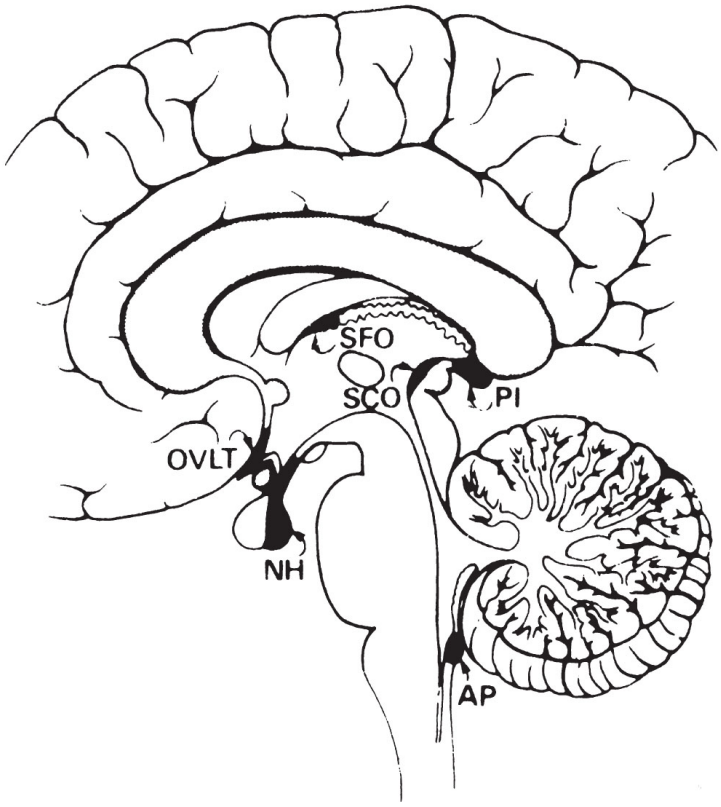


Figure 1.3: Circumventricular organs (CVO).

A schematic diagram showing the locations of the brain CVOs and their close vicinity to the brain ventricular system. AP; area postrema, NH; neurohypophysis, OVLT; vascular organ of the lamina terminalis, PI; pineal, SFO; subfronical organ. Diagram taken from (Ganong 2000).

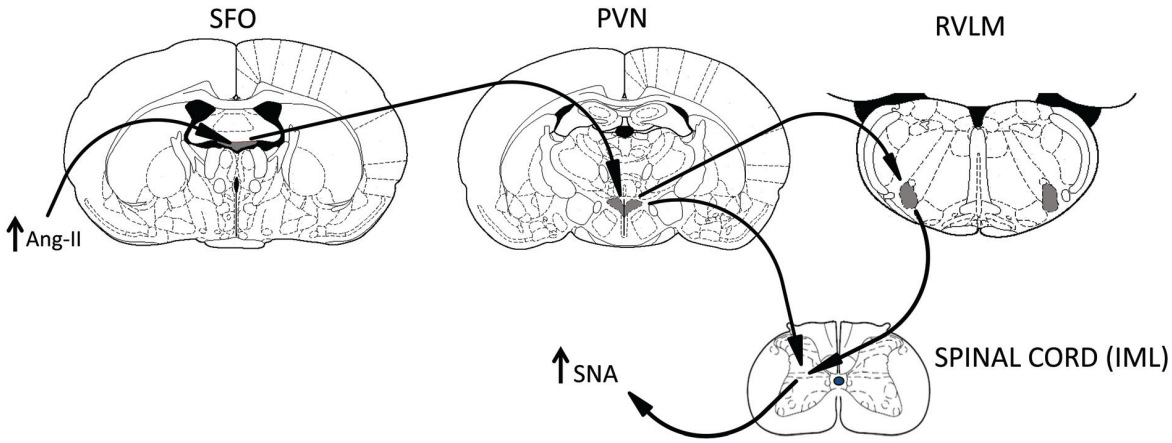


Figure 1.4: CVOs communicating with peripherally circulating factors.

A schematic diagram showing an example of how CVOs might be accessed via blood-borne factors in the circulation. The example in the diagram shows how circulating angiotensin II can activate cardiovascular brain regions. The pathway involves angiotensin II acting on the SFO, activating projections to the PVN, resulting in the activation of the sympathetic preganglionic neurons of the IML, increasing SNA. The area postrema (AP) may also utilise this same pathway, as it projects to both the PVN and the RVLM, and circulating angiotensin II activates the AP and elevate BP. IML; interomediolateral column, PVN; paraventricular nucleus, RVLM; rostral ventrolateral medulla, SFO; subfronical organ, SNA; sympathetic nerve activity. Diagram taken from (Braga, Medeiros et al. 2011).

1.2.4 Neurochemical Properties of the Cardiovascular Brain Centers

Cardiovascular control centres in the brain are fairly well characterised and express a wide range of receptors for various neurotransmitters and neuromodulators. These neurotransmitters and neuromodulators constitute a wide range of amino acids, peptide, metabolites and inflammatory mediators. Previous studies demonstrate the expression of both the transmitters/modulators and their receptors in cardiovascular brain regions. The neurochemical properties of the cardiovascular centres of the brain will be discussed in detail below.

1.2.4.1 Classical Neurotransmitters

L-glutamate and gamma-aminobutyric acid (GABA) are the primary excitatory and inhibitory amino acid neurotransmitters utilised by the central nervous system respectively (DeFelipe 1993, Martin and Olsen 2000, Petroff 2002). Densities of amino acid receptors such as excitatory L-glutamate receptors (namely, NMDA and AMPA receptors) and inhibitory GABA receptors are expressed in many cardiovascular brain regions including the PVN and the RVLM (Strack, Sawyer et al. 1989, Crestani, Alves et al. 2010, Bowman, Kumar et al. 2013). The blockade of these receptors with antagonists alters SNA and BP, suggesting that they play an important role in the maintenance of the CVS (Chen, Haywood et al. 2003, Carillo, Oliveira-Sales et al. 2012). For example, inhibiting glutamatergic receptors in the PVN with kynurenate reduces sympatho-excitation (Badoer, Ng et al. 2003). In addition, stimulation of the cardiovascular brain regions increases the endogenous release of these neurotransmitters (Talman, Perrone et al. 1980, Lawrence and Jarrott 1994). Thus, the direct microinjection of these amino acid into specific cardiovascular centres in the brain results in changing SNA and BP (Li, Jackson et al. 2006). For example, the local microinjection of glutamate into the RVLM elevates BP in both anaesthetised (Dampney, Goodchild et al. 1985, McAllen 1986, McAllen

and Dampney 1989) and conscious animals (Bachelard, Gardiner et al. 1990). In fact, there is no doubt that these classical amino acids are utilised as neurotransmitters by neurons of the cardiovascular centres of the brain; however, modulation of the excitability of these neurons may be the mediated by neuromodulators such as neuropeptides (i.e. vasopressin and oxytocin) and metabolites (i.e. adenosine) (Hallbeck, Larhammar et al. 2001, Yang, Wheatley et al. 2002, Stern 2004, Kc, Balan et al. 2010).

1.2.4.2 Peptides and hormones

A number of peptides, such as vasopressin, oxytocin and angiotensin II modulate a number of central cardiovascular regions (Hokfelt, Elde et al. 1978). Receptor densities for vasopressin, oxytocin and angiotensin II are found to be expressed in many central cardiovascular nuclei (Aguilera, Kiss et al. 1995, Vaccari, Lolait et al. 1998, Barnes, DeWeese et al. 2003, Bailey, Jin et al. 2006), as well as the expression of these peptides in the neurons of those brain regions (Hallbeck, Larhammar et al. 2001, Lee, Ryu et al. 2013). For example, approximately 80% of PVN neurons projecting to the RVLM express oxytocin, whereas only 20% express vasopressin, and about 47% of these neurons express more than 2 peptides (Lee, Ryu et al. 2013). These peptides are present in many hypothalamic presynaptic terminals and are shown to modulate neuronal responses to either blunt or augment the cardiovascular responses (Michelini and Morris 1999, Michelini 2007, Michelini and Stern 2009, Stern, Sonner et al. 2012). For example, increased vasopressin transmission from the PVN to the RVLM is shown to augment sympathetic outflow (Kc, Balan et al. 2010). Thus; the microinjection of these peptides into specific central cardiovascular regions alters SNA and BP (Undesser, Hasser et al. 1985, Yang, Wheatley et al. 2002). For example; the microinjection of vasopressin in the PVN induces sympatho-excitation to the kidney (Yang, Wheatley et al. 2002).

1.2.4.3 Metabolites

Adenosine and adenosine triphosphate (ATP) are examples of metabolites utilised by the central nervous system (Burnstock 1997, Burnstock and Knight 2017). Receptors for these metabolites are known as purinoceptors (Buell, Collo et al. 1996) and are found to be expressed in many brain regions controlling the CVS (Yao, Barden et al. 2000, Yao, Barden et al. 2001, Yao, Gourine et al. 2003). Approximately 14-29% of PVN neurons projecting the RVLM express purinoceptors (Cham, Owens et al. 2006). Interestingly; antagonising purinoceptors in the PVN of conscious rats leads to elevating BP (Cruz, Bonagamba et al. 2010). Suggesting that these metabolites are utilised as signalling molecules in brain, rather than just a by-product of metabolism. Indeed, many reports show that they influence neurotransmission (Deuchars, Atkinson et al. 2001, Sperlágh, Köfalvi et al. 2002), and are involved in fast excitatory synaptic transmission between neurons (Edwards, Gibb et al. 1992, Evans, Derkach et al. 1992). In fact, stimulation of glutamatergic receptors triggers transient ATP release (Dissing-Olesen, LeDue et al. 2014). Thus, the microinjection of ATP into the PVN increases BP and SNA (Busnardo, Ferreira-Junior et al. 2013, Ferreira-Neto, Yao et al. 2013).

1.2.4.4 Inflammatory mediators

Inflammatory mediators such as pro-inflammatory cytokines and chemoattractants are the focus of recent studies in autonomic regulation. In the last decade, emerging evidence suggests that receptors for several chemokines are expressed in many brain regions controlling the CVS (Banisadr, Gosselin et al. 2005, Rostene, Kitabgi et al. 2007, Ruchaya, Antunes et al. 2014). For example; receptors for the chemoattractant fractalkine (CX3CL1) are expressed on PVN neurons (Ruchaya, Antunes et al. 2014). These inflammatory mediators are capable of modulating the activity of neurons. For example, CXCL12 modulates the firing pattern of vasopressin neurons (Callewaere, Banisadr et al. 2006), and CCL2 modulates the GABAergic

currents in spinal cord neurons (Gosselin, Varela et al. 2005). Thus, the microinjection of specific inflammatory mediators into specific cardiovascular brain regions increases SNA and BP (Wei, Yu et al. 2015, Wei, Yu et al. 2017, Yu, Wei et al. 2017). Indeed; the microinjection of TNF-α and IL-1β into the SFO elicits SNA and BP increases (Wei, Yu et al. 2015, Wei, Yu et al. 2017), and the microinjection of CX3CL1 into the PVN increases BP (Ruchaya, Antunes et al. 2014). Therefore, there is a growing body of evidence to suggest a role for inflammatory mediators in cardiovascular regulation. Indeed, it has been implicated in the pathogenesis of cardiovascular diseases such as hypertension.

1.3 Inflammatory Mediators in Hypertension

A hallmark of hypertension is the upregulation of inflammatory mediators in brain regions controlling CVS (Shi, Diez-Freire et al. 2010). Microglia, the resident immune cells of the CNS, exhibit an activated pro-inflammatory phenotype in the PVN of hypertensive rats (Shi, Diez-Freire et al. 2010). Activation of microglia increases the production of a number of pro-inflammatory cytokines, such as TNF-α and IL-1β, which are elevated in the PVN of hypertensive rats (Shi, Diez-Freire et al. 2010, Shi, Raizada et al. 2010, Shi, Gan et al. 2011). Since there is a strong association between pro-inflammatory cytokines in brain cardiovascular control centres and hypertension, the next section will focus on the role that these various cytokines play in maintaining hypertension.

1.3.1 Pro-inflammatory Cytokines in Hypertension

Studies by Yu-Ming Kang's group and collaborators reveal a wide range of pro-inflammatory cytokines to be elevated in a number of experimental animal models of hypertension. Animal models of primary (essential) hypertension demonstrate significant upregulation of TNF-α, IL-1β, IL-6, and CCL2 in the PVN of spontaneously hypertensive rats (SHR) in comparison to normotensive, control, Wistar-Kyoto rats (WKY) (Jia, Kang et al. 2014, Song, Jia et al. 2014, Yu, Zhang et al. 2015, Li, Li et al. 2016). Similarly, in secondary (renovascular) models of hypertension, the levels of TNF-α, IL-1β, IL-6, and CCL2 are significantly elevated in the RVLM of kidney clipped animals (2K1C) in comparison to sham controls (Li, Qin et al. 2014). Finally, the levels of these cytokines are also elevated in the PVN of experimental models of hypertension (angiotensin II mediated hypertension) (Kang, Ma et al. 2009, Sriramula, Cardinale et al. 2013, Kang, Zhang et al. 2014, Su, Qin et al. 2014), and in diet induced hypertension (high salt diet) (Gao, Yu et al. 2016). Thus, these studies establish an association between the upregulation of pro-inflammatory cytokines in regions such as the

PVN and the RVLM in animal models of hypertension. In addition, these studies further demonstrate an attenuation in the hypertensive phenotype and the restoration of pro-inflammatory cytokine upregulation, by antagonising the RAS (Kang, Zhang et al. 2014, Li, Qin et al. 2014), TNF-α receptors (Sriramula, Cardinale et al. 2013, Song, Jia et al. 2014, Yu, Wei et al. 2017), IL-1β receptors (Lu, Jiang et al. 2017), and the downstream secondary messenger of pro-inflammatory cytokines, NF-$_K$B (Yu, Zhang et al. 2015). Taken together this collection of studies by the Kang group and collaborators establish that; (1) pro-inflammatory cytokines production is upregulated in the cardiovascular centres of the brain in a variety of rodent models of hypertension and that, (2) the blockade of receptors for pro-inflammatory cytokines rescues the hypertensive phenotype.

1.3.2 Immune Cells in Hypertension

Immune cells are a source of pro-inflammatory cytokine production. These cells are activated, recruited and infiltrate the cardiovascular organs in many animal models of hypertension (Hilgers, Hartner et al. 2000, Guzik, Hoch et al. 2007, Marvar, Thabet et al. 2010, Matsuda, Umemoto et al. 2015). For example, T-cells (lymphocytes) infiltrate and release pro-inflammatory cytokines in the aortic walls of angiotensin II mediated hypertension (Guzik, Hoch et al. 2007, Marvar, Thabet et al. 2010). Furthermore, macrophages (monocytes) infiltrate the hearts and the kidneys of angiotensin II-induced hypertension and renovascular model of hypertension in rats (Hilgers, Hartner et al. 2000, Matsuda, Umemoto et al. 2015). In the brain, microglia are the source of pro-inflammatory cytokine production, and previous studies demonstrate the increased production of pro-inflammatory cytokines by microglia in cardiovascular brain regions of animal models of hypertension (Shi, Diez-Freire et al. 2010, Shi, Raizada et al. 2010, Shi, Gan et al. 2011, Shen, Li et al. 2015). Thus, this raises the questions of whether peripherally circulating immune cells can infiltrate into cardiovascular

brain centres in hypertension. Indeed, both monocytes and lymphocytes have been shown to infiltrate into the brain of hypertensive animals (Santisteban, Ahmari et al. 2015, Cédile, Wlodarczyk et al. 2017). Blood derived monocytes which circulate in the systemic circulation infiltrate into the PVN of both SHR and angiotensin II mediated hypertension (Santisteban, Ahmari et al. 2015). Whether or not immune cell recruitment to the cardiovascular regions of the brain play a role in mediating hypertension warrants further investigation.

Table 1.1: Levels of inflammatory mediators in animal models of hypertension.

IM	BM	Plasma/Blood	CSF	PVN	RVLM
TNF-α	- SHR + Ang II U 2K1C	U SHR U Ang II U 2K1C	U SHR U Ang II U 2K1C	+ SHR + Ang II U 2K1C	U SHR U Ang II + 2K1C
IL-6	U SHR U Ang II U 2K1C	+ SHR + Ang II + 2K1C	U SHR U Ang II U 2K1C	+ SHR + Ang II U 2K1C	U SHR U Ang II + 2K1C
IL-1β	+ SHR + Ang II U 2K1C	+ SHR + Ang II + 2K1C	U SHR U Ang II U 2K1C	+ SHR + Ang II U 2K1C	U SHR U Ang II + 2K1C
CCL2	+ SHR + Ang II U 2K1C	+ SHR + Ang II U 2K1C	+ SHR U Ang II U 2K1C	+ SHR + Ang II U 2K1C	U SHR U Ang II + 2K1C
Microglia Activation	N/A N/A N/A	N/A N/A N/A	N/A N/A N/A	+ SHR + Ang II U 2K1C	U SHR U Ang II U 2K1C
Monocytes Infiltration	N/A N/A N/A	N/A N/A N/A	N/A N/A N/A	+ SHR +Ang II U 2K1C	U SHR U Ang II U 2K1C
Lymphocyte Infiltration	N/A N/A N/A	N/A N/A N/A	N/A N/A N/A	U SHR + Ang II U 2K1C	U SHR U Ang II U 2K1C

Key: +; increased, -; no change, U; unknown, **N/A**; not applicable, 2K1C; 2 kidney-1 clip model of hypertension, Ang II; angiotensin II mediated hypertension, BM; bone marrow, CSF; cerebrospinal fluid, IM; Inflammatory mediator, PVN; paraventricular nucleus of the hypothalamus, RVLM; rostral ventrolateral medulla, SHR; spontaneous hypertensive rats.

1.3.3 Potential Role for CCL2?

The chemokine CCL2 is a pro-inflammatory chemokine, known for its role as a chemoattractant involved in the chemotaxis of immune cells. Hence it is also known as monocyte chemoattractant protein-1 (MCP-1) (Deshmane, Kremlev et al. 2009). Not only are the levels of CCL2 increased in different animal models of hypertension, it is also increased in the serum of hypertensive patients and significantly correlates to BP elevations (Antonelli, Fallahi et al. 2012). Furthermore, in both SHR and angiotensin II mediated hypertension, CCL2 elevation shows a significant gradient from bone marrow<serum<CSF (Fig. 1.5), suggesting a formation of a CCL2 chemotactic gradient towards the brain to activate and recruit immune cells to infiltrate into the cardiovascular brain regions (Santisteban, Ahmari et al. 2015). The fact that depleting immune cells reduces BP in hypertensive animals further support this contention (Santisteban, Ahmari et al. 2015). Thus, the involvement of CCL2 in the chemotaxis and the infiltration of immune cells into the brain in hypertension, warrants further investigation.

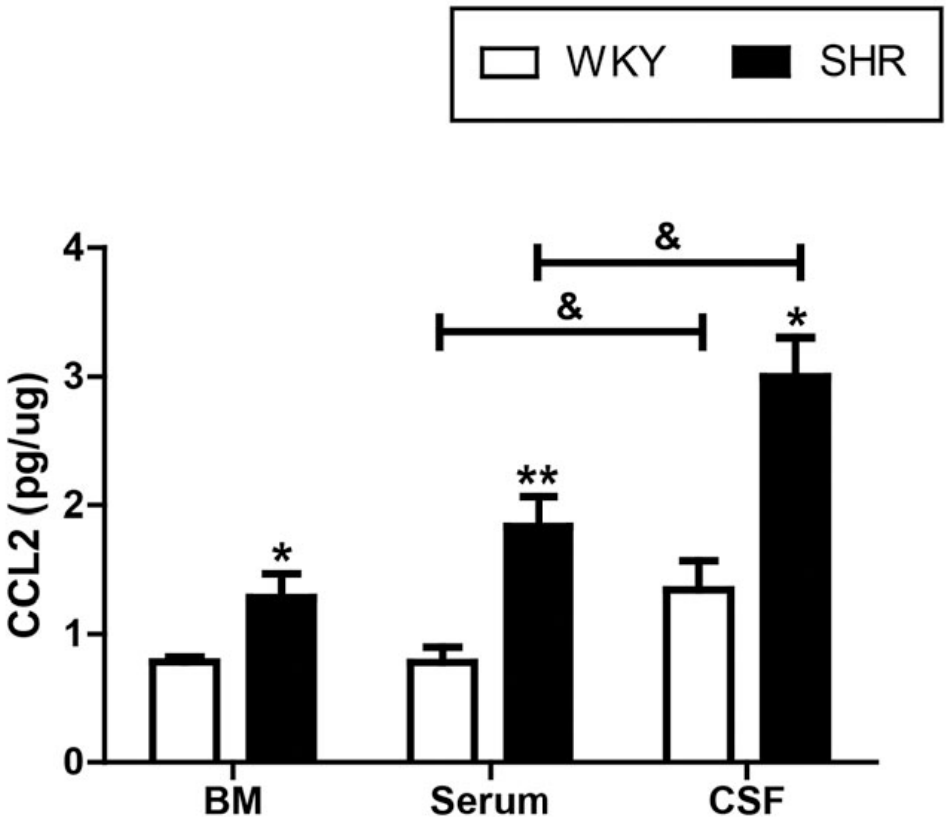


Figure 1.5: Levels of CCL2 in bone marrow, serum and CSF of SHR.

The bar graph shows the levels of CCL2 in bone marrow, plasma and CSF of SHR in comparison to normotensive WKY. BM; bone marrow, CSF; cerebrospinal fluid, SHR; spontaneous hypertensive rats, WKY; Wistar-Kyoto rats. $^{*}P<0.05$, $^{**}P<0.01$ in comparison to WKY, $^{\&}P<0.05$ in comparison to serum, n=4 per group. Figure regenerated from (Santisteban, Ahmari et al. 2015).

1.4 Chemokines and Hypertension

1.4.1 What are Chemokines?

Chemokines are small proteins that form a large family of peptides (6-10 KDa) whose main function is to regulate cell trafficking (Rollins 1997, Deshmane, Kremlev et al. 2009, Zlotnik and Yoshie 2012). The first chemokine was described in 1977 with the purification of the secreted platelet factor 4 (PF4/CXCL4) (Walz, Wu et al. 1977). Since then about 50 chemokines and 20 chemokine receptors have been described (Rollins 1997). Chemokines and their receptors are extensively studied in the immune response, as they activate immune cells and cause them to move toward a chemokine concentration gradient (chemotaxis/chemoattraction) (Zlotnik and Yoshie 2012). Chemokines have a common structure, which comprises of three domains. The first domain is a highly flexible N-terminal domain, constrained by disulphide bonds. The second domain is a loop which leads to 3 antiparallel β-pleated sheets. The third domain is an α-helix which overlies the antiparallel β-pleated sheets. Chemokines can be further subdivided into four subfamilies; CXC, C-C, CX3C, and C, on the basis of the number and the location of cysteine residues within the N-terminus (Rollins 1997, Deshmane, Kremlev et al. 2009, Zlotnik and Yoshie 2012).

1.4.2 Chemokine (C-C motif) Ligand 2 (CCL2)

Chemokine (C-C motif) Ligand 2 (CCL2) was the first C-C chemokine discovered in humans (Van Coillie, Van Damme et al. 1999). CCL2 is implicated in the antiviral and the immune response (Zlotnik and Yoshie 2012). The cognate receptor for CCL2 is termed C-C Chemokine receptor type 2 (CCR2), which is a G-protein coupled receptor (Deshmane, Kremlev et al. 2009, Bose and Cho 2013). CCL2 and CCR2 receptors are both expressed and produced in the brain, and further co-localize to specific cardiovascular brain regions, such as the PVN and the RVLM (Wittendorp, Boddeke et al. 2004, Banisadr, Gosselin et al. 2005, Hinojosa, Garcia-Bueno et al. 2011, Morioka, Tokuhara et al. 2013). Moreover, lymphocyte and monocyte infiltration into areas such as the PVN, is mediated through CCL2-CCR2 signalling (Ataka, Asakawa et al. 2013, Santisteban, Ahmari et al. 2015, Cédile, Wlodarczyk et al. 2017). Thus in the brain, CCL2 can regulate a number of physiological and endocrine functions (Rostene, Kitabgi et al. 2007), such as the modulation of stress responses (Reyes, Walker et al. 2003), body temperature (Tavares and Minano 2004), water balance (Callewaere, Banisadr et al. 2006) and feeding (Guyon, Banisadr et al. 2005). As such, it is possible that CCL2-CCR2 signalling in the brain also regulates SNA and BP.

1.4.3 Expression of CCL2 and its Receptor CCR2

CCL2 is produced and secreted by a wide range of cell types including endothelial, fibroblasts, epithelial, smooth muscle, mesangial, astrocytic, monocytic and microglial cells (Cushing, Berliner et al. 1990, Standiford, Kunkel et al. 1991, Brown, Strieter et al. 1992, Barna, Pettay et al. 1994). Whereas CCR2 receptors are mainly expressed by mononuclear immune cells and vascular smooth muscle cells (Bartoli, Civatte et al. 2001). However, monocytes/macrophages are found to be the major source of CCL2 (Yoshimura, Robinson et al. 1989, Yoshimura, Yuhki et al. 1989). CCL2 secretion is induced in response to injury,

oxidative stress, growth factors and pro-inflammatory cytokines, where CCL2 secretion forms a chemotactic gradient towards the stimulus. This process is known as chemotaxis; where monocytes/macrophages are activated recruited by CCL2 to infiltrate from the peripheral circulation, into the tissue, and move towards the stimulus through the CCL2 chemotactic gradient (Ajuebor, Flower et al. 1998). In fact, abnormalities in monocytes recruitment and cytokine expression is observed in CCL2 knockout mice (Lu, Rutledge et al. 1998). In addition, CCL2 expression is associated with the development of polarized T-cell responses (Chensue, Warmington et al. 1995, Handel and Domaille 1996).

1.4.3.1 Distribution and Production in the Brain

In the rat brain both CCL2 and CCR2 receptors are both expressed in many areas including; telencephalon, diencephalon, mesencephalon, brainstem, basal ganglia, hippocampus and the amygdala (Banisadr, Gosselin et al. 2005, Banisadr, Gosselin et al. 2005). This expression is found in both neurons and glia, which is in agreement with studies from human brain tissue (Meng, Oka et al. 1999, Coughlan, McManus et al. 2000). Interestingly, the expression of CCL2 and CCR2 receptors is found in many brain regions implicated in controlling the CVS, including the PVN and the brainstem (Banisadr, Gosselin et al. 2005, Banisadr, Gosselin et al. 2005). While CCL2 is synthesised and secreted by neurons (Banisadr, Gosselin et al. 2005, Gosselin, Varela et al. 2005), microglia and astrocytes are believed to be another source of CCL2 production (Fig. 1.6) (Wittendorp, Boddeke et al. 2004, Madrigal, Garcia-Bueno et al. 2010, Baamonde, Hidalgo et al. 2011, Hinojosa, Garcia-Bueno et al. 2011, Morioka, Tokuhara et al. 2013). In fact, microglia activation induces the production of CCL2 (Morioka, Tokuhara et al. 2013). As such, it is highly likely that the endogenous production of CCL2 in the brain may be a driver for the recruitment of immune cells to cardiovascular brain regions in hypertension.

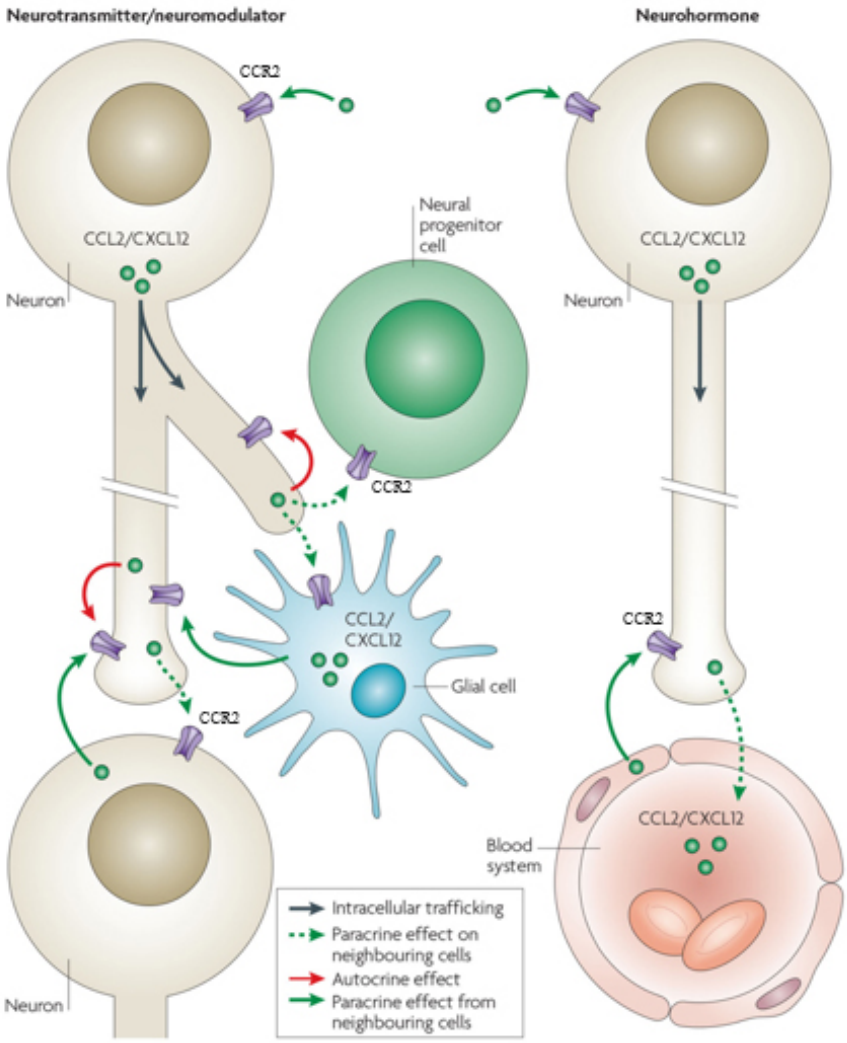


Figure 1.6: Expression of CCL2 and CCR2 receptors in brain cells.

This schematic diagram shows the expression of CCR2 receptors on neurons and glial cells. It depicts the production and secretion of CCL2 by neurons, glial cells, and circulating blood cells. Diagram taken from (Rostene, Kitabgi et al. 2007).

1.4.4 CCL2 in Hypertension

The study of hypertension in animals involves a number of animal models ranging from models of primary (essential) to secondary hypertension. The two kidneys – one clip (2K1C) or Goldblatt model is a model of secondary (renovascular) hypertension. In this model, hypertension is induced by the partial obstruction of one renal artery via a clip. The partial stenosis of the renal artery in this renovascular model of hypertension causes elevations in components of RAS, resulting in elevated SNA and blood pressure (Goldblatt, Lynch et al. 1934). Similarly, the angiotensin II-mediated model of hypertension, causes BP elevations through the subcutaneous infusion of angiotensin II, mimicking the aberrant activation of RAS (Zimmerman, Lazartigues et al. 2004). In addition, the SHR; a genetic model of hypertension, is classified as primary (essential) model of hypertension, where BP spontaneously increases at 5-6 weeks of age (Simms, Paton et al. 2008). Interestingly, in all these different rodent models of hypertension, SNA elevations are observed prior to the development of BP increases or hypertension. Generally, in these models, hypertension normally starts to develop at week 4 and is fully established by week 8. However, previous studies demonstrate elevations in SNA by week 3, prior to development of high BP (Zimmerman, Lazartigues et al. 2004, Simms, Paton et al. 2008, Zoccal, Simms et al. 2008, Oliveira-Sales, Toward et al. 2014, Oliveira-Sales, Colombari et al. 2016). Therefore, this might suggest that neurochemical changes in the brain leading to elevated SNA may occur prior to the development and the establishment of hypertension. Potentially, CCL2 upregulation and immune cell recruitment into cardiovascular brain regions may be occurring at the early stages of the hypertension, possibly mediating increases SNA and BP elevations.

1.4.4.1 CCL2 in Animal Models of Hypertension

While the only evidence for CCL2 upregulation in clinical studies comes from the observation that serum CCL2 levels correlate to BP increases in hypertensive patients (Antonelli, Fallahi et al. 2012), CCL2 in animal models of hypertension has been studied more extensively. It is well documented in many studies that plasma levels of CCL2 are increased in both primary and secondary models of hypertension (Sriramula, Cardinale et al. 2013, Li, Qin et al. 2014, Song, Jia et al. 2014). Surprisingly a 3-fold increase in CCL2 levels is reported within the PVN of hypertensive animals (Sriramula, Cardinale et al. 2013, Li, Qin et al. 2014, Song, Jia et al. 2014). Furthermore, a CCL2 chemotactic gradient from circulation to the CSF is observed in hypertensive animals (Santisteban, Ahmari et al. 2015). However, these studies only report CCL2 levels when hypertension is already established. Hence, establishing the temporal profile of CCL2 upregulation throughout the progression of hypertension will answer the question of whether CCL2 is playing a role in inducing the hypertensive phenotype. Similar to SNA elevations in hypertension, it is possible that CCL2 elevations precede BP increases in hypertension. This is supported by findings in the renovascular model of hypertension, where, CCL2 levels in the aortic wall are increased by day 7 following kidney clipping (Hilgers, Hartner et al. 2000, Xie, Sun et al. 2006). As such, it is possible that CCL2 levels elevate and form a chemotactic gradient towards the brain prior to increased BP in hypertension. Whereby the blockade of receptors for CCL2 may have anti-hypertensive effects. This is supported by previous studies which demonstrated that selective antagonism of CCR2 receptors reduce BP in hypertensive animals (Elmarakby, Quigley et al. 2007, Chan, Moore et al. 2012, Chang, Li et al. 2014, Wang, Zhu et al. 2015). Interestingly, the study by Chan *et al*., showed that the antagonism of CCR2 receptors, through the intraperitoneal administration of the CCR2 antagonist (INCB3344) reduced BP by approximately 20 mmHg (Chan, Moore et al. 2012).

1.4.4.2 CCL2 & Neuronal Activity

There is no doubt that CCL2 can modulate neuronal activity. Further to finding that CCR2 receptors are found to co-localised with classical neurotransmitters on neurons, CCL2 is also found to modulate neuronal activity (Banisadr, Gosselin et al. 2005, Banisadr, Gosselin et al. 2005). In primary cultured neurons from various brain regions of the rat, CCL2 is shown to elicit Ca^{2+} transients (Banisadr, Gosselin et al. 2005, van Gassen, Netzeband et al. 2005). More interestingly, CCL2 inhibits GABA-induced currents in primary cultures spinal cord neurons in a dose dependent manner (Gosselin, Varela et al. 2005), and evokes NMDA and AMPA receptor sensitisation (Baamonde, Hidalgo et al. 2011). Thus, one can postulate that increased levels of CCL2 in brain regions controlling the CVS may be involved in the neurotransmitter imbalances and the activation of cardiovascular brain regions as observed in hypertensive animals (Jia, Kang et al. 2014, Song, Jia et al. 2014, Yu, Zhang et al. 2015, Li, Li et al. 2016).

1.4.4.3 CCL2 and Microglia/Astrocytes

Both microglia and astrocytes can influence neuronal activity (Walz 1989, Hatten and Mason 1990, Ullian, Sapperstein et al. 2001) and are implicated in activating sympathetic nerves (Arnoux and Audinat 2015, Du, Jiang et al. 2015, Shen, Li et al. 2015). For example, specific optogenetic stimulation of RVLM astrocytes increases renal sympathetic nerve activity (Marina, Tang et al. 2013). Furthermore, both microglia and astrocytes synthesise and produce CCL2 (Wittendorp, Boddeke et al. 2004, Madrigal, Garcia-Bueno et al. 2010, Baamonde, Hidalgo et al. 2011, Hinojosa, Garcia-Bueno et al. 2011, Morioka, Tokuhara et al. 2013), and are activated in the brains of hypertensive animals (Aiyar, Daines et al. 2001, Tomassoni, Avola et al. 2004, Shi, Diez-Freire et al. 2010, Shi, Raizada et al. 2010, Shen, Li et al. 2015). As such, it is possible that CCL2 modulates the activity of glia in hypertension.

1.4.4.4 CCL2 and Immune Cells

Immune cell recruitment to the brain is mainly driven by CCL2 (Marvar, Thabet et al. 2010, Ataka, Asakawa et al. 2013, Santisteban, Ahmari et al. 2015). As discussed previously, these circulating immune cells are a potential source of pro-inflammatory cytokine production in the brain, that elevates both SNA and BP (Shi, Diez-Freire et al. 2010, Shi, Gan et al. 2011, Santisteban, Ahmari et al. 2015, Shen, Li et al. 2015). Furthermore, as SNA is elevated prior to the development of BP elevation in hypertension (Oliveira-Sales, Colombari et al. 2016), recruitment of circulating immune cells to the brain could occur prior to the increased BP in hypertension. The dynamics of immune cell recruitment to brain in an experimental autoimmune encephalitis (EAE) model suggest the involvement of infiltrating immune cells at the early stages of the model. A study by Ajami and colleagues, demonstrated that immune cells infiltrate the CNS during the early stages of experimental EAE, triggering EAE (Ajami, Bennett et al. 2011). Therefore, this raises the question of whether similar dynamics occur in hypertension, where immune cells are recruited by CCL2 into the brain to elevate SNA at the early stages of hypertension.

1.5 Proposed Role of CCL2 in Hypertension

A hallmark of hypertension is the upregulation of pro-inflammatory cytokines; such as TNF−α, IL-1β, IL-6, in the brain regions that control the CVS of hypertensive animals (Jia, Kang et al. 2014, Song, Jia et al. 2014, Yu, Zhang et al. 2015, Li, Li et al. 2016). Upregulation of pro-inflammatory cytokines causes neuro-transmitter imbalances and oxidative stress which activate those regions, leading to elevations in SNA and BP (Francis, Zhang et al. 2004, Wei, Yu et al. 2015). In further support of the important role pro-inflammatory cytokines play in hypertension, studies have demonstrated that the blockade of receptors for pro-inflammatory cytokines rescues the hypertensive phenotype (Sriramula, Cardinale et al. 2013, Song, Jia et al. 2014, Yu, Wei et al. 2017). While the source of pro-inflammatory cytokine production in the brain is the resident glia of the CNS (Shi, Diez-Freire et al. 2010, Shi, Raizada et al. 2010), circulating immune cells may also be a potential source of pro-inflammatory cytokine production. These circulating immune cells infiltrate into brain regions controlling the CVS in hypertension (Santisteban, Ahmari et al. 2015, Cédile, Wlodarczyk et al. 2017). Furthermore, immune cells are activated and recruited by the chemokine CCL2 (Chensue, Warmington et al. 1995, Handel and Domaille 1996, Ajuebor, Flower et al. 1998). Whereby, the blockade of CCR2 receptors in the periphery prevents the activation of immune cells and reduces BP in hypertensive rats (Aiyar, Disa et al. 1999, Elmarakby, Quigley et al. 2007, Chan, Moore et al. 2012, Chang, Li et al. 2014, Wang, Zhu et al. 2015). Hence, it is possible that CCL2 is involved in recruiting immune cells to the cardiovascular brain region in hypertension. Thus, I propose that the chemokine CCL2 is involved in the recruitment of circulating immune cells into the PVN, inducing and inflammatory cascade, thereby activating SNA and increasing BP. Therefore, I sought to investigate the cardiovascular role and the underlying mechanisms of CCL2 in central cardiovascular control.

In hypertension, SNA is elevated prior to any BP increases in the 2K1C model of hypertension (Oliveira-Sales, Toward et al. 2014, Oliveira-Sales, Colombari et al. 2016), SHR (Simms, Paton et al. 2008, Zoccal, Simms et al. 2008), and in humans (Smith, Graham et al. 2002, Grassi 2004, Grassi 2004, Smith, Graham et al. 2004). Furthermore, CCL2 levels are increased in peripheral tissue prior to the development of BP elevations in animal models of hypertension (Hilgers, Hartner et al. 2000, Xie, Sun et al. 2006). Thus, I propose that CCL2 levels are increased during the development of hypertension causing circulating immune cells to invade the PVN, prior to the development of BP elevations or the establishment of hypertension in rats. As such, I aim to investigate the temporal profile of CCL2 elevations and immune cell recruitment to the PVN throughout the development of hypertension.

Peripheral blockade of CCR2 receptors reduces BP. This is demonstrated by a number of studies in many animal models of hypertension (Elmarakby, Quigley et al. 2007, Chan, Moore et al. 2012, Chang, Li et al. 2014, Wang, Zhu et al. 2015). However, as I proposed that CCL2 acts in the brain, I aim to investigate the effects of blocking CCR2 receptors in the brain on BP in hypertensive animals.

1.6 Hypothesis and Aims

In light of the strong link between CCL2 levels, pro-inflammatory cytokine upregulation, recruitment of immune cell, and the elevation of SNA and BP in hypertension, I hypothesise that CCL2 is involved in the pathophysiology of hypertension through recruiting immune cells into brain regions that control the cardiovascular system. More specifically, I propose that CCL2 plays a key role in the development, progression and maintenance of hypertension. Hence, I have established 3 main aims:

1. To investigate the cardiovascular role of CCL2 in the PVN.
2. To elucidate the temporal profile of CCL2 levels centrally and peripherally, and the degree of immune cell recruitment in a hypertensive animal model.
3. To investigate the effects of the long-term blockade of CCR2 receptors in the brain on blood pressure in a hypertensive animal model.

frontiers in Physiology

MINI REVIEW
published: 02 August 2019
doi: 10.3389/fphys.2019.00984

Chemoattraction and Recruitment of Activated Immune Cells, Central Autonomic Control, and Blood Pressure Regulation

*Khalid Elsaafien[1], Willian S. Korim[1], Anthony Setiadi[1], Clive N. May[1] and Song T. Yao[1,2]**

[1]Discovery Science, Florey Institute of Neuroscience and Mental Health, Parkville, VIC, Australia, [2]Florey Department of Neuroscience and Mental Health, The University of Melbourne, Parkville, VIC, Australia

Inflammatory mediators play a critical role in the regulation of sympathetic outflow to cardiovascular organs in hypertension. Emerging evidence highlights the involvement of immune cells in the regulation of blood pressure. However, it is still unclear how these immune cells are activated and recruited to key autonomic brain regions to regulate sympathetic outflow to cardiovascular organs. Chemokines such as C-C motif chemokine ligand 2 (CCL2), and pro-inflammatory cytokines such as tumor necrosis factor alpha (TNF-α) and interleukin 1 beta (IL-1β), are upregulated both peripherally and centrally in hypertension. More specifically, they are upregulated in key autonomic brain regions that control sympathetic activity and blood pressure such as the paraventricular nucleus of the hypothalamus and the rostral ventrolateral medulla. Furthermore, this upregulation of inflammatory mediators is associated with the infiltration of immune cells to these brain areas. Thus, expression of pro-inflammatory chemokines and cytokines is a potential mechanism promoting invasion of immune cells into key autonomic brain regions. In pathophysiological conditions, this can result in abnormal activation of brain circuits that control sympathetic nerve activity to cardiovascular organs and ultimately in increases in blood pressure. In this review, we discuss emerging evidence that helps explain how immune cells are chemoattracted to autonomic nuclei and contribute to changes in sympathetic outflow and blood pressure.

Keywords: neuroinflammation, chemoattraction, immune system, autonomic nervous system, hypertension

OPEN ACCESS

Edited by:
Vaughan G. Macefield, Baker Heart and Diabetes Institute, Australia

Reviewed by:
J. Thomas Cunningham, University of North Texas Health Science Center, United States
Melissa Mary Jean Farnham, Heart Research Institute, Australia

Correspondence:
Song T. Yao
song.yao@florey.edu.au

Specialty section:
This article was submitted to Integrative Physiology, a section of the journal Frontiers in Physiology

Received: *31 May 2019*
Accepted: *15 July 2019*
Published: *02 August 2019*

Citation:
Elsaafien K, Korim WS, Setiadi A, May CN and Yao ST (2019) Chemoattraction and Recruitment of Activated Immune Cells, Central Autonomic Control, and Blood Pressure Regulation. Front. Physiol. 10:984. doi: 10.3389/fphys.2019.00984

INTRODUCTION

The autonomic nervous system plays a major role in blood pressure regulation whereby dysfunction can lead to hypertension. Brain regions lacking a functional blood-brain barrier (BBB), known as circumventricular organs (CVOs), can sense and respond to circulating factors such as blood-borne hormones, like angiotensin II. This can lead to elevated sympathetic discharge and blood pressure (BP) (Nunes and Braga, 2011; Zubcevic et al., 2017). CVOs, such as the subfornical organ (SFO) and the area postrema (AP), regulate sympathetic outflow by changing the activity of neurons in the paraventricular nucleus of the hypothalamus (PVN) and the rostral ventrolateral medulla in the brainstem (RVLM) (van der Kooy and Koda, 1983; Dampney et al., 1987; Braga et al., 2011). Both the PVN and the RVLM are implicated in

the regulation of sympathetic outflow to cardiovascular organs *via* direct projections to sympathetic preganglionic neurons (SPNs) located in the spinal cord (Strack et al., 1989a,b; Schramm et al., 1993). Thus, these brain regions play an important role in regulating homeostatic levels of sympathetic outflow to the cardiovascular organs such that activation of the AP, by inflammatory mediators such as tumor necrosis factor alpha (TNF-α), for example, can lead to increases in both cardiac and renal sympathetic nerve activity (Korim et al., 2018).

The upregulation of pro-inflammatory mediators is associated with human hypertension (Chrysohoou et al., 2004; Antonelli et al., 2012). Studies in experimental rodent models of hypertension confirm this finding. Moreover, they further show that upregulation of a wide range of pro-inflammatory mediators occurs in key brain regions known to regulate sympathetic outflow to cardiovascular organs (Shen et al., 2015). These pro-inflammatory cytokines include TNF-α, interleukin 1 beta (IL-1β), interleukin 6 (IL-6), and pro-inflammatory chemokines such as C-C motif chemokine ligand 2 (CCL2). These mediators are upregulated in the PVN and RVLM, in models of both primary and secondary hypertension (Li et al., 2014; Song et al., 2014). Selective blockade of these inflammatory mediators in the central nervous system reduces BP in animal models of hypertension (Li et al., 2014; Song et al., 2014). These studies indicate that upregulation of pro-inflammatory mediators in brain regions that control cardiovascular function contributes to sustained BP increase in hypertension. However, the factors leading to upregulation of these mediators in critical brain areas in the context of cardiovascular control remain unclear.

Recently, focus has shifted to the role of immune cells in the development of hypertension (Bomfim et al., 2018; Caillon et al., 2018; Carnagarin et al., 2018). Resident immune cells in the central nervous system (microglia) are responsible for local inflammatory processes in the brain (Shen et al., 2015). In fact, chronic central infusion of minocycline, an anti-inflammatory antibiotic that reduces microglia activation, reduces central inflammation and BP in hypertension (Shi et al., 2010). There is also evidence that peripheral bone marrow immune cells are involved in inducing brain inflammation, leading to a hypertensive phenotype (Santisteban et al., 2015). Interestingly, when the bone marrow of spontaneously hypertensive rats (SHRs) is ablated and replaced with bone marrow from normotensive Wistar Kyoto rats (WKYs), central inflammation is attenuated, leading to BP reduction (Santisteban et al., 2015). This evidence suggests that peripheral immune cells play an important role in central inflammation and the development of hypertension.

Infiltrating immune cells are activated and recruited by pro-inflammatory chemokines, such as CCL2 (Deshmane et al., 2009). Interestingly, CCL2 is upregulated in the PVN of hypertensive rodents. This upregulation of CCL2 was linked to the presence of infiltrating immune cells in the PVN of these animals (Wang et al., 2018). Moreover, there is a clear gradient of CCL2 levels in hypertensive animals, whereby the lowest levels are detected in bone marrow and the highest levels are detected in the cerebrospinal fluid (CSF) of rodents (Santisteban et al., 2015). Hence, this forms a distinct chemotactic gradient, such that immune cells are recruited to specialized cardiovascular control regions of the brain. Once there, they initiate an inflammatory cascade, which impairs sympathetic control and mediates sustained increases in BP.

In this review, we discuss the evidence supporting brain chemoattraction and the involvement of immune cells in regulating sympathetic outflow to cardiovascular organs. We will focus on the effects of chemoattraction of immune cells to induce inflammatory cascades in key autonomic brain centers that control cardiovascular function, and the potential role of these changes in the development of hypertension.

UPREGULATION OF BRAIN PRO-INFLAMMATORY CYTOKINES AND CHEMOATTRACTION OF IMMUNE CELLS ON THE REGULATION OF BLOOD PRESSURE

Upregulation of Brain Pro-inflammatory Cytokines in Hypertension

Increases in BP in rodent models of hypertension are associated with the upregulation of pro-inflammatory mediators, both peripherally and centrally. Recent studies demonstrate that a number of pro-inflammatory mediators are elevated in different rodent models of hypertension (Jia et al., 2014; Song et al., 2014; Yu et al., 2015; Li et al., 2016). For example, there are significantly higher levels of TNF-α, IL-1β, IL-6, and CCL2 in the PVN of SHRs, a model of primary hypertension, compared with normotensive WKYs. Similarly, in a model of secondary hypertension (renovascular; two kidney-one clip, 2 K-1C), the levels of TNF-α, IL-1β, IL-6, and CCL2 are elevated in the RVLM (Li et al., 2014). Furthermore, the levels of these pro-inflammatory mediators are also elevated in the PVN of angiotensin II-induced hypertensive rat models (Kang et al., 2009, 2014; Sriramula et al., 2013; Su et al., 2014), as well as in high salt diet-induced hypertension (Gao et al., 2016; Wang et al., 2018). The downstream effect of this increased inflammation is thought to contribute to altered neuronal signaling caused by imbalances in neurotransmitter and neuromodulator levels in key autonomic brain centers. For instance, glutamate and norepinephrine are upregulated whereas GABA was downregulated within both the PVN and the RVLM of hypertensive animals (Jia et al., 2014; Song et al., 2014; Yu et al., 2015; Li et al., 2016). Thus, changes in the activity of neurons in key autonomic brain nuclei may contribute to elevated sympathetic nerve activity (SNA) and increases in BP.

Blockade of receptors for pro-inflammatory mediators within cardiovascular brain regions reduces BP in rodent models of hypertension. Recently, we showed that blockade of TNF-α receptors (TNFR1) in the AP reduces BP in the 2 K-1C model of hypertension (Korim et al., 2018). Others have also demonstrated that non-selective blockade of TNF-α receptors (Sriramula et al., 2013; Song et al., 2014), IL-1β receptors (Lu et al., 2017), and the downstream secondary messenger of pro-inflammatory cytokines NF-κB (Yu et al., 2015) in the PVN of hypertensive rats reduced BP. Interestingly, antagonism of pro-inflammatory

cytokine receptors within the central nervous system not only reduced SNA and BP in hypertension, but also appeared to restore the neurotransmitter imbalances and excessive activation of cardiovascular brain regions (Sriramula et al., 2013; Song et al., 2014; Lu et al., 2017). Thus, the dysregulation of pro-inflammatory mediator levels within key autonomic centers appears to be associated with the development of hypertension.

Exogenous application of pro-inflammatory cytokines into specific central cardiovascular control centers of normotensive animals increases SNA and BP. For example, microinjections of TNF-α and IL-1β into the SFO (Wei et al., 2015) and in the PVN (Shi et al., 2011) increased renal SNA and BP. Furthermore, our group has recently shown that the microinjection of TNF-α into the AP increases both renal and cardiac SNA and BP (Korim et al., 2018). Interestingly, we found receptors for TNF-α to be expressed on AP neurons projecting to the RVLM – a cardiovascular brain region known for containing neurons directly projecting to SPNs (Strack et al., 1989a,b; Schramm et al., 1993). These neurons appear to be chronically activated in hypertensive animals and are also active following microinjection of TNF-α into the AP (Korim et al., 2018). These studies provide a direct causal relationship whereby activation of neurons by pro-inflammatory mediators, within important central cardiovascular control regions such as the AP, increases the sympathetic outflow and BP. Indeed, we have also previously demonstrated that the AP is critical in driving the increased cardiac SNA in an ovine model of heart failure (Abukar et al., 2018). Taken together, these studies provide compelling evidence to support a link between increases in brain pro-inflammatory mediators and the dysregulation of SNA and BP in hypertension.

C-C Motif Chemokine Ligand 2 and the Chemoattraction of Immune Cells in Hypertension

Chemokines are pro-inflammatory mediators and chemotactic cytokines, whose main function is to regulate cell trafficking (Rollins, 1997; Deshmane et al., 2009; Zlotnik and Yoshie, 2012). These proteins create a concentration gradient and activate immune cells, causing them to move up this chemotactic gradient (Zlotnik and Yoshie, 2012). The chemokine CCL2 (also known as monocyte chemoattractant protein-1 or MCP-1), and its cognate receptor C-C Chemokine receptor type 2 (CCR2), is one of the most extensively studied chemokines. While CCL2 can be secreted by a variety of cell types, including endothelial cells and vascular smooth muscle cells (Bartoli et al., 2001), the main source of CCL2 is believed to be monocytes/macrophages (Yoshimura et al., 1989a,b). CCL2 is secreted in response to injury, oxidative stress, growth factors, and expression of other pro-inflammatory cytokines – where CCL2 secretion forms a gradient toward these stimuli. This process is termed chemotaxis, where CCL2 recruits circulating monocytes/macrophages to the respective chemical stimulus in the inflamed tissue or site of injury (Ajuebor et al., 1998). Evidence that CCL2 plays a vital role in the process of monocyte recruitment and cytokine expression is demonstrated by the finding that these are abnormal in CCL2 knockout mice (Lu et al., 1998). Interestingly, both CCL2 and its receptor, CCR2, are expressed and produced in the brain, specifically in central autonomic control centers such as the PVN and the RVLM (Wittendorp et al., 2004; Banisadr et al., 2005; Hinojosa et al., 2011; Morioka et al., 2013). However, the extent to which CCL2 and the chemoattraction of immune cells contribute to increased SNA and BP in the development of hypertension is still unknown and requires further investigation.

There is some evidence suggesting the involvement of increased chemoattraction of immune cells by CCL2 into cardiovascular brain centers during the development of hypertension. For example, selective antagonism of CCR2 receptors reduces BP in rodent models of hypertension (Aiyar et al., 1999; Elmarakby et al., 2007; Chan et al., 2012; Chang et al., 2014; Wang et al., 2015). Furthermore, studies in models of both primary and secondary hypertension reveal upregulation of CCL2 both peripherally and centrally (Sriramula et al., 2013; Li et al., 2014; Song et al., 2014), with a 3-fold elevation in the levels of CCL2 within the PVN of hypertensive animals (Sriramula et al., 2013; Li et al., 2014; Song et al., 2014). Upregulation of CCL2 occurs in the bone marrow, serum, and cerebrospinal fluid of SHRs compared with normotensive WKYs (Santisteban et al., 2015). Interestingly, the increase in CCL2 levels in SHRs forms a gradient from the bone marrow (lowest concentrations) toward the cerebrospinal fluid (highest concentrations) (Santisteban et al., 2015), possibly forming a chemotactic gradient toward the central nervous system. Thus, it seems that CCL2 chemoattracts immune cells and triggers an inflammatory cascade within the brain, leading to increases in BP.

THE NEURO-IMMUNE-INFLAMMATORY MODEL OF HYPERTENSION

In hypertension, increased circulating levels of angiotensin II is a potential cause for increased levels of brain CCL2 (Matsuda et al., 2015). A hallmark of hypertension is the upregulation of renin-angiotensin system and increased levels of angiotensin II (Goldblatt et al., 1934; Crowley et al., 2006, 2010). While not all human essential hypertension is angiotensin II mediated, the serum levels of CCL2 are increased in hypertensive patients (Antonelli et al., 2012). Interestingly, treating these patients with angiotensin II receptor blockers, which reduces blood pressure, also reduces plasma levels of CCL2 (Marketou et al., 2011), suggesting a link between angiotensin II and increased levels of CCL2. Similarly, in a rodent renovascular model of hypertension, peripheral blockade of receptors for angiotensin II attenuates peripheral CCL2 production (Xie et al., 2006). Moreover, *in vitro* studies show that angiotensin II can directly stimulate the production of CCL2 from monocytes and vascular smooth muscle cells (Chen et al., 1998; Tsou et al., 2007). In addition, systemic angiotensin II infusion increases CCR2 receptor expression in circulating monocytes – which is blunted by blocking angiotensin II receptors (Ishibashi et al., 2004). Recent studies further show that application of angiotensin II to primary hypothalamic neurons induces increased CCL2 mRNA and CCL2 protein levels in the cell culture media (Santisteban et al., 2015).

As such, the stimulation of receptors for angiotensin II on peripheral circulating monocytes, vascular smooth muscle cells, and even on neurons induces the production of CCL2 in these cells.

Increased levels of CCL2 lead to the disruption of the BBB and facilitate immune cell infiltration into the brain tissue. While the BBB prevents immune cells from entering the brain, we have previously suggested that this structure is disrupted in hypertension (Setiadi et al., 2018). The regulation of BBB permeability involves tight junction proteins expressed on endothelial cells (Begley and Brightman, 2003). CCL2 is known to disrupt the BBB, through dysregulation of tight junction proteins such as ZO-1, ZO-2, occludin, and claudin-5 (Stamatovic et al., 2009; Roberts et al., 2012). *In vitro* studies have demonstrated that the application of CCL2 to primary mouse brain endothelial cell cultures reorganizes and redistributes tight junction proteins, increasing the permeability of the BBB (Stamatovic et al., 2003, 2009). Hence, CCL2 can directly disrupt the BBB by regulating the distribution of tight junction proteins. In SHRs, increased BBB permeability in the PVN and RVLM facilitates the entry of circulating angiotensin II into these brain structures (Biancardi et al., 2013). Interestingly, *in vitro* studies using primary human brain endothelial cells corroborate *in vitro* animal studies by showing that CCL2 can disrupt tight junction proteins expressed on endothelial cells cultured from human brains (Roberts et al., 2012). Furthermore, the application of CCL2 to primary human brain endothelial cell cultures induces the expression of cell adhesion molecules, such as PECAM-1 on the surface membrane of endothelial cells, which is required for facilitating transmigration of immune cells through endothelial cells (Muller et al., 1993; Roberts

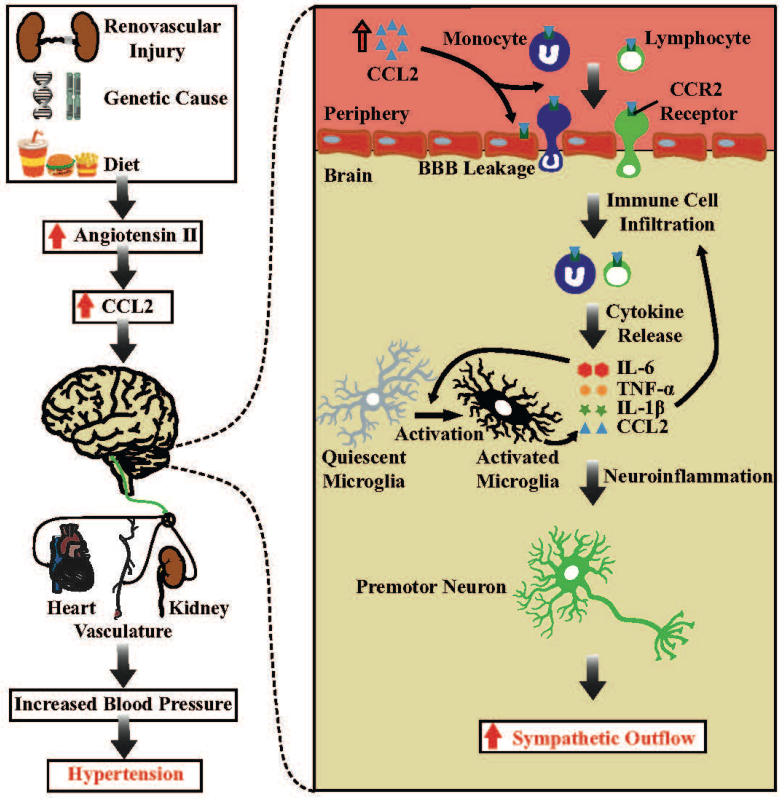


FIGURE 1 | Chemoattraction of immune cells in the brain, autonomic dysfunction, and hypertension. Schematic diagram showing the potential role of chemoattraction of immune cells and their components in determining increases in sympathetic nerve activity and blood pressure. Increased circulating levels of angiotensin II leads to production of the chemokine CCL2. CCL2 can act directly on the BBB, increasing the permeability of endothelial cells and recruiting immune cells to the brain tissue. The resulting overexpression of pro-inflammatory cytokines produces sustained activation of cardiovascular sympathetic neurons and increases blood pressure. Abbreviations: BBB, blood brain barrier; CCL2, C-C motif chemokine ligand 2; CCR2, C-C Chemokine receptor type 2; IL-1β, interleukin 1 beta; IL-6, interleukin 6; TNF-α, tumor necrosis factor alpha.

et al., 2012). Thus, not only can CCL2 reorganize the distribution of tight junction proteins expressed on endothelial cells to increase BBB permeability, it can also induce the expression of cell adhesion molecules on the surface membrane of endothelial cells to facilitate immune cell entry into brain tissue (**Figure 1**).

The recruitment and infiltration of immune cells into distinct brain regions can induce an inflammatory cascade resulting in the local upregulation of pro-inflammatory cytokines. The recruitment of activated immune cells into brain areas, including the PVN, results in the production and the upregulation of pro-inflammatory cytokines such as TNF-α, IL-1β, and IL-6 (Santisteban et al., 2015; Zubcevic et al., 2017; Sharma et al., 2019). These pro-inflammatory cytokines are capable of directly activating neurons and increasing sympathetic outflow and BP (Shi et al., 2011; Wei et al., 2015; Korim et al., 2018). Furthermore, the upregulation of pro-inflammatory cytokines and chemoattraction of activated immune cells also leads to activation of microglial cells (Santisteban et al., 2015; Zubcevic et al., 2017; Sharma et al., 2019). As microglia are the resident immune cells of the brain, activation of microglia leads to further release of pro-inflammatory mediators (Shi et al., 2010; Shen et al., 2015), therefore establishing an inflammatory state and escalating the inflammatory process centrally. Such a chronic inflammatory state results in further activation of immune cells, further neuroinflammation, and further rises in BP, leading to severe hypertension (Marvar et al., 2010). Whereas the blockade of receptors for pro-inflammatory cytokines in the brain (Sriramula et al., 2013; Song et al., 2014; Lu et al., 2017) prevents the activation of microglia (Shi et al., 2010), the recruitment of peripheral macrophages to the brain (Santisteban et al., 2015) and completely reverses the increased levels of peripheral and central pro-inflammatory cytokines and chemokines, leading to a reduced BP in hypertensive rats.

In summary, we propose a possible mechanism by which an inflammatory state in brain areas that control cardiovascular function is established, resulting in impaired BP control and hypertension. We propose that the increased levels of angiotensin II in the circulation results in the production and release of CCL2. This chemokine produces a chemotactic gradient that recruits immune cells toward the central nervous system. In addition, CCL2 increases BBB permeability and promotes the recruitment of activated immune cells. These immune cells initiate an inflammatory cascade where several pro-inflammatory mediators are released locally. Pro-inflammatory mediators activate neurons directly or indirectly by involving microglial transmission, which relays excitatory synapses to cardiovascular sympathetic premotor neurons in the ventrolateral medulla (Brown and Guyenet, 1985). The excitation of these neuronal subsets increases SNA and BP. These findings suggest that sustained activation of autonomic circuits contributes to the development of increased SNA and BP in neurogenic hypertension. Hence, chronic chemoattraction and recruitment of immune cells into key cardiovascular control regions might be a potential pathophysiological mechanism responsible for impaired BP control and hypertension (**Figure 1**).

CONCLUSION

In this review, we discussed recent findings that support our proposal of a potential mechanism to explain the contribution of neuroinflammation and chemoattraction mediated by CCL2, in brain regions that control cardiovascular function, as a cause of the sustained increase in sympathetic tone and BP in hypertension. This mechanism likely involves the recruitment and the infiltration of immune cells by chemokines to key autonomic brain areas. In future, targeting brain immune cells or the chemoattraction of immune cells may serve as a new avenue for developing antihypertensive treatments. In fact, in the pre-clinical setting, blockade of receptors for CCL2 or preventing immune cells from being activated reduces BP, in addition to slowing the development of atherosclerosis and vascular hypertrophy (Aiyar et al., 1999; Bush et al., 2000; Elmarakby et al., 2007; Chan et al., 2012; Chang et al., 2014; Santisteban et al., 2015; Wang et al., 2015). However, more thorough investigations are required to determine the mechanism by which chemoattraction and immune cells interact with the central nervous system, during the development and maintenance of hypertension.

AUTHOR CONTRIBUTIONS

KE drafted the manuscript and Figure. WK, AS, CM, and SY critically revised the intellectual content. All authors conceived and discussed the content of the manuscript, approved the final version of the manuscript, and agreed to be accountable for all aspects of the work.

FUNDING

This work was supported by the National Health and Medical Research Council of Australia (GNT 1079680 to SY; GNT 1128108 to CM and SY), the High Blood Pressure Research Council of Australia, the Rebecca L Cooper Medical Foundation (WK), and the Victorian Government through the Operational Infrastructure Scheme. KE and AS are supported by the Australian Government Research Training Program Scholarships. SY is supported by an Australian Research Council Future Fellowship (FT170100363).

REFERENCES

Abukar, Y., Ramchandra, R., Hood, S. G., McKinley, M. J., Booth, L. C., Yao, S. T., et al. (2018). Increased cardiac sympathetic nerve activity in ovine heart failure is reduced by lesion of the area postrema, but not lamina terminalis. *Basic Res. Cardiol.* 113:35. doi: 10.1007/s00395-018-0695-9

Aiyar, N., Disa, J., Stadel, J. M., and Lysko, P. G. (1999). Calcitonin gene-related peptide receptor independently stimulates 3′,5′-cyclic adenosine monophosphate and Ca2+ signaling pathways. *Mol. Cell. Biochem.* 197, 179–185.

Ajuebor, M. N., Flower, R. J., Hannon, R., Christie, M., Bowers, K., Verity, A., et al. (1998). Endogenous monocyte chemoattractant protein-1 recruits monocytes in the zymosan peritonitis model. *J. Leukoc. Biol.* 63, 108–116. doi: 10.1002/jlb.63.1.108

Antonelli, A., Fallahi, P., Ferrari, S., Ghiadoni, L., Virdis, A., Mancusi, C., et al. (2012). High serum levels of CXC (CXCL10) and CC (CCL2) chemokines in untreated essential hypertension. *Int. J. Immunopathol. Pharmacol.* 25, 387–395. doi: 10.1177/039463201202500208

Banisadr, G., Gosselin, R. D., Mechighel, P., Kitabgi, P., Rosene, W., and Parsadaniantz, S. P. M. (2005). Highly regionalized neuronal expression of monocyte chemoattractant protein-1 (MCP-1/CCL2) in rat brain: evidence for its colocalization with neurotransmitters and neuropeptides. *J. Comp. Neurol.* 489, 275–292. doi: 10.1002/cne.20598

Bartoli, C., Civatte, M., Pellissier, J., and Figarella-Branger, D. (2001). CCR2A and CCR2B, the two isoforms of the monocyte chemoattractant protein-1 receptor are up-regulated and expressed by different cell subsets in idiopathic inflammatory myopathies. *Acta Neuropathol.* 102, 385–392. doi: 10.1007/s004010100394

Begley, D. J., and Brightman, M. W. (2003). "Structural and functional aspects of the blood-brain barrier" in *Peptide transport and delivery into the central nervous system.* (Birkhäuser, Basel: Springer), 39–78.

Biancardi, V. C., Son, S. J., Ahmadi, S., Filosa, J. A., and Stern, J. E. (2013). Circulating angiotensin II gains access to the hypothalamus and brain stem during hypertension via breakdown of the blood–brain barrier. *Hypertension* 63, 572–579. doi: 10.1161/HYPERTENSIONAHA.113.01743

Bomfim, G. F., Cau, S. B. A., Bruno, A. S., Fedoce, A. G., and Carneiro, F. S. (2018). Hypertension: a new treatment for an old disease? Targeting the immune system. *Br. J. Pharmacol.* 176, 2028–2048. doi: 10.1111/bph.14436

Braga, V. A., Medeiros, I. A., Ribeiro, T. P., Franca-Silva, M. S., Botelho-Ono, M. S., and Guimaraes, D. D. (2011). Angiotensin-II-induced reactive oxygen species along the SFO-PVN-RVLM pathway: implications in neurogenic hypertension. *Braz. J. Med. Biol. Res.* 44, 871–876. doi: 10.1590/s0100-879x2011007500088

Brown, D., and Guyenet, P. G. (1985). Electrophysiological study of cardiovascular neurons in the rostral ventrolateral medulla in rats. *Circ. Res.* 56, 359–369.

Bush, E., Maeda, N., Kuziel, W. A., Dawson, T. C., Wilcox, J. N., DeLeon, H., et al. (2000). CC chemokine receptor 2 is required for macrophage infiltration and vascular hypertrophy in angiotensin II–induced hypertension. *Hypertension* 36, 360–363. doi: 10.1161/01.HYP.36.3.360

Caillon, A., Paradis, P., and Schiffrin, E. L. (2018). Role of immune cells in hypertension. *Br. J. Pharmacol.* 176, 1818–1828. doi: 10.1111/bph.14427

Carnagarin, R., Matthews, V., Zaldivia, M. T., Peter, K., and Schlaich, M. P. (2018). The bidirectional interaction between the sympathetic nervous system and immune mechanisms in the pathogenesis of hypertension. *Br. J. Pharmacol.* 176, 1839–1852. doi: 10.1111/bph.14481

Chan, C. T., Moore, J. P., Budzyn, K., Guida, E., Diep, H., Vinh, A., et al. (2012). Reversal of vascular macrophage accumulation and hypertension by a CCR2 antagonist in deoxycorticosterone/salt-treated mice. *Hypertension* 60, 1207–1212. doi: 10.1161/HYPERTENSIONAHA.112.201251

Chang, A. Y., Li, F. C., Huang, C.-W., Wu, J. C., Dai, K.-Y., Chen, C.-H., et al. (2014). Interplay between brain stem angiotensins and monocyte chemoattractant protein-1 as a novel mechanism for pressor response after ischemic stroke. *Neurobiol. Dis.* 71, 292–304. doi: 10.1016/j.nbd.2014.08.005

Chen, X.-L., Tummala, P. E., Olbrych, M. T., Alexander, R. W., and Medford, R. M. (1998). Angiotensin II induces monocyte chemoattractant protein-1 gene expression in rat vascular smooth muscle cells. *Circ. Res.* 83, 952–959. doi: 10.1161/01.RES.83.9.952

Chrysohoou, C., Pitsavos, C., Panagiotakos, D. B., Skoumas, I., and Stefanadis, C. (2004). Association between prehypertension status and inflammatory markers related to atherosclerotic disease* The ATTICA Study. *Am. J. Hypertens.* 17, 568–573. doi: 10.1016/j.amjhyper.2004.03.675

Crowley, S. D., Gurley, S. B., Herrera, M. J., Ruiz, P., Griffiths, R., Kumar, A. P., et al. (2006). Angiotensin II causes hypertension and cardiac hypertrophy through its receptors in the kidney. *Proc. Natl. Acad. Sci. USA* 103, 17985–17990. doi: 10.1073/pnas.0605545103

Crowley, S. D., Song, Y.-S., Sprung, G., Griffiths, R., Sparks, M., Yan, M., et al. (2010). A role for angiotensin II type 1 receptors on bone marrow-derived cells in the pathogenesis of angiotensin II–dependent hypertension. *Hypertension* 55, 99–108. doi: 10.1161/HYPERTENSIONAHA.109.144964

Dampney, R. A., Czachurski, J., Dembowsky, K., Goodchild, A. K., and Seller, H. (1987). Afferent connections and spinal projections of the pressor region in the rostral ventrolateral medulla of the cat. *J. Auton. Nerv. Syst.* 20, 73–86.

Deshmane, S. L., Kremlev, S., Amini, S., and Sawaya, B. E. (2009). Monocyte chemoattractant protein-1 (MCP-1): an overview. *J. Interf. Cytokine Res.* 29, 313–326. doi: 10.1089/jir.2008.0027

Elmarakby, A. A., Quigley, J. E., Olearczyk, J. J., Sridhar, A., Cook, A. K., Inscho, E. W., et al. (2007). Chemokine receptor 2b inhibition provides renal protection in angiotensin II–salt hypertension. *Hypertension* 50, 1069–1076. doi: 10.1161/HYPERTENSIONAHA.107.098806

Gao, H.-L., Yu, X.-J., Qi, J., Yi, Q.-Y., Jing, W.-H., Sun, W.-Y., et al. (2016). Oral CoQ10 attenuates high salt-induced hypertension by restoring neurotransmitters and cytokines in the hypothalamic paraventricular nucleus. *Sci. Rep.* 6:30301. doi: 10.1038/srep30301

Goldblatt, H., Lynch, J., Hanzal, R. F., and Summerville, W. W. (1934). Studies on experimental hypertension I. The production of persistent elevation of systolic blood pressure by means of renal ischemia. *J. Exp. Med.* 59, 347–379.

Hinojosa, A. E., Garcia-Bueno, B., Leza, J. C., and Madrigal, J. L. (2011). Regulation of CCL2/MCP-1 production in astrocytes by desipramine and atomoxetine: involvement of alpha2 adrenergic receptors. *Brain Res. Bull.* 86, 326–333. doi: 10.1016/j.brainresbull.2011.09.014

Ishibashi, M., Hiasa, K.-I., Zhao, Q., Inoue, S., Ohtani, K., Kitamoto, S., et al. (2004). Critical role of monocyte chemoattractant protein-1 receptor CCR2 on monocytes in hypertension-induced vascular inflammation and remodeling. *Circ. Res.* 94, 1203–1210. doi: 10.1161/01.RES.0000126924.23467.A3

Jia, L. L., Kang, Y. M., Wang, F. X., Li, H. B., Zhang, Y., Yu, X. J., et al. (2014). Exercise training attenuates hypertension and cardiac hypertrophy by modulating neurotransmitters and cytokines in hypothalamic paraventricular nucleus. *PLoS One* 9:e85481. doi: 10.1371/journal.pone.0085481

Kang, Y.-M., Ma, Y., Zheng, J.-P., Elks, C., Sriramula, S., Yang, Z.-M., et al. (2009). Brain nuclear factor-kappa B activation contributes to neurohumoral excitation in angiotensin II-induced hypertension. *Cardiovasc. Res.* 82, 503–512. doi: 10.1093/cvr/cvp073

Kang, Y.-M., Zhang, D.-M., Yu, X.-J., Yang, Q., Qi, J., Su, Q., et al. (2014). Chronic infusion of enalaprilat into hypothalamic paraventricular nucleus attenuates angiotensin II-induced hypertension and cardiac hypertrophy by restoring neurotransmitters and cytokines. *Toxicol. Appl. Pharmacol.* 274, 436–444. doi: 10.1016/j.taap.2013.12.001

Korim, W. S., Elsaafien, K., Basser, J. R., Setiadi, A., May, C. N., and Yao, S. T. (2018). In renovascular hypertension, TNF-α type-1 receptors in the area postrema mediate increases in cardiac and renal sympathetic nerve activity and blood pressure. *Cardiovasc. Res.* 115, 1092–1101. doi: 10.1093/cvr/cvy268

Li, H.-B., Li, X., Huo, C.-J., Su, Q., Guo, J., Yuan, Z.-Y., et al. (2016). TLR4/MyD88/NF-κB signaling and PPAR-γ within the paraventricular nucleus are involved in the effects of telmisartan in hypertension. *Toxicol. Appl. Pharmacol.* 305, 93–102. doi: 10.1016/j.taap.2016.06.014

Li, H.-B., Qin, D.-N., Ma, L., Miao, Y.-W., Zhang, D.-M., Lu, Y., et al. (2014). Chronic infusion of lisinopril into hypothalamic paraventricular nucleus modulates cytokines and attenuates oxidative stress in rostral ventrolateral medulla in hypertension. *Toxicol. Appl. Pharmacol.* 279, 141–149. doi: 10.1016/j.taap.2014.06.004

Lu, P., Jiang, S.-J., Pan, H., Xu, A.-L., Wang, G.-H., Ma, C.-L., et al. (2017). Short hairpin RNA interference targeting interleukin 1 receptor type I in the paraventricular nucleus attenuates hypertension in rats. *Pflugers Arch.* 470, 1–10. doi: 10.1007/s00424-017-2081-0

Lu, B., Rutledge, B. J., Gu, L., Fiorillo, J., Lukacs, N. W., Kunkel, S. L., et al. (1998). Abnormalities in monocyte recruitment and cytokine expression in monocyte chemoattractant protein 1–deficient mice. *J. Exp. Med.* 187, 601–608. doi: 10.1084/jem.187.4.601

Marketou, M. E., Kontaraki, J. E., Tsakountakis, N. A., Zacharis, E. A., Kochiadakis, G. E., Arfanakis, D. A., et al. (2011). Differential effect of telmisartan and amlodipine on monocyte chemoattractant protein-1 and peroxisome proliferator-activated receptor-gamma gene expression in peripheral monocytes in patients with essential hypertension. *Am. J. Cardiol.* 107, 59–63. doi: 10.1016/j.amjcard.2010.08.048

Marvar, P. J., Thabet, S. R., Guzik, T. J., Lob, H. E., McCann, L. A., Weyand, C., et al. (2010). Central and peripheral mechanisms of T-lymphocyte activation and vascular inflammation produced by angiotensin II–induced hypertension. *Circ. Res.* 107, 263–270. doi: 10.1161/CIRCRESAHA.110.217299

Matsuda, S., Umemoto, S., Yoshimura, K., Itoh, S., Murata, T., Fukai, T., et al. (2015). Angiotensin II Activates MCP-1 and induces cardiac hypertrophy

and dysfunction via toll-like receptor 4. *J. Atheroscler. Thromb.* 22, 833–844. doi: 10.5551/jat.27292

Morioka, N., Tokuhara, M., Harano, S., Nakamura, Y., Hisaoka-Nakashima, K., and Nakata, Y. (2013). The activation of P2Y6 receptor in cultured spinal microglia induces the production of CCL2 through the MAP kinases-NF-kappaB pathway. *Neuropharmacology* 75, 116–125. doi: 10.1016/j.neuropharm.2013.07.017

Muller, W. A., Weigl, S. A., Deng, X., and Phillips, D. M. (1993). PECAM-1 is required for transendothelial migration of leukocytes. *J. Exp. Med.* 178, 449–460.

Nunes, F. C., and Braga, V. A. (2011). Chronic angiotensin II infusion modulates angiotensin II type I receptor expression in the subfornical organ and the rostral ventrolateral medulla in hypertensive rats. *J. Renin-Angiotensin-Aldosterone Syst.* 12, 440–445. doi: 10.1177/1470320310394891

Roberts, T. K., Eugenin, E. A., Lopez, L., Romero, I. A., Weksler, B. B., Couraud, P.-O., et al. (2012). CCL2 disrupts the adherens junction: implications for neuroinflammation. *Lab. Investig.* 92, 1213–1233. doi: 10.1038/labinvest.2012.80

Rollins, B. J. (1997). Chemokines. *Blood* 90, 909–928.

Santisteban, M. M., Ahmari, N., Carvajal, J. M., Zingler, M. B., Qi, Y., Kim, S., et al. (2015). Involvement of bone marrow cells and neuroinflammation in hypertension. *Circ. Res.* 117, 178–191. doi: 10.1161/CIRCRESAHA.117.305853

Schramm, L. P., Strack, A. M., Platt, K. B., and Loewy, A. D. (1993). Peripheral and central pathways regulating the kidney: a study using pseudorabies virus. *Brain Res.* 616, 251–262.

Setiadi, A., Korim, W. S., Elsaafien, K., and Yao, S. T. (2018). The role of the blood–brain barrier in hypertension. *Exp. Physiol.* 103, 337–342. doi: 10.1113/EP086434

Sharma, R. K., Yang, T., Oliveira, A. C., Lobaton, G. O., Aquino, V., Kim, S., et al. (2019). Microglial cells impact gut microbiota and gut pathology in angiotensin II-induced hypertension. *Circ. Res.* 124, 727–736. doi: 10.1161/CIRCRESAHA.118.313882

Shen, X. Z., Li, Y., Li, L., Shah, K. H., Bernstein, K. E., Lyden, P., et al. (2015). Microglia participate in neurogenic regulation of hypertension. *Hypertension* 66, 309–316. doi: 10.1161/HYPERTENSIONAHA.115.05333

Shi, P., Diez-Freire, C., Jun, J. Y., Qi, Y., Katovich, M. J., Li, Q., et al. (2010). Brain microglial cytokines in neurogenic hypertension. *Hypertension* 56, 297–303. doi: 10.1161/HYPERTENSIONAHA.110.150409

Shi, Z., Gan, X. B., Fan, Z. D., Zhang, F., Zhou, Y. B., Gao, X. Y., et al. (2011). Inflammatory cytokines in paraventricular nucleus modulate sympathetic activity and cardiac sympathetic afferent reflex in rats. *Acta Physiol.* 203, 289–297. doi: 10.1111/j.1748-1716.2011.02313.x

Song, X.-A., Jia, L.-L., Cui, W., Zhang, M., Chen, W., Yuan, Z.-Y., et al. (2014). Inhibition of TNF-α in hypothalamic paraventricular nucleus attenuates hypertension and cardiac hypertrophy by inhibiting neurohormonal excitation in spontaneously hypertensive rats. *Toxicol. Appl. Pharmacol.* 281, 101–108. doi: 10.1016/j.taap.2014.09.004

Sriramula, S., Cardinale, J. P., and Francis, J. (2013). Inhibition of TNF in the brain reverses alterations in RAS components and attenuates angiotensin II-induced hypertension. *PLoS One* 8:e63847. doi: 10.1371/journal.pone.0063847

Stamatovic, S. M., Keep, R. F., Kunkel, S. L., and Andjelkovic, A. V. (2003). Potential role of MCP-1 in endothelial cell tight junctionopening': signaling via Rho and Rho kinase. *J. Cell Sci.* 116, 4615–4628. doi: 10.1242/jcs.00755

Stamatovic, S. M., Keep, R. F., Wang, M. M., Jankovic, I., and Andjelkovic, A. V. (2009). Caveolae-mediated internalization of occludin and claudin-5 during CCL2-induced tight junction remodeling in brain endothelial cells. *J. Biol. Chem.* 284, 19053–19066. doi: 10.1074/jbc.M109.000521

Strack, A., Sawyer, W., Hughes, J., Platt, K., and Loewy, A. (1989a). A general pattern of CNS innervation of the sympathetic outflow demonstrated by transneuronal pseudorabies viral infections. *Brain Res.* 491, 156–162.

Strack, A. M., Sawyer, W. B., Platt, K. B., and Loewy, A. D. (1989b). CNS cell groups regulating the sympathetic outflow to adrenal gland as revealed by transneuronal cell body labeling with pseudorabies virus. *Brain Res.* 491, 274–296.

Su, Q., Qin, D.-N., Wang, F.-X., Ren, J., Li, H.-B., Zhang, M., et al. (2014). Inhibition of reactive oxygen species in hypothalamic paraventricular nucleus attenuates the renin–angiotensin system and proinflammatory cytokines in hypertension. *Toxicol. Appl. Pharmacol.* 276, 115–120. doi: 10.1016/j.taap.2014.02.002

Tsou, C.-L., Peters, W., Si, Y., Slaymaker, S., Aslanian, A. M., Weisberg, S. P., et al. (2007). Critical roles for CCR2 and MCP-3 in monocyte mobilization from bone marrow and recruitment to inflammatory sites. *J. Clin. Invest.* 117, 902–909. doi: 10.1172/JCI29919

van der Kooy, D., and Koda, L. Y. (1983). Organization of the projections of a circumventricular organ: the area postrema in the rat. *J. Comp. Neurol.* 219, 328–338.

Wang, M.-L., Kang, Y.-M., Li, X.-G., Su, Q., Li, H.-B., Liu, K.-L., et al. (2018). Central blockade of NLRP3 reduces blood pressure via regulating inflammation microenvironment and neurohormonal excitation in salt-induced prehypertensive rats. *J. Neuroinflammation* 15:95. doi: 10.1186/s12974-018-1131-7

Wang, Y., Zhu, M., Xu, H., Cui, L., Liu, W., Wang, X., et al. (2015). Role of the monocyte chemoattractant protein-1/CC chemokine receptor 2 signaling pathway in transient receptor potential vanilloid type 1 ablation-induced renal injury in salt-sensitive hypertension. *Exp. Biol. Med.* 240, 1223–1234. doi: 10.1177/1535370214565970

Wei, S.-G., Yu, Y., Zhang, Z.-H., and Felder, R. B. (2015). Proinflammatory cytokines upregulate sympathoexcitatory mechanisms in the subfornical organ of the rat. *Hypertension* 65, 1126–1133. doi: 10.1161/HYPERTENSIONAHA.114.05112

Wittendorp, M. C., Boddeke, H. W. G. M., and Biber, K. (2004). Adenosine A(3) receptor-induced CCL2 synthesis in cultured mouse astrocytes. *Glia* 46, 410–418. doi: 10.1002/glia.20016

Xie, Q.-Y., Sun, M., Yang, T.-L., and Sun, Z.-L. (2006). Losartan reduces monocyte chemoattractant protein-1 expression in aortic tissues of 2K1C hypertensive rats. *Int. J. Cardiol.* 110, 60–66. doi: 10.1016/j.ijcard.2005.07.046

Yoshimura, T., Robinson, E., Tanaka, S., Appella, E., and Leonard, E. (1989a). Purification and amino acid analysis of two human monocyte chemoattractants produced by phytohemagglutinin-stimulated human blood mononuclear leukocytes. *J. Immunol.* 142, 1956–1962.

Yoshimura, T., Yuhki, N., Moore, S. K., Appella, E., Lerman, M. I., and Leonard, E. J. (1989b). Human monocyte chemoattractant protein-1 (MCP-1) full-length cDNA cloning, expression in mitogen-stimulated blood mononuclear leukocytes, and sequence similarity to mouse competence gene JE. *FEBS Lett.* 244, 487–493.

Yu, X.-J., Zhang, D.-M., Jia, L.-L., Qi, J., Song, X.-A., Tan, H., et al. (2015). Inhibition of NF-κB activity in the hypothalamic paraventricular nucleus attenuates hypertension and cardiac hypertrophy by modulating cytokines and attenuating oxidative stress. *Toxicol. Appl. Pharmacol.* 284, 315–322. doi: 10.1016/j.taap.2015.02.023

Zlotnik, A., and Yoshie, O. (2012). The chemokine superfamily revisited. *Immunity* 36, 705–716. doi: 10.1016/j.immuni.2012.05.008

Zubcevic, J., Santisteban, M. M., Perez, P. D., Arocha, R., Hiller, H., Malphurs, W. L., et al. (2017). A single angiotensin II hypertensive stimulus is associated with prolonged neuronal and immune system activation in Wistar-Kyoto rats. *Front. Physiol.* 8:592. doi: 10.3389/fphys.2017.00592

Conflict of Interest Statement: The authors declare that the research was conducted in the absence of any commercial or financial relationships that could be construed as a potential conflict of interest.

Copyright © 2019 Elsaafien, Korim, Setiadi, May and Yao. This is an open-access article distributed under the terms of the Creative Commons Attribution License (CC BY). The use, distribution or reproduction in other forums is permitted, provided the original author(s) and the copyright owner(s) are credited and that the original publication in this journal is cited, in accordance with accepted academic practice. No use, distribution or reproduction is permitted which does not comply with these terms.

2. General Methods and Materials

2.1 Animals

2.1.1 Ethics Approval

Animals were purchased from the Animal Resource Centre (ARC, Western Australia). All experimental protocols used in this study were performed in accordance with the Prevention of Cruelty to Animals Act. Australia 1986. These protocols comply to (1) the "Guiding Principles for Research Involving Animals and Human Beings" (2) and the guidelines set by the Australian Code of Practice for the Care and Use of Animals for Scientific Purposes, 2007 (National Health and Medical Research Council of Australia) and were approved by the Florey Institute of Neuroscience and Mental Health Animal Ethics Committee (ethics number 15-013). Every attempt was made to minimize animal suffering, discomfort and reduce the number of animals needed to obtain reliable results.

2.1.2 Animal Strain and Housekeeping

Male Sprague-Dawley rats, spontaneously hypertensive rats (SHR), and Wistar-Kyoto (WKY), between 10-12 weeks of age were used in the studies described in this thesis. Each animal weighed between 250-300 grams upon arrival. Rats were given free access to food (Standard laboratory rat chow, Barastoc, Australia) and tap water. Animals were housed in temperature-controlled room (22±2 ˚C), two rats in each cage in the animal facility at the Howard Florey Laboratories, Florey Institute of Neuroscience and Mental Health. Rats were housed under a 12:12 hour light / dark cycle (lights off at 7:00 P.M. and lights on at 7:00 A.M.). Rats were allowed at least 5 days to acclimatize to the animal housing facilities before being used for experimental purposes.

2.2 Surgical Protocols

2.2.1 General

Rats were weighed at the beginning of each experiment and were deeply anaesthetised with sodium pentobarbitone (60mg/kg intraperitoneally; Troy Laboratories Pty Ltd, Australia) for acute experiments, or with ketamine/medetomidine (75 mg/kg; 0.5 mg/kg) for recovery surgeries. Once the animals had reached a surgical plane of anaesthesia (i.e. absence of a hind paw withdrawal reflex following a noxious pinch and blink reflex to corneal stimulation with a cotton tip), surgical procedures began. All surgical instruments and the incision region were sterilised with 80% ethanol (Chem Supply, Australia). At the conclusion of all recovery surgeries, animals were given 0.1 ml of meloxicam (5mg/ml, Troy Laboratories PTY. Limited, Australia) intramuscularly, and a triple antibiotic powder (Tricin, 250 iu/g Bactiricin zinc, 5mg/g Neomycin sulfate, 5000 iu/g Polymyxin B sulfate, 50 g, Jutox Pty Ltd, Australia) was applied onto the sutured incisions and the animals were left to recover in clean warmed cage.

2.2.2 Rat Models of Hypertension

Spontaneously hypertensive rats (SHR) and normotensive Wistar-Kyoto (WKY) were purchased from the Animal Resource Centre (ARC, Western Australia). Both SHR and WKY were between 10-12 weeks of age (300-400g) and were allowed at least 5 days to acclimatize to the animal housing facilities before being used for experimental purposes.

For the renovascular model (two kidney- one clip; 2K1C), male Sprague-Dawley rats (250-400g) were used (Goldblatt, Lynch et al. 1934). General anaesthesia was induced with ketamine/medetomidine (75 mg/kg; 0.5 mg/kg). An incision was made to the abdomen, and linae alba was incised to expose the abdomen. The small intestines were pushed aside using a wet cotton buds to expose the left kidney. Once the kidney was exposed, and the renovascular

bundle was cleared, the renal artery was separated from the renal vein. A silver clip (Silver foil, 0.25 mm, Sigma-Aldrich, USA) was then used to partially occlude the left renal artery, permitting partial perfusion of the kidney. The abdominal muscles and the incision were then sutured (Silk 4-0 U.S.P, 45 cm, USA). Animals were then allowed to develop hypertension over their respective periods.

2.2.3 Femoral Cannulation

Once the animals have reached a surgical plane of anaesthesia an incision was made to the femoral region and the subcutaneous tissue was bluntly dissected to expose the femoral neurovascular bundle. Retractors were used to pull the skin aside to expose the femoral neurovascular bundle. Forceps were then used to separate the femoral nerve from the femoral vessels. After that the femoral artery and the femoral vein were separated using forceps. Two silk threads (Mersilk 2-0 U.S.P, Look, USA) were then placed around the vessel and pulled to opposite ends of the expose vessel. The silk threads were clamped with haemostats, which helped in lifting the vessel. A 25-gauge needle (Terumo needle, 25G x 1inch, 0.50x25mm, Terumo, Japan) was then used to pierce the vessel and a cannula (polyethylene tubing, internal diameter 0.58mm, outer diameter 0.96mm, Silverwater BC, Australia) was then inserted into the vessel. Approximately 4 cm of the cannula was advanced into the vessel. The threads placed around each vessel were then tied to secure the cannula in the vessel for the whole duration of the experiment. Heparinised saline (10 U/mL) was used to flush the cannulae. The free end of the femoral artery cannula was connected to a pressure transducer to record blood pressure. The femoral vein cannula was used for the intravenous infusion of supplementary doses of pentobarbitone sodium (20mg/kg i.v. as required) upon observing a corneal or a pedal reflex. For blood pressure recording in conscious animals, the free end of the femoral artery cannula

tunnelled subcutaneously and externalised at the base of the neck. The femoral region and the base of the neck were then sutured (Silk 4-0 U.S.P, 45 cm, Look, USA).

2.2.4 Telemetry Implantation

General anaesthesia was induced with ketamine/medetomidine (75 mg/kg; 0.5 mg/kg). An incision was made to the abdomen, and linae alba was incised to expose the abdomen. The small intestines were then pushed using wet cotton buds to expose the abdominal aorta and the inferior vena cava. The abdominal aorta was then separated from the inferior vena cava. Two silk threads (Mersilk 2-0 U.S.P, Look, USA) were then placed around the vessel and pulled to opposite ends to expose vessel. The silk threads were clamped with haemostats, which helped in lifting the vessel. A 25-gauge needle (Terumo needle, 25G x 1inch, 0.50x25mm, Terumo, Japan) was then used to pierce the vessel. Once an opening was made into the abdominal aorta; the probe of the radio-telemetry transmitter (DSI, USA) was then inserted was then inserted into the vessel. Approximately about 4 mm of the probe was advanced into the vessel. The threads were then carefully removed, and a cellulose patch (DSI, USA) was then placed on the opening of the abdominal aorta. A few drops of tissue adhesive (Physiotel tissue adhesive, 3 ml, DSI, USA) were then placed on the cellulose patch, so that the opening is closed, and the probe is secured. The probe of the radio-telemetry transmitter was filled with an anti-coagulant gel (Pressure Implant Re-gel syringe, 5 ml, DSI, USA) to prevent blood clotting in the probe. The radio-telemetry transmitter was then secured into the abdominal muscles, abdomen was then closed and sutured (Silk 4-0 U.S.P, 45 cm, Look, USA).

2.2.5 Renal Sympathetic Nerve Preparation

After a flank incision, retractors were used to pull the skin aside to allow a better view of the exposed kidney retroperitoneally. With the aid of an operating microscope, the renal nerve was carefully dissected free of surrounding tissue under mineral oil. The nerve was then placed onto bipolar silver hook electrodes, and the region was then flooded with paraffin oil. RSNA was amplified (x10000; Neurolog, Digitimer, Hertfordshire, UK) and filtered (50-1000 Hz). Signals were sampled at 10000 Hz, and digitized using a Power1401 (Cambridge Electronic Design, Cambridge, UK), using Spike2 v7.02 software. Neurograms were quantified by rectifying and time-averaging the signal using 1 second constant, followed by subtraction of the noise level (0%), and normalization adopting 100% as baseline. To ensure the quality and the validity of the signal, pulse modulation of the signal was determined, and baroreflex modulation of RSNA was also determined following intravenous administration of phenylephrine 5 μg/kg (Figure 2.1) (Hart, Head et al. 2017).

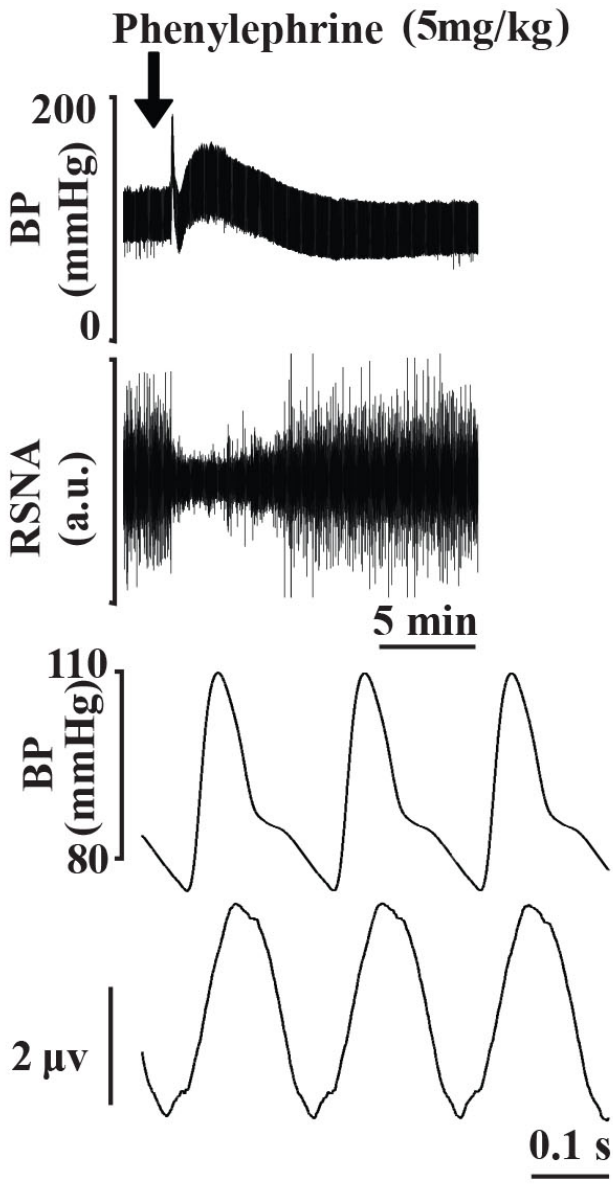


Figure 2.1: Baroreflex modulation of RSNA.

Top: Pulsatile arterial pressure (BP) and renal sympathetic nerve activity (RSNA) following intravenous administration of phenylephrine 5 µg/kg. Bottom: Pulse modulation of RSNA.

2.2.6 Cranial Surgery for Central Microinjections

Once anaesthetised and the head area shaved, animals were placed in a stereotaxic frame (David Kopf, USA). Each ear bar was inserted into the animal's ear canal and the nose clamp was tightened. A scalpel blade was used to make an incision on the dorsal aspect of the head, and using wet cotton buds, the periosteum was removed so that the skull sutures could be easily visualised. Using the stereotaxic arm, bregma was identified and the coordinates in the anterior-posterior and medial-lateral planes were taken. The coordinates for the drilling site were obtained from the rat brain atlas, depending on the region of interest (Paxinos G 2007). A small electric hand drill (Dremel, USA) was used to drill a small burr hole (approximately 2 mm in diameter) to expose the dorsal surface of the brain overlying the region of injection.

2.2.7 PVN Microinjection

Once a small burr hole is drilled into the skull overlying the PVN, a 5-barrell glass micropipette (Sigma-Aldrich, USA) was loaded with various drugs of interest. The glass micropipette was then carefully positioned in a pipette holder supported by the stereotaxic arm, and the coordinates for bregma were obtained again. From the coordinates of bregma, the PVN coordinates were obtained (1.8 mm posterior to bregma and 0.3 mm lateral to the midline). The glass micropipette was the inserted into the PVN (to a depth of 8.5 mm ventral to dorsal surface of the brain).

For PVN microinjections in conscious animals, a guide cannula (guide cannula, 20GA, Plastic one INC, USA) was inserted into the drilled hole, 1 mm dorsal to the PVN (7.5 mm ventral to the brain surface). Screws and dental cement were used to secure the guide cannula. The scalp was then sutured around the guide cannula leaving it externalised. Animals were then allowed five days of recovery, before performing PVN microinjections. Microinjections into

the PVN were performed using an injector (injector, Plastic one INC, USA) connected to a Hamilton syringe (Hamilton syringe, 25 µl syringe, Anspec INC, USA).

At the end of the experiment Evans blue dye was injected in the same site as drugs injected into the PVN, to mark the injection site. All PVN microinjections were validated and mapped respectively (Figure 2.2).

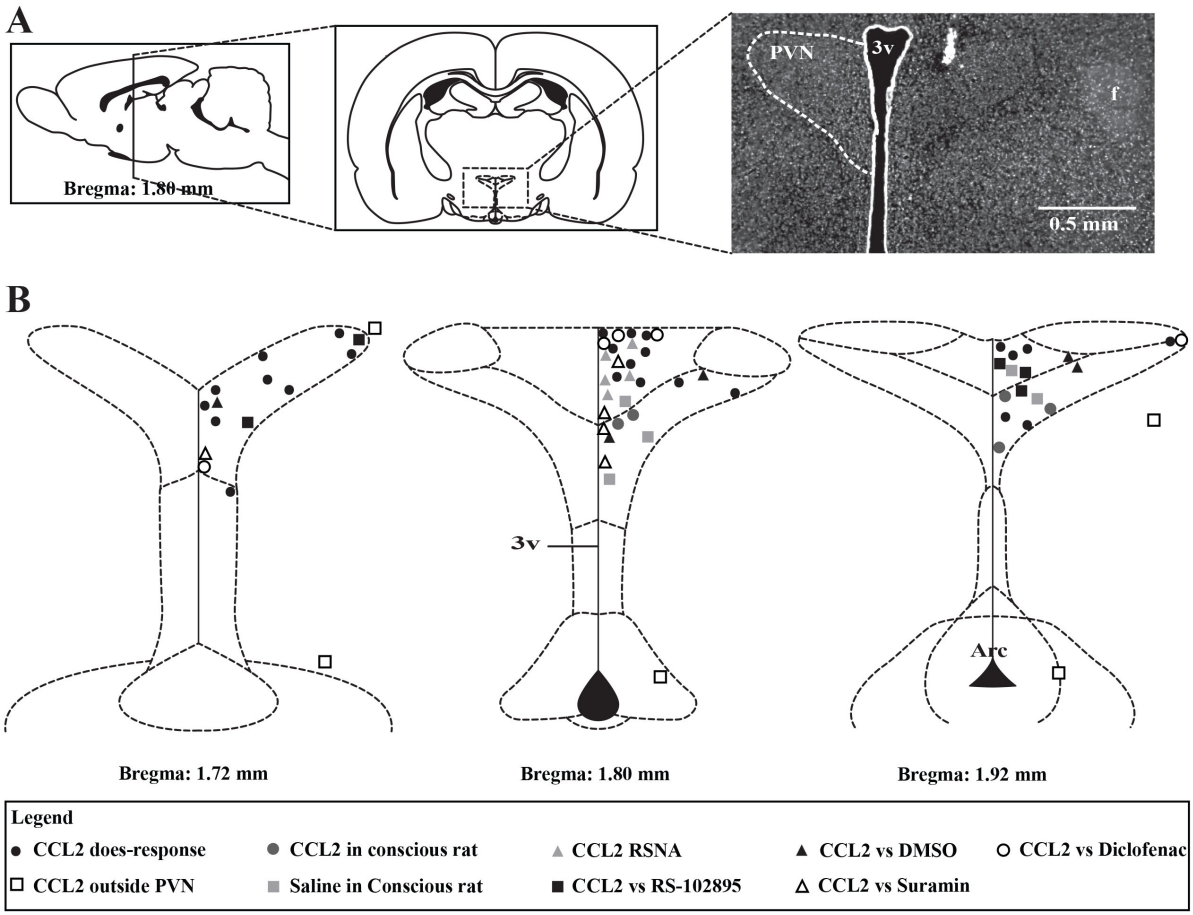


Figure 2.2: Validation of PVN microinjections.

(A) Representative photomicrograph of a PVN microinjection site. **(B)** A schematic coronal diagram mapping all PVN microinjection sites. 3v; third ventricle, Arc; arcuate nucleus, f; fornix, PVN; paraventricular nucleus of the hypothalamus. Schematic Diagrams are regenerated from (Paxinos G 2007).

2.2.8 RVLM Microinjection

Following anaesthesia, the head was shaved, and an incision was made from the level of the occipital ridge to approximately T3. Using forceps, the posterior neck muscles (upper trapezius and splenius capitis) were separated via blunt dissection along the midline. After the muscles were separated, retractors were used to pull the muscles and the skin aside. With the aid of an operating microscope, the atlanto-occipital membrane was identified, and incised to expose the brain stem. A cotton bud was used to clear the cerebrospinal fluid. The rostral ventrolateral medulla (RVLM) was approached from the brainstem and obex was used as a reference point. A single glass micropipette (Sigma-Aldrich, USA) was loaded with cholera toxin B subunit (CTb). The stereotaxic arm was placed on a 30-degree angle. Using the operating microscope, obex was identified. Coordinates were taken in the medial-lateral plane and the dorsal-ventral plane. The coordinates for the RVLM injection were calculated (2.2 mm lateral to obex, 4.6 mm ventral to brainstem surface) (Paxinos G 2007). The glass micropipette was inserted into the RVLM. The micropipette was connected to an air compressor, to help control the amount and speed of the CTb injected into the RVLM. CTb (approximately 20 nl) was injected into the RVLM, and the glass micropipette was left in the RVLM for ten minutes to minimise back-tracking. The glass micropipette was then quickly withdrawn, and the incision was sutured (Silk 4-0 U.S.P, 45 cm, USA). Animals were then left for seven days to recover, before they were perfused, and brains were collected for immunohistochemical studies. RVLM microinjection sites were validated using post-mortem histology and were mapped respectively (Figure 2.3).

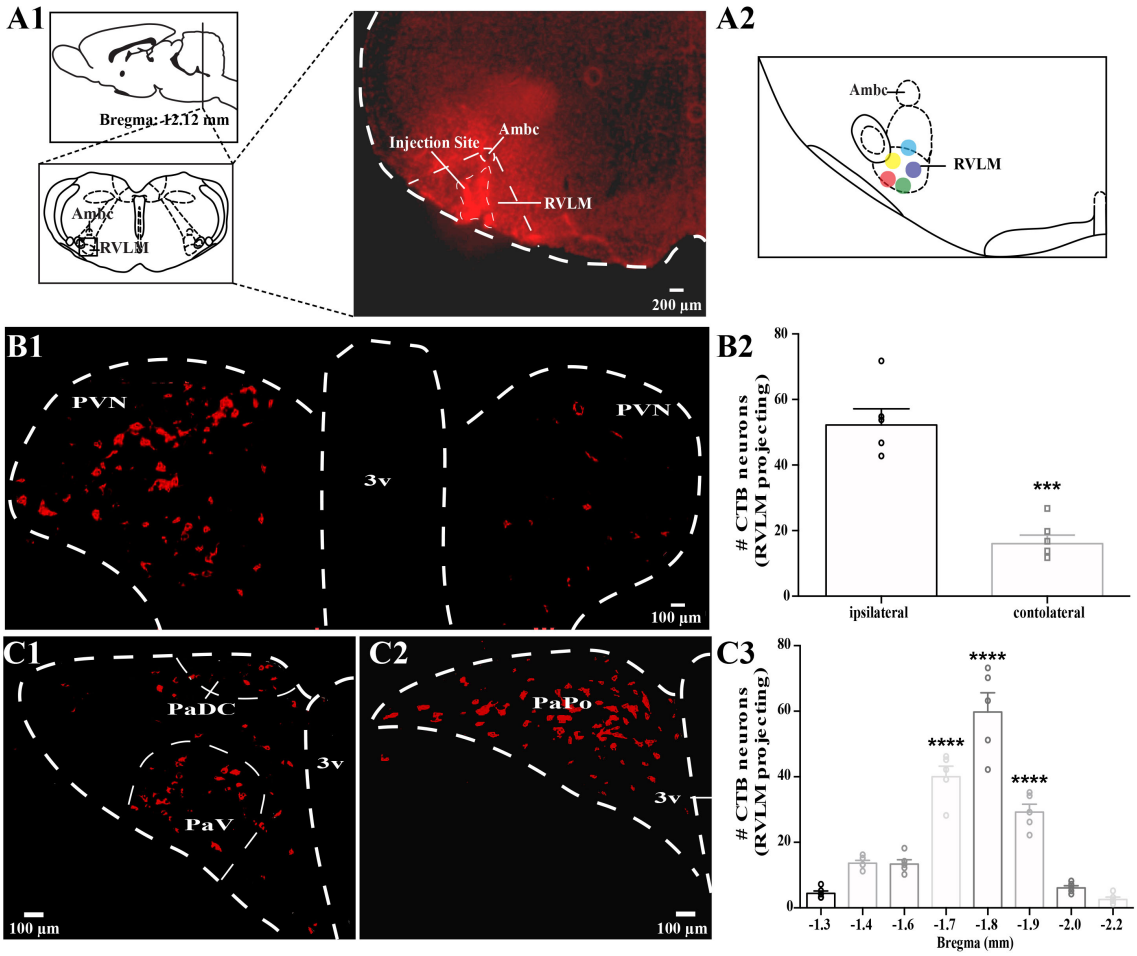


Figure 2.3: Validity of retrograde tracing using CTb.

(A1) Representative photomicrograph of RVLM injection site with CTb. **(A2)** A schematic diagram mapping all injection sites. **(B1)** Photomicrograph of CTb positive neurons in the PVN, and **(B2)** grouped cell count of CTb positive neurons, depicting more positive neurons labelled ipsilaterally. **(C1-C2)** Photomicrographs of CTb positive neurons at different levels from bregma, depicting the majority of labelled neurons to be localized to the PaDC, PaV, PaPo regions of the PVN, and **(C3)** grouped cell count of CTb positive neurons at different levels from bregma. 3v; third ventricle, Ambc; compact part of the nucleus ambiguous, PaDC; dorsal cap of PVN, PaPo; medial PVN, PaV; ventral PVN, $^{***}P\leq0.001$; student t-test of ipsilateral vs. contralateral, $^{****}P\leq0.0001$; one-way ANOVA of different levels from bregma (n=5 rats per group). Schematic diagrams modified from (Paxinos G 2007).

2.2.9 ICV Microinjection

Once the skull was drilled, as described above, a single glass micropipette (Sigma-Aldrich, USA) was loaded with drugs of interest. The glass micropipette was then carefully positioned in a pipette holder supported by the stereotaxic arm, and the coordinates for bregma were obtained. From the coordinates of bregma, the coordinates for the left lateral ventricle were obtained (0.5 mm posterior to bregma and 1.4 lateral to the midline). The glass micropipette was the inserted into the lateral ventricle (to a depth of 3.7 mm ventral to dorsal surface of the brain). The volume of the microinjection was 1 µl.

2.2.10 Osmotic Minipump Implantation

After shaving the animals head and exposing the dorsal surface of the skill, a hole was drilled in the skull superior to left lateral cerebroventricle (0.5 mm posterior to bregma, and 1.4 mm lateral to the midline). A guide cannula (guide cannula, 20GA, Plastic one INC, USA) was inserted into the drilled hole, 3.7 mm ventral to the brain surface, into the left lateral ventricle. Screws and dental cement were used to secure the guide cannula. A 4-week osmotic minipump (2.5 µl/hour, 28 days, Alzet, USA), was connected to the infusion cannula via the catheter tube. The osmotic minipump was then implanted subcutaneously between the scapula, and the incision was then sutured (Silk 4-0 U.S.P, 45 cm, USA). Microinjection into the lateral ventricle were validated histologically, post-mortem (Figure 2.4).

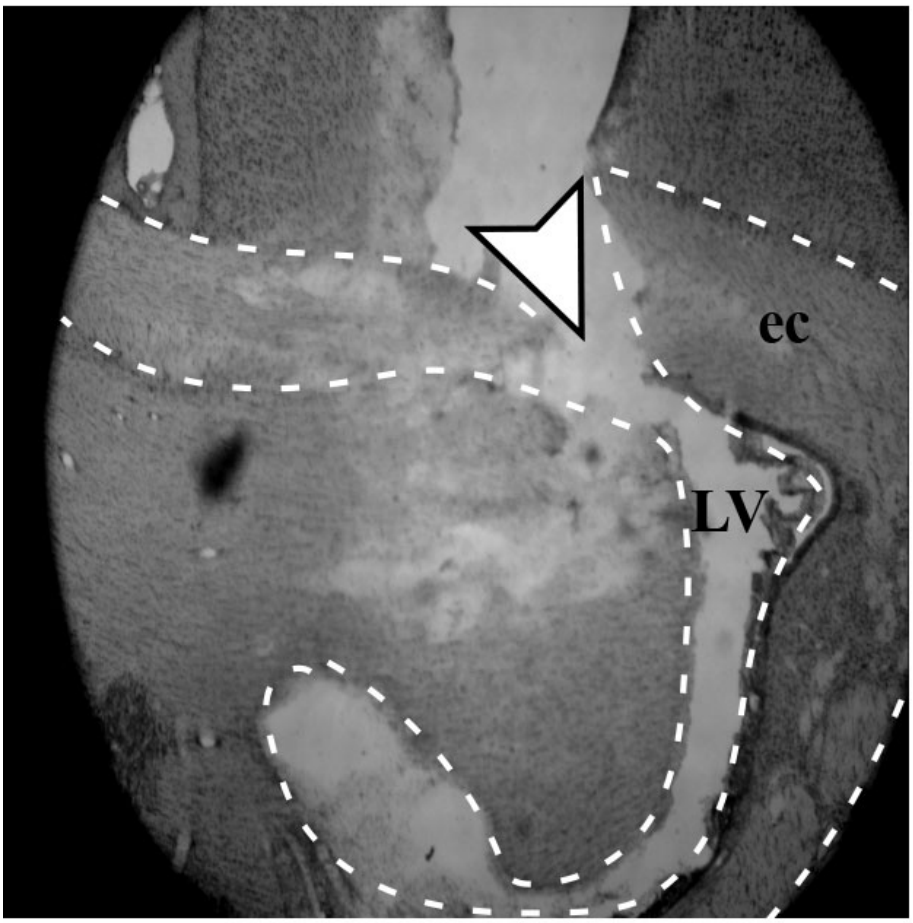


Figure 2.4: Validity of intra-cerebroventricular (ICV) infusions.

The validity of ventricular infusion was determined by post-mortem histology, were the breakage of the external capsule (ec), indicates the position of the infusion cannula into the left lateral ventricle (LV).

2.2.11 Drugs

The table below lists all the drugs and agents and their respective doses used in all the studies described in this thesis.

Table 2.1: List of all experimental drugs used in all series of experiments presented by this thesis.

Drug	Description	Dose	Dose based on	Company
CCL2	Recombinant rat CCL2/JE/MCP-1, 3144-JE/CF, derived from myeloma cell line	3.5 nM 7.0 nM 14.0 nM 35.5 nM 71.0 nM	(Soares, Ott et al. 2013)	R&D systems, USA
RS-102895	CCR2 antagonist	70 µM	(Aiyar, Daines et al. 2001)	Tocris, Australia
Suramin	Non-selective P2x antagonist	10 mM	(Inoue, Nakazawa et al. 1991)	Sigma Aldrich, USA
Diclofenac	Non-steroidal anti-inflammatory drug	5 mg/kg	(Todd and Sorkin 1988)	Sigma Aldrich, USA
Saline	Sodium chloride	0.9%	N/A	Baxter healthcare Pty Ltd, Australia
DMSO	Dimethyl sulfoxide	33.7%	N/A	Sigma Aldrich, USA
CTb	Cholera toxin subunit B	1 mg/ml	N/A	Sigma Aldrich, USA
Evans Blue	Evans Blue dye	2%	N/A	Sigma Aldrich, USA

2.3 Tissue Collection

2.3.1 Cerebrospinal Fluid Sample Collection

Following anaesthesia, an incision was made from the level of the occipital ridge to approximately T3. With the aid of an operating microscope, posterior neck muscles were separated and retracted to expose atlanto-occipital membrane. Once the atlanto-occipital membrane was exposed, a 25-gauge needle (Terumo needle, 25G x 1inch, 0.50x25mm, Terumo, Japan) was used to pierce through the membrane and withdraw cerebrospinal fluid. Once samples were collected, they were stored in a -80 ^{o}C for further biochemical analysis.

2.3.2 Plasma Sample Collection

Following recording of blood pressure and CSF sample collection, the arterial line was used to collect blood samples. Blood samples were collected from the arterial line in 1.7 ml microtubes (1.7 ml microtubes, Axygen, USA), and were then centrifuged (Velocity 14R refrigerated centrifuge, Dynamic Scientific, China) (4^{o}C, 2000 rpm, 30 minutes), to separate blood into a plasma layer, white blood cell layer, and a red blood cell layer. The plasma was then carefully collected from the centrifuged blood sample and was stored in a -80^{o}C for further biochemical assay studies.

2.3.3 Transcardial Perfusion

After the induction of deep anaesthesia (80mg/kg i.p.), animals were transcardially perfusion. Animals were positioned in the supine position in a fume hood. Using a scalpel blade an incision was made from the neck to the pelvis region. The skin was the separated from the muscles around the rib cage. The xiphoid process of sternum was then clamped with a haemostat and was lifted. A midline cut using a large scissor was made, followed by two lateral

cuts. This provided access to the abdomen. The xiphoid process was lifted up again to expose the diaphragm. The diaphragm was cut in a similar way used for gaining access to the abdomen. Two lateral cuts were then made to the diaphragm across all ribs. The diaphragm was the then lifted away to expose the mediastinum. The thymus was then dissected out along with connective tissue surrounding the heart. Heparin (0.2ml, 1000U/ml) was then injected into the left ventricle of the heart to prevent clots. A 15-gauge needle (Terumo needle, 15G x 1inch, 0.50x25mm, Terumo, Japan) was then inserted into the left ventricle and advanced 2-3mm into the ascending aorta. The right atrium was cut, and then 250 ml of 0.1M phosphate buffered saline (PBS) was pumped at 150 mmHg pressure. This was followed by 250 ml of 4% (w/v) paraformaldehyde (PFA), at a perfusion pressure of 150 mmHg.

2.3.4 Brain Collection Tissue

2.3.4.1 Perfused Brains

Following transcardial perfusion the animals were decapitated, and an incision was made to the dorsal surface of the head, from the plane of the eyes all the way to the occipital ridge using a scalpel blade. The skin was then pulled aside and rongeurs were used to remove the muscles that attach to vertebrae and to the occipital ridge. The vertebrae were then carefully removed with rongeurs without causing any damage to the spinal cord or the brainstem. The occipital bone was then carefully removed followed by the removal of the parietal and frontal bones. The dura mater was then peeled off. A thin spatula was then used to sever the cranial nerves. The brain was then placed in 4% PFA solution for four hours at four degrees Celsius. After 4 hours, the brain was transferred into a 20% sucrose solution (w/v in PBS) for 24 hours at 4^{o} Celsius before it was processed for immunohistochemical studies.

2.3.4.2 Fresh Brains

For the series of experiments in anaesthetised rats, the injection site was confirmed at the end of each experiment with 2% Evans blue dye (w/v in PBS) (i.e. injected into the PVN). After that the animal was decapitated the brain was rapidly removed as described above and the forebrain was frozen in powdered dry ice. After the brains were completely frozen, they were wrapped in foil and stored at -80ºC prior to histological processing to confirm the injection sites.

2.3.4.3 Brain Micro-punches

For the serious of experiments involving fluorescence activated cell sorting (FACS), the thorax was crushed under deep anaesthesia, to terminate pumping of blood. This was done by a single blow to the posterior thorax using a metal rod. The animal was quickly decapitated, and the brain was then removed and placed in chilled artificial cerebrospinal fluid (aCSF). The dura was them peeled and the brain was then dissected into a hypothalamic block and a medulla block. These blocks were sectioned in aCSF using a vibratome (Leica Microsystems, Germany) to obtain 1 mm thick sections. Following sectioning, a 1 ml syringe was then filled with aCSF, and with the aid of a microscope, micro-punches of the PVN were obtained from the hypothalamic block, and micro-punches of the AP, and the RVLM were obtained from the medulla block. Micro-punched tissue was then placed in 1.7 ml microtubes (1.7 ml microtubes, Axygen, USA) filled with aCSF. Microtubes were then snap frozen using liquid nitrogen and stored -80ºC for further flow cytometric analysis.

2.3.5 Heart and Kidney Collection

Following transcardial perfusion, the kidneys and the hearts were dissected free from the surrounding tissue. The renal artery, vein, and nephrons were cut to remove the kidneys, and heart great vessels were incised to remove the heart from situ. Both hearts and kidneys were then placed in 10% neutral buffered formalin (Amber Scientific, Australia) at room temperature for further histological analysis.

2.4 Immunohistochemical Studies

2.4.1 Immunofluorescence Labelling

Following the induction of anaesthesia with pentobarbitone sodium (60 mg/kg; i.p); animals were transcardially perfused using 250 ml of 0.1M phosphate buffered saline (PBS) and 250 ml of 4% (w/v) paraformaldehyde (PFA). Brains were then collected and fixed in 4% PFA solution for four hours at 4^{o}C, followed by cryoprotection in a 20% sucrose solution (w/v in PBS) for 24 hours at 4^{o}C. Brains were then coronally sectioned (30 μm) using a cryostat (CM1800, Leica Microsystems, Germany) and transferred into 24 well culture plates (Thermofisher, Denmark) containing 0.1M PBS. Sections were washed and incubated in PBS-0.3% Triton-X 100 on a shaker for fifteen minutes at room temperature, to facilitate antibody penetration. Sections were then incubated in the primary antibodies (see table 2.2 for the list of primary antibodies used in this thesis), for one hour on the shaker at room temperature. Sections were then transferred to a refrigerator (4^{o}C) for 24 hours. On the following day, sections were washed in 0.1 M PBS three times, each time for five minutes on a shaker at room temperature. Sections were then incubated in the secondary antibodies (donkey anti rabbit, mice, goat) at 1:500 (Jackson ImmunoResearch laboratories, INC. USA), for one hour on a shaker at room temperature. After that sections were washed in 0.1 M PBS three times, each time for five

minutes on a shaker at room temperature. Sections were then incubated in streptavidin conjugated with fluorophores (AlexaFluor-488,594,680) at 1:500 (Jackson ImmunoResearch laboratories, INC. USA) for one hour on a shaker at room temperature. Finally, sections were washed in 0.1 M PBS three more times (3 x 5 mins). Sections were then mounted on gel-subbed slides (76 x 26mm; Menzel-Glaser, 50 slides, Germany) and left for 10-15 minutes to dry at room temperature before they were cover-slipped (24 x 50 mm; #1 coverslips, Menzel-Glaser, Germany), using anti-fade mountant (FluoroShield™ mountant containing DAPI; Sigma-Aldrich), and nail polish was used to seal the slides.

Table 2.2: List of all primary antibodies used in all series of experiments presented by this thesis.

Antibody	Description	Species raised in	Dilution	Company
Anti- CTb	Marks neurons that uptake CTb	Goat	1:10,000	Sigma Aldrich, USA
Anti- CCR2	Marks cells expressing CCR2 receptors	Rabbit	1:30,000	Novus Biological, USA
Anti- NeuN	Marks Neurons	Mice	1:1000	Sigma Aldrich, USA
Anti- CD11b	Marks macrophages	Mice	1:1000	Bio-Rad Laboratories, USA
Anti- GFAP	Marks astrocytes	Rabbit	1:10,000	DAKO, USA
Anti- CD8	Marks CD+ T cells	Mice	1:10,000	Bio-Rad Laboratories, USA
Anti- RECA-1	Marks rat's endothelial cells	Mice	1:1000	Bio-Rad Laboratories, USA
Anti- C-Fos	Marks activated neurons	Rabbit	1:5000	Synaptic Systems, Germany
Anti- TH	Marks neurons expressing tyrosine hydroxylase	Rabbit	1:1000	R&D Systems, USA
Anti- nNos	Marks neurons expressing nitric oxide synthase	Rabbit	1:1000	Sigma Aldrich, USA

2.4.1.1 Tyramide Signal Amplification (TSA)

For immunofluorescence where antibodies were raised in the same species, a TSA protocol was used. Firstly, sections were incubated in 0.01% hydrogen peroxide (H_2O_2, 500 ml, Selby Scientific Limited, Victoria), for fifteen minutes on a shaker at room temperature. Sections were washed in 0.1 M PBS two times, each time for ten minutes. Sections were then incubated in the primary antibody (raised in the same species as another primary antibody); at a 10x lower dilution than normally used. The incubation lasted for 24 hours at 4°C. After 24 hours, the sections were washed in 0.1M PBS for ten minutes and in TNT for another ten minutes. After that, sections were blocked with TNB blocking buffer for 30-45 minutes. Sections were then incubated in an HRP-conjugated secondary antibody at 1:500, for 30 minutes on a shaker at room temperature. Sections were then rinsed twice in TNT, each time for twenty minutes. Sections were then incubated in fluorophores tyramide diluted in amplification diluent (TSA™-Plus Fluorescein System, PerkinElmer, Australia) at 1:100 for a maximum of ten minutes at room temperature. Sections were then washed two times in TNT, each time for 20 minutes, and in 0.1 M PBS two times for 20 minutes. Sections were then ready to begin standard immunohistochemistry (with another antibody raised in the same species) as described above.

2.4.2 Histological Analysis of Injection Sites

Tissue was coronally sectioned (40 μm) using a cryostat (CM1800, Leica Microsystems, Germany), and then mounted on gel-subbed slides (76x26mm; Menzel-Glaser, 50 slides, Germany) and left for 10-15 minutes to dry at room temperature. Slides were then incubated in 1% neutral red (Sigma-Aldrich, USA) for five minutes, and washed with water to remove the excess stain. Slides were then incubated serially in ethanol (Chem Supply, Australia); 50%, 70%, 90%, 95%, 100% respectively for one minute in each concentration, to

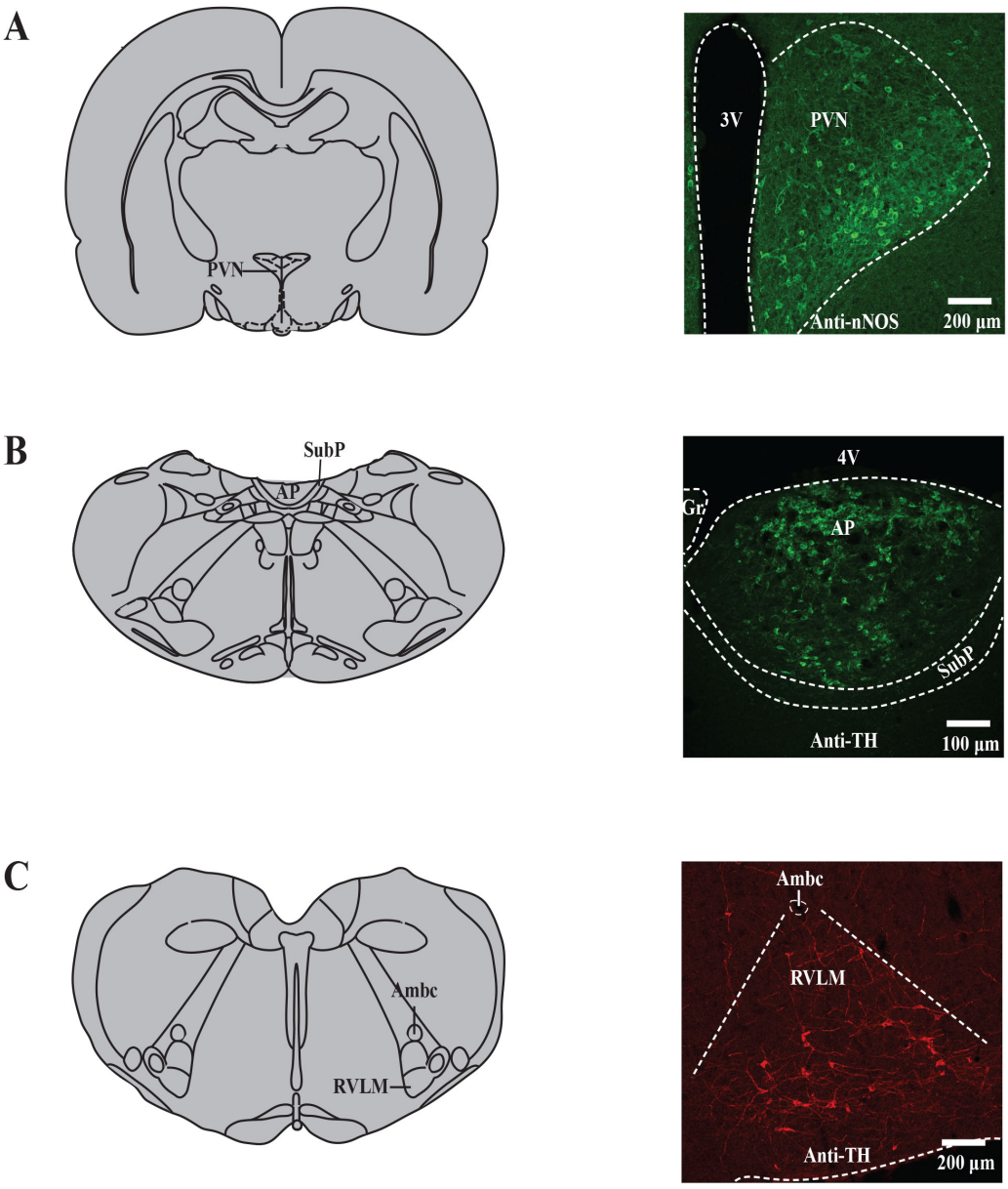
dehydrate the sections. Following dehydration, slides were incubated in histolene (Grade HDS, Australia) for one minute, before slides were coverslipped (24 x 50 mm; #1 coverslips, Menzel-Glaser, Germany), using DePeX (DePeX mounting media, BDH PROLABO, South Africa).

2.4.3 Photomicroscopy and Figure Preparation

The processed sections from microinjections (histological sections) were examined on a Nikon E800 microscope equipped with Nikon CFI plan optics. Photomicrographs were taken with an Olympus digital camera (DP70, Olympus, Japan) using DP Controller software (V2.1.1, Olympus, Japan), saved as JPEG images at 300 dpi resolution. For the immunofluorescence studies, a stereology/fluorescent microscope (Leica DMLB2^{TM}, Leica GmbH, Wetzlar, Germany) was used to examine the sections containing the PVN, AP and RVLM. Images were taken at 1600x1200 pixel resolution and saved as JPEG images using a microfire^{TM} camera in conjunction with PictureFrame software (Optronics, CA, USA). For figure production a confocal laser-scanning microscope (Leica TCS SP8^{TM}; Leica GmbH, Wetzlar, Germany) was used to obtain 1024x1024 pixel resolution images of the PVN, AP and RVLM labelled for CTb, CCR2, NeuN, CD11b, GFAP, RECA-1, C-Fos, CD8, TH, nNos in conjunction with Leica Application Suite Advanced Fluorescence software (LSAF AF version 3.0, Leica GmbH, Wetzlar, Germany). Images were saved as Leica Image files (.lif) then converted into JPEG using FIJI open source image analysis software (NIH, USA). All confocal images were taken at constant settings for each image to allow for post-image capture analysis. All images were post-processed with Adobe Photoshop CS2 (Adobe Systems, Mountain View, CA, USA) either for overlaying channels or converting file types. Other analyses such as cell counting and the addition of scale bars were performed using ImageJ or FIJI (NIH, USA).

2.4.4 Identifying Brain Regions

To identify brain regions such as the PVN, RVLM, and AP, sections were labelled with markers readily expressed by the neurons of the brain corresponding region. Markers for neuronal nitric oxide synthase (nNOS) were used as markers to identify the PVN (Figure 2.5A) (Yamaguchi, Okada et al. 2009). Whereas tyrosine hydroxylase (TH) was used to identify the AP (Figure 2.5B), and the RVLM (Figure 2.5C) (Strack, Sawyer et al. 1989). Once these regions were identified using the above described methods, regions were sampled and examined for other markers used or labelled for in the immunohistochemical experiments.



<u>Figure 2.5:</u> Methodology used to identify different brain regions.

Representative photomicrographs of the PVN labelled with neuronal nitric oxide synthase (nNOS) (**A**), the AP labelled with tyrosine hydroxylase (TH) **(B)**, and the RVLM labelled with TH **(C)**. 3V; third ventricle, 4V; fourth ventricle, Ambc; compact part of the nucleus ambiguus, AP; area postrema, nNOS; neuronal nitric oxide synthase, PVN; paraventricular nucleus of the hypothalamus, RVLM; rostral ventrolateral medulla, SubP; subpostremal area, TH; tyrosine hydroxylase. Schematic diagrams are regenerated from (Paxinos G 2007).

2.4.5 Validation of Immunohistochemistry

To label blood derived monocytes, CD11b was used as a marker for ~~macrophages~~ myeloid-derived cells. CD11b labels both infiltrating myeloid cells (monocytes and macrophages) and resident macrophages (microglia). To distinguish between resident microglia and circulating macrophages, sections were co-labelled with CCR2, as CCR2 receptors are only expressed on circulating macrophages and not resident macrophages (Figure 2.6) (Ataka, Asakawa et al. 2013).

For the validity of the C-Fos staining, nuclear staining by the C-Fos antibody was compared to DAPI nuclear stain. C-Fos is a protein expressed by the nucleus following the activation of a neurons (Dragunow and Faull 1989), therefore C-Fos labelling should be contained in the nucleus and hence confirmed by co-localisation with DAPI nuclear stain (Figure 2.7).

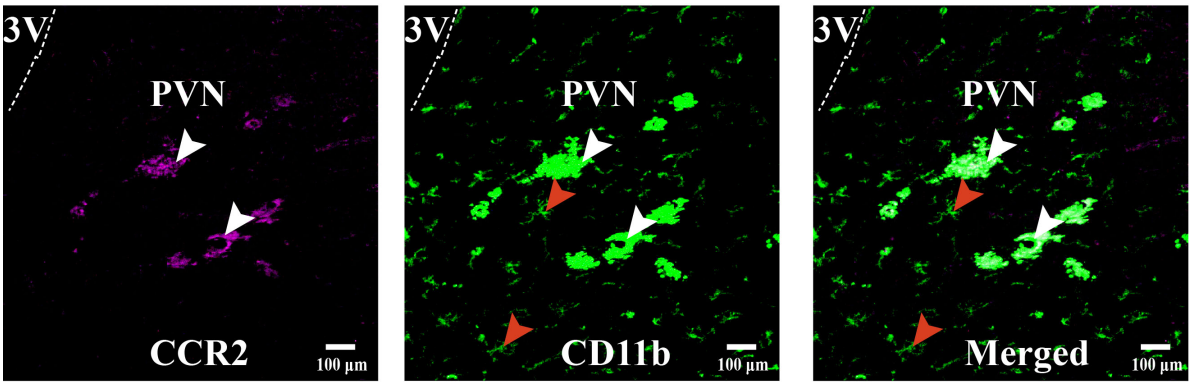


Figure 2.6: Distinguishing circulating macrophages from resident macrophages (microglia).

Representative photomicrographs of the PVN microinjected with CCL2 and labelled with CD11b as a marker for macrophages and CCR2. White arrows represent circulating macrophages infiltrating from circulation into PVN tissue expressing CCR2 receptors, whereas the red arrows represent resident microglia which do not express CCR2 receptors. 3V; third ventricle, PVN; paraventricular nucleus, (Green= CD11b labelled with AlexaFluor-488, Purple= CCR2 labelled with AlexaFluor-680).

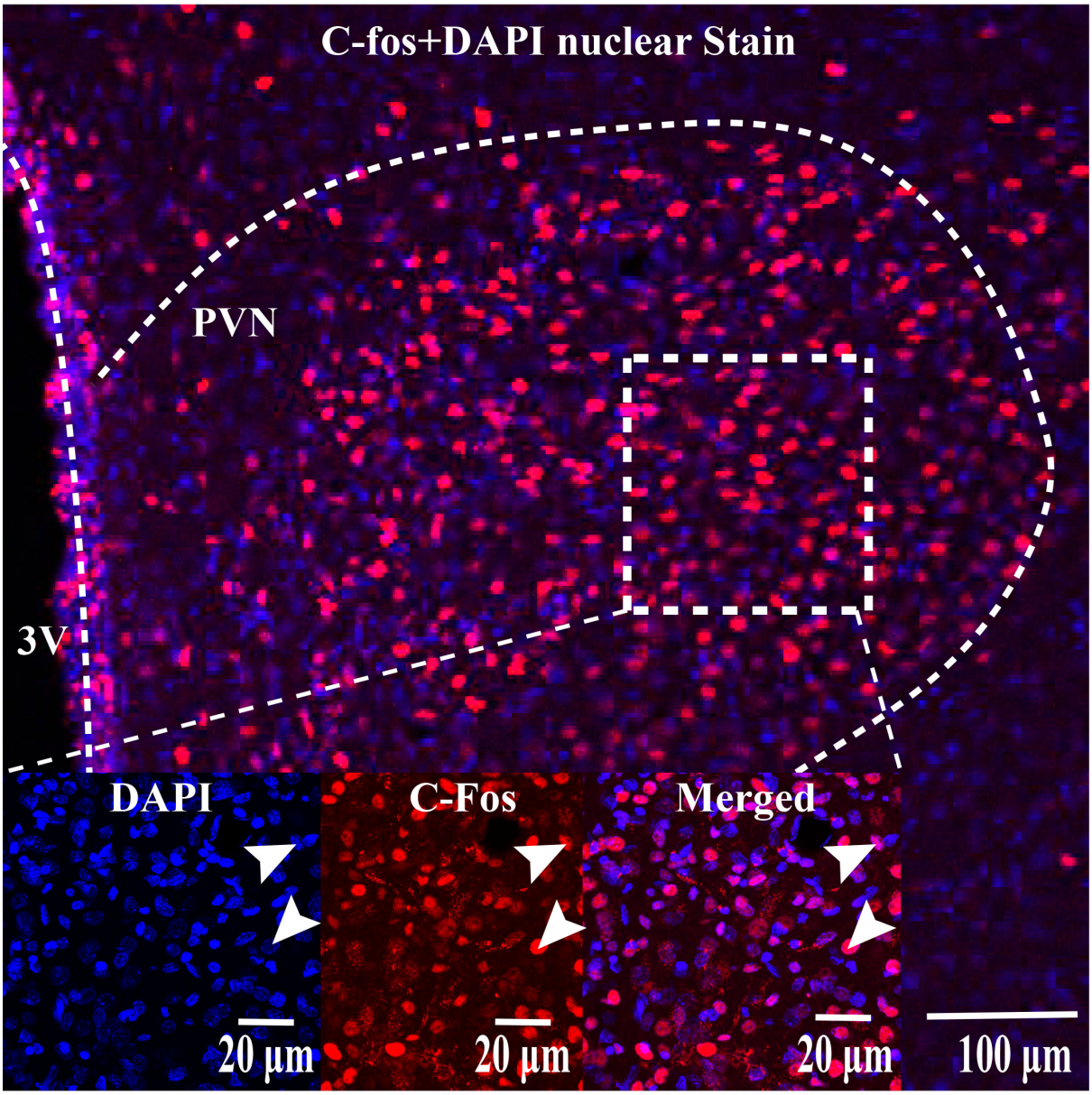


Figure 2.7: Validation of C-fos labelling.

PVN section labelled with C-fos and DAPI nuclear stain, following the microinjection of CCL2 into the PVN. White arrows show an example of a nuclei positive for both C-fos and DAPI, confirming the specificity of the C-fos antibody in labelled the nucleus of activated neurons. PVN; paraventricular nucleus, 3V; third ventricle, (Red= C-Fos labelled with AlexaFluor-594, Blue= DAPI nuclear stain).

2.5 Biochemical Assays

2.5.1 Enzyme-Linked Immunosorbent Assay (ELISA)

Rat MCP-1 Picokine™ ELISA kit (BoosterBio, USA) was used to detect the levels of CCL2 in the plasma and CSF. Samples from both plasma and CSF were diluted at 1:4 in the sample diluent buffer (60 µl of the sample in 180 µl in the diluent buffer). Standard solutions were then made and diluted in the sample diluent buffer at 1000, 500, 250, 125, 62.5, 31.2, 15.6 pg/ml. The samples and the 7 standard solutions, were then aliquoted at 0.1 ml in a 96-well plate pre-coated with anti-rat MCP-1 antibody, leaving two blank wells. Samples and standard solutions were run in duplicates. The plate was then sealed with an adhesive cover and incubated at 37°C for 90 minutes. Plate content was then discarded, and 0.1 ml of biotinylated anti-rat MCP-1 antibody (1:100) was aliquoted into each well and incubated at 37°C for 60 minutes. Plate content was then discarded, and the plate was then washed with 0.01M PBS 3 times. After that, 0.1 ml of ABC working solution (Avidin-Biotin-Peroxidase, 1:100) was aliquoted into each well and incubated at 37°C for 30 minutes. Plate content was then discarded, and plate was washed 5 times in 0.01M PBS. Each well was then incubated in 90 µl of TMB colour in the dark at 37°C for 20 minutes. Finally, a 0.1 ml of TMB stop solution was aliquoted into each well, and the plate was immediately taken to a microplate spectrophotometer reader (Bio-Rad, USA), and read at 450 nm. Optical densities obtain from the plate (including standard solutions, samples, and blank wells), were then transferred into a template (available at www.ELISAanalysis.com), were the concentration of MCP-1 in each well was determined from the standard solution curve. Final concentrations were then multiplied by the dilution factor.

2.5.2 Flow Cytometry

Punches of the PVN, AP, and RVLM were mechanically digested using a blade to mince the tissue. Minced tissue was then placed in chilled 0.1 mol/L PBS and centrifuged for 20 minutes (4^{o}C; 220 rpm). The supernatant was discarded, and 1 ml of digestive enzyme cocktail was added (TrypLE Express; Life Technologies Corporation, USA, and Liberase TL Research Grade; Roche, Germany), and incubated at 37^{o}C for 30 minutes. The suspension was then centrifuged (4^{o}C; 950 rpm), supernatant was discarded, and the pellet was resuspended in 600 µl of 0.1 mol/L PBS. Cell suspension was then filtered through a 70 µm cell strainer. Conjugated antibodies at 1:200 (Mice anti-Rat CD45-APC/Fire750; Biolegend, mice anti-rat CD11b-PE/CY5; Abcam, mice anti-rat CD3-BV421; Biosciences) were then added to the suspension and incubated for 30 minutes before samples were analysed using a CytoFlex S analyser (Beckman Coulter, USA). Total events in flow cytometry were 100,000 events. Events were firstly plotted on a forward scatter by area (FSC-A), against a side scatter by area (SSC-A). A region identified as region containing white blood cells was gated and plotted on a forward scatter by area (FCS-A) against a forward scatter by height (FCS-H), were single cells were then gated. Events highly positive for $CD45^{+hi}$ (hematopoietic cell marker) were then gated and plotted for their expression of $CD11b^{+}$ events (macrophages), against $CD3^{+}$ events (T lymphocytes). An FCS Express 6 Flow software was then used to quantify $CD45^{+hi}CD11b^{+}$ events (macrophages) and $CD45^{+hi}CD3^{+}$ events (T lymphocytes). The protocol was adapted and modified from a previously published report on single cell isolation and FACS from brain tissue (Pösel, Möller et al. 2016). Viability of the cell suspension isolated from the PVN, AP, and RVLM was validated using DAPI nuclear stain (Figure 2.8). Validity and specificity of the antibodies used in this protocol, and $CD45^{+hi}CD11b^{+}$ / $CD45^{+hi}CD3^{+}$ events were confirmed using a whole white blood sample isolated from rat blood (Figure 2.9). Validation from the

whole white blood sample was compared to a PVN sample and was used as a template for the experiments (Figure 2.10).

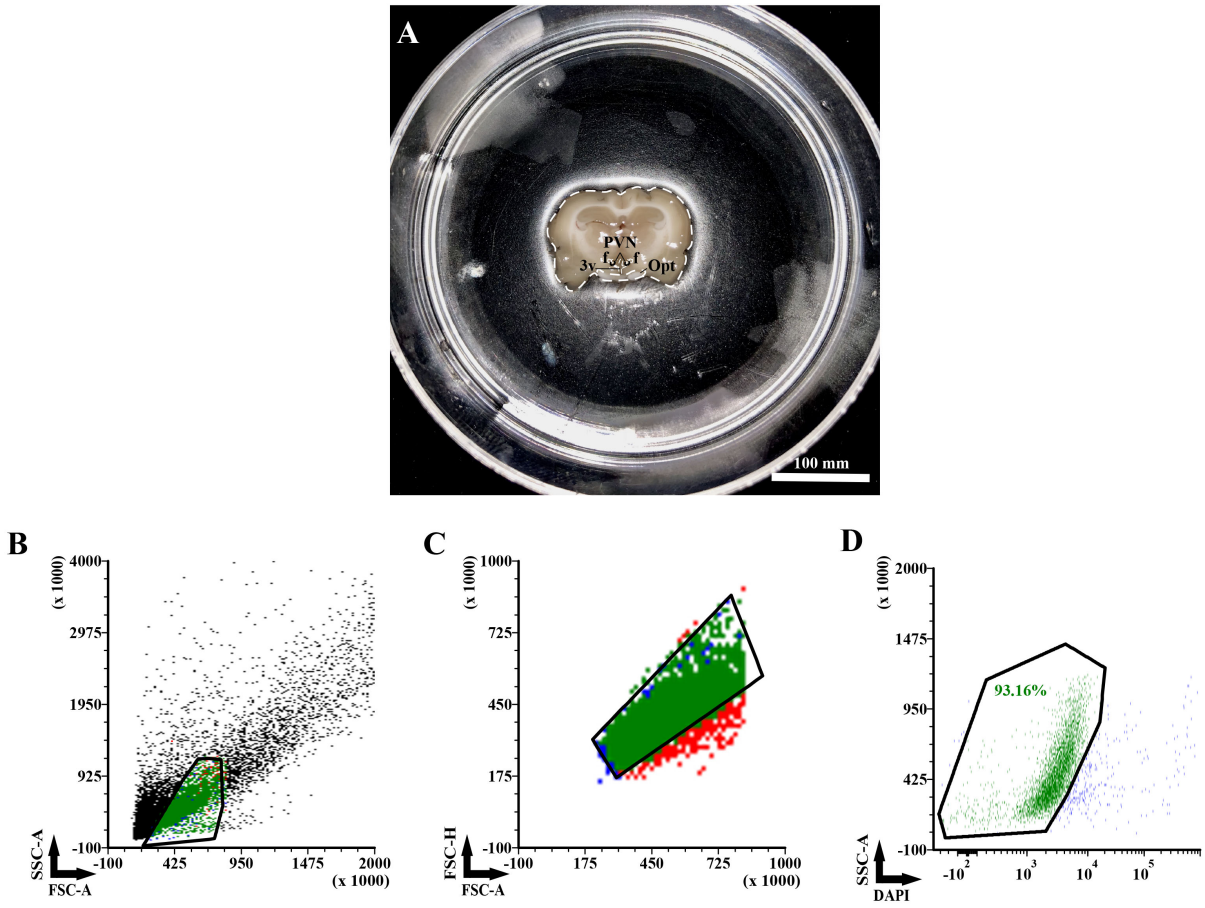


Figure 2.8: Viability of single cell suspension isolated from the PVN.

(A) Representative image of micro-punches obtained from the PVN. **(B-D)** Representative flow cytometry charts of PVN tissue; showing percentage of events negative for DAPI (viable cells) in the sample; total flow cytometry events; 100,000. 3v; third ventricle, f; fornix, Opt; optic chiasm, PVN; paraventricular nucleus of the hypothalamus.

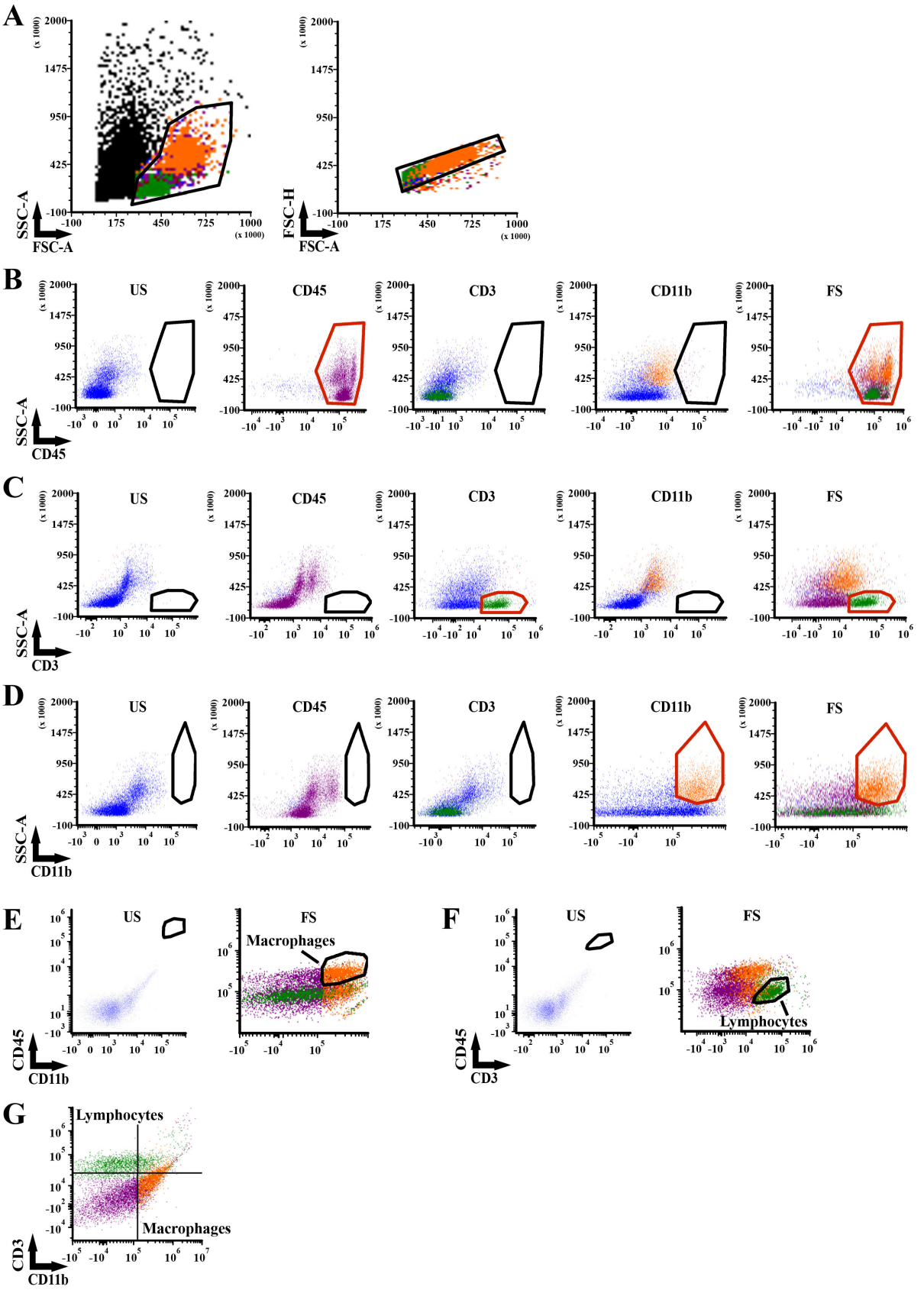
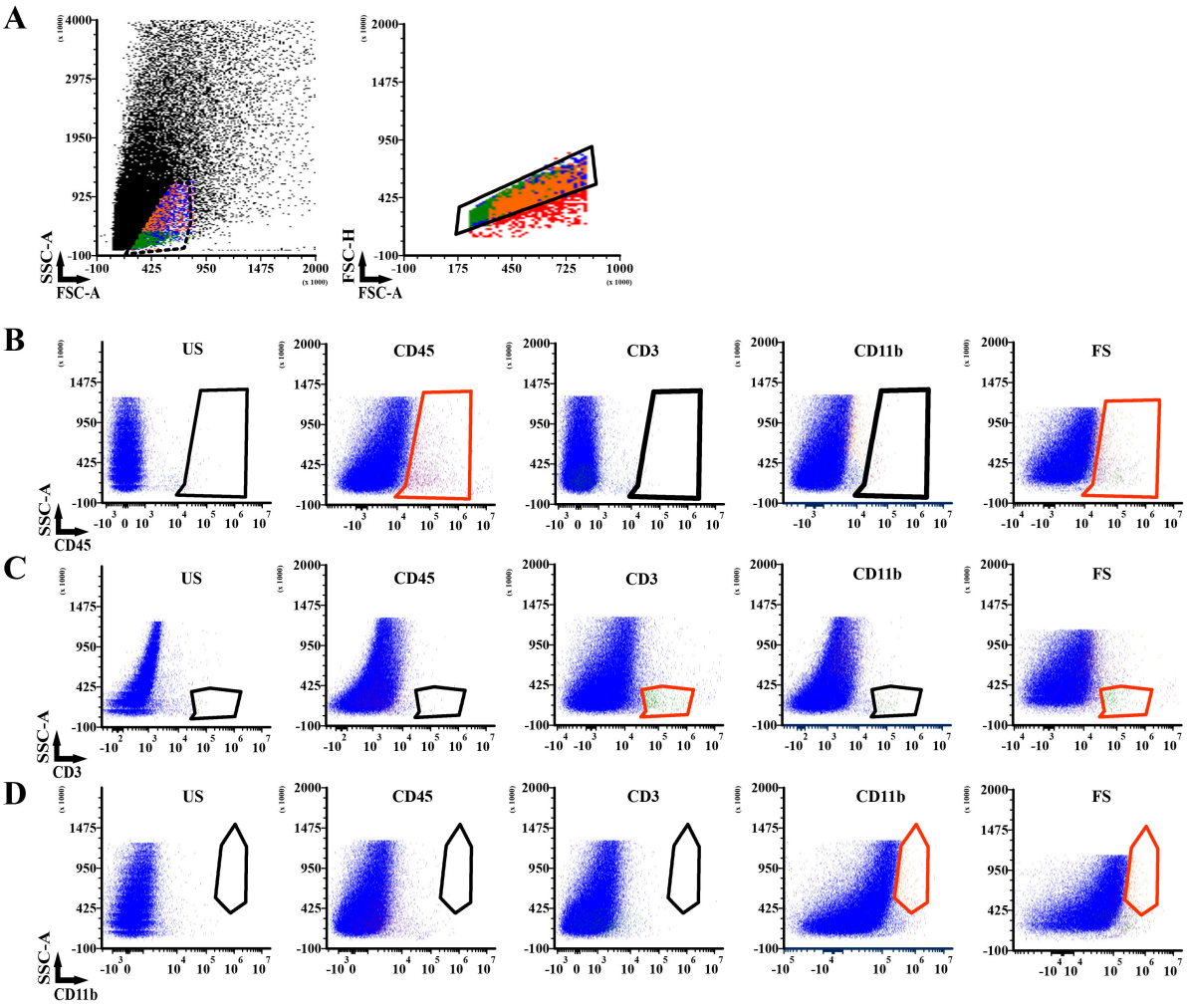

A
SSC-A
FSC-A
FSC-H
FSC-A
B
US
CD45
CD3
CD11b
FS
SSC-A
CD45
C
US
CD45
CD3
CD11b
FS
SSC-A
CD3
D
US
CD45
CD3
CD11b
FS
SSC-A
CD11b
E
US
FS
Macrophages
CD45
CD11b
F
US
FS
Lymphocytes
CD45
CD3
G
Lymphocytes
Macrophages
CD3
CD11b

Figure 2.9: Validity of flow cytometry antibodies using a whole white blood sample.

Representative flow cytometry charts of a whole white blood sample, with samples labelled with only a single antibody **(B-D)**; showing a specific shift for only that antibody. **(E-G)** Fully stained white blood samples; showing specific shifts for macrophages and monocytes. US; unstained sample, FS; fully stained sample. Total events by flow cytometry; 100,000 events.



<u>Figure 2.10:</u> Validity of flow cytometry antibodies and positive events in the PVN.

Representative flow cytometry charts of samples labelled with only a single antibody **(B-D)**; showing a specific shift for only that antibody. US; unstained sample, FS; fully stained sample. Total events by flow cytometry; 100,000 events.

2.6 Experimental Protocols

2.6.1 Hypertensive Animal Experimental Series

Anaesthesia was induced by ketamine/medetomidine (75 mg/kg; 0.5 mg/kg), and the left renal artery was clipped. Following induction of the kidney clip (2K1C model), animals were divided into 2 groups (sham controls and 2K1C) to allow hypertension to be developed over their respective periods. The time points were one week, two weeks, and four weeks; based on previous studies showing the development of blood pressure elevation in the 2K1C model by the third-fourth week after the kidney clip induction (Oliveira-Sales, Toward et al. 2014, Oliveira-Sales, Colombari et al. 2016). Once each group reached the respective time point, animals were firstly anaesthetized, and the femoral artery was cannulated, tunnelled subcutaneously and externalized at the base of the neck. Following a four-hour recovery period, blood pressure was then recorded consciously for 15 minutes. Animals were anaesthetized to obtain CSF and plasma samples for further biochemical assay analysis. At the end of the protocol animals were either perfused for brain collection for further immunohistochemical studies or culled for fresh brain tissue collection for flow cytometry studies. Hearts and kidneys were also collected and weighed (Figure 2.11 & 2.12). SHR and WKY followed a similar protocol to animals in the 2K1C study, once they were acclimatized.

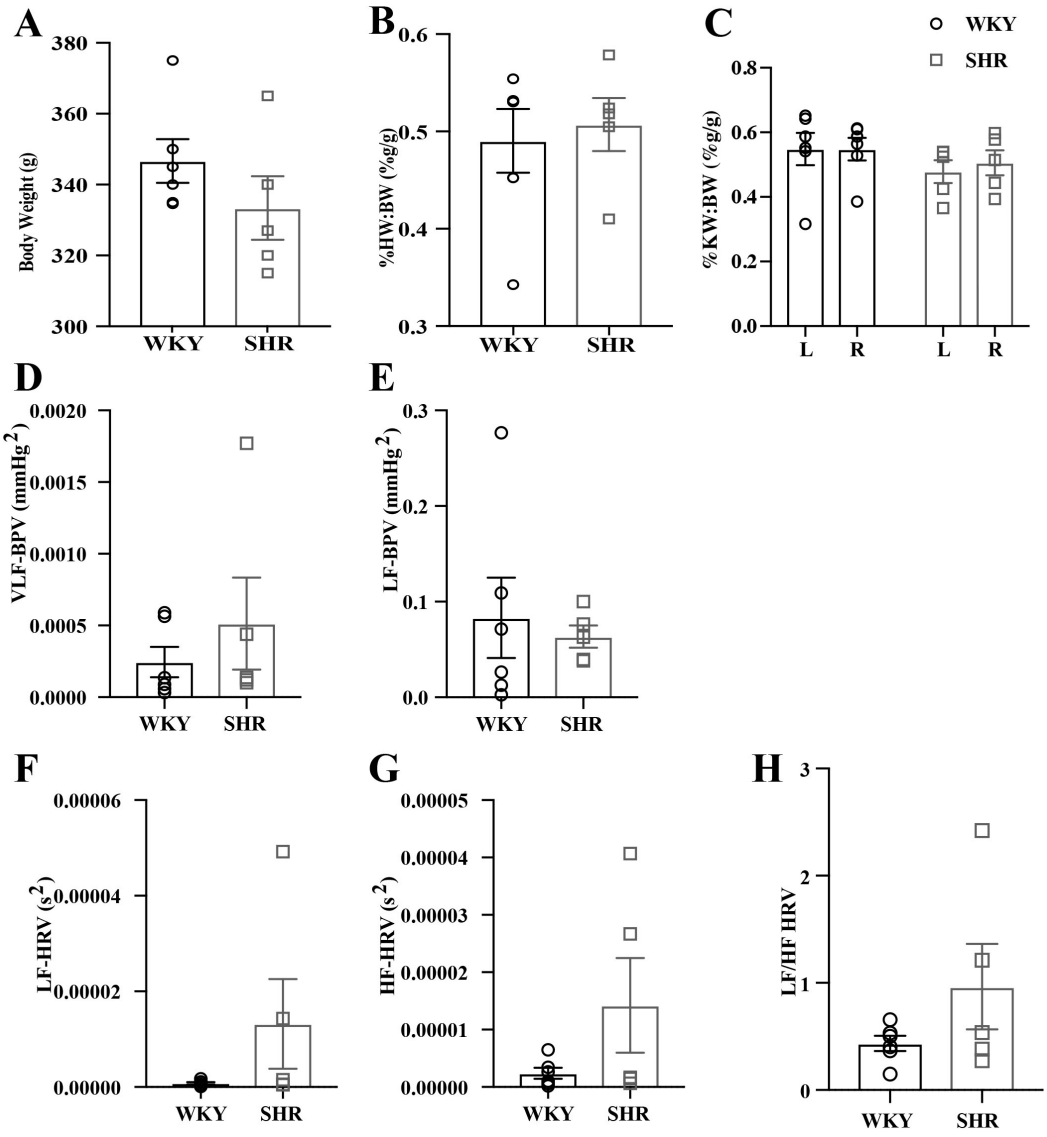


Figure 2.11: Body, heart, and kidney weights, and spectral analysis of the primary model of hypertension.

Average body weights **(A)** heart weight to body weight ratio, **(B)** and left and right kidney weight to body weight ratio. **(C)** Spectral frequency analysis of very low frequency of blood pressure variability, **(D)** low frequency of blood pressure variability **(E)**, low frequency of heart rate variability, **(F)** high frequency of heart rate variability **(G)**, ratio of low frequency to high frequency heart rate variability **(H)**. Student's t-test of SHR vs. WKY; $p>0.05$ (n=5 rats per group).

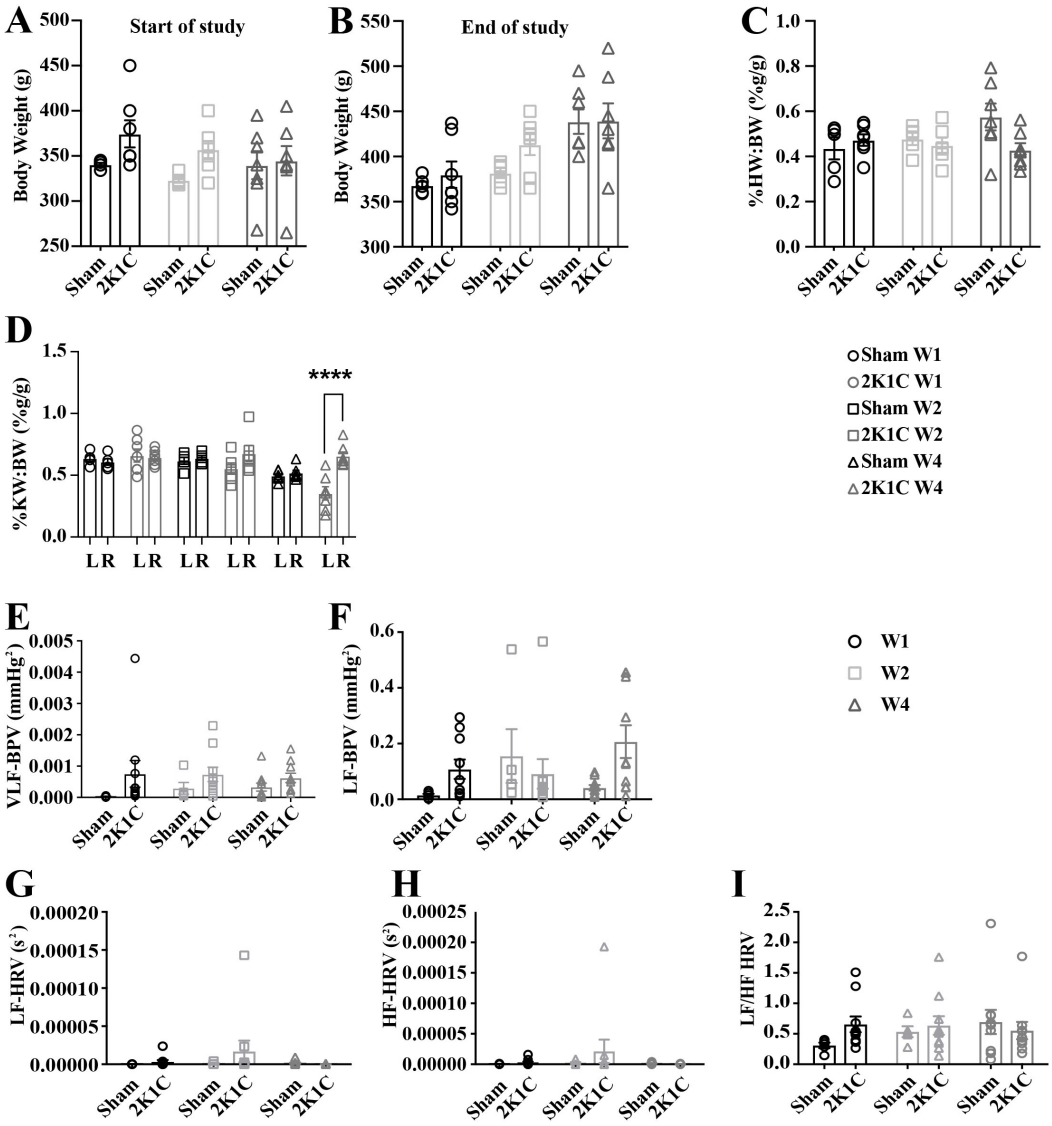


Figure 2.12: Body, heart, and kidney weights, and the spectral analysis of the renovascular model of hypertension.

Average body weights **(A-B)** heart weight to body weight ratio, **(C)** and left and right kidney weight to body weight ratio. **(D)** Spectral frequency analysis of very low frequency of blood pressure variability, **(E)** low frequency of blood pressure variability **(F)**, low frequency of heart rate variability, **(G)** high frequency of heart rate variability, **(H)** ratio of low frequency to high frequency heart rate variability **(I)**. Two-way ANOVA of Left kidney (L) vs right kidney (R); $p<0.0001$ (n=5-10 per group).

2.6.2 Anaesthetized Animals Experimental Series

Anaesthesia was induced by sodium pentobarbitone (60mg/kg intraperitoneally; Troy Laboratories Pty Ltd, Australia). Following femoral cannulation and implantation of electrodes for recording renal sympathetic nerve activity recording, the PVN was microinjected with: (1) different doses of CCL2 (3.5 nM, 7.0 nM, 14.0 nM, 35.5 nM, 71.0 nM) (2) Saline (0.9% NaCl), (3) DMSO (33.7% w/v), (4) RS-102895 (70 μM), (5) Suramin (10 mM) (6) Diclofenac (5 mg/kg), while MAP, HR, RSNA, were simultaneously recorded. At the end of each experiment, the PVN was microinjected with 2% Evan's blue dye to mark the injection sites, animals were culled, and brains were collected for further histological analysis. All microinjections in the PVN of anaesthetized animal experimental series had a volume of 50 nl.

For intracerebroventricular (ICV) microinjections, the lateral ventricle was microinjected with (1) CCL2 (71 nM) or (2) Saline (0.9% NaCl), while MAP was simultaneously recorded. At the end of each experiment, the thorax of the animal was crushed, animals were culled, and micro-punches were collected for further flow cytometric analysis. All microinjections in the lateral ventricles of anaesthetized animal experimental series had a volume of 1 μl.

2.6.3 Conscious Animal Experimental Series

Firstly, a guide cannula was implanted above the PVN and animals were allowed to recover for five days. After recovery, the femoral vessels were cannulated and the cannulae externalized, and animals were allowed to recover for one day. Finally, animals were injected with CCL2 (35.5 nM) or saline (0.9% NaCl) using a Hamilton syringe. Ninety minutes after the injection, animals were anaesthetized with pentobarbitone sodium (60 mg/kg; i.p) perfused, and the brain was collected for further immunohistochemical analysis. All microinjections in the PVN in the conscious animal experimental series were made at a volume of 1 μl.

2.6.4 Tracer Study

Following the microinjection of the RVLM with CTb (1 mg/ml), animals were allowed to recover for approximately seven days; which also allows CTb to be retrogradely up taken by neurons projecting to the RVLM. Animals were then transcardially perfused and brain tissue was sectioned at 30 μm. Immunohistochemistry was then performed labelling for CTb and other markers such as CCR2 and GFAP. All RVLM microinjections in the conscious animal experimental series had a volume of 10 nl.

2.6.5 Antagonizing CCR2 in Hypertensive Animal Experimental Series

Anaesthesia was induced by ketamine/medetomidine (75 mg/kg; 0.5 mg/kg), and radiotelemetry transmitters were implanted. Following radio-telemetry transmitter implants; animals were left to recover for seven days. Following recovery, animals were subjected to either kidney clipping or Sham surgery. Kidney clipped animals were then divided into two groups where one group received an infusion of RS-102895 (70 μM) or vehicle (aCSF), into the lateral ventricle; via an osmotic minipump implant (2.5 μl/hour, 28 days, Alzet, USA). The three groups; sham, 2K1C-Veh, and 2K1C -RS102895 were then allowed to rest at the animal house for a period of eight weeks, while blood pressure was simultaneously recorded. At the end of the infusion period, animals were anaesthetized, plasma and CSF samples were collected, then animals were transcardially perfused and brains, hearts and kidneys collected.

2.7 Statistical Analysis

Blood pressure, heart rate, renal sympathetic nerve activity, and spectral analysis were acquired using Spike 2 (v7.16; Cambridge Electronic Design, Cambridge, UK) data acquisition system, whereas all immunohistochemical analysis were performed using ImageJ or FIJI (NIH, USA). The values from analyses were then transferred into an excel data sheet (Microsoft Corp, WA, USA), before they were transferred into GraphPad Prism 7 (Graphpad Software INC., CA, USA) for statistical analysis. All parametric statistical analyses were performed using student's t-test, one-way, or two-way ANOVA, with the Bonferroni correction. All data is represented as mean ± SEM. $P<0.05$ was used to determine statistically significant differences.

2.7.1 Physiological Responses Analysis

2.7.1.1 Blood Pressure, Heart Rate, and Renal Sympathetic Nerve Activity

Mean arterial pressure (MAP) was acquired from the raw pulse arterial pressure channel using a custom (hal.s2s) script. Whereas neurograms from renal sympathetic nerve activity (RSNA), were quantified by rectifying and time-averaging the signal using 1 second constant, followed by subtraction of the noise level (0%), and normalization adopting 100% as baseline.

For the anaesthetized animal experimental series, MAP and RSNA were averaged at 30 second intervals, 2 minutes prior to microinjections, during the microinjection, and 10 minutes after the microinjection. Data was then averaged across time and compared between different treatments, and a two-way ANOVA was used to obtain statistical significance of $P<0.05$.

For the conscious animal experimental series, MAP was averaged at 60 second intervals, 10 minutes prior to microinjections, during the microinjection, and 50 minutes after the microinjection. Data was then averaged across time and compared between different treatments, and a two-way ANOVA was used to obtain Statistical significance of $P<0.05$.

For the hypertensive animal experimental series, MAP, DBP, SBP, and HR acquired across the 15-minute recording period was averaged, and data was then compared between different time groups, and a two-way ANOVA was used to obtain Statistical significance of $P<0.05$.

For the series of experiments where CCR2 was blocked in hypertensive rats, MAP was acquired through a 24-hour recording twice a week. The 24-hour recording allowed acquiring of the light and the dark cycle. Analysis was performed on recordings from 2, 3, 4 ,5 pm for the light cycle, and 2, 3, 4,5 am for the dark cycle. Values of MAP, DBP, SBP, and HR were averaged for one light cycle and one dark cycle. Data was then compared between different time groups, and a two-way ANOVA was used to obtain Statistical significance of $P<0.05$.

2.7.1.2 Spectral Analysis

Spectral analysis method was adapted from (Oliveira-Sales, Toward et al. 2014, Oliveira-Sales, Colombari et al. 2016) and acquired using Spike 2 (v7.16; Cambridge Electronic Design, Cambridge, UK). Spectral analysis was used to determine heart rate variability (HRV) and blood pressure variability (BPV). The time difference between peaks of each wave was used to calculate for HRV, and value difference between peaks of each wave was used to calculate for BRV. For HRV low frequency bands (LF) represent sympathetic drive to the heart, and high frequency bands (HF) represent both sympathetic and parasympathetic drive to the heart. Whereas for BPV, very low frequency bands (VLF) represent hormonal vasomotor drive to vasculature, and LF bands represent sympathetic vasomotor drive to the vasculature.

2.7.2 Immunohistochemical Analysis

All immunohistochemical analysis including; counting C-fos nuclei, CTb positive cells, TH neurons, CD11b/CD8 positive cells, were performed in FIJI (NIH, USA) using a multipoint tool. Data was then averaged and compared between different groups/treatments; and a one-way ANOVA was used to obtain statistical significance of $P<0.05$ (unless otherwise stated in the thesis).

2.7.2.1 Microglia Quantification & Skeleton Analysis

For quantification of microglial activation in different brain regions two different previously described methods were used; including a manual and a semi-automated quantification technique. All microglial quantification and analysis were performed in FIJI (NIH, USA). The first method of microglial activation quantification is previously described and validated in the literature (Rana, Stebbing et al. 2010, Shi, Diez-Freire et al. 2010). This method relies on the morphology of the microglia; as resting/quiescent microglia tend to have longer and many processes/branches, whereas activated/ramified microglia tend to have retracted and less processes/branches (Figure. 2.13). For this method; a multipoint tool is used in FIJI, which allows the quantification of microglia and potentially activated microglia in a specific region. A percentage of the number of activated microglia/total number of microglia is then determined.

The second methods is a skeleton analysis script in FIJI, described by (Morrison and Filosa 2013). In brief, an image is firstly converted into an 8-bit binary image and then thresholded. A skeleton function in FIJI is then run on the image, where all microglia in the image is converted into a skeleton figure, where each skeleton represents single microglia with all its process/branches. Finally, an analyse skeleton function is then run on the skeletonized image, where the analysis counts each individual skeleton, the total number of branches, and

the average process/branch length (Figure 2.14). Data was then averaged and compared between different groups/treatments; and a one-way ANOVA was used to obtain statistical significance of $P<0.05$.

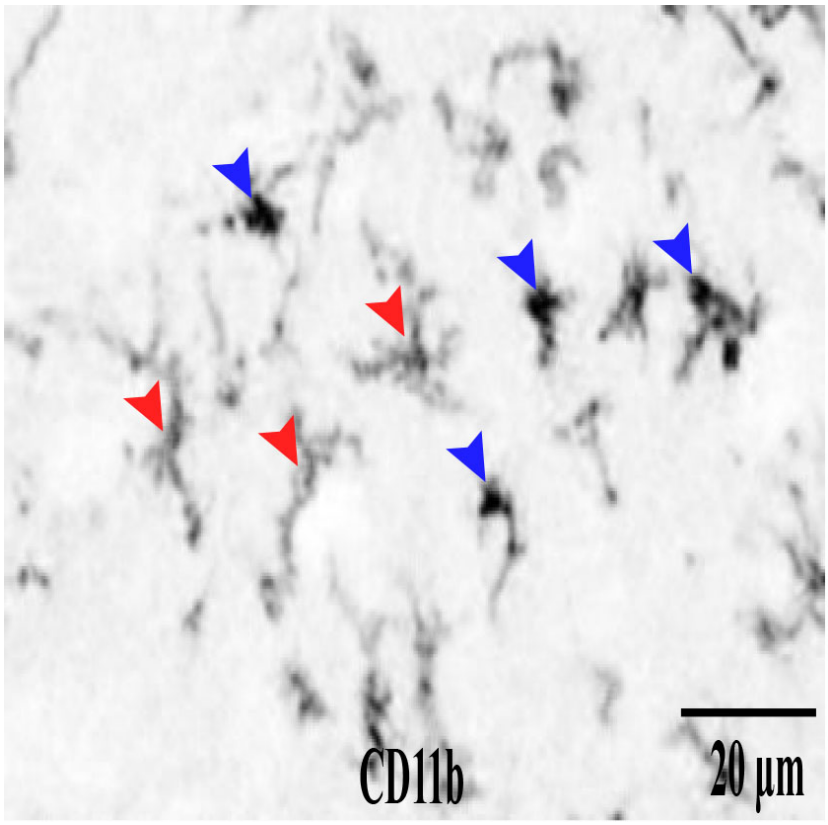


Figure 2.13: Morphology of resting and activated microglia.

Representative high-power photomicrograph taken of microglia labelled with CD11b from PVN section of a hypertensive animals. Red arrows show the morphology of resting microglia; where the cell is large with many long processes. Blue arrows show the morphology of activated microglia; where the cell is small with retracted and fewer process.

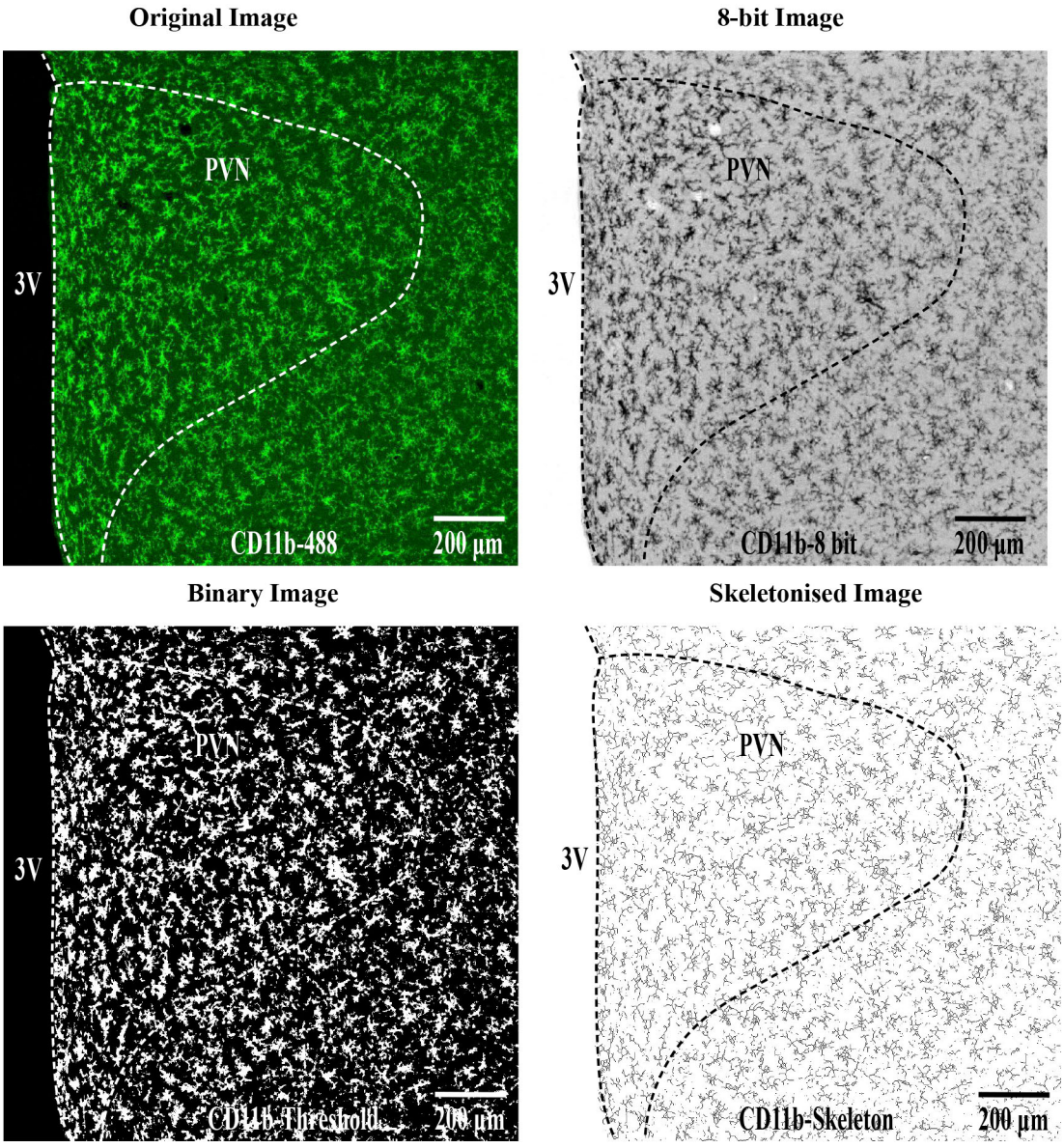


Figure 2.14: Skeleton analysis for microglia.

Skeletal analysis used for microglial activation quantification in this thesis. Firstly, the image is acquired through a confocal microscope, and is then converted into an 8-bit image in FIJI. The image is then thresholded to convert to a binary image, where a skeleton script is then run on the image to skeletonise each microglia in the image. 3v; third ventricle, PVN; paraventricular nucleus of the hypothalamus.

3. Chemoattraction of Immune Cells via CCL2-CCR2 signalling into the Hypothalamic Paraventricular Nucleus Drives Sympathetic Nerve Activation and Causes Hypertension

Remark: This chapter is being submitted for publication by *Circulation Research*.

3.1 Abstract

Rationale: Recruitment of activated immune cells to autonomic brain regions is linked to neural inflammation in hypertension. In rodent models of hypertension, immune cells infiltrate the paraventricular nucleus of the hypothalamus (PVN); and CCL2, a pro-inflammatory chemokine involved in activating and recruiting immune cells, is increased by 3-fold in the PVN of these animals. However, how recruitment of immune cells to the PVN regulates sympathetic outflow and blood pressure (BP), in hypertension, is unclear.

Objective: To determine whether CCL2- mediated immune cell recruitment into the PVN elicits sympathetically-mediated elevations in BP during hypertension.

Methods and Results: The quantity of immune cells, measured by flow cytometry, in the PVN was greater in both a primary and a secondary rat models of hypertension. Furthermore, plasma and cerebrospinal fluid CCL2 levels and immune cell recruitment in the PVN were elevated in renovascular pre-hypertensive rats. In anaesthetized rats, CCL2 recruited immune cells to the PVN and elicited dose-dependent increases in renal sympathetic nerve activity (RSNA) and BP. The BP increase in response to CCL2 was also observed in conscious freely-moving rats.

Conclusions: Upregulation of CCL2 and immune cell infiltration to the PVN evokes sustained increases in RSNA and BP in hypertension.

Key words: CCL2, immune cells, neuroinflammation, blood pressure, sympathetic nerve activity, paraventricular nucleus, hypertension.

3.2 Introduction

Sympathetic nerve activity (SNA) is elevated in human hypertension (Smith, Graham et al. 2004). In both hypertensive humans and animal models of hypertension, SNA is increased before blood pressure (BP) (Mancia and Grassi 2014, Oliveira-Sales, Colombari et al. 2016). Regulation of SNA involves autonomic brain regions including the paraventricular nucleus of the hypothalamus (PVN), which communicates with the sympathetic nervous system and cardiovascular organs via direct neural projections and neuro-humoral mechanisms, respectively (Strack, Sawyer et al. 1989). In fact, magnetic resonance imaging of hypertensive rats demonstrates an increase in neuronal activity in the PVN (Zubcevic, Santisteban et al. 2017). Hence, establishing the underlying central (PVN) mechanisms that contribute to neurogenic hypertension is essential to better understand the pathophysiology of this disease.

Inflammation in the PVN plays an important role in the development and establishment of hypertension (Sharma, Yang et al. 2019). Pro-inflammatory cytokines, including tumour necrosis factor alpha (TNF-α), and interleukin 1 beta (IL-1β), are upregulated within the PVN in animal models of hypertension (Shi, Diez-Freire et al. 2010, Shen, Li et al. 2015). When these cytokines are microinjected into the PVN, arterial pressure, and renal and cardiac SNA are increased (Shi, Gan et al. 2011). Recently, it has been suggested that the immune system plays a key role in increasing brain inflammation and subsequently neural activity in hypertension (Zubcevic, Santisteban et al. 2014, Zubcevic, Santisteban et al. 2017, Elsaafien, Korim et al. 2019). Interestingly, depletion of peripheral immune cells derived from bone marrow reduced neural inflammation in animal models of hypertension (Santisteban, Ahmari et al. 2015). Furthermore, immune cell infiltration is associated with upregulation of pro-inflammatory cytokines in the PVN (Wang, Kang et al. 2018). There is evidence that the chemokine C-C motif chemokine ligand 2 (CCL2) activates and recruits immune cells (Ajuebor, Flower et al. 1998, Lu, Rutledge et al. 1998), and is upregulated in the

bone marrow, plasma, cerebrospinal fluid (CSF), and the PVN of hypertensive animals (Santisteban, Ahmari et al. 2015, Wang, Kang et al. 2018, Ahmari, Santisteban et al. 2019). In the PVN of hypertensive animals, it is reported that the CCL2 is increased by approximately 3-fold (Wang, Kang et al. 2018). However, whether the recruitment of immune cells by CCL2 into the PVN contributes to the increases SNA and BP in hypertension remains to be elucidated.

In the present study, we hypothesize that CCL2 excites rostral ventrolateral medulla-projecting PVN neurons indirectly via recruitment of immune cells to increase SNA and BP leading to and sustaining hypertension. Using a combination of *in vivo* electrophysiology, neuropharmacological, histological, anatomical, and biochemical techniques we determined: (1) the temporal profile of CCL2 upregulation and immune cell recruitment to the PVN throughout the development of renovascular hypertension; (2) whether recruitment of immune cells to the PVN by CCL2 increases SNA and BP; and (3) the underlying molecular and neural mechanisms driving these increases. We believe that the findings here support the current "neuro-immune axis" theory for the development of hypertension (Zubcevic, Santisteban et al. 2014, Zubcevic, Santisteban et al. 2017, Elsaafien, Korim et al. 2019).

3.3 Methods and Materials

The authors declare that all supporting data in the article and supplement are available from the corresponding author upon reasonable request.

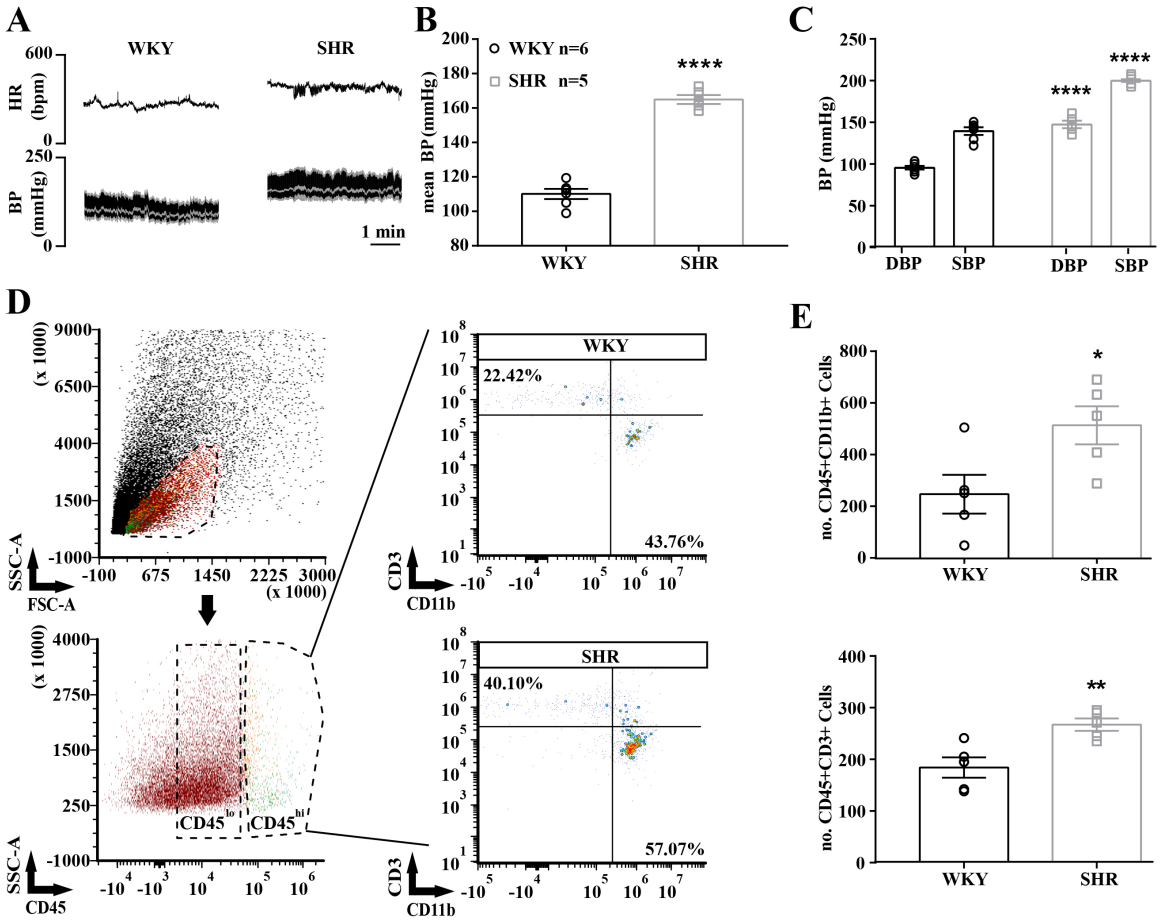
Experiments were approved by the Animal Ethics Committee of the Florey Institute of Neuroscience, which adhered to the Australian Code for the Care and Use of Animals for Scientific Purposes. All animals were housed in a temperature-controlled room (22 ± 2 ˚C) with a 12:12-hour light-dark cycle and had free access to food and tap water. Induction of hypertension in the renovascular model was as previously described (Korim, Elsaafien et al. 2018). Blood pressure (BP) was recorded in primary and secondary models of hypertension and their respective controls, prior to being euthanized for the collection of tissue for analysis. In anaesthetized animals, BP was recorded through femoral cannulation, and renal sympathetic nerve activity (RSNA) was recorded using a bipolar silver hook electrode, both procedures have been previously described (Korim, Elsaafien et al. 2018). All PVN microinjections were made in a volume of 50 nl. Values are expressed as mean ± SEM, and data were analyzed using parametric statistics, where $P<0.05$ was considered statistically significance. Full details of all experimental parameters are described in chapter 2.

3.4 Results

3.4.1 Immune Cell Profile in the PVN of a Primary Rat Model of Hypertension

Spontaneously hypertensive rats (SHR) exhibited higher mean blood pressure (mean BP; 110±3 vs. 165±3 mmHg, $p<0.05$, n= 5-6), diastolic blood pressure (DBP; 96±2 vs. 148±4 mmHg, WKY vs. SHR respectively, $p<0.05$, n= 5-6), and systolic blood pressure (SBP; 140±5 vs. 200±2 mmHg, WKY vs. SHR respectively, $p<0.05$, n= 5-6), in comparison with their, control, Wistar Kyoto (WKY) counterparts (Figure 3.1A-C).

Flow cytometric analysis of SHR PVN showed elevations in the number of immune cells in comparison with WKY (Figure 3.1D-E). The number of $CD45^{+hi}CD11b^{+}$ cells was higher in the PVN of SHR (247±75 vs. 514±74 cells, WKY vs. SHR respectively, $p<0.05$, n=5; Figure 3.1E). Similarly, $CD45^{+hi}CD3^{+}$ cell (lymphocytes) count was greater in the PVN of SHR (184±20 vs. 267±12 cells, WKY vs. SHR respectively, $p<0.05$, n=5; Figure 3.1E). Regression analysis showed that the number of $CD45^{+hi}CD11b^{+}$ cells in the PVN was positively correlated with mean BP ($r^2= 0.412$, $p<0.05$, n=10) or SBP ($r^2= 0.554$, $p<0.05$, n=10; Supplementary Figure 3.1). Similarly, a positive correlation was found between the number of PVN $CD45^{+hi}CD3^{+}$ cells and mean BP ($r^2= 0.588$, $p<0.01$, n=10) or SBP ($r^2= 0.517$, $p<0.05$, n=10; Supplementary Figure 3.1). Together, these results support the hypothesis that in a model of primary hypertension, immune cells are activated, recruited and infiltrate into the PVN.



<u>Figure 3.1:</u> Immune cells are activated and recruited to the paraventricular nucleus of the hypothalamus (PVN) in hypertension.

(A) Representative recordings of heart rate (HR) and pulsatile blood pressure (BP), **(B)** mean blood pressure (mean BP) **(C)** and diastolic and systolic blood pressure (DBP, SBP), in normotensive Wistar-Kyoto (WKY) and spontaneously hypertensive rats (SHR). **(D)** Representative flow cytometry charts of PVN tissue; total events; 100,000. **(E)** Cell count of macrophages (CD11b+ cells) and lymphocytes (CD3+ cells) by FACS. *P≤ 0.05, **P≤0.01, ****P≤0.0001; student's t-test of SHR vs. WKY (n= 5-6 rats per group).

3.4.2 Immune Cell Profile in the PVN of Renovascular Hypertensive Rats

Goldblatt, 2-Kidney-1-Clip (2K1C) rats were used as a model of renovascular hypertension (Oliveira-Sales, Toward et al. 2014) , whilst sham surgery was used as a control. 2K1C rats showed a significant increase in mean BP four weeks after clipping (week 1: 120±2 vs. 137±7 mmHg, week 2: 118±4 vs. 140±9 mmHg, week 4: 121±5 vs. 160±4 mmHg, Sham vs. 2K1C respectively, week 1-2: $p>0.05$, week 4: $p<0.05$, n=5-10; Figure 3.2A-B). Similarly, SBP was elevated at week 4 (week 1: 140±3 vs. 171±10 mmHg, week 2: 142±4 vs. 159±11 mmHg, week 4: 132±8 vs. 181±7 mmHg, Sham vs. 2K1C respectively, week 1-2: $p>0.05$, week 4: $p<0.05$, n=5-10; Figure 3.2A-B), but DBP did not change (week 1: 111±3 vs. 121±6 mmHg, week 2: 106±4 vs. 130±8 mmHg, week 4: 109±4 vs. 130±8 mmHg, Sham vs. 2K1C respectively, $p>0.05$, n=5-10; Figure 3.2A-B). Plasma levels of CCL2 were elevated by week one after clipping and remained increased throughout the following 3 weeks (week 1: 260±125 vs. 1313±190 pg/ml, week 2: 327±242 vs. 1245±152 pg/ml, week 4: 330±84 vs. 1739±333 pg/ml, Sham vs. 2K1C respectively, $p<0.05$, n=5; Figure 3.2C). However, only at week-2 were the cerebrospinal fluid (CSF) levels of CCL2 significantly elevated in the of 2K1C rats (week 1: 515±100 vs. 1246±90 pg/ml, week 2: 337±63 vs. 1776±204 pg/ml, week 4: 349±133 vs. 1069±359 pg/ml, Sham vs. 2K1C respectively, week 1 & 4: $p>0.05$, week 2: $p<0.05$ n=5; Figure 3.2C).

Flow cytometric analysis showed increases in the number of immune cells within the PVN of 2K1C animals during the early stage of hypertension (Figure 3.2D-E). The number of $CD45^{+hi}CD11b^{+}$ cells was higher in PVN tissue of 2K1C groups during week-1 and week-2 (week 1: 103±32 vs. 533±69 cells, week 2: 91±26 vs. 491±84 cells, week 4: 107±33 vs. 268±58 cells, Sham vs. 2K1C respectively, week1-2: $p<0.05$, week 4: $p>0.05$, n=5, Figure 3.2E); whereas $CD45^{+hi}CD3^{+}$ cell numbers were greater in 2K1C groups at week-4 (week 1: 418±48 vs. 252±38 cells, week 2: 132±24 vs. 52±11 cells, week 4: 60±27 vs. 226±18 cells,

Sham vs. 2K1C respectively, week 1-2; $p>0.05$, week 4: $p<0.05$, n=5; Figure 3.2E). Regression analysis showed that plasma CCL2 was positively correlated to mean BP ($r^2= 0.268$, $p<0.01$, n=30) or to the number of $CD45^{+hi}CD11b^{+}$ cells in the PVN ($r^2= 0.163$, $p<0.01$, n=30; Supplementary Figure 3.2). Overall, these results indicate that in hypertension immune cells are recruited by CCL2 into the PVN early, prior to the onset of hypertension (the pre-hypertensive stage).

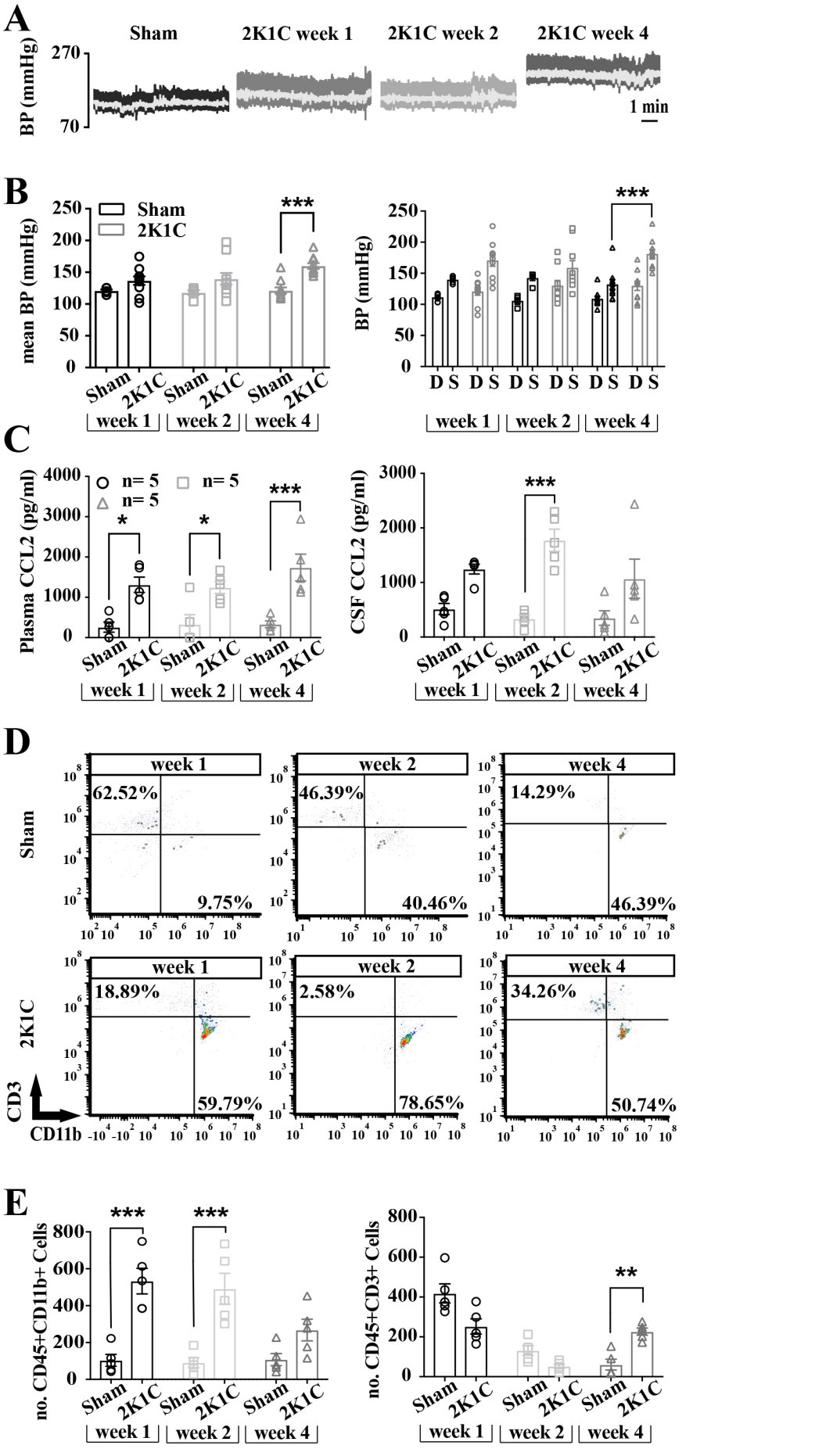

A
Sham
2K1C week 1
2K1C week 2
2K1C week 4
BP (mmHg)
270
70
1 min
B
mean BP (mmHg)
Sham
2K1C
***
BP (mmHg)
D S D S D S D S D S D S
week 1
week 2
week 4
C
Plasma CCL2 (pg/ml)
n= 5
n= 5
n= 5
*
*
***
CSF CCL2 (pg/ml)
***
D
Sham
2K1C
week 1
week 2
week 4
62.52%
9.75%
46.39%
40.46%
14.29%
46.39%
18.89%
59.79%
2.58%
78.65%
34.26%
50.74%
CD3
CD11b
E
no. CD45+CD11b+ Cells
***
***
no. CD45+CD3+ Cells
**

Figure 3.2: Recruitment and activation of immune cells by CCL2 precede blood pressure increases in hypertension.

(A) Representative recordings of pulsatile blood pressure (BP) **(B)** and mean BP, diastolic blood pressure (D), and systolic blood pressure (S) of sham-operated control, and 2 kidney-1 clip (2K1C) rats at different time points. **(C)** Temporal profile of plasma and CSF levels of CCL2 in control and 2K1C hypertensive rats. **(D)** Representative flow cytometry charts of PVN tissue; total events; 100,000. **(E)** Cell count of macrophages and lymphocytes by FACS. $^{*}P \leq 0.05$, $^{**}P \leq 0.01$, $^{***}P \leq 0.001$, two-way ANOVA of 2K1C vs. Sham (n= 5-10 rats per group).

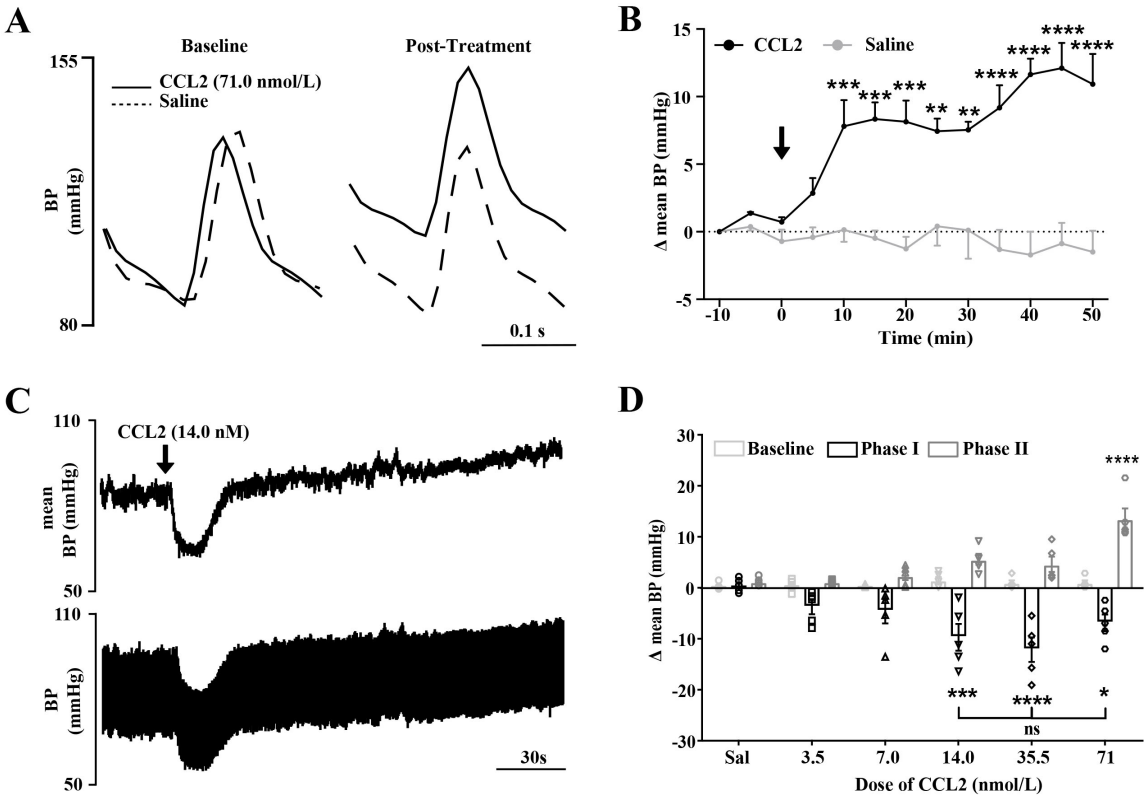
3.4.3 Cardiovascular Effects of Exogenous Application of CCL2 into the PVN of Conscious and Anaesthetized Rats

To establish whether CCL2 induces changes in BP, CCL2 (71 nmol/L) was microinjected into the PVN of conscious freely-moving animals. Unilateral microinjection produced an increase in BP; consisting of an initial increase in mean BP with a rapid onset, followed by a sustained pressor response, reaching its peak at ~45 minutes (+12±2 Δ mmHg, $p<0.05$; n=5; Figure 3.3A-B).

In anesthetized rats, microinjection of CCL2 (3.5-71 nmol/L) into the PVN produced a dose-dependent, biphasic response in BP (Figure 3.3C), first eliciting a rapid short-lasting decrease in mean BP (Phase I: 3.5 nmol/L: -4±1 Δ mmHg, 7 nmol/L: -5±2 Δ mmHg, 14 nmol/L: -10±3 Δ mmHg, 35.5 nmol/L: -12±2 Δ mmHg, 71 nmol/L: -7±2 Δ mmHg, $p<0.05$, n=5; Figure 3.3D) followed by a prolonged and sustained increase in mean BP (Phase II: 3.5 nmol/L: +1±0.2 Δ mmHg, 7 nmol/L: +2±1 Δ mmHg, 14 nmol/L: +6±1 Δ mmHg, 35.5 nmol/L: +5±2 Δ mmHg, 71 nmol/L: +14±2 Δ mmHg, $p<0.05$, n=5; Figure 3.3D). Administration of vehicle (0.9% saline) did not change mean BP (phase I: +0.4±0.3 Δ mmHg, phase II: +1.2±0.4 Δ mmHg, $p>0.05$, n=5; Supplementary Figure 3.3), nor did the administration of CCL2 (71 nmol/L) in areas adjacent to the PVN (phase I: +0.3±0.1 Δ mmHg, phase II: +0.7±0.2 Δ mmHg, $p>0.05$, n=5; Supplementary Figure 3.3).

In contrast to the response in conscious animals, in pentobarbitone anesthetized rats, the first phase of the CCL2 response was a depressor response. The contrasting phase I was due to the use of the CNS depressant anaesthetic; pentobarbitone (Barker and Ransom 1978). We confirmed this by microinjecting L-glutamate (10 mmol/L) into the PVN; which produced a depressor response in anaesthetized rats and a pressor response in conscious rats (Supplementary Figure 3.4). All PVN microinjections were validated through post-mortem

histological analysis, and all microinjections were mapped respectively (Supplementary Figure 3.5).



<u>Figure 3.3:</u> CCL2 in the PVN produces a biphasic blood pressure response.

PVN microinjection with CCL2 is marked by a black arrow. **(A)** Representative wave form averages of BP following PVN microinjection in conscious animals. **(B)** Time course changes of mean BP in conscious rats. **(C)** Representative recordings of mean BP and pulsatile BP following administration of CCL2 (14.0 nmol/L) into the PVN of anesthetized rats. **(D)** Δ mean BP following different doses of CCL2 into the PVN of anaesthetized rats. $^{*}P \leq 0.05$, $^{**}P \leq 0.01$, $^{***}P \leq 0.001$, $^{****}P \leq 0.0001$, ns; not significant, two-way ANOVA of CCL2 vs. saline (n=5 rats per group).

3.4.4 Sympathetic Responses to Activation of CCL2-mediated Activation of CCR2 Receptors in the PVN

In order to determine whether the increases in BP were accompanied by sympathetic activation, we performed whole-animal electrophysiological recordings of renal sympathetic nerve activity (RSNA). Microinjection of CCL2 (71 nmol/L) into the PVN evoked a biphasic response in RSNA and mean BP; consisting of brief sympatho-inhibition and fall in BP (phase I: 85±2% RSNA and -9±4 Δ mmHg; $p<0.05$n=5; Figure 3.4A and E-F) followed by a prolonged and sustained increase in RSNA and mean BP (phase II: 126±7% and +10±1 Δ mmHg; $p<0.05$, n=5 Figure 3.4A and E-F). Furthermore, there was increased c-fos expression in the PVN following CCL2 administration compared with 0.9% saline (control) injected rats (24±7 vs. 98±3 nuclei, saline vs. CCL2 respectively, $p<0.05$, n=5; Supplementary Figure 3.6). These parallel changes in BP and RSNA suggest that the changes in BP elicited by CCL2 are sympathetically mediated.

To establish if the BP responses were specific to CCR2 activation, the selective antagonist (RS-102895; 70 μmol/L) was microinjected into the PVN five minutes prior to CCL2 (71 nmol/L). Antagonism of CCR2 receptors abolished both the inhibitory and excitatory phases of the RSNA response (phase I: 101±1%, phase II: 102±3%; $p<0.05$, n=5; Figure 3.4B and E-F) and the decrease and increase in BP (phase I: -1±1 Δ mmHg, phase II: -4±2 Δ mmHg; $p<0.05$, n=5; Figure 3.4B and E-F). Confirmation of arterial baroreceptor control of RSNA was demonstrated by the ongoing pulse-modulation and inhibition in response to baroreceptor loading with phenylephrine (5 μg/kg, i.v.) (Supplementary Figure 3.3).

3.4.5 Location of CCR2 Receptors in the PVN

To further determine the brain mechanisms underlying the sympathetic responses elicited by CCL2, we performed immunohistochemical studies identifying the location of

CCR2 receptors. Immunohistochemistry revealed that in the PVN, CCR2 were mostly expressed on astrocytes that made close appositions with RVLM-projecting PVN neurons, identified by retrograde transport of cholera toxin b (CTb) from the RVLM to the PVN (Figure 3.4G). CCR2 were highly expressed in PVN astrocytes, but minimal co-localization was observed with neurons expressing CTb, (confirmed with the neuronal marker NeuN or the microglia marker CD11b; Supplementary Figure 3.7). Validity and specificity of retrograde labelling from the RVLM were verified through immunobiological labelling of RVLM injection sites (Supplementary Figure 3.8). These results suggest that the changes to RSNA induced by CCL2 injections into the PVN is partly mediated by stimulation of receptors expressed on astrocytes, which in turn activates RVLM-projecting PVN neurons and sympathetic preganglionic neurons responsible for resting sympathetic tone (Strack, Sawyer et al. 1989).

3.4.6 Cardiovascular Responses to PVN Injections of CCL2 After Blockade of Purinergic Transmission

As glutamate-purinergic co-transmission is commonly found between brain astrocytes and neurons (Gordon, Baimoukhametova et al. 2005), we examined the effect of blocking purinergic receptors within the PVN. Microinjections of the non-selective P2X antagonist, suramin (10 mmol/L), into the PVN five minutes prior to CCL2 (71 nmol/L) abolished the initial decreases in RSNA and mean BP elicited by CCL2 (103±1% vs. 85±2%, and +2±1 Δ mmHg vs. -9±4 Δ mmHg, CCL2 after suramin vs. CCL2 respectively, $p<0.05$, n=4-5; Figure 3.4C and E-F). However, the administration of suramin did not affect the second phase of sustained increase in RSNA and mean BP in response to CCL2 (130±4% vs. 126±7%, and +10±2 Δ mmHg vs. +10±1 Δ mmHg, CCL2 after suramin vs. CCL2 respectively, $p<0.05$, n=4-

5; Figure 3.4C and E-F); therefore, suggesting that astrocytic purinergic transmission to PVN neurons mediates the first rapid and initial inhibitory phase of the CCL2 response.

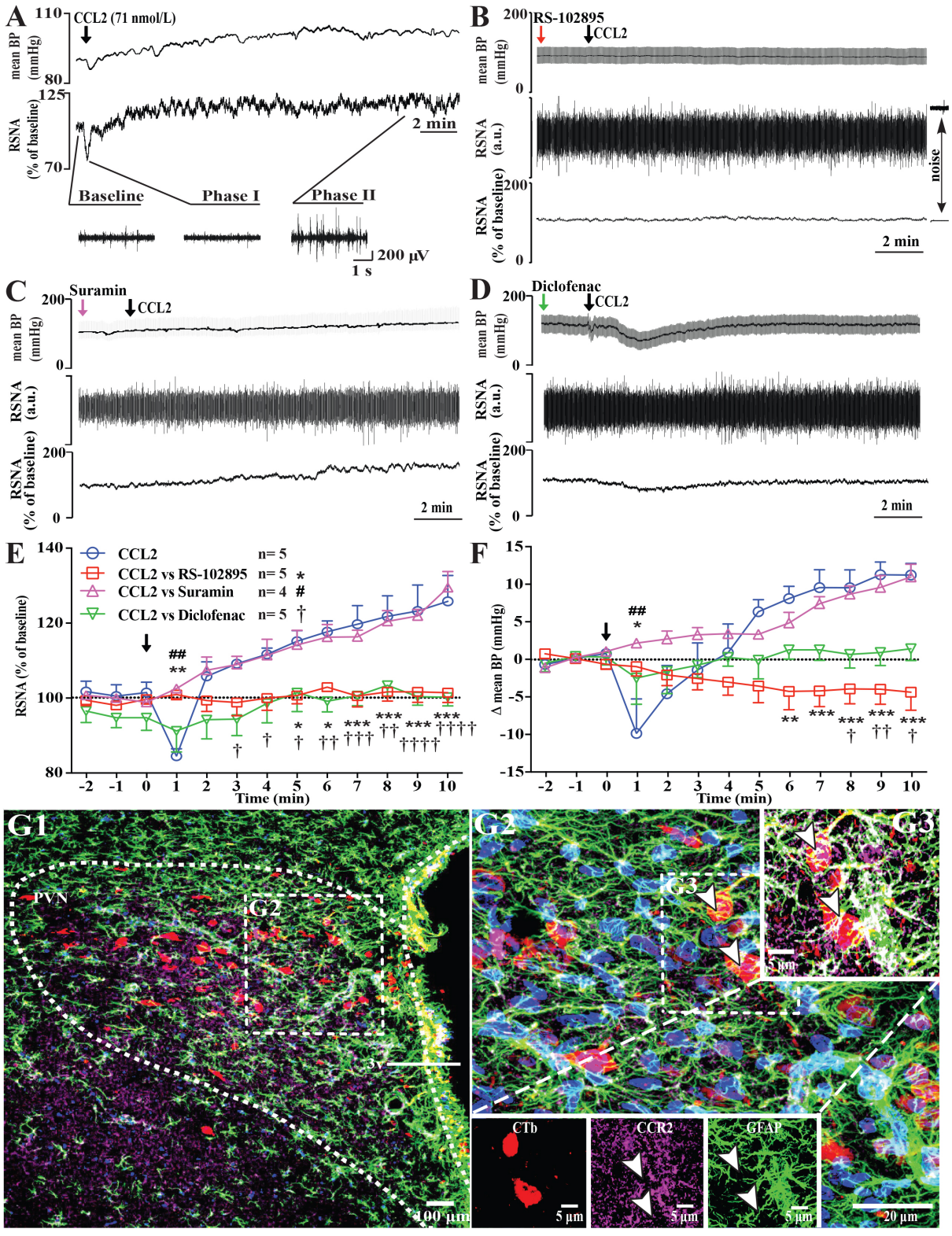

A
CCL2 (71 nmol/L)
mean BP (mmHg)
RSNA (% of baseline)
2 min
Baseline
Phase I
Phase II
200 µV
1 s
B
RS-102895
CCL2
RSNA (a.u.)
noise
2 min
C
Suramin
CCL2
D
Diclofenac
E
CCL2 n= 5
CCL2 vs RS-102895 n= 5
CCL2 vs Suramin n= 4
CCL2 vs Diclofenac n= 5
RSNA (% of baseline)
Time (min)
F
Δ mean BP (mmHg)
G1
PVN
3V
100 µm
G2
G3
CTb
CCR2
GFAP
5 µm
20 µm

Figure 3.4: CCL2 evokes sympathetic mediated responses in BP.

PVN microinjection of CCL2 is marked by a black arrow. **(A)** Representative recordings of BP and averaged renal sympathetic nerve activity (RSNA), following PVN CCL2 (71 nmol/L) injection. Representative recordings of BP and RSNA following administration of **(B)** RS-102985 (CCR2 antagonist; 70 μmol/L; marked by a red arrow) into the PVN, **(C)** suramin (10 mmol/L; marked by a pink arrow) into the PVN, **(D)** and systemic injection of the anti-inflammatory agent diclofenac (5 mg/kg; marked by a green arrow); prior to CCL2 administration. Time course changes in %RSNA **(E)** and Δ mean BP **(F)**. (**G)** Representative micrographs of the PVN showing CCR2 expressing astrocytes (GFAP) in close apposition to CTb positive RVLM-projecting neurons (white arrows). 3v; third ventricle, PVN; paraventricular nucleus of the hypothalamus. $^{*}P\leq 0.05$, $^{**}P\leq 0.01$, $^{***}P\leq 0.001$; two-way ANOVA of CCL2 vs. RS-102985; $^{\#\#}P\leq 0.01$; two-way ANOVA of CCL2 vs. suramin, $^{\dagger}P\leq 0.05$, $^{\dagger\dagger}P\leq 0.01$, $^{\dagger\dagger\dagger}P\leq 0.001$, $^{\dagger\dagger\dagger\dagger}P\leq 0.0001$; two-way ANOVA of CCL2 vs. diclofenac (n=4-5 rats per group).

3.4.7 Changes in the Profile of Immune Cells in Response to PVN Injections of CCL2 in Normotensive Rats

To determine whether CCL2 recruits immune cells from the circulation to the PVN, we labelled the tissue with the microvasculature marker (RECA-1) after injecting CCL2 (71 nmol/L) into the left PVN. Both macrophage ($CD11b^{+}$) and mononuclear immune cells ($CD8^{+}$) were clustered around the blood vessels in the brain parenchyma in the left PVN (Figure 3.5C). No immune cells were labelled within the contralateral (right) PVN – used as control (Figure 3.5A-B). Additionally, no immune cells were recruited to the PVN following microinjection of 0.9% saline (Supplementary Figure 3.9). Flow cytometric quantification of the immune cells infiltrating the PVN (Figure 3.5D) demonstrated that in comparison with saline, CCL2 increased the numbers of $CD45^{+hi}CD11b^{+}$ cells (myeloid cells; 55±27 vs. 492±189 cells, saline vs. CCL2 respectively, $p<0.05$, n=8; Figure 3.5E) and $CD45^{+hi}CD3^{+}$ cells (T lymphocytes; 45±14 vs. 138±32, saline vs. CCL2 injection, $p<0.05$, n=8; Figure 3.5E) in the PVN.

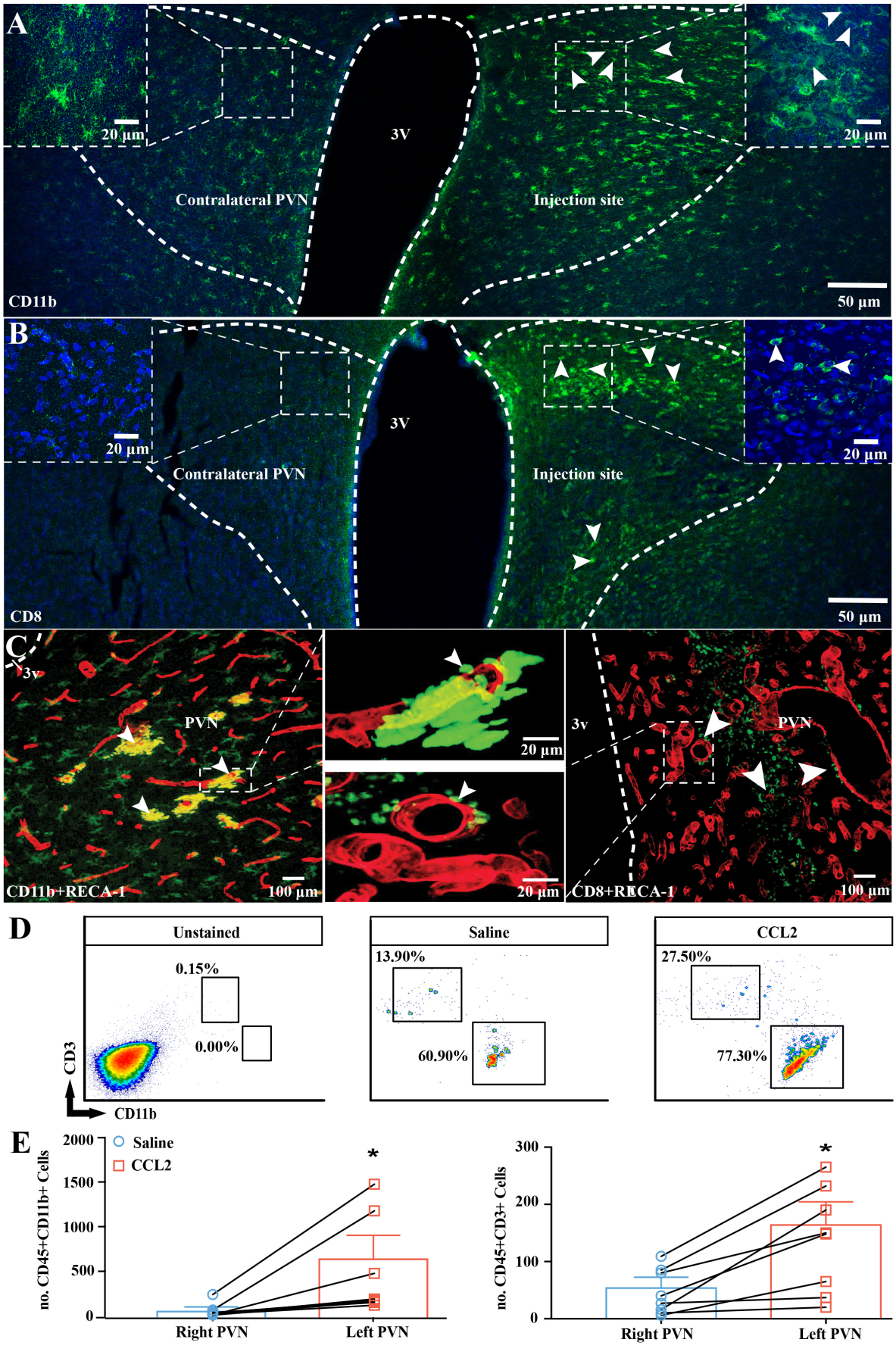

A
20 µm
3V
Contralateral PVN
Injection site
20 µm
CD11b
50 µm
B
20 µm
3V
Contralateral PVN
Injection site
20 µm
CD8
50 µm
C
3v
PVN
CD11b+RECA-1
100 µm
20 µm
20 µm
3v
PVN
CD8+RECA-1
100 µm
D
Unstained
0.15%
0.00%
CD3
CD11b
Saline
13.90%
60.90%
CCL2
27.50%
77.30%
E
Saline
CCL2
no. CD45+CD11b+ Cells
2000
1500
1000
500
0
*
Right PVN
Left PVN
no. CD45+CD3+ Cells
300
200
100
0
*
Right PVN
Left PVN

Figure 3.5: CCL2 recruits immune cells that infiltrate into the PVN.

Representative confocal images of the PVN following unilateral CCL2 (71 nmol/L) microinjection. **(A-B)** Representative confocal images of PVN, labelled with **(A)** macrophage marker (CD11b; green) **(B)** or mononuclear immune cell marker (CD8; green), **(C)** and confocal images of the PVN labelled with the microvasculature marker (RECA-1; red), and the macrophage marker (CD11b; green, left) or the mononuclear immune cell marker (CD8; green, right), white arrows; infiltrating immune cells into PVN tissue. **(D)** Representative flow cytometry charts of PVN tissue; total events; 100,000. **(E)** Cell count of macrophages and lymphocytes by FACS following either saline (right PVN) or CCL2 (left PVN) microinjection into PVN. 3v= third ventricle, PVN; paraventricular nucleus of the hypothalamus, US, unstained sample, $^{*}P \leq 0.05$; student's t-test of CCL2 vs. saline (n= 8 rats per group).

3.4.8 Anti-inflammatory Treatment Blocks the Sympathetic Responses to CCL2 Microinjection into the PVN

To determine the effects of anti-inflammatory treatment on the actions of CCL2 in the PVN, we pre-treated animals with a non-steroidal anti-inflammatory agent, diclofenac (5 mg/kg, i.v.), 20 minutes prior to microinjection of CCL2 (71 nmol/L) into the PVN. Diclofenac completely inhibited the infiltration of macrophages (Figure 3.6A-B and E) and mononuclear immune cells (Figure 3.6C-D and E) into the PVN and abolished the second phase response of increased RSNA and BP (101±3% vs. 120±5%, and +1±1 Δ mmHg vs. +9±2 Δ mmHg, CCL2 after diclofenac vs. CCL2 respectively, $p<0.05$, n=5; Figure 3.4D and E-F) to CCL2 injection into the PVN. This suggests that the second phase of the CCL2 response is caused by the infiltration of immune cells and neuroinflammation in the PVN. Peripheral immune cells in the spleen and the thymus were found to express CCR2 receptors in naïve control rats (Supplementary Figure 3.10).

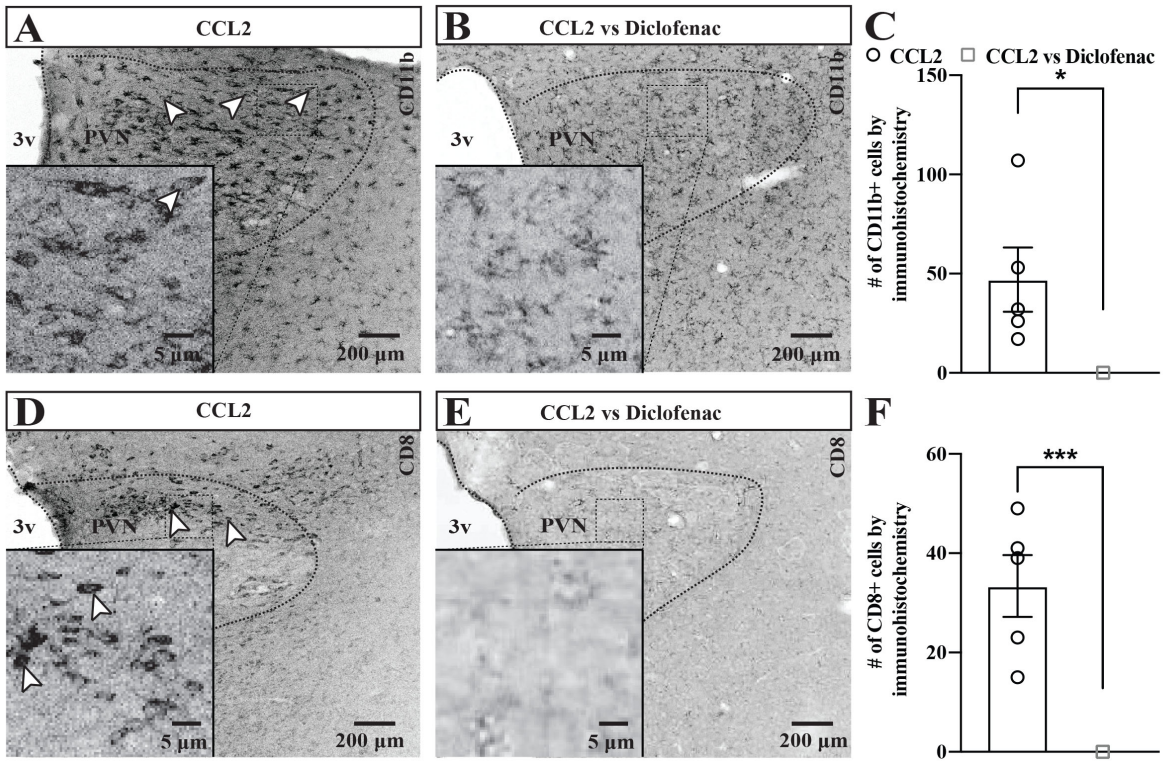


Figure 3.6: Infiltration of immune cells into the PVN mediates and maintains the second phase of the CCL2 response.

(A-B) CD11b immunoreactivity showing macrophage infiltration into the PVN at the site microinjected with CCL2 (A), and no recruitment following diclofenac pre-treatment (B). **(C)** Cell count of $CD11b^{+}$ macrophages by immunohistochemistry following either PVN CCL2 (control) or CCL2 following systemic diclofenac. **(D-E)** CD8 immunoreactivity showing mononuclear immune cell infiltration into the PVN after CCL2 injection (D), and no recruitment following diclofenac pre-treatment (E). **(F)** $CD8^{+}$ mononuclear immune cells by immunohistochemistry. White arrows; recruitment of immune cells into the PVN. 3v; third ventricle, PVN; paraventricular nucleus of the hypothalamus. $^{*}P \leq 0.05$, $^{**}P \leq 0.01$; one-way ANOVA of CCL2 vs. CCL2 following diclofenac (n= 5 rats per group).

3.5 Discussion

In this study, we show that the chemokine CCL2 recruited immune cells that infiltrate the PVN to evoke increases in RSNA and BP. Furthermore, the recruitment of immune cells occurred prior to rats developing hypertension in our renovascular 2K1C rat model. To our knowledge, this is the first report demonstrating that CCL2-CCR2 signalling can recruit immune cells to the PVN, eliciting increases in SNA and BP in hypertension. The results here support the "neuro-immune axis" theory in hypertension (Abboud, Harwani et al. 2012, Zubcevic, Santisteban et al. 2014, Harwani 2018), where the immune system and increased neuroinflammation drives increases in SNA and BP (Elsaafien, Korim et al. 2019).

We (Korim, Elsaafien et al. 2018) and others (Shi, Gan et al. 2011, Wei, Yu et al. 2015) have demonstrated previously that the administration of pro-inflammatory cytokines into autonomic brain regions increases SNA and BP. Furthermore, activation of immune cells contributes to neural inflammation and BP elevation in hypertension (Jun, Zubcevic et al. 2012, Zubcevic, Jun et al. 2013). Thus, the present study addressed the question of whether the recruitment of immune cells into the PVN by CCL2 can have effects on SNA and BP in hypertension.

We found that levels of CCL2 are increased in the plasma and CSF of prior to the development of hypertension. Previous studies only measured CCL2 levels at the end stage of hypertension and found it to be elevated in plasma and CSF (Santisteban, Ahmari et al. 2015, Wang, Kang et al. 2018). CCL2 is a chemokine involved in the inflammatory response, and is released to recruit circulating immune cells (Rollins 1997). Activation of CCR2 receptors by CCL2 recruits and activates immune cells to move through a chemotactic gradient towards a stimulus (Ajuebor, Flower et al. 1998, Lu, Rutledge et al. 1998). Activated immune cells induce an inflammatory cascade in tissue by secreting pro-inflammatory cytokines (Ishibashi, Hiasa et al. 2004). In hypertension, a stimulus for CCL2 upregulation is angiotensin II (Crowley,

Song et al. 2010). *In vitro*, angiotensin II application to primary hypothalamic neuronal cultures increases CCL2 levels (Santisteban, Ahmari et al. 2015). This increase in CCL2 levels allows the formation of a chemotactic gradient towards the CSF bathing the central nervous system (Santisteban, Ahmari et al. 2015), increasing CCL2 by approximately 3-fold in the PVN of hypertensive animals (Wang, Kang et al. 2018). We found that CCL2 levels are elevated in the plasma and CSF prior to BP increases in renovascular hypertension, suggesting that CCL2-mediated recruitment of immune cells into the PVN might contribute to the development of hypertension.

We have shown that $CD11b^+$ and $CD3^+$ immune cells were recruited to the PVN in both primary and secondary animal models of hypertension. This finding is consistent with similar observations in primary and secondary models of hypertension (Santisteban, Ahmari et al. 2015, Wang, Kang et al. 2018, Ahmari, Santisteban et al. 2019). We found the number of macrophages ($CD11b^+$) in the PVN was increased prior to BP elevation in hypertension, and their levels remained increased throughout the development of hypertension. Previous studies show macrophages to be recruited to the central nervous system in established hypertension (Santisteban, Ahmari et al. 2015, Wang, Kang et al. 2018). Furthermore, the innate immune response in the periphery is active in pre-hypertensive rats (Harwani, Chapleau et al. 2012). Importantly, in the present study, we reveal the temporal profile of macrophage infiltration into the PVN and show that infiltration precedes, and indeed, might cause hypertension. Whereas, we only observed lymphocyte ($CD3^+$) recruitment to the PVN once hypertension was established, previous studies showed that elevations in BP results in the recruitment of T-lymphocytes (Marvar, Thabet et al. 2010). Our findings show that macrophages are recruited early during the development of hypertension, whereas lymphocytes are recruited in response to elevated BP. Activated immune cells enhance the inflammatory response by secreting pro-inflammatory cytokines; such as TNF-α and IL-1β (Ishibashi, Hiasa et al. 2004, Jun, Zubcevic

et al. 2012, Santisteban, Ahmari et al. 2015). Those cytokines are upregulated in the PVN of hypertensive animals (Kang, Ma et al. 2009, Li, Qin et al. 2014), and can increase SNA and BP when administered directly in the PVN (Shi, Gan et al. 2011). Therefore, we propose that CCL2 mediates the early recruitment of macrophages into the PVN to increase SNA and BP; leading to the development of hypertension.

We also demonstrate that CCL2 in the PVN increases BP in both conscious, freely-behaving and pentobarbitone anaesthetized rats. For the first time, we show that CCL2 causes sustained increases in BP. Previous studies only provided a link between CCL2 and elevations in BP. For example, plasma levels of CCL2 are positively correlated to BP levels in hypertensive patients (Antonelli, Fallahi et al. 2012). Additionally, in animal models of hypertension CCL2 is upregulated in the plasma (Santisteban, Ahmari et al. 2015), PVN (Kang, Ma et al. 2009), and RVLM(Li, Qin et al. 2014). Moreover, we show that exogenous application of CCL2 into the PVN increases RSNA and BP. These findings fit with what we know about the neurocircuitry of the PVN, since this nucleus contains subpopulations of neurons that project to the RVLM (Shafton, Ryan et al. 1998), which contains cardiovascular sympathetic preganglionic neurons responsible for generating sympathetic tone to cardiovascular organs (Strack, Sawyer et al. 1989).

Injection of CCL2 into the PVN evoked a dose-dependent biphasic response in RSNA and BP. Phase I was an initial rapid response followed by a slow sustained phase II response (elevated RSNA and BP). These responses were observed in both conscious and pentobarbitone anaesthetized rats. Similar observations, though not for CCL2, have been previously reported, where activation of brain regions involved in cardiovascular control elicited a rapid response followed by slow sustained effects (Scislo and O'Leary 2000). Interestingly, we noted that the initial phase was a pressor response in conscious animals, and a depressor response in anaesthetized animals. This difference is caused by the anaesthesia, since pentobarbitone

depresses neuronal excitability, activates post-synaptic GABA-receptor coupled Cl^- conductance and depresses post-synaptic glutamate excitability (Barker and Ransom 1978). As such, exciting sympathetic neurons may lead to sympatho-inhibitory responses rather than sympatho-excitation in pentobarbitone anaesthetized rats. We confirmed this through exciting the PVN with L-glutamate and observed a pressor response in conscious rats, and a depressor response in pentobarbitone anaesthetized rats. To confirm that the biphasic response was elicited through CCL2 signalling, we demonstrated that blocking CCR2 receptors in the PVN abolished the changes in RSNA and BP during both the inhibitory and excitatory phases. These findings indicate that CCL2-CCR2 signalling in the PVN evokes rapid responses followed by sustained increases in RSNA and BP.

We found that CCL2 induced astrocytic-ATP-mediated activation of PVN neurons alters RSNA and BP with a rapid onset. We showed that stimulation of CCR2 receptors expressed on PVN astrocytes induces ATP-mediated activation of RVLM-projecting PVN neurons. This mediated the rapid "phase I" of the response in RSNA and BP, as the prior blockade of PVN P2X purinergic receptors abolished the responses in phase I. This is consistent with similar observations in previous studies demonstrating that the stimulation of astrocytes in the RVLM activates sympatho-excitatory neurons via ATP, increasing renal and cardiac SNA with a rapid onset (Marina, Tang et al. 2013). Furthermore, activation of astrocytes in the RVLM results in ATP-mediated rapid depolarization of C1 neurons. Similarly, injection of ATP into the PVN induces dose-dependent rapid elevations in SNA in a decorticate, un-anesthetized, arterially perfused in situ preparation (Ferreira-Neto, Yao et al. 2013). Therefore, ATP released by activated astrocytes results in the rapid depolarization of PVN neurons mediating increases in SNA and BP with a rapid onset.

Phase II was characterized by a slow, sustained increase in RSNA and BP mediated by recruitment of immune cells into the PVN. Activation of CCR2 receptors

expressed on immune cells facilitates the infiltration of macrophages and lymphocytes to the PVN. Preventing this with diclofenac abolished the second phase of the response to CCL2. We further confirmed that diclofenac blocked the infiltration of immune cells in to the PVN evoked by CCL2. This suggests that the recruitment of activated immune cells to the PVN induces a slow inflammatory cascade that stimulates RSNA and increases BP. Activation of immune cells through CCL2-CCR2 signalling likely initiates an inflammatory response through immune cell secretion of pro-inflammatory cytokines; such as TNF-α and IL-1β (Ishibashi, Hiasa et al. 2004, Jun, Zubcevic et al. 2012, Santisteban, Ahmari et al. 2015). In the brain, increased production of cytokines mediates increases in SNA and BP (Shi, Gan et al. 2011, Wei, Yu et al. 2015, Korim, Elsaafien et al. 2018). In fact, administration of TNF-α or IL-1β into the PVN mediates sustained increases in cardiac and renal SNA and BP (Shi, Gan et al. 2011). Moreover, in CCR2 receptor knockout mice there is impaired recruitment of macrophages in hypertension (Bush, Maeda et al. 2000). Furthermore, the depletion of immune cells reduces neural inflammation and BP (Santisteban, Ahmari et al. 2015). In addition, antagonism of peripheral CCR2 receptors in hypertensive animals reduced the activation immune cells, decreased peripheral inflammation and reduced BP (Elmarakby, Quigley et al. 2007, Chan, Moore et al. 2012). Taken together these findings suggest that CCL2-CCR2 signalling plays a critical role in immune cell recruitment mediating neural inflammation and BP elevation in hypertension.

In the present study, we propose a role for CCL2-CCR2 signalling in mediating recruitment of immune cells into the PVN, evoking increases in SNA and BP. Peripheral CCL2 is upregulated in response to circulating angiotensin II in hypertension (Crowley, Song et al. 2010), while peripheral blockade of angiotensin II receptors in hypertension, reduces CCL2 levels (Ishibashi, Hiasa et al. 2004). Furthermore, CCL2 mRNA and CCL2 protein levels increase upon the application of angiotensin II to primary hypothalamic neuronal culture

(Santisteban, Ahmari et al. 2015). The increase in CCL2 levels stimulates CCR2 receptors expressed on immune cells facilitating their infiltration into tissue (Ajuebor, Flower et al. 1998, Lu, Rutledge et al. 1998). In hypertension CCL2 forms a chemotactic gradient guiding immune cells to infiltrate into autonomic brain regions, including the PVN (Santisteban, Ahmari et al. 2015, Wang, Kang et al. 2018). To allow immune cell infiltration into the PVN, CCL2 induces the internalization of tight junction proteins expressed on endothelial cells, making the blood brain barrier (BBB) more permeable (Stamatovic, Keep et al. 2009, Roberts, Eugenin et al. 2012). Once activated, immune cells gain access to the PVN, release cytokines and initiate an inflammatory cascade (Ishibashi, Hiasa et al. 2004, Jun, Zubcevic et al. 2012, Santisteban, Ahmari et al. 2015), leading to sustained increases in SNA and BP (Shi, Gan et al. 2011). Our results demonstrate that CCL2-CCR2 signalling recruits immune cells into the PVN prior to the development of hypertension. Therefore, we propose CCL2-CCR2 signalling is important for the infiltration of immune cells into the PVN which ultimately leads to elevated SNA and BP and the development of hypertension (Figure 3.7). This is consistent with previous studies demonstrating that the peripheral blockade of CCR2 receptors reduces the inflammatory response, leading to reduced BP in hypertensive animals (Bush, Maeda et al. 2000, Elmarakby, Quigley et al. 2007, Chan, Moore et al. 2012).

3.6 Conclusion

In conclusion, our study provides new evidence that in models of primary and secondary hypertension the chemokine CCL2 recruits immune cells to the PVN to increase SNA and BP, leading to the development of hypertension (Elsaafien, Korim et al. 2019). As such, specific blockade of immune cell entry into autonomic brain regions may serve as a potential therapeutic target for the treatment of hypertension.

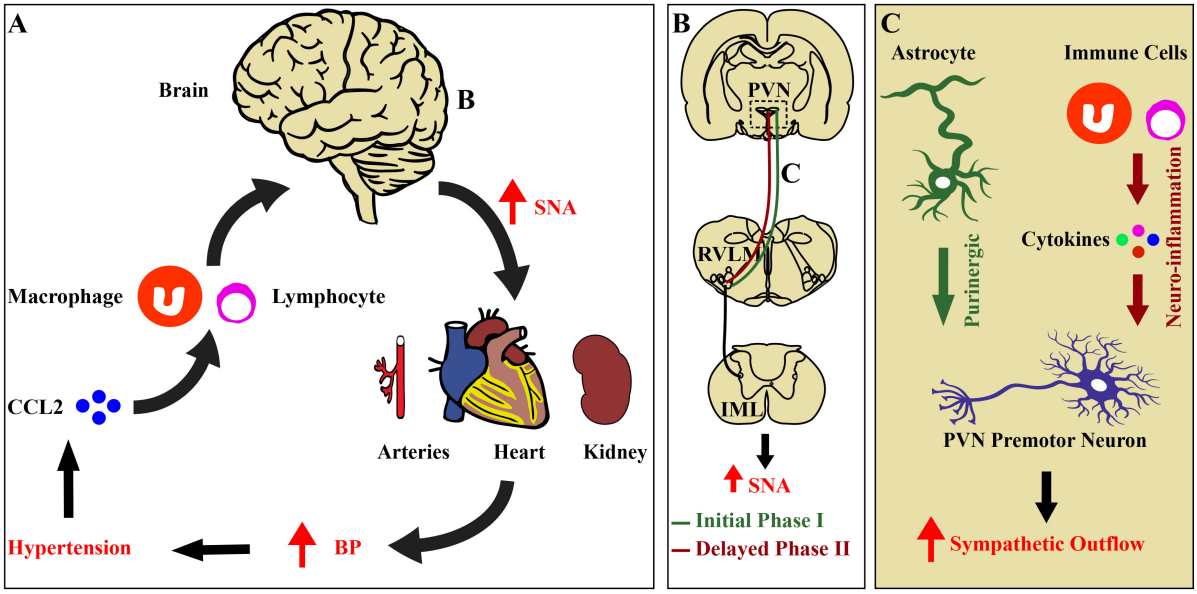


Figure 3.7: The Chemoattraction of immune cells by CCL2 into the PVN induces neuroinflammation and sustained BP increases in hypertension.

Schematic diagram of the proposed mechanisms by which immune cells facilitate the development of hypertension. **(A)** Upregulation of CCL2 activates, recruits and promotes immune cells infiltration into the PVN. This activates the PVN, increasing sympathetic outflow to cardiovascular organs leading to increases in BP and the development of hypertension. **(B)** Activation of PVN premotor neurons excites IML projecting RVLM neurons – increasing SNA. **(C)** CCL2 excites PVN premotor neurons via two mechanisms; Astrocytic purinergic mediated mechanisms result in the initial increase in SNA (green), and the neuro-inflammatory process mediated by the infiltration of immune cells induces the delayed prolonged increase in SNA (red). BP; blood pressure, CCL2; C-C motif chemokine ligand 2, IML; intermediolateral column of the spinal cord, PVN; paraventricular nucleus of the hypothalamus, RVLM; rostral ventrolateral medulla, SNA; sympathetic nerve activity.

3.7 Novelty and Significance

What is known?

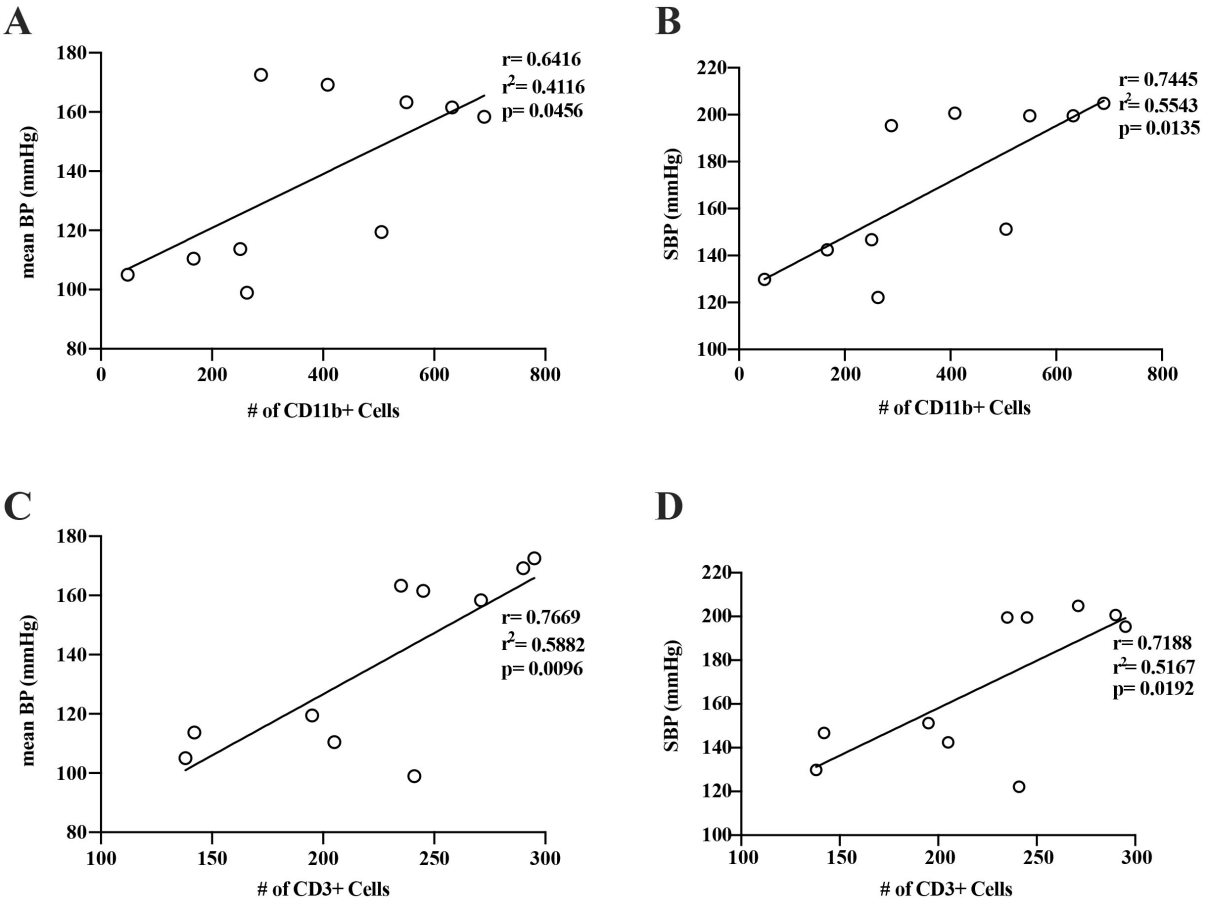
- Neural inflammation in brain regions that control sympathetic nerve activity is involved in the pathogenesis of hypertension.
- Immune cell infiltration into autonomic brain regions is linked to neural inflammation in hypertension.
- CCL2 has been identified as a chemokine involved in recruiting immune cells and is upregulated in hypertension.

What New Information Does This Article Contribute?

- This study uncovers the underlying mechanism by which CCL2 recruits immune cells to the paraventricular nucleus (PVN) to increase sympathetic nerve activity (SNA) and blood pressure (BP).
- It establishes the temporal profile of CCL2 upregulation and immune cell infiltration into the PVN during the development of hypertension.
- It demonstrates for the first time, the importance of CCL2 in driving immune cell infiltration into the brain parenchyma which leads to ultimately to hypertension.

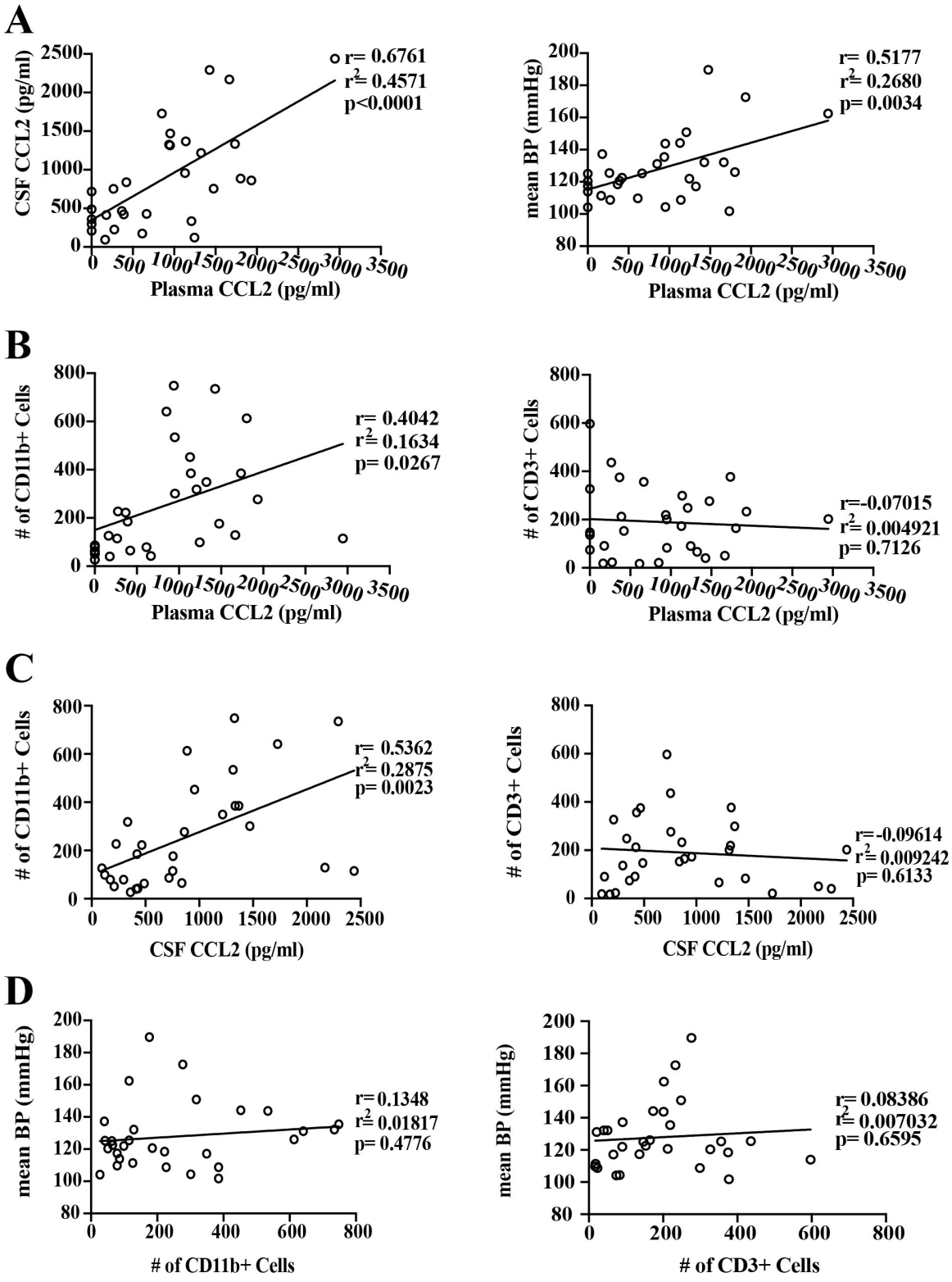
Hypertension is associated with enhanced neural inflammation coupled with augmented sympathetic drive. However, what regulates this inflammation and sympatho-excitation is still unknown. The present study provides evidence that the chemokine CCL2 mediates the recruitment of immune cells to the PVN, which increases sympathetic drive and BP. Upregulation of CCL2 leads to immune cell infiltration to the PVN during the development of hypertension. Targeting CCL2 and immune cell activation in the brain creates new possibilities for therapeutic interventions in hypertension.

Supplemental Material



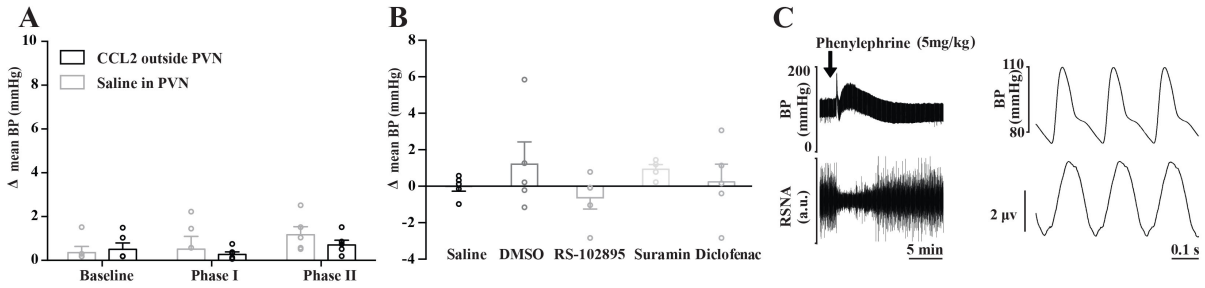
<u>Supplementary Figure 3.1:</u> Correlations between PVN immune cells and BP in the primary model of hypertension.

Simple regression in both WKY and SHR between CD45+^{hi}CD11b+ cells (macrophages) and MAP **(A)**, or SBP **(B),** and between CD45+^{hi}CD3+ cells (lymphocytes) and MAP **(C)**, or SBP **(D)**. MAP; mean arterial pressure, SBP; systolic blood pressure, SHR and WKY groups, n=10.


A
CSF CCL2 (pg/ml)
Plasma CCL2 (pg/ml)
r= 0.6761
r2= 0.4571
p<0.0001
mean BP (mmHg)
Plasma CCL2 (pg/ml)
r= 0.5177
r2= 0.2680
p= 0.0034
B
# of CD11b+ Cells
Plasma CCL2 (pg/ml)
r= 0.4042
r2= 0.1634
p= 0.0267
# of CD3+ Cells
Plasma CCL2 (pg/ml)
r=-0.07015
r2= 0.004921
p= 0.7126
C
# of CD11b+ Cells
CSF CCL2 (pg/ml)
r= 0.5362
r2= 0.2875
p= 0.0023
# of CD3+ Cells
CSF CCL2 (pg/ml)
r=-0.09614
r2= 0.009242
p= 0.6133
D
mean BP (mmHg)
# of CD11b+ Cells
r= 0.1348
r2= 0.01817
p= 0.4776
mean BP (mmHg)
# of CD3+ Cells
r= 0.08386
r2= 0.007032
p= 0.6595

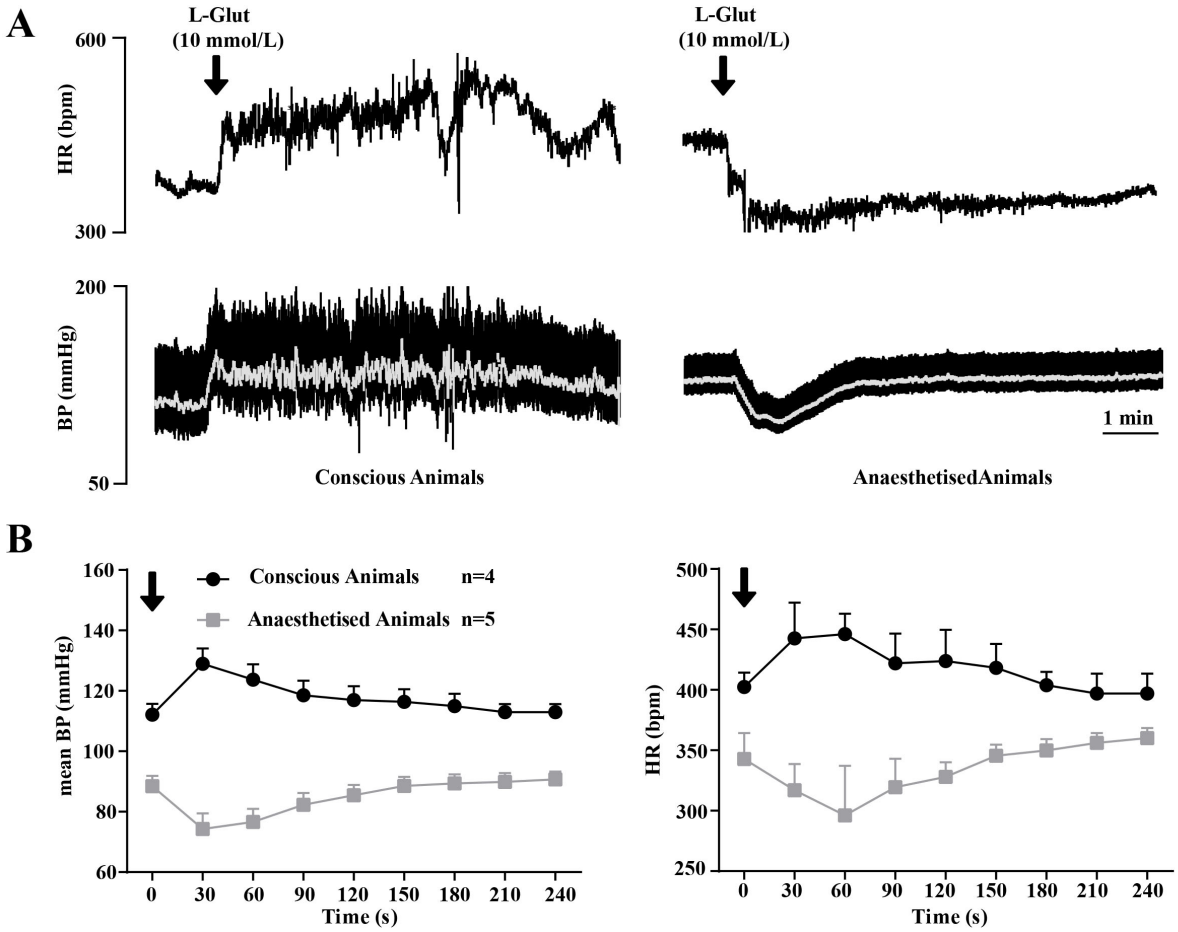
<u>Supplementary Figure 3.2:</u> Correlations between PVN immune cells, CCL2 levels and BP in the renovascular model of hypertension.

(A) Simple regression between CCL2 levels in plasma and CSF or MAP, **(B)** and between plasma levels of CCL2 and $CD45^{+hi}CD11b^{+}$ cells (macrophages), $CD45^{+hi}CD3^{+}$ cells (lymphocytes), or $CD45^{+hi}$ cells. **(C)** Simple regression between CSF levels of CCL2 and macrophages, or lymphocytes. **(D)** Simple regression between MAP macrophages, or lymphocytes. CSF; cerebrospinal fluid, MAP; mean arterial pressure, SBP; systolic blood pressure, Sham and 2K1C groups, n=30.



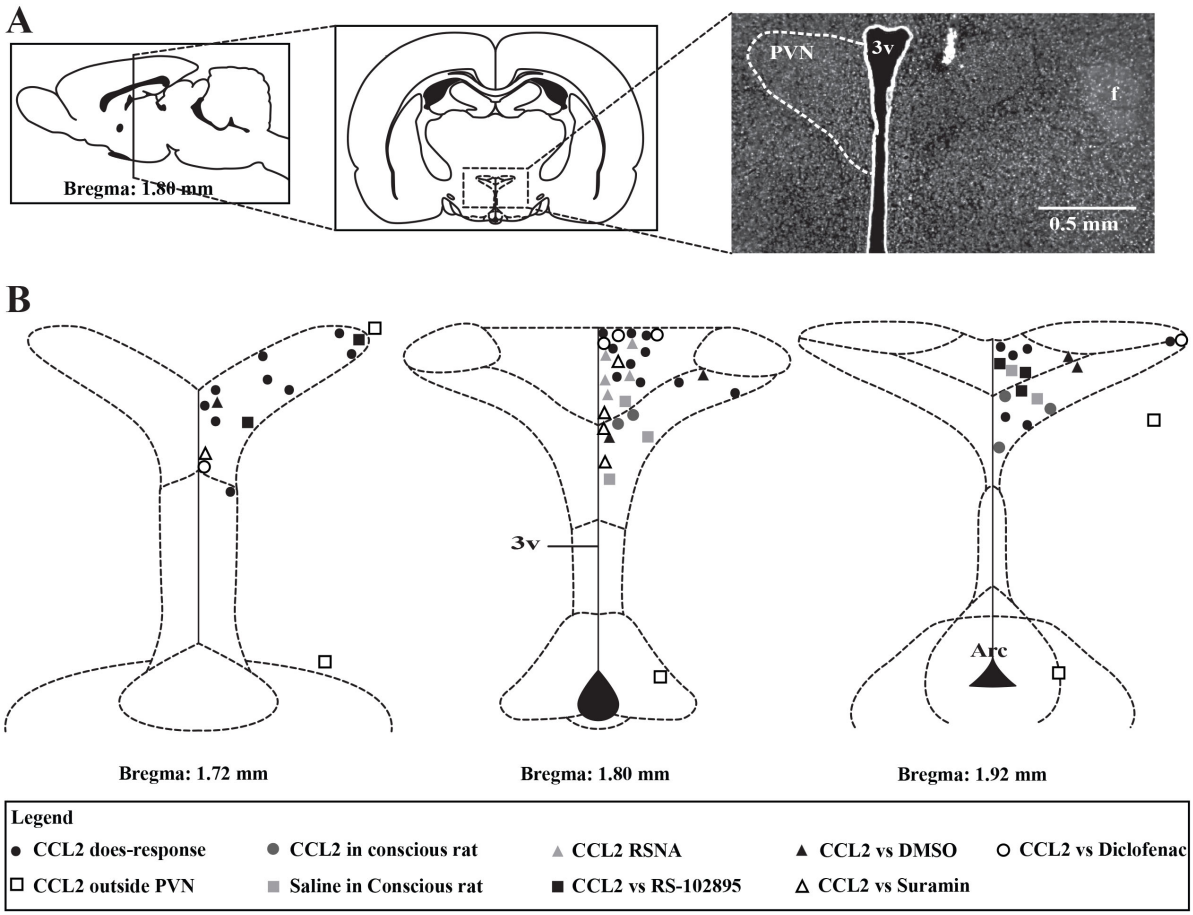
Supplementary Figure 3.3: Baseline controls of drugs microinjected into the PVN.

(A) Grouped MAP of CCL2 (71 nmol/L) microinjected outside the PVN (□ in online figure V), and saline. **(B)** Baseline MAP effects of PVN administration of saline, DMSO, RS-102895, suramin or diclofenac. **(C)** Baroreflex modulation of RSNA. BP and RSNA following intravenous administration of phenylephrine 5 µg/kg, and pulse modulation of RSNA (n= 5 rats per group).



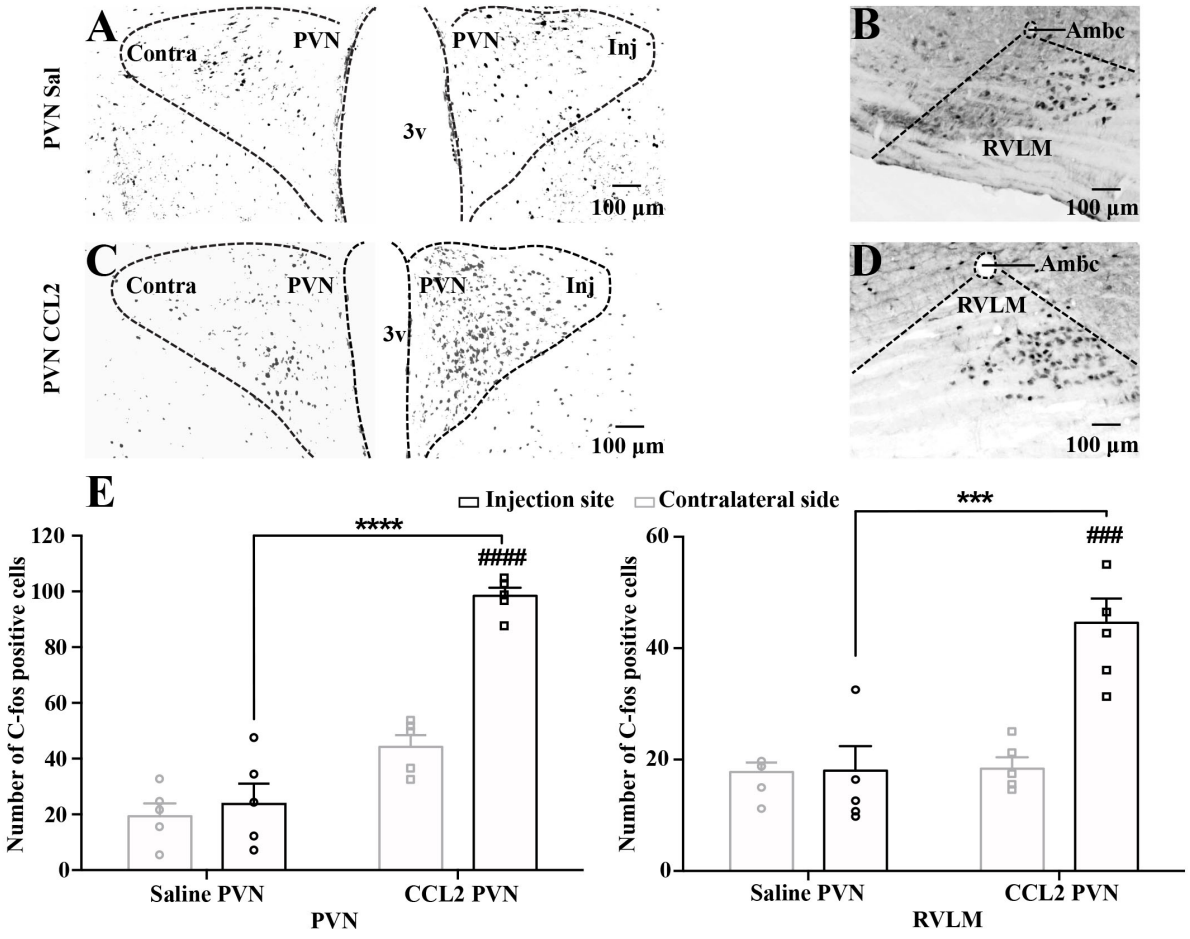
<u>Supplementary Figure 3.4:</u> L-glutamate PVN microinjection in anaesthetized and conscious rats.

(A) Representative recordings of HR and MAP, **(B)** and time course changes in MAP and HR following PVN microinjection with L-glutamate (10 mmol/L) in conscious rats in comparison to saline.



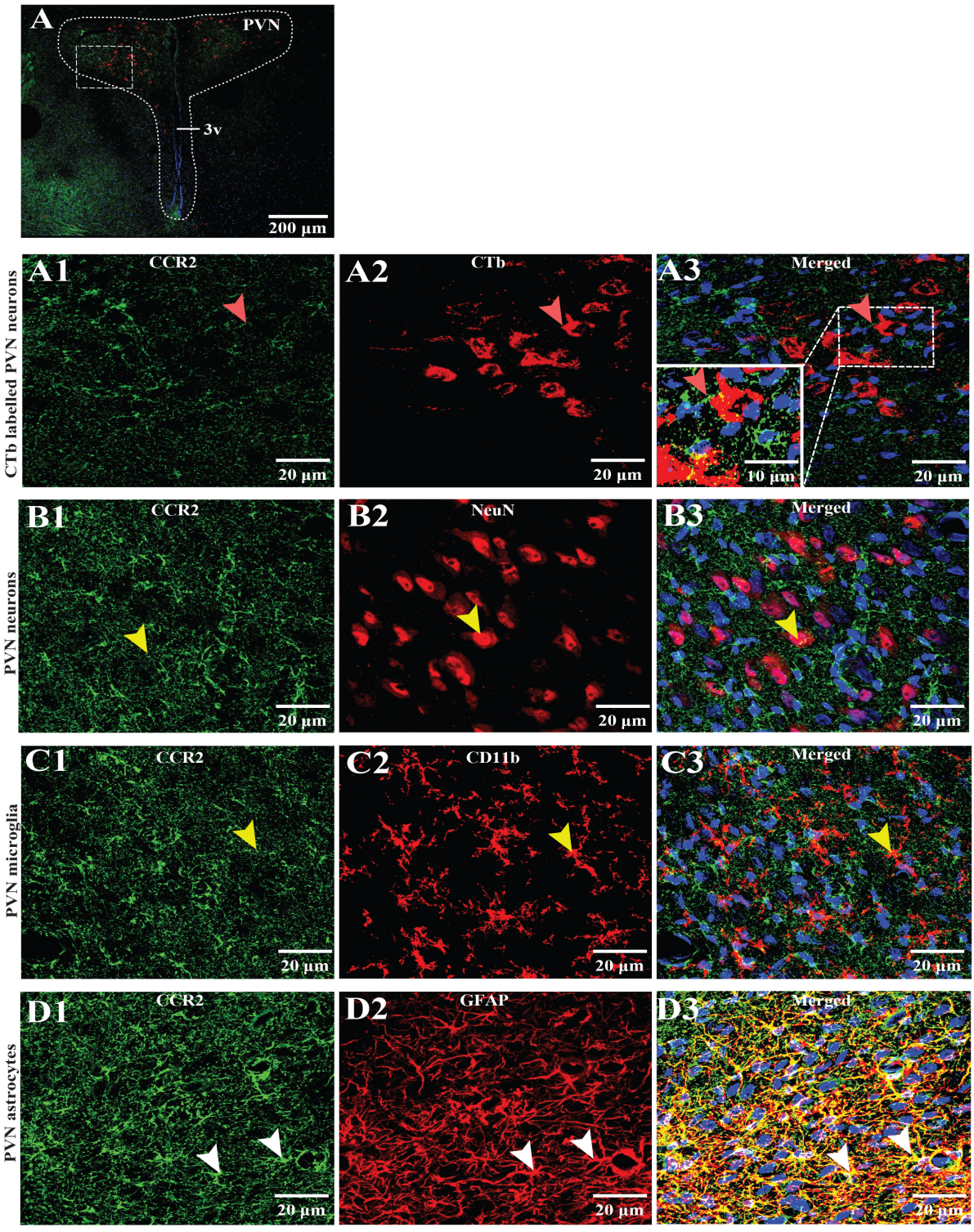
Supplementary Figure 3.5: Validation of PVN microinjections.

(A) Representative photomicrograph of a PVN injection site. **(B)** A schematic coronal diagram mapping all PVN injection sites. 3v; third ventricle, Arc; Arcuate nucleus, f; fornix, PVN; paraventricular nucleus of the hypothalamus. Schematic diagrams modified from (Paxinos G 2007).



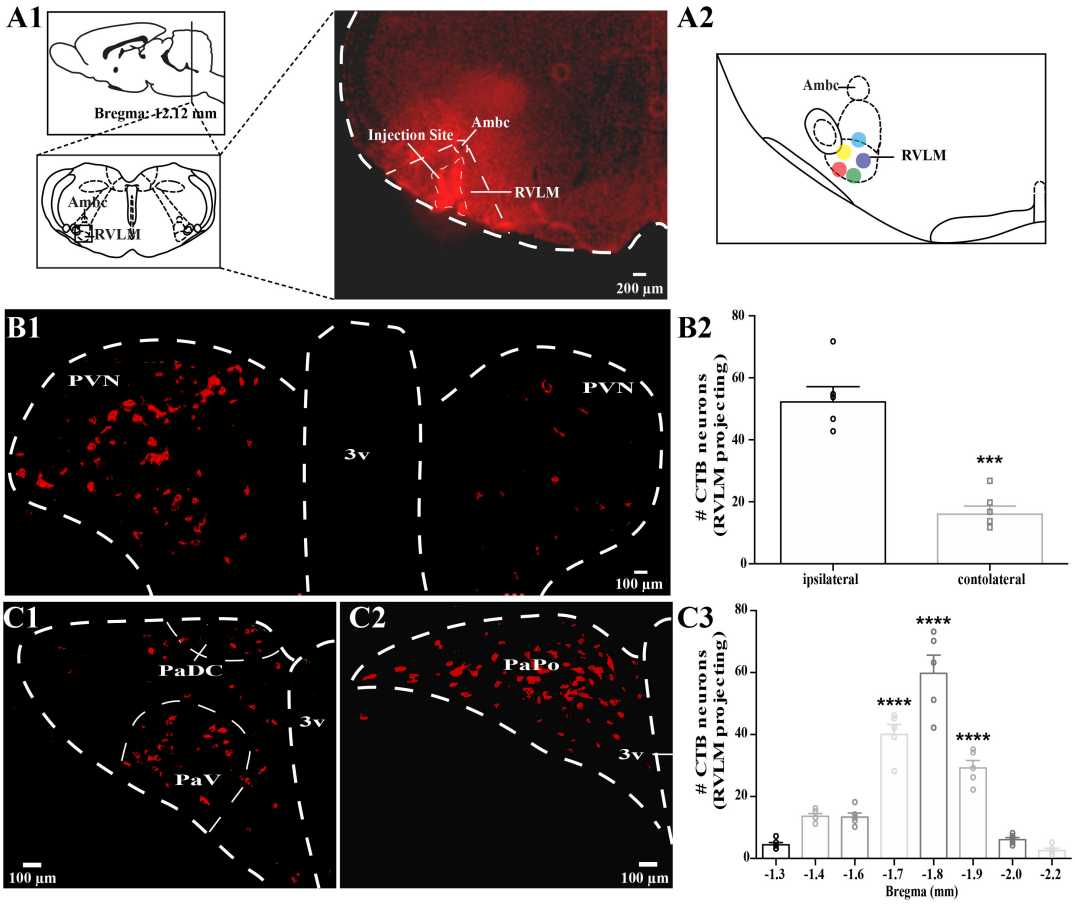
<u>Supplementary Figure 3.6:</u> C-fos in the PVN and the RVLM following PVN microinjections with CCL2.

(A-D) Photomicrographs of the PVN (A and C) and the RVLM (B and D) labelled with the neuronal activation marker c-fos following PVN microinjection with saline (A-B) or CCL2 (C-D). **(E)** Count of c-fos positive nuclei in the PVN and the RVLM following PVN microinjection with saline or CCL2. 3v; third ventricle, Ambc; compact part of the nucleus ambiguous, PVN; paraventricular nucleus of the hypothalamus, RVLM; rostral ventrolateral medulla, $^{***}P\leq0.001$, $^{****}P\leq0.0001$; one-way ANOVA of CCL2 vs. saline, $^{###}P\leq0.001$, $^{####P}\leq0.0001$; one-way ANOVA of injected vs. contralateral site (n=5 rats per group).


A
PVN
3v
200 µm
CTb labelled PVN neurons
A1
CCR2
20 µm
A2
CTb
20 µm
A3
Merged
10 µm
20 µm
PVN neurons
B1
CCR2
20 µm
B2
NeuN
20 µm
B3
Merged
20 µm
PVN microglia
C1
CCR2
20 µm
C2
CD11b
20 µm
C3
Merged
20 µm
PVN astrocytes
D1
CCR2
20 µm
D2
GFAP
20 µm
D3
Merged
20 µm

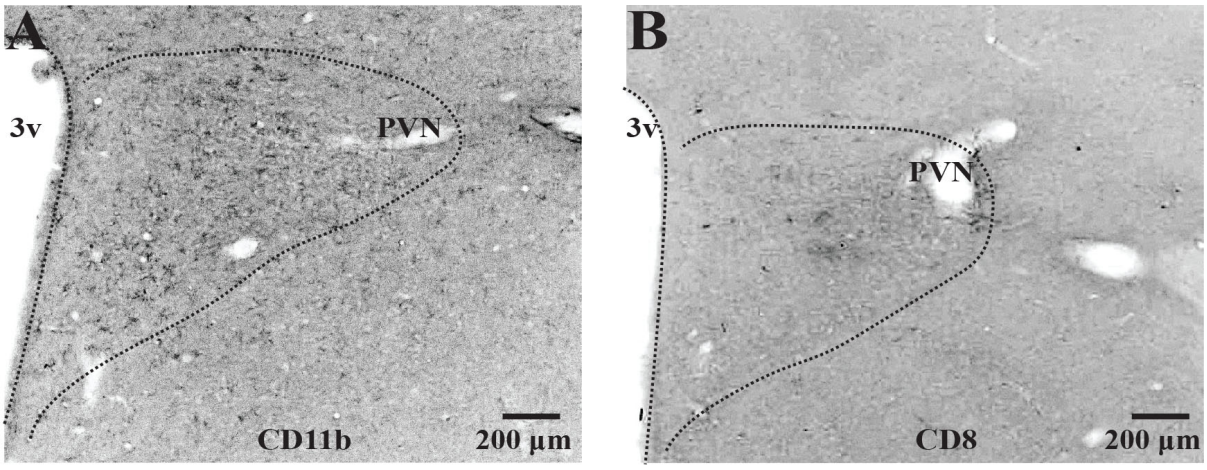
<u>Supplementary Figure 3.7:</u> Colocalization of CCR2 receptors with other cell types in the PVN.

(A) Low power photomicrograph of the PVN. **(A1-A3)** High power photomicrographs of the PVN labelled with CTb and CCR2. Red arrows = close apposition of CCR2 to CTb neurons. **(B1-B3)** High power photomicrographs of the PVN labelled with the neuronal marker NeuN and CCR2. **(C1-C3)** High power photomicrographs of the PVN labelled with the microglia marker CD11b and CCR2. Yellow arrows; minimal expression of CCR2 receptors. **(D1-D3)** Representative photomicrographs of the PVN labelled with the astrocytic marker GFAP and CCR2. White arrows; co-localization of CCR2 and GFAP. 3v; third ventricle, PVN; paraventricular nucleus of the hypothalamus.



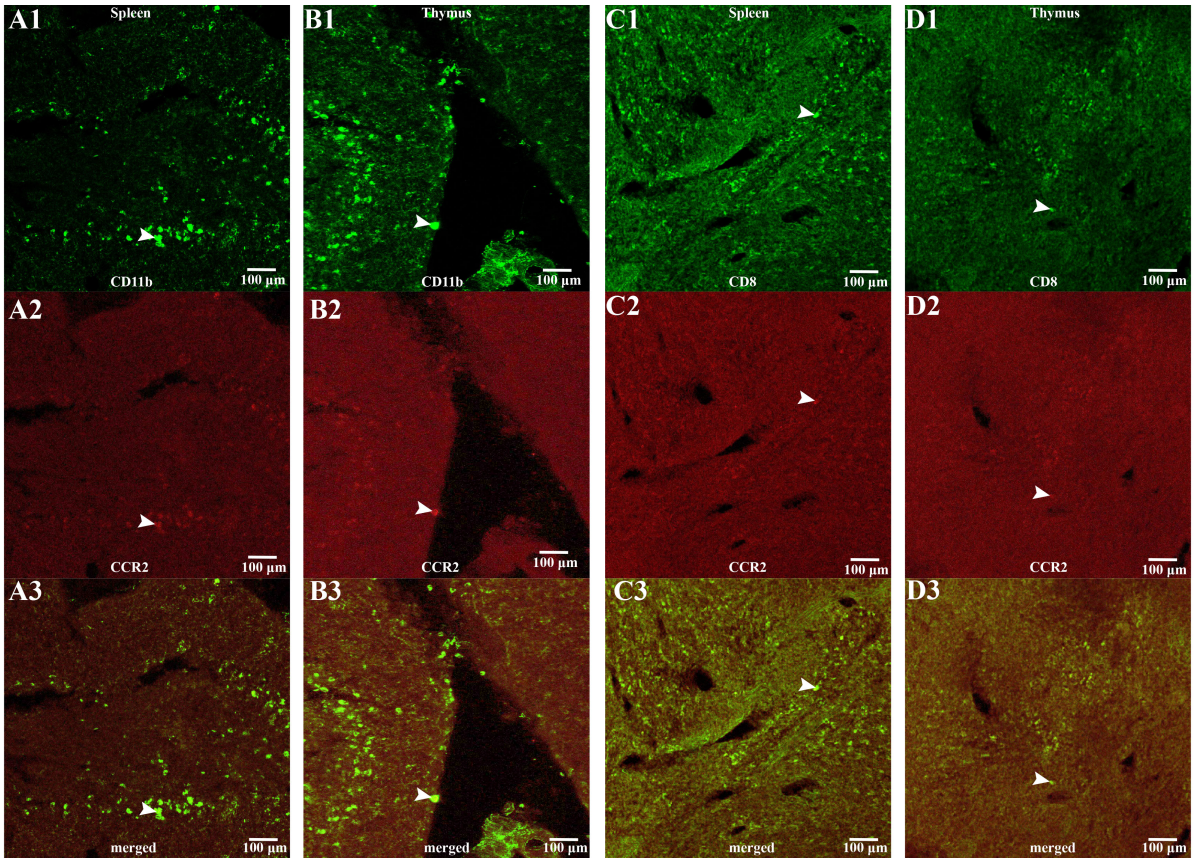
<u>Supplementary Figure 3.8</u>: Validation of RVLM microinjections.

(A1) Representative photomicrograph of RVLM injection site (CTb). **(A2)** A schematic coronal diagram mapping all injection sites. **(B1)** Representative photomicrograph of CTb positive neurons in the PVN, **(B2)** and grouped cell count of CTb positive neurons in the PVN, depicting more positive neurons labelled with CTb ipsilaterally following microinjection of CTb into the RVLM. **(C1-C2)** Photomicrographs of CTb positive neurons at different levels from bregma, depicting the majority of labelled neurons to be localized to the PaDC, PaV, PaPo regions of the PVN, **(C3)** and grouped cell count of CTb positive neurons at different levels from bregma. 3v; third ventricle, Ambc; compact part of the nucleus ambiguous, PaDC; dorsal cap of PVN, PaPo; medial PVN, PaV; ventral PVN, PVN; paraventricular nucleus of the hypothalamus, RVLM; rostral ventrolateral medulla. $^{***}P\leq0.001$; student t-test of ipsilateral vs. contralateral, $^{****}P\leq0.0001$; one-way ANOVA of different levels from bregma (n=5 rats per group). Schematic diagrams modified from (Paxinos G 2007).



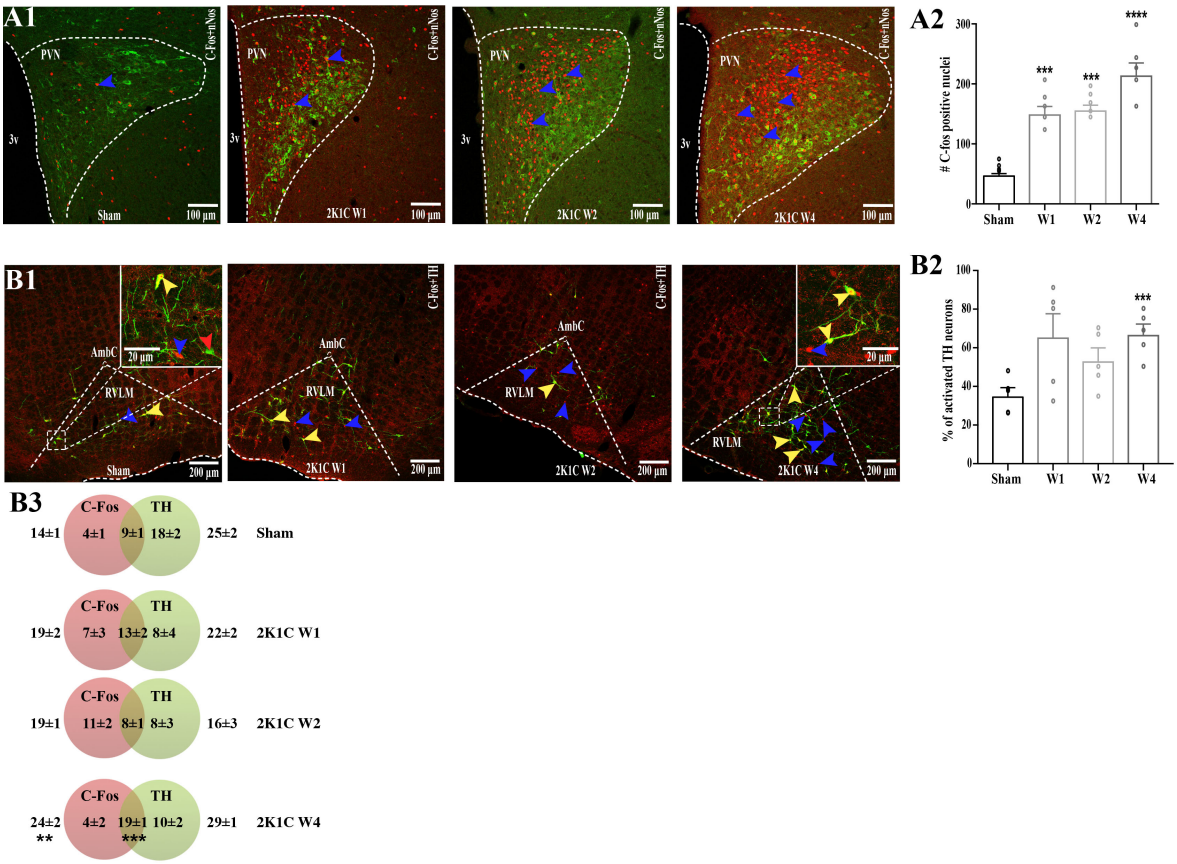
<u>Supplementary Figure 3.9</u>: Immune profile in PVN microinjected with saline.

(A) Representative micrograph of a PVN microinjected with saline and labelled with the macrophage marker CD11b **(A)**, or the mononuclear immune cell marker CD8 **(B)**. 3v; third ventricle, PVN; paraventricular nucleus of the hypothalamus.



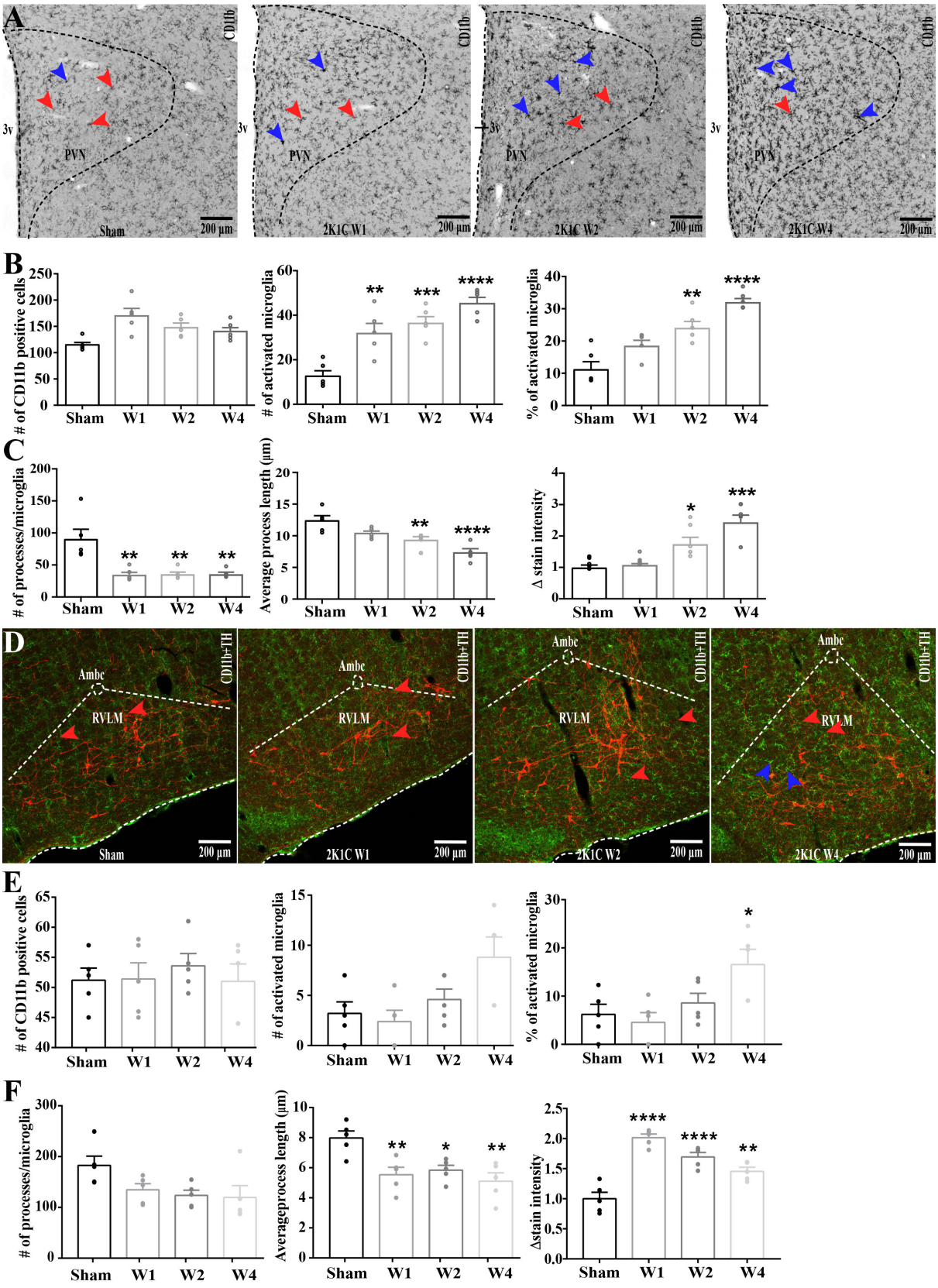
Supplementary Figure 3.10: CCR2 expression in splenic and thymic immune cells.

Representative photomicrograph of a spleen **(A)** or a thymus **(B)** section showing macrophages labelled with CD11b and CCR2 receptors, or mononuclear immune cells labelled with CD8 **(C-D)**. White arrows; co-localization with CCR2 receptors.



<u>Supplementary Figure 3.11:</u> C-fos activity in the PVN and the RVLM of the renovascular model of hypertension.

(A1) Representative photomicrographs of the PVN, **(A2)** and the count of the number of c-fos positive nuclei in the PVN. **(B1)** Representative photomicrographs of the RVLM, **(B2)** and the percentage of tyrosine hydroxylase (TH) c-fos positive double labelling in the RVLM, **(B3)** and a Venn diagram showing the number of c-fos positive nuclei, TH positive neurons, and double positive neurons. Blue arrow; c-fos positive nuclei, yellow arrow; TH/C-fos double positive neuron, red arrow; TH positive/c-fos negative neuron. $^{**}P \leq 0.01$, $^{***}P \leq 0.001$**;** one-way ANOVA of 2K1C vs. sham (n=5 rats per group).


A
CD11b
3v
PVN
Sham
2K1C W1
2K1C W2
2K1C W4
200 µm
B
# of CD11b positive cells
# of activated microglia
% of activated microglia
Sham
W1
W2
W4
C
# of processes/microglia
Average process length (µm)
Δ stain intensity
D
CD11b+TH
Ambc
RVLM
E
F
Averageprocess length (µm)
Δstain intensity

Supplementary Figure 3.12: Microglia activation in the PVN and the RVLM of the renovascular model of hypertension.

(A) Representative photomicrographs of the PVN, **(B)** % of the activated microglia using manual quantification, **(C)** and semi-automated FIJI quantification to indicate microglia activation in the PVN. **(D)** Representative photomicrographs of the RVLM, **(E)** % of the activated microglia using manual quantification, **(F)** and semi-automated FIJI quantification to indicate microglia activation in the RVLM. Blue arrow; activated microglia, red arrow; quiescent microglia. $^{**}P \leq 0.01$, $^{***}P \leq 0.001$**;** one-way ANOVA of 2K1C vs. sham (n=5 rats per group).

4. Blockade of the C-C Motif Chemokine Receptor Type 2 in the Brain Attenuates Blood Pressure Increases in Renovascular Hypertension

Remark: This chapter is in revision following peer review by *Journal of the American College of Cardiology (JACC)*.

4.1 Abstract

In neurogenic hypertension, activated macrophages are recruited to the paraventricular nucleus of the hypothalamus (PVN). The chemokine (C-C motif) ligand 2 (CCL2) and its cognate receptor, C-C motif chemokine receptor type 2 (CCR2), are involved in the activation and the recruitment of both macrophages and lymphocytes. Peripheral blockade of CCR2 receptors reduces blood pressure (BP) in rodent models of hypertension. However, it remains unclear whether the blockade of brain CCR2 receptors can reduce BP in hypertension. In this study we sought to determine whether blockade of CCR2 receptors, in the brain, reduces BP in renovascular hypertensive rats. We used the 2-kidney-1-clip model of renovascular hypertension. After renal artery clipping, these animals were subjected to constant infusion of a selective CCR2 antagonist (RS-102895; 70 μmol/L) into a lateral cerebral ventricle, using an osmotic minipump (2.5 μl/hour). BP was recorded via radio-telemetry for 8 weeks. The antagonism of brain CCR2 receptors prevented the increases in BP and macrophage recruitment in the PVN. There was also a significant reduction in the number of activated microglia and neurons in the brains of treated rats. Conversely, the administration of CCL2 (71 nmol/L) into a lateral cerebral ventricle of naïve rats resulted in recruitment of macrophages to the PVN and increased BP. Our findings show that in a renovascular model of hypertension blockade of brain CCR2 receptors prevents macrophage recruitment and activation of microglia and neurons in the PVN and reduces BP. These findings suggest that macrophage recruitment in the PVN is critical for the development of renovascular hypertension.

Key words: CCR2 receptors, hypertension, blood pressure, paraventricular nucleus, macrophages, neuroinflammation

4.2 Introduction

There is evidence that altered regulation of central autonomic function contributes to the development of angiotensin II-mediated and renovascular hypertension (Oliveira-Sales, Toward et al. 2014, Zubcevic, Santisteban et al. 2017). In particular, altered activity of neurons in the paraventricular nucleus of the hypothalamus (PVN) (Santisteban, Ahmari et al. 2015, Zubcevic, Santisteban et al. 2017)**,** the rostral ventrolateral medulla in the brainstem (RVLM) (Zubcevic, Santisteban et al. 2017, Korim, Elsaafien et al. 2018) and the area postrema (AP) (Zubcevic, Santisteban et al. 2017, Korim, Elsaafien et al. 2018). Neurons in the PVN, RVLM, and AP can increase sympathetic nerve activity (SNA), via neuronal projections to the cardiovascular organs, mediating increases in blood pressure (BP) (van der Kooy and Koda 1983, Dampney, Czachurski et al. 1987, Strack, Sawyer et al. 1989, Schramm, Strack et al. 1993).

Inflammation within the PVN, RVLM and AP plays important roles in the development of hypertension (Shi, Gan et al. 2011, Korim, Elsaafien et al. 2018). Pro-inflammatory cytokines are upregulated within the PVN and the RVLM in different rodent models of hypertension (Shi, Diez-Freire et al. 2010, Li, Qin et al. 2014). A major source of cytokine production in the brain of hypertensive rats is microglia (Shi, Diez-Freire et al. 2010). However, it was recently demonstrated that circulating macrophages can infiltrate the brain and might constitute a potential source of cytokines in the brains of hypertensive rats (Ishibashi, Hiasa et al. 2004, Santisteban, Ahmari et al. 2015, Wang, Kang et al. 2018). The chemokine (C-C motif) ligand 2 (CCL2) and its cognate receptor C-C motif chemokine receptor 2 (CCR2) play a pivotal role in the activation and the recruitment of macrophages (Lu, Rutledge et al. 1998). Administration of a selective CCR2 antagonist in the drinking water of hypertensive rats was shown to reduce the levels of pro-inflammatory cytokines and infiltrating macrophages in the kidney and the aortic vascular wall, and importantly to decrease BP (Bush,

Maeda et al. 2000, Elmarakby, Quigley et al. 2007, Chan, Moore et al. 2012). However, it is unclear to what extent these effects are dependent on peripheral or central inhibition of CCR2 receptors, and the effect of the selective blockade of CCR2 receptors in the brain on inflammation, macrophage recruitment and the development of hypertension has not been examined.

In this study, we hypothesize that CCL2-CCR2 signalling recruits macrophages to the PVN, inducing an inflammatory cascade that increases BP in hypertension. To examine this, we used a combination of hemodynamic recordings, biochemical assays, fluorescence activated cell sorting, and immunohistochemical studies to determine the effects of brain CCR2 receptor blockade on the increase in BP and the recruitment of macrophages and lymphocytes to autonomic brain regions in renovascular hypertension.

4.3 Methods and Materials

4.3.1 Experimental Protocol

The authors declare that all supporting data in the article and supplement are available from the corresponding author upon reasonable request.

Experiments were approved by the Florey Institute of Neuroscience and Mental Health Animal Ethics Committee and conformed to guidelines set out by the National Health and Medical Research Council of Australia. Male Sprague-Dawley rats were purchased from the Australian Resources Centre (ARC, Perth, Australia). Radio-telemetry transmitters (Data Sciences International, St Paul, MN) were implanted into the abdominal aorta. Following recovery, rats were subjected to either a implantation of a left renal artery clip (2 kidney-1clip; 2K1C) or a sham surgery, as previously described (Korim, Elsaafien et al. 2018). 2K1C animals received an infusion of either the CCR2 antagonist (RS-102895; 70 μmol/L) or the vehicle (artificial cerebrospinal fluid (aCSF)) into a lateral cerebral ventricle with an osmotic minipump (2.5 μl/hour, ALZET, Cupertino, CA). Sham (n=5), 2K1C-Veh (n=5), and 2K1C-RS (n=5) groups were infused for 8 weeks, while BP was simultaneously recorded twice a week (24 hours for each recording period). At the end of the protocol these animals were transcardially perfused, and brains were collected and fixed for immunohistochemical analysis.

An additional group of animals that included Sham (n=5), 2K1C-Veh (n=5), and 2K1C-RS (n=5) were infused into a lateral cerebral ventricle with RS-102895 or the vehicle for 8 weeks and then were euthanized, and micro-punches of the PVN, AP, and RVLM were collected for flow cytometric analysis. Plasma, CSF, hearts, kidneys and spleens were also collected.

In an acute experiment, naïve male Sprague-Dawley rats were an injection (1 μL) of either saline (0.9% NaCl; n=5) or CCL2 (71 nmol/L; n=5) into a lateral cerebral ventricle,

while blood pressure was recorded via a femoral cannulation for 30 min, as previously described (Korim, Elsaafien et al. 2018). Animals were then euthanized, and micro-punches of the PVN were collected for flow cytometric analysis. Full details of all experimental parameters are described in chapter 2.

4.3.2 Immunohistochemical Analysis

Brain sections were cut at 30 μm thickness to obtain sections of the PVN, RVLM and AP. Sections were labelled with the microglia marker CD11b at 1:1000 dilution (mouse anti-rat CD11b, Bio-Rad Laboratories, Gladesville, Australia), to examine the activation state of microglia as previously described (Korim, Elsaafien et al. 2018). To quantify the number of activated neurons, sections were labelled with the neuronal activation marker c-Fos at 1:1000 dilution (rabbit anti-rat c-Fos, Synaptic Systems, Goettingen, Germany). A confocal laser-scanning microscope (Leica TCS SP8^{TM}; Leica GmbH, Wetzlar, Germany) was used to obtain images for analysis in FIJI open source image analysis software (NIH).

4.3.3 Enzyme-Linked Immunosorbent Assay (ELISA)

Levels of CCL2 in plasma and CSF samples were detected using a rat MCP-1 Picokine^{TM} ELISA kit (BosterBio, Pleasanton, CA). Samples were diluted at 1:4 in the sample diluent buffer, and manufacturer's instructions were followed. The plate was read at 450 nm using a microplate spectrophotometer reader (Bio-Rad), so that optical densities from samples are obtained to construct a standard curve for the determination of the concentrations of CCL2 in each sample.

4.3.4 Fluorescence Activated Cell Sorting

Tissue obtained from the PVN, AP, and RVLM was homogenized manually through tissue mincing, and enzymatically through the incubation in a digestive enzyme cocktail at 37ºC (TrypLE Express; Life Technologies Corporation, and Liberase TL Research Grade; Roche). The cell suspension was then filtered through a 70 μm cell strainer. Conjugated antibodies at 1:200 (mice anti-rat CD45-APC/Fire750; BioLegend, mice anti-rat CD11b-PE/CY5; Abcam, and mice anti-rat CD3-BV421; Biosciences) were then added to the suspension. Samples were then analysed using a CytoFlex S analyser (Beckman Coulter, Sydney, Australia).

4.3.5 Statistical Analysis

Parametric statistical analysis was performed using one-way, or two-way ANOVA, with the Bonferroni correction. All data are presented as mean± SEM. $P<0.05$ was used to determine statistically significant differences between groups. MBP, SBP, DBP, and HR were recorded for 24-hours twice a week; to acquire both the light and the dark cycle. Analysis was performed on recordings extracted at 2, 3, 4 ,5 pm for the light cycle, and 2, 3, 4, 5 am for the dark cycle. Values of MBP, DBP, SBP, and HR were averaged for one light cycle and one dark cycle and compared between the different groups overtime using a two-way ANOVA. One-way ANOVA was used to compare data from immunohistochemical, FACS, and ELISA studies between the different groups. Student's t-test was used to compare FACS data between saline and CCL2 injected groups in the acute experiment.

4.4 Results

4.4.1 Blockade of Brain CCR2 Receptors Inhibits the Increase in BP in Renovascular Hypertension

During the first weeks after surgery, mean blood pressure (MBP) was increased in clipped compared with sham-clipped rats (Sham 96±3 mmHg, 2K1C-Veh 134±12 mmHg, 2K1C-RS 130±9 mmHg, $p<0.05$, n= 5; Figure 4.1B). Following the first week, the MBP of the clipped rats receiving central infusion of the CCR2 antagonist (RS-102895) decreased compared with the MBP of vehicle treated rats (2K1C-Veh 154±9 mmHg, 2K1C-RS 118±10 mmHg, $p<0.05$, n= 5; Figure 4.1B). During the second week MBP in both clipped groups decreased compared with MBP levels of the first week (Sham 98±2 mmHg, 2K1C-Veh 119±9 mmHg, 2K1C-RS 107±8 mmHg, $p>0.05$, n= 5; Figure 4.1B). In the third week, we observed the onset of a sustained increase in MBP in rats receiving the vehicle, which plateaued during the 4^{th}-5^{th} weeks. The MBP remained elevated until the 8^{th} week (Sham 98±1 mmHg, 2K1C-Veh 140±7 mmHg at week 8, $p<0.05$, n= 5; Figure 4.1A-B); whereas it was reduced by RS102895, returning to sham levels by the 4^{th}-5^{th} week; and this decrease in MBP was maintained up to the 8^{th} week (2K1C-Veh 140±7 mmHg, 2K1C-RS 100±4 mmHg at week 8, $p<0.05$, n= 5; Figure 4.1A-B) when the experimental endpoint was reached. Similar changes were observed in systolic (SBP) and diastolic (DBP) blood pressures during both the light and dark cycles (Figure 4.1C-D). However, no significant differences in heart rate (HR) were observed across the groups ($p>0.05$, n= 5, Figure 4.1E).

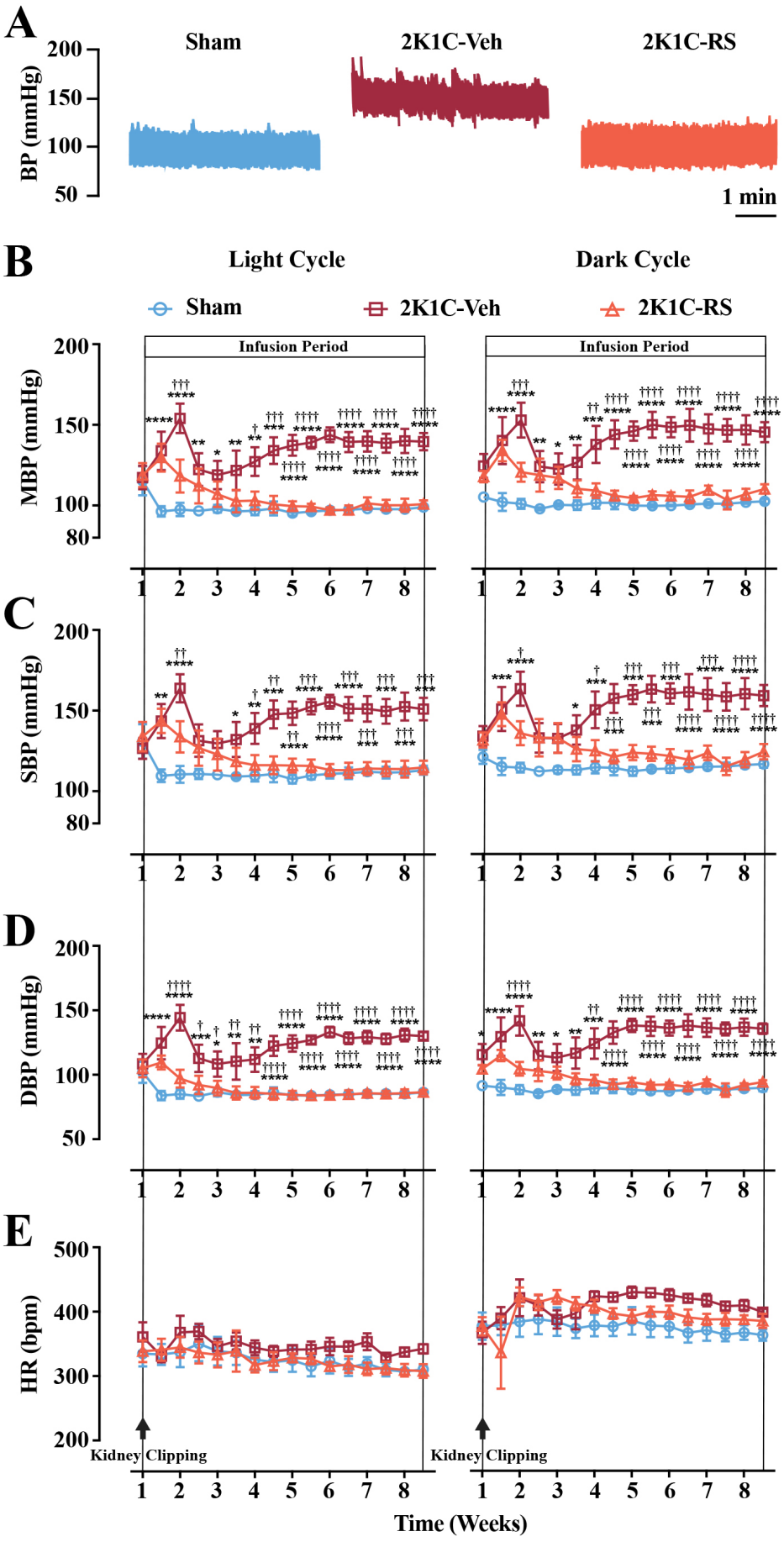
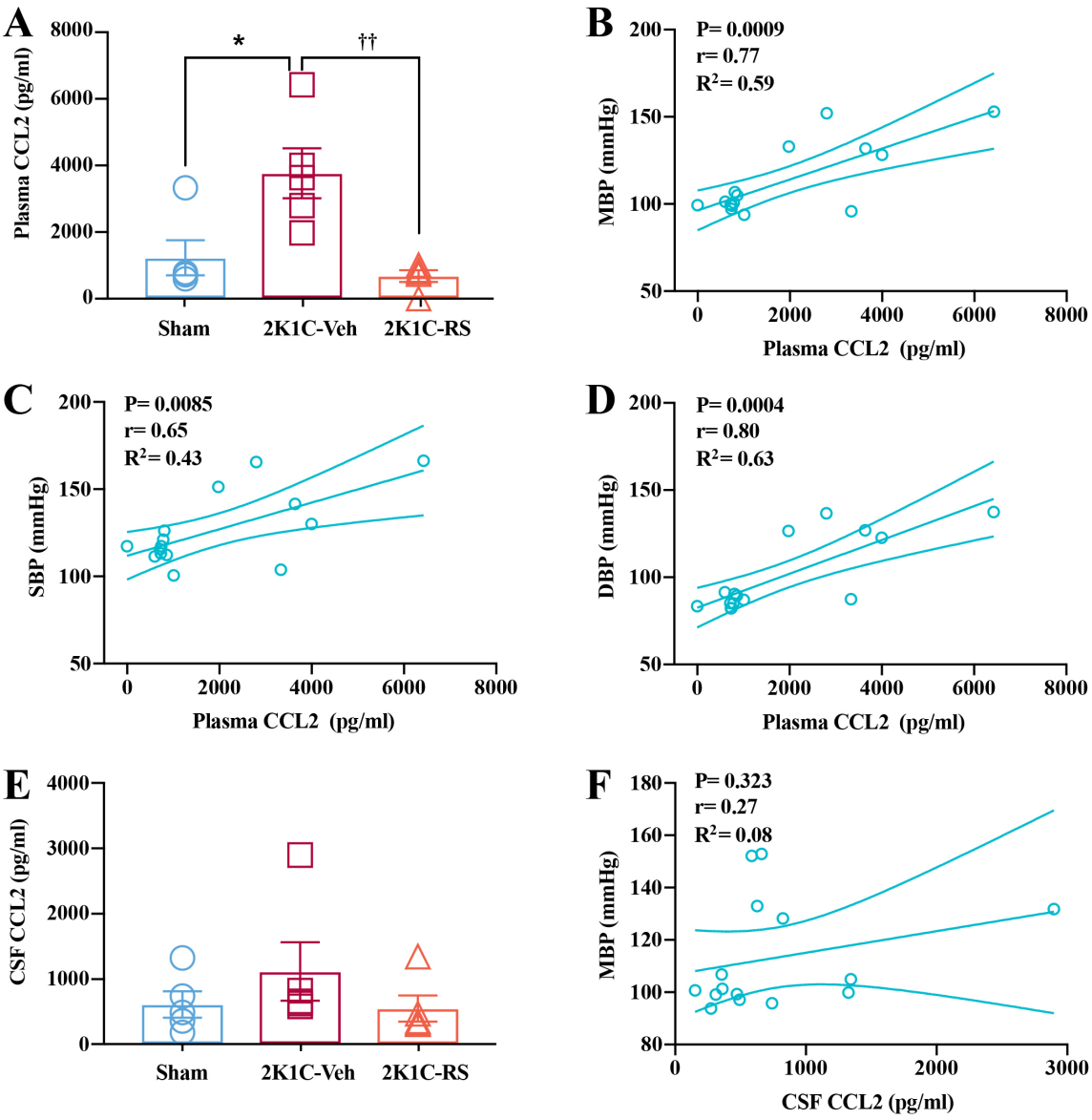

A
Sham
2K1C-Veh
2K1C-RS
BP (mmHg)
200
150
100
50
1 min
B
Light Cycle
Dark Cycle
Sham
2K1C-Veh
2K1C-RS
Infusion Period
MBP (mmHg)
C
SBP (mmHg)
D
DBP (mmHg)
E
HR (bpm)
Kidney Clipping
Time (Weeks)

Figure 4.1: Central blockade of CCR2 receptors prevents blood pressure increases in renovascular hypertension.

(A) Representative recordings of pulsatile blood pressure (BP) in sham controls and 2K1C rats receiving a vehicle infusion (aCSF, 2K1C-Veh), or 2K1C rats receiving the CCR2 antagonist infusion (RS-102895; 70 μmol/L, 2K1C-RS). Time course changes of mean blood pressure (MBP; **B**), systolic blood pressure (SBP; **C**), diastolic blood pressure (DBP; **D**), and heart rate (HR; **E**). $^{*}P\leq 0.05$, $^{**}P\leq 0.01$, $^{***}P\leq 0.001$, $^{****}P\leq 0.0001$; two-way ANOVA of sham vs. 2K1C-Veh, $^{\dagger}P\leq 0.05$, $^{\dagger\dagger}P\leq 0.01$, $^{\dagger\dagger\dagger}P\leq 0.001$, $^{\dagger\dagger\dagger\dagger}P\leq 0.0001$; two-way ANOVA of sham vs. 2K1C-RS, (n=5 rats per group).

4.4.2 Blockade of Brain CCR2 Receptors Prevents the Increase in Plasma CCL2 in Renovascular Hypertension

Plasma levels of CCL2 increased in 2K1C renovascular hypertensive rats (Sham 1232±526 pg/ml, 2K1C-Veh 3767±751 pg/ml, $p<0.05$, n= 5; Figure 4.2A). Blockade of brain CCR2 receptors prevented the increase in plasma levels of CCL2 in 2K1C hypertensive rats (2K1C-Veh 3767±751 pg/ml, 2K1C-RS 682±176 pg/ml, $p<0.05$, n= 5; Figure 4.2A). Changes in plasma levels of CCL2 correlated with changes in MBP (R^2= 0.59, P= 0.0009, n=15; Figure 4.2B), SBP (R^2= 0.43, P= 0.0085, n=15; Figure 4.2C), and DBP (R^2= 0.63, P= 0.0004, n=15; Figure 4.2D). However, no significant differences were found in the levels of CCL2 in the cerebrospinal fluid (CSF) between all groups (Sham 615±202 pg/ml, 2K1C-Veh 1119±447 pg/ml, 2K1C-RS 552±201 pg/ml, $p>0.05$, n= 5; Figure 4.2E). Additionally, no correlation was found between CSF levels of CCL2 and MAP (R^2= 0.08, P= 0.323, n=15; Figure 4.2F).



<u>Figure 4.2:</u> Central blockade of CCR2 receptors prevents increases of plasma CCL2 in renovascular hypertension.

(A) Plasma levels of CCL2 in sham, 2K1C-Veh, and 2K1C-RS. Correlation between plasma CCL2 levels and **(B)** MBP, **(C)** SBP, **(D)** DBP in all groups. **(E)** Cerebrospinal fluid (CSF) levels of CCL2 in sham, 2K1C-Veh, and 2K1C-RS. **(F)** Correlation between CSF CCL2 levels and MBP in all groups. $^{*}P \leq 0.05$; one-way ANOVA of sham vs. 2K1C-Veh, $^{\dagger\dagger}P \leq 0.01$; one-way ANOVA of sham vs. 2K1C-RS, (n=5 rats per group).

4.4.3 Blockade of Brain CCR2 Receptors Prevents the Recruitment of Macrophages to the PVN of Renovascular Hypertensive Rats

To determine if the blockade of brain CCR2 receptors prevents the recruitment of macrophages and lymphocytes into autonomic brain regions of 2K1C hypertensive rats, flow cytometric analysis was performed on tissue from the PVN, AP, and RVLM. The total number of $CD45^{+hi}CD11b^{+}$ cells (myeloid cells) was higher in the PVN of renovascular hypertensive rats receiving vehicle compared with rats in which CCR2 receptors were blocked (Sham 102±52 cells, 2K1C-Veh 481±64 cells, 2K1C-RS 65±7 cells, $p<0.05$, n= 5; Figure 4.3A&D). In contrast, in hypertensive rats there were no significant differences in the number of $CD45^{+hi}CD11b^{+}$ cells in the RVLM (Sham 377±76 cells, 2K1C-Veh 374±48 cells, 2K1C-RS 423±74 cells, $p>0.05$, n= 5; Figure 4.3C&D), although there was a tendency for the levels to be increased in the AP (Sham 36±9 cells, 2K1C-Veh 966±375 cells, 2K1C-RS 263±237 cells, $p>0.05$, n= 5; Figure 4.3B&D); however, this difference did not reach significance.

There were no differences between the groups in the total number of $CD45^{+hi}CD3^{+}$ cells (T lymphocytes) in the PVN (Sham 38±11 cells, 2K1C-Veh 30±10 cells, 2K1C-RS 12±3 cells, $p>0.05$, n= 5; Figure 4.3A&E) or AP (Sham 40±9 cells, 2K1C-Veh 37±8 cells, 2K1C-RS 39±22 cells, $p>0.05$, n= 5; Figure 4.3B&E). However, in the RVLM the number of lymphocytes was higher in renovascular hypertensive rats regardless of treatment (Sham 14±10 cells, 2K1C-Veh 68±5 cells, 2K1C-RS 72±9 cells, $p<0.05$, n= 5; Figure 4.3C&E).

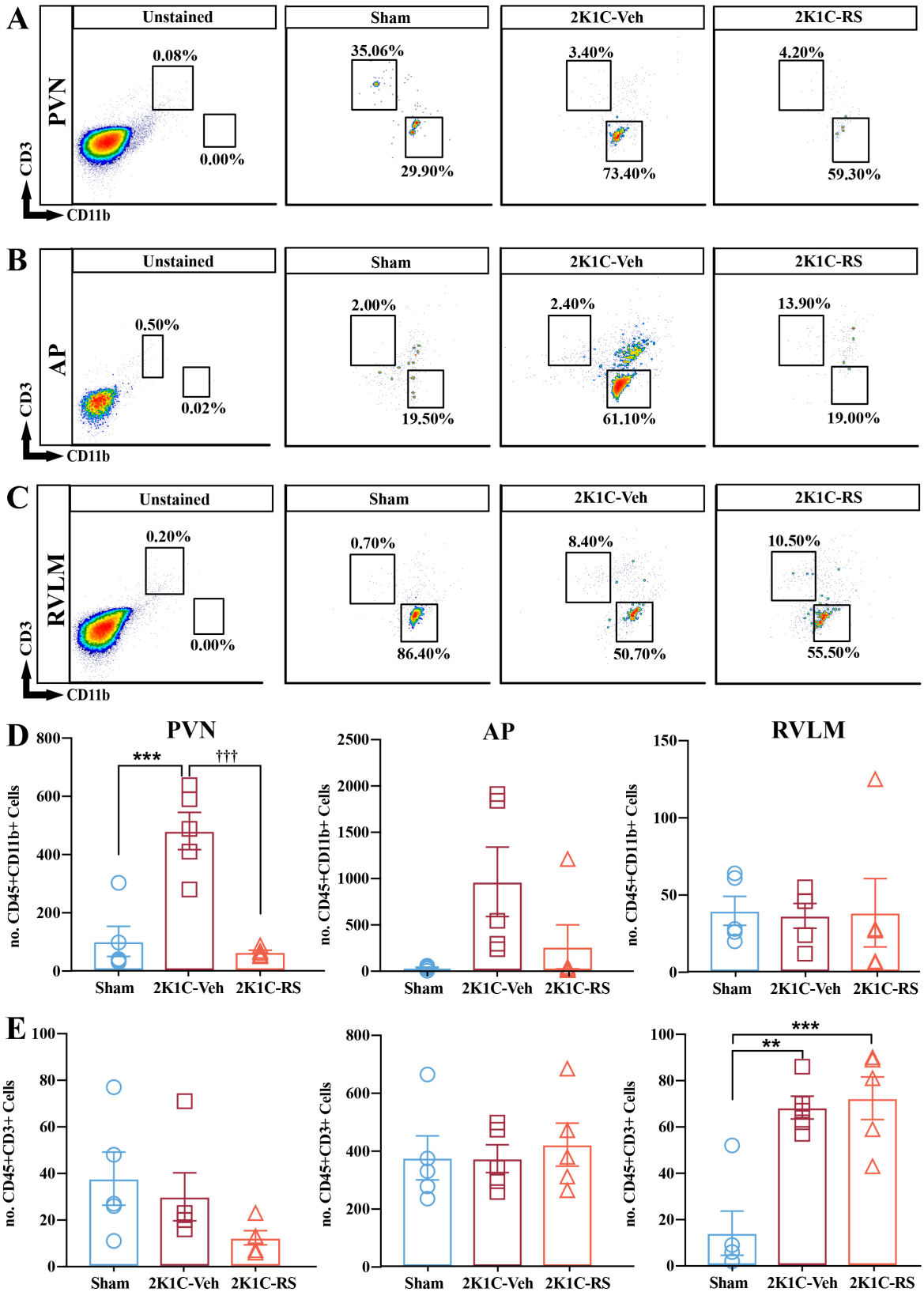

A
Unstained
Sham
2K1C-Veh
2K1C-RS
PVN
CD3
CD11b
0.08%
0.00%
35.06%
29.90%
3.40%
73.40%
4.20%
59.30%
B
AP
0.50%
0.02%
2.00%
19.50%
2.40%
61.10%
13.90%
19.00%
C
RVLM
0.20%
0.00%
0.70%
86.40%
8.40%
50.70%
10.50%
55.50%
D
PVN
AP
RVLM
no. CD45+CD11b+ Cells
***
†††
Sham
2K1C-Veh
2K1C-RS
E
no. CD45+CD3+ Cells
**
***

Figure 4.3: Central blockade of CCR2 receptors prevents macrophage recruitment to the PVN of renovascular hypertensive rats.

Representative flow cytometric charts of **(A)** PVN, **(B)** AP, and **(C)** RVLM of sham, 2K1C-Veh, and 2K1C-RS, total events; 100,000. Cell count of macrophages ($CD11b^+$ cells; **D**) and lymphocytes ($CD3^+$ cells; **E**). $^{**}P \leq 0.01$, $^{***}P \leq 0.001$; one-way ANOVA of sham vs. 2K1C-Veh, $^{\dagger\dagger\dagger}P \leq 0.001$; one-way ANOVA of sham vs. 2K1C-RS, (n=5 rats per group).

4.4.4 Blockade of Brain CCR2 Receptors Reduces Microglia Activation in the PVN of Renovascular Hypertensive Rats

To determine if the blockade of brain CCR2 receptors prevents local inflammation in cardiovascular centres of the brain induced by kidney hypoperfusion, sections of the PVN, AP and RVLM were labelled with the microglia marker CD11b. In the PVN, the proportion of activated microglia was higher in vehicle-treated renovascular hypertensive rats compared with CCR2 receptor antagonist treated rats (Sham 10±2 %, 2K1C-Veh 18±2 %, 2K1C-RS 6±1 %, $p<0.05$, n= 5; Figure 4.4A&D). In the AP, the percentage of activated microglia was higher in renovascular hypertensive rats regardless of the treatment compared with normotensive rats (Sham 5±1 %, 2K1C-Veh 15±4 %, 2K1C-RS 8±2 %, $p<0.05$, n= 5; Figure 4.4B&D). No differences in the RVLM were found between groups (Sham 7±2 %, 2K1C-Veh 9±2 %, 2K1C-RS 10±2 %, $p<0.05$, n= 5; Figure 4.4C&D).

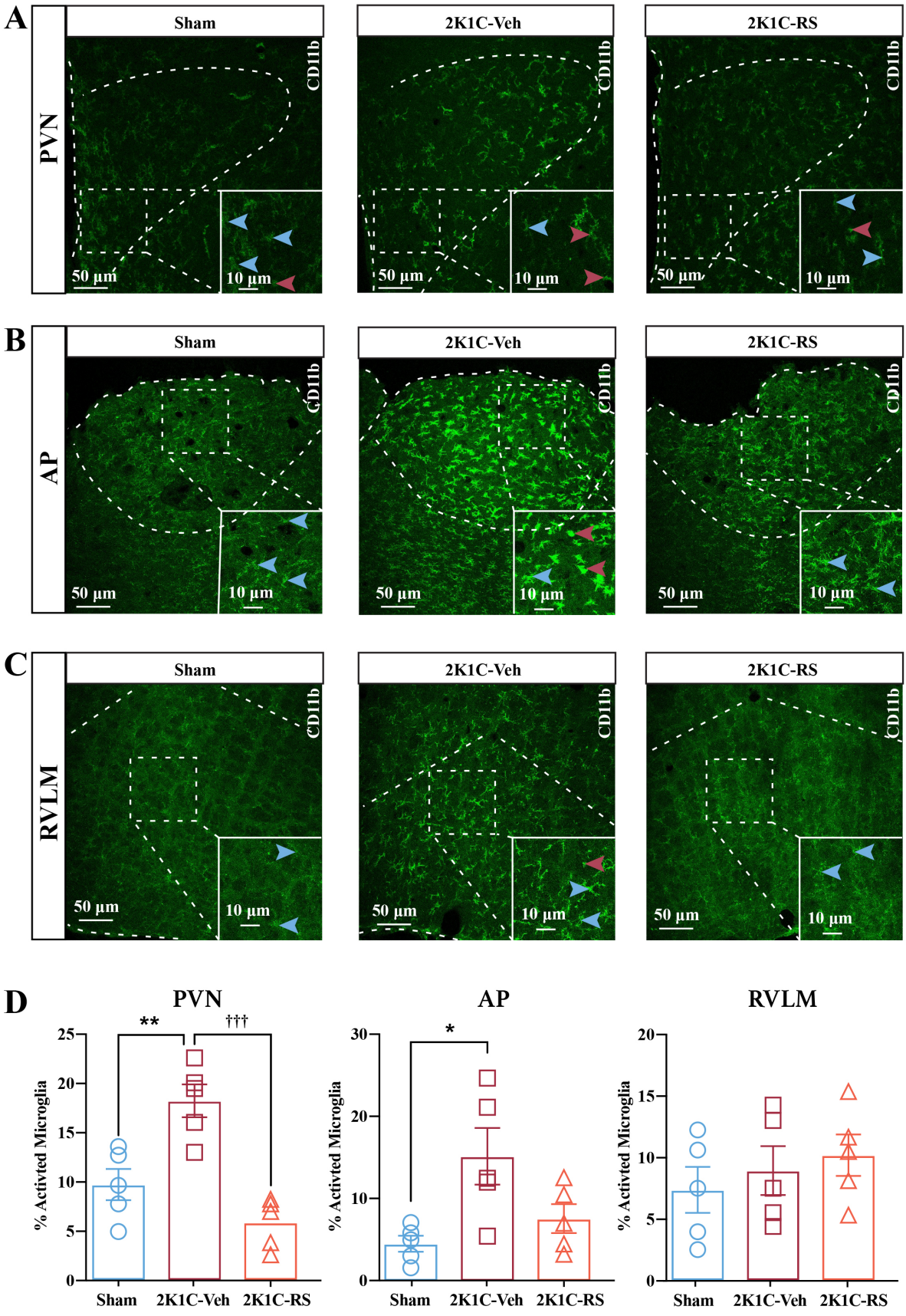

A
PVN
Sham
2K1C-Veh
2K1C-RS
CD11b
50 µm
10 µm
B
AP
C
RVLM
D
PVN
AP
RVLM
% Activted Microglia
**
†††
*
Sham
2K1C-Veh
2K1C-RS

Figure 4.4: Central blockade of CCR2 receptors prevents microglia activation in the PVN of renovascular hypertensive rats.

Representative images of **(A)** PVN, **(B)** AP, and **(C)** RVLM labelled with the microglia marker CD11b, in sham, 2K1C-Veh, and 2K1C-RS. **(D)** Average percentage of activated microglia in the PVN, AP, and RVLM. $^{*}P \leq 0.05$, $^{**}P \leq 0.01$; one-way ANOVA of sham vs. 2K1C-Veh, $^{\dagger\dagger\dagger}P \leq 0.001$; one-way ANOVA of sham vs. 2K1C-RS, (n=5 rats per group).

4.4.5 Blockade of Brain CCR2 Receptors Prevents Neuronal Activation in Autonomic Nuclei in Renovascular Hypertension

We also examined if central blockade of CCR2 receptors reduced the neuronal activation of brain regions that occurs in renovascular hypertension. CCR2 receptor blockade prevented the increase in c-Fos expression in the PVN (Sham 84±15 nuclei, 2K1C-Veh 201±13 nuclei, 2K1C-RS 56±9 nuclei; $p<0.05$, n= 5; Figure 4.5A&D), in the AP (Sham 14±4 nuclei, 2K1C-Veh 59±11 nuclei, 2K1C-RS 13±4 nuclei; $p<0.05$, n= 5; Figure 4.5B&D), and in the RVLM (Sham 7±2 nuclei, 2K1C-Veh 14±1 nuclei, 2K1C-RS 7±1 nuclei; $p<0.05$, n= 5; Figure 4.5C&D).

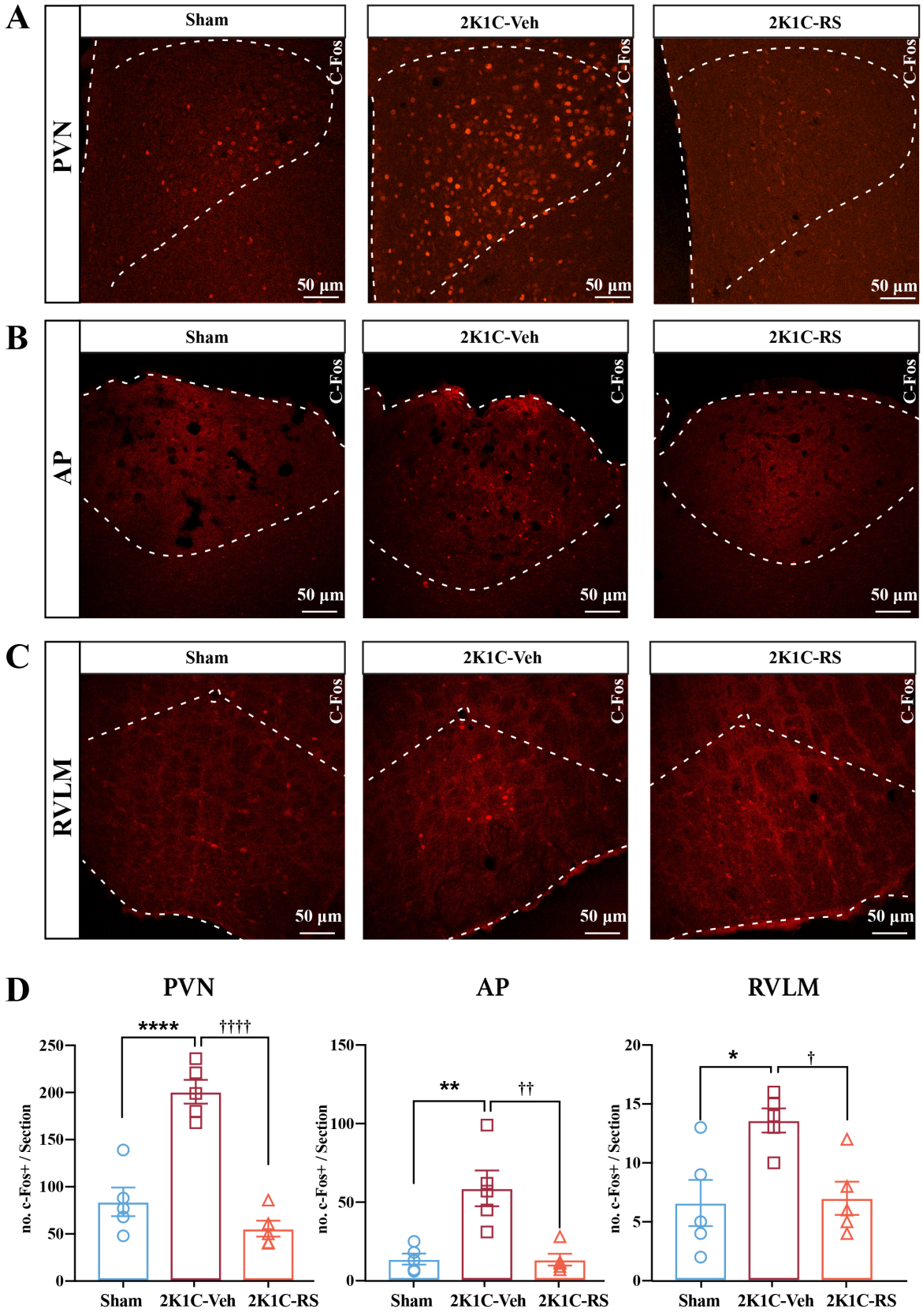

A
PVN
Sham
2K1C-Veh
2K1C-RS
C-Fos
50 µm
B
AP
Sham
2K1C-Veh
2K1C-RS
C-Fos
50 µm
C
RVLM
Sham
2K1C-Veh
2K1C-RS
C-Fos
50 µm
D
PVN
AP
RVLM
no. c-Fos+ / Section
****
††††
**
††
*
†
Sham
2K1C-Veh
2K1C-RS

Figure 4.5: Central blockade of CCR2 receptors prevents neuronal activation in renovascular hypertension.

Representative photomicrographs of **(A)** PVN, **(B)** AP, and **(C)** RVLM labelled with the neuronal activation marker c-Fos, in sham, 2K1C-Veh, and 2K1C-RS cohorts. **(D)** Average number of activated neurons in the PVN, AP, and RVLM. $^{*}P\leq0.05$, $^{**}P\leq0.01$, $^{****}P\leq0.0001$; one-way ANOVA of sham vs. 2K1C-Veh, $^{\dagger}P\leq0.05$, $^{\dagger\dagger}P\leq0.01$, $^{\dagger\dagger\dagger\dagger}P\leq0.0001$; one-way ANOVA of sham vs. 2K1C-RS, (n=5 rats per group).

4.4.6 Cardiovascular Effects of the Injection of CCL2 into a Lateral Cerebral Ventricle in Normotensive Rats

To determine if increasing the levels of CCL2 in the brain could recruit macrophages to the PVN and elicit increases in BP, we injected CCL2 (71 nmol/L) into a lateral cerebral ventricle of naïve, normotensive rats. Administration of CCL2 increased MBP (Saline - 5±3 Δ mmHg, CCL2 + 7±1 Δ mmHg, at time= 30 min, $p<0.05$, n=5; Figure 4.6A) and HR (Saline - 3±12 Δ bpm, CCL2 + 40±10 Δ bpm, at time= 30 min, $p<0.05$, n=5; Figure 4.6B). The total number of $CD45^{+hi}CD11b^{+}$ cells (macrophages) was higher in the PVN following CCL2 compared with saline injected controls (Saline 82±22 cells, CCL2 222±14 cells, $p<0.05$, n=5; Figure 4.6C-D). In contrast, no differences were found in the total number of $CD45^{hi+}CD3^{+}$ (lymphocytes) following CCL2 injection compared with saline injected controls (Saline 51±12 cells, CCL2 25±10 cells, $p>0.05$, n=5; Figure 4.6E-F).

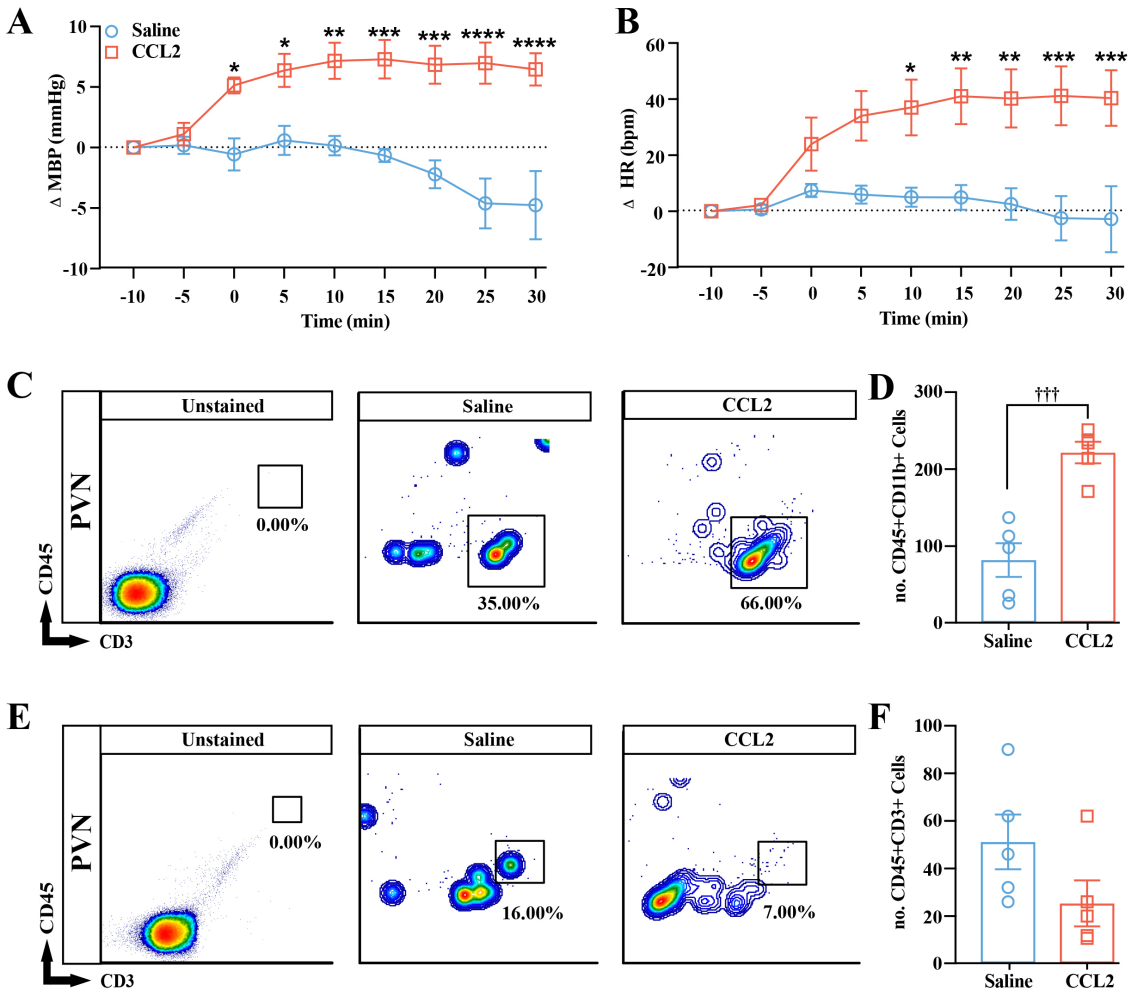


Figure 4.6: Central administration of CCL2 recruits' macrophages to the PVN and increases blood pressure.

Time course changes in **(A)** mean arterial pressure (MBP) and **(B)** heart rate (HR) following the injection of CCL2 (70 nmol/L) or vehicle (0.9% saline) into a lateral cerebral ventricle. Injections began between time = -5 and 0 min. **(C-F)** Representative flow cytometry charts of PVN macrophages ($CD11b^+$ cells; **C**) and lymphocytes ($CD3^+$ cells; **E**) in the PVN, and cell count of macrophages (**D**) and lymphocytes (**F**). $^{*}P\leq0.05$, $^{**}P\leq0.01$, $^{***}P\leq0.001$ $^{****}P\leq0.0001$; two-way ANOVA of saline vs. CCL2, $^{\dagger\dagger\dagger}P\leq0.001$; student's t-test of saline vs. CCL2, (n=5 rats per group).

4.5 Discussion

In this study we show that, in a rat model of renovascular hypertension, blockade of brain CCR2 receptors prevented the increase in plasma CCL2; the recruitment of circulating macrophages to the PVN; the activation of microglia in the PVN; neural activation in the PVN and the development of hypertension. Furthermore, we demonstrated in normotensive rats that injection of CCL2 into a lateral cerebral ventricle increased the number of macrophages in the PVN and raised blood pressure. Our results, indicating that the immune system and increased neuroinflammation contribute to increases in neural activation and BP, support the theory that the neuro-immune axis plays an important role in development of hypertension (Abboud, Harwani et al. 2012, de Kloet, Krause et al. 2013, Zubcevic, Santisteban et al. 2014, Harwani 2018, Elsaafien, Korim et al. 2019). In view of the evidence that circulating macrophages and lymphocytes, recruited by CCL2-CCR2 signalling (Elsaafien, Korim et al. 2019), can play a role in the development of hypertension (Marvar, Thabet et al. 2010, Jun, Zubcevic et al. 2012, Zubcevic, Jun et al. 2013, Santisteban, Ahmari et al. 2015, Ahmari, Santisteban et al. 2019), we investigated whether blocking central CCR2 receptors can reduce BP in a renovascular model of hypertension.

Our findings are consistent with previous reports in which the peripheral blockade of CCR2 receptors reduced BP in many rodent models of hypertension (Bush, Maeda et al. 2000, Elmarakby, Quigley et al. 2007, Chan, Moore et al. 2012). Previous studies have demonstrated that the administration of a selective CCR2 antagonist in the drinking water of hypertensive rats decreases BP (Bush, Maeda et al. 2000, Elmarakby, Quigley et al. 2007, Chan, Moore et al. 2012). The findings of these reports demonstrate that the peripheral blockade of CCR2 receptors, reduces the elevated levels of pro-inflammatory cytokines and infiltrating macrophages in the kidney (Elmarakby, Quigley et al. 2007) and the aortic vascular wall (Bush, Maeda et al. 2000, Chan, Moore et al. 2012). However, it is unclear whether these

effects are also mediated by the inhibition of CCR2 receptors in the brain. Thus, the present study demonstrates the importance of CCL2-CCR2 signalling in the brain in mediating the hypertensive phenotype. In renovascular hypertensive rats the initial transient increase in BP, seen immediately after clipping, is driven by the kidneys through the release of renin and angiotensin in the circulation (Martinez-Maldonado 1991). The sustained increase in BP occurs during the third week and plateaus by the fifth week (Martinez-Maldonado 1991, Oliveira-Sales, Toward et al. 2014). Similar hemodynamic changes were observed in our control renovascular hypertensive rats. We demonstrated that continuous infusion of a CCR2 antagonist into a lateral cerebral ventricle prevented the establishment of hypertension. CCR2 receptors are abundantly expressed on circulating macrophages, and are activated by the chemokine CCL2 to facilitate their entry to the brain (Lu, Rutledge et al. 1998). In hypertensive rats, macrophages are recruited to the PVN (Wang, Kang et al. 2018), and blocking this invasion of macrophages to the PVN reduced BP in angiotensin II- induced hypertension (Santisteban, Ahmari et al. 2015). Evidence that CCL2-CCR2 is required for the recruitment of macrophages is supported by the finding that macrophage recruitment is impaired in CCR2 knockout mice (Lu, Rutledge et al. 1998). Therefore, it is likely that in renovascular hypertension the selective blockade of brain CCR2 receptors reduced BP by inhibiting the recruitment of circulating macrophages to the PVN.

Blockade of brain CCR2 receptors also prevented increases in the plasma levels of CCL2 in the 2K1C hypertensive rats. Serum levels of CCL2 are increased in hypertensive patients (Antonelli, Fallahi et al. 2012) and in the plasma of renovascular hypertensive rats (Li, Qin et al. 2014). In fact, in angiotensin II- induced hypertension, increased levels of CCL2 form a chemotactic gradient towards the central nervous system (Santisteban, Ahmari et al. 2015). This gradient attracts macrophages to the brain through a CCL2-CCR2 mediated signalling mechanism (Lu, Rutledge et al. 1998, Santisteban, Ahmari et al. 2015). By contrast,

reducing BP in hypertension leads to a reduction in plasma levels of CCL2 (Li, Qin et al. 2014, Santisteban, Ahmari et al. 2015, Wang, Yu et al. 2018), and a correllation between BP and the plasma levels of CCL2 has been demonstrated (Antonelli, Fallahi et al. 2012). For example, infusion of the anti-inflammatory drug, pentoxyfilline, into the brain of hypertensive rats reduces BP and plasma levels of CCL2 (Sriramula, Cardinale et al. 2013). Similarly, in the present study we found that blockade of CCR2 receptors in the brain of renovascular hypertensive rats reduced plasma levels of CCL2 and also BP. Although we found the plasma levels of CCL2 increased in response to kidney hypoperfusion and the subsequent hypertension, there was no change in the levels of CCL2 in the CSF. This suggests that, in the brain, CCL2 is likely to be produced locally within specific brain regions and is not secreted into the CSF. This is supported by findings that in both the 2K1C and angiotensin II-induced rat models of hypertension, CCL2 is increased by approximately 3-fold in the PVN (Sriramula, Cardinale et al. 2013, Li, Qin et al. 2014). These data suggest that in the renovascular model of hypertension high levels of CCL2 in the PVN facilitate the invasion of macrophages, whilst blockade of CCR2 receptors prevents the invasion of macrophages, as demonstrated in our study.

We demonstrated that $CD45^{+hi}CD11b^{+}$ macrophages were recruited to the PVN of hypertesive rats and that blocking CCR2 receptors with a selective antagonist, RS102895, prevented the recruitment of macrophages into the PVN of hypertensive rats. This finding is consistent with the obervation that macrophages infiltrate the PVN in angiotensin II- induced hypertension (Santisteban, Ahmari et al. 2015, Wang, Kang et al. 2018). However, we did not observe recruitment of $CD45^{+hi}CD3^{+}$ lymphocytes to the PVN, whereas recruitment of lymphocytes was increased in the RVLM of the renovascular hypertensive rats. Previous studies have demonstrated the importance of the innate immune system during the pre-hypertensive stage (Harwani, Chapleau et al. 2012), and adaptive immunity during the

establishment of hypertension (Ahmari, Santisteban et al. 2019). This heterogeneity in the recruitment of the different immune subtypes suggests that the innate immune system may be involved in mediating hypertension, whereas the adaptive immune system is involved in sustaining the hypertension. In support of this notion, previous studies demonstrate a pronounced increase in the innate immune cell population at the pre-hypertensive stage (Harwani, Chapleau et al. 2012). Whereas lymphocytes are recruited in response to increases in blood pressure (Marvar, Thabet et al. 2010), and they infiltrate into the brain once hypertension is established despite the fact that neuro-inflammation had occurred prior to the lymphocyte invasion (Ahmari, Santisteban et al. 2019). Thus, there seems to be a heterogeneity in the recruitment of the different arms of the immune system during the progression and the development of hypertension, where the early recruitment of macrophages establishes an inflammatory state in the brain that increases BP (Harwani, Chapleau et al. 2012, Santisteban, Ahmari et al. 2015), and the late recruitment of lymphocytes sustains the elevation of BP (Marvar, Thabet et al. 2010, Ahmari, Santisteban et al. 2019). Similarly, our present results also suggest that immune cells are selectively recruited to the different autonomic regions of the brain. In the present study, we found that macrophage recruitment was specific to the PVN, not in the RVLM, although there was a trend towards a significant increase in the AP. This selectivity might be due to the fact that PVN is a highly vascularized brain region in which the blood-brain barrier becomes permeable in hypertension (Biancardi, Son et al. 2013), or that there is increased production of CCL2 specifically in the PVN of hypertensive rats (Wang, Kang et al. 2018). Together these findings suggest that CCL2-CCR2 signalling recruits circulating macrophages in the PVN (Wang, Kang et al. 2018), which increase the production of pro-inflammatory cytokines (Ishibashi, Hiasa et al. 2004, Santisteban, Ahmari et al. 2015).

The local release of pro-inflammatory cytokines and inflammatory mediators by the recruited macrophages are likely to activate microglia (Matsumoto, Dohgu et al. 2018) and

establish a local inflammatory state within the PVN (Shi, Diez-Freire et al. 2010, Santisteban, Ahmari et al. 2015, Sharma, Yang et al. 2019). Indeed, we found microglia to be activated in the PVN of renovascular hypertensive rats, confirming the establishment of a local inflammatory state within the PVN. In addition, we found that the infusion of a CCR2 antagonist into a lateral cerebral ventricle attenuated the recruitment of macrophages. This is similar to previous findings showing that peripheral blockade of CCR2 receptors reduced macrophage recruitment and inflammation in the kidneys and the aortic vascular wall in hypertensive rats (Bush, Maeda et al. 2000, Elmarakby, Quigley et al. 2007). Thus, blocking CCR2 receptors to prevent the establishment of a local inflammatory state, as indicated by fewer activated microglia, likely accounted for the prevention of the development of hypertension in renovascular hypertensive rats.

Previous reports demonstrate that the PVN, AP, and RVLM are activated in renovascular 2K1C rats (Li, Qin et al. 2014, Korim, Elsaafien et al. 2018). We found that antagonism of brain CCR2 receptors reduced the neuronal activation in the PVN, AP, and RVLM of renovascular hypertensive rats. Cytokines produced locally by recruited macrophages are capable of activating premotor neurons to increase SNA and BP (Shi, Gan et al. 2011, Korim, Elsaafien et al. 2018). It is possible that this immune-inflammatory process in the PVN excited efferent projections from the PVN and AP to the RVLM (van der Kooy and Koda 1983, Dampney, Czachurski et al. 1987, Strack, Sawyer et al. 1989, Schramm, Strack et al. 1993). Supporting the critical role of CCR2 receptors in this response, we demonstrated that CCR2 antagonism prevented the neuroinflammation, the neural activation and the development of hypertension in renovascular rats.

In order to determine whether CCL2 has the capacity to recruit macrophages to the PVN, we injected CCL2 into a lateral cerebral ventricle in normotensive rats, which would be expected to have low endogenous levels of CCL2 in the brain as demonstrated previously in

normotensive rats (Wang, Kang et al. 2018). This treatment resulted in the recruitment of macrophages to PVN, eliciting increases in BP. These findings are consistent with those in renovascular hypertensive rats, where plasma CCL2 levels were increased and macrophages were recruited to the PVN. We therefore propose that CCL2-CCR2 signalling plays an important role in recruiting macrophages to the PVN (Figure 4.7). The recruited macrophages synthesize and secrete pro-inflammatory cytokines (Ishibashi, Hiasa et al. 2004, Santisteban, Ahmari et al. 2015), which activate microglia (Matsumoto, Dohgu et al. 2018) and establish a local inflammatory state within the PVN (Shi, Diez-Freire et al. 2010, Santisteban, Ahmari et al. 2015, Sharma, Yang et al. 2019). The increased production of pro-inflammatory cytokines and the established inflammatory state activates neurons in the PVN and increases SNA to the cardiovascular organs (Shi, Gan et al. 2011, Korim, Elsaafien et al. 2018), leading to increases in BP and the development of hypertension (Figure 4.7). In summary, in renovascular hypertension inhibition of CCL2-CCR2 signalling in the brain prevents the recruitment of macrophages to the PVN and the activation of neurons in the PVN, resulting in prevention of the development of hypertension.

4.6 Perspectives

The present study shows that antagonism of brain CCR2 receptors prevented macrophage recruitment to the PVN and reduced the number of activated microglia and neurons in the PVN, inhibiting the development of hypertension. This highlights the importance of CCL2-CCR2 signalling in recruiting macrophages to the PVN to establish a local inflammatory state. This inflammatory state leads to the excitation of PVN neurons that ultimately leads to increasing BP. Finally, targeting central CCR2 receptors might be explored to develop future therapeutic antihypertensive interventions.

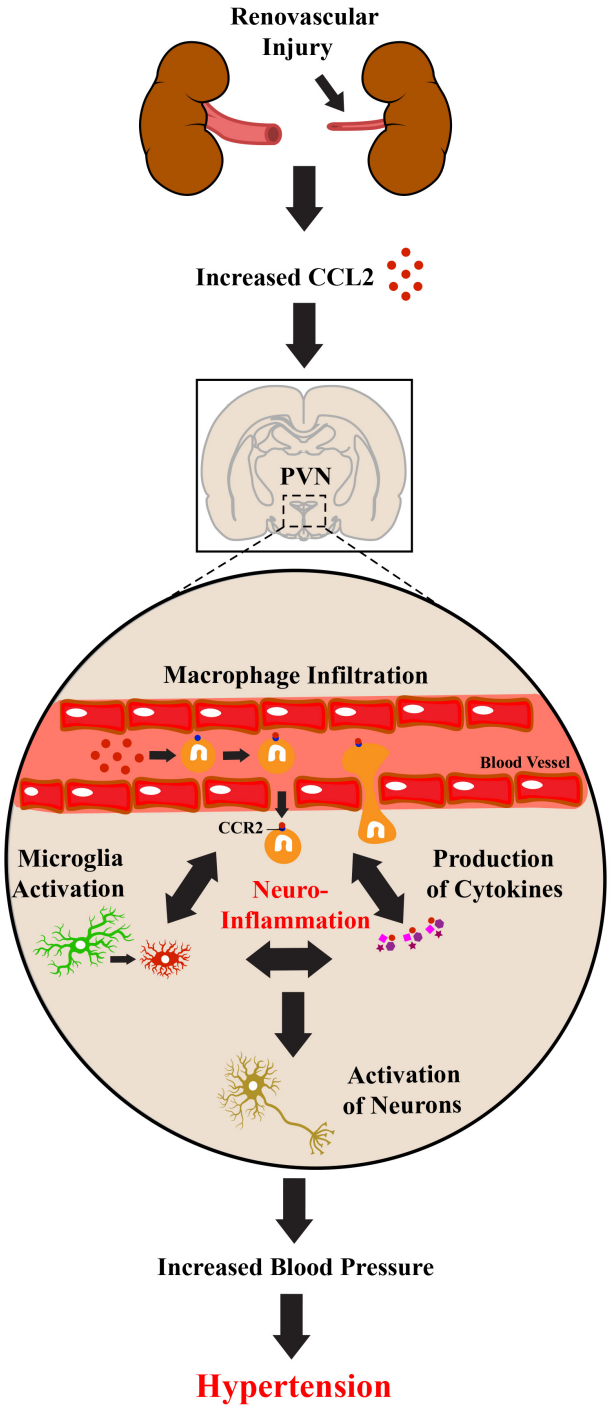


Figure 4.7: CCL2-CCR2 Signalling in the PVN causes Hypertension.

The proposed mechanism of action by which CCL2-CCR2 signalling in the PVN recruits' macrophages to invade the paraventricular nucleus of hypothalamus (PVN); inducing an inflammatory cascade that activates the neurons of the PVN, causing hypertension.

4.7 Novelty and Significance

What Is New?

- This study demonstrates that CCR2 receptors in the brain play a critical role in recruiting macrophages to central cardiovascular nuclei to mediate the development of hypertension in renovascular rats.
- The paraventricular nucleus of the hypothalamus is a key brain region targeted by circulating macrophages to establish a state of inflammation.
- Blockade of brain CCR2 receptors prevents the recruitment of macrophages to the paraventricular nucleus and reduces blood pressure in renovascular hypertensive rats.

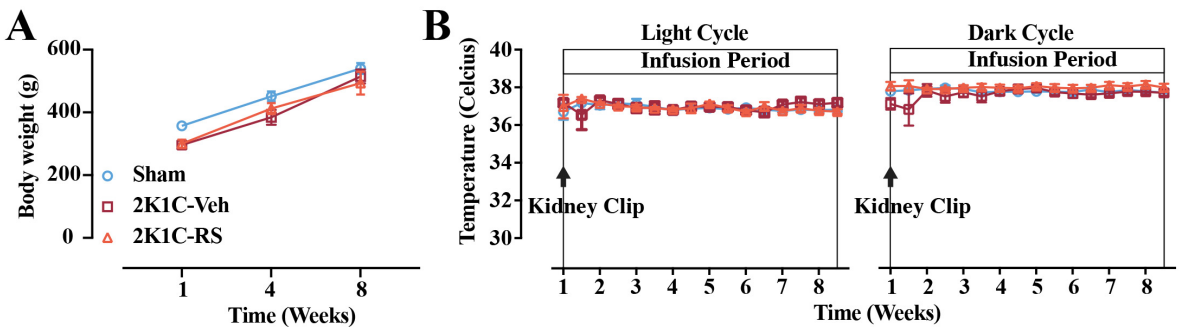
What Is Relevant?

- Circulating macrophages play a pivotal role in the development of renovascular hypertension by infiltrating the paraventricular nucleus of the hypothalamus.

Summary

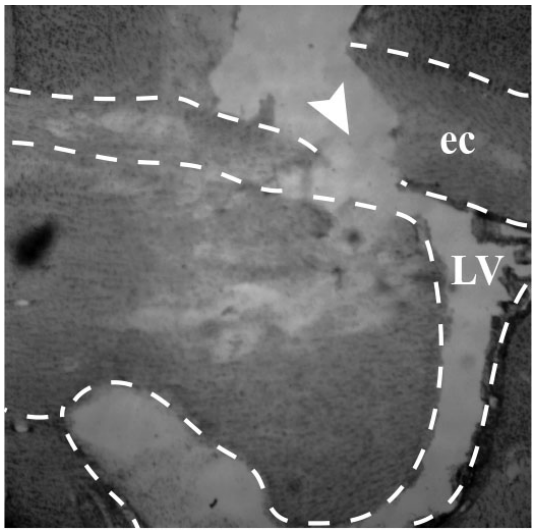
This study demonstrates that circulating macrophages are involved in the development of renovascular hypertension via a CCL2-CCR2 mediated mechanism within the paraventricular nucleus of the hypothalamus.

Supplemental Material



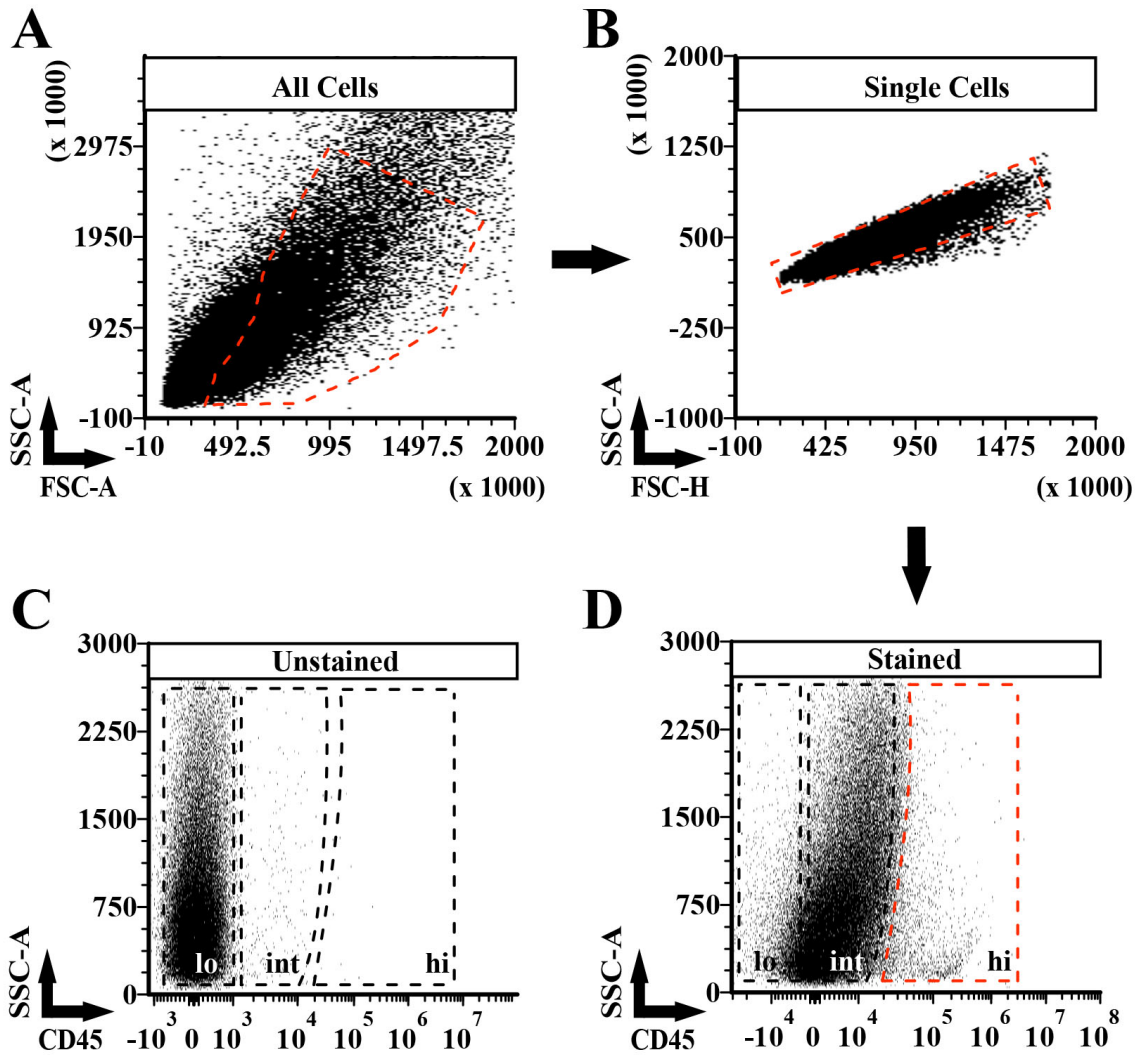
<u>Supplementary Figure 4.1:</u> Body weights and temperatures overtime in renovascular hypertensive.

(A) Average body weight, and **(B)** temperature in sham controls, 2K1C rats receiving a vehicle infusion (aCSF, 2K1C-Veh), or 2K1C rats receiving the CCR2 antagonist infusion (RS-102895; 70 µmol/L, 2K1C-RS). (n=5 per group).



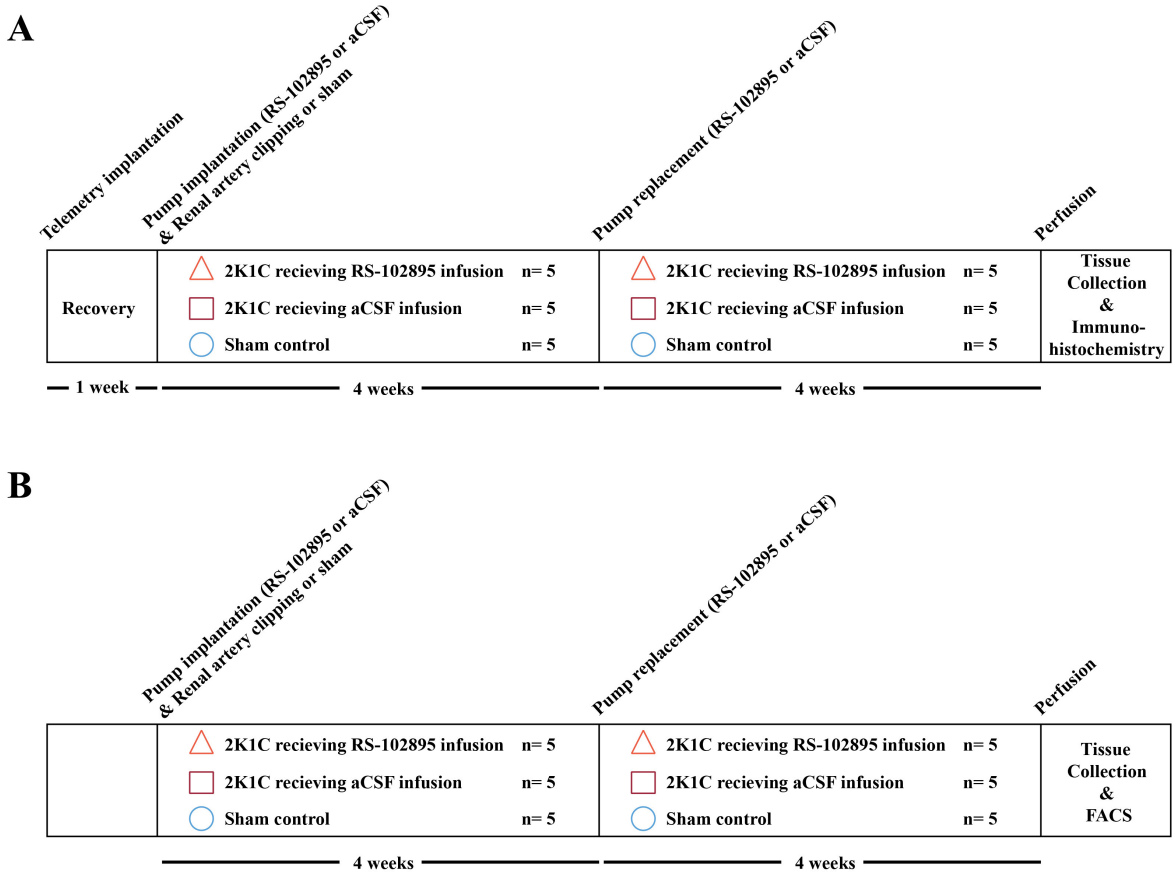
<u>Supplementary Figure 4.2:</u> Validation of intra-cerebroventricular (ICV) infusions.

The validity of ventricular infusion through the osmotic minipump was determined by post-mortem histology, were the rupture of the external capsule (ec), indicates the position of the infusion cannula into the left lateral ventricle (LV).



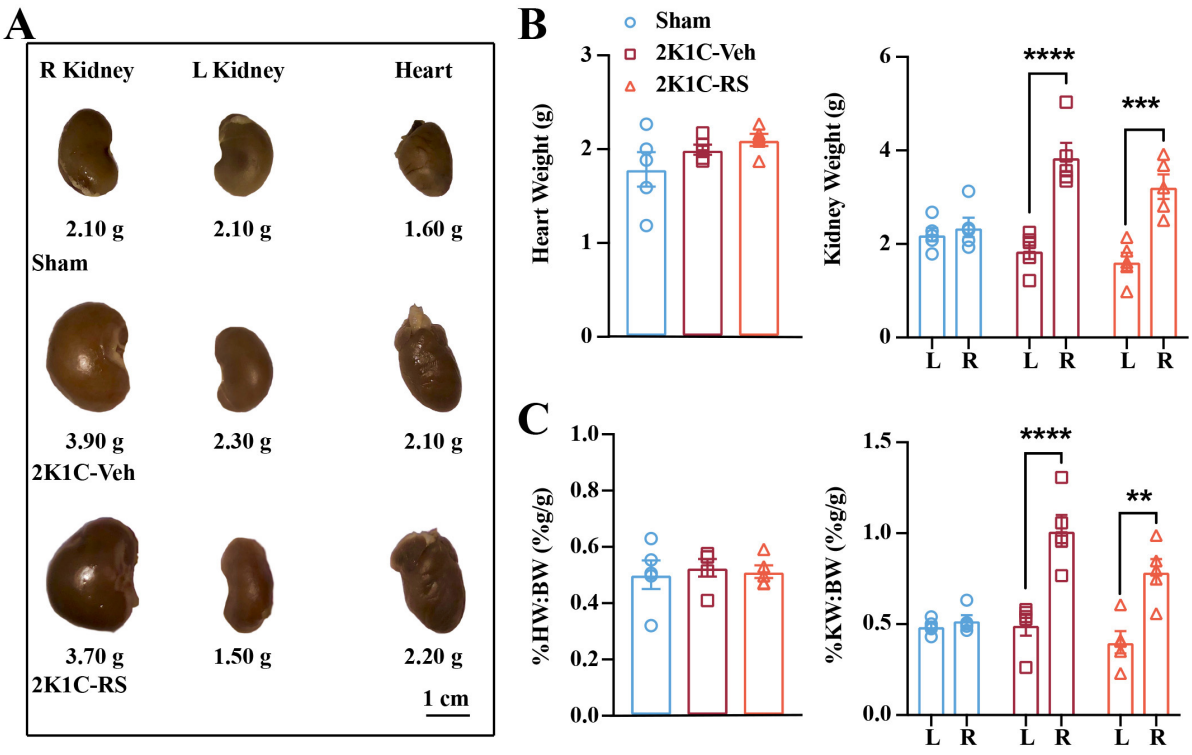
<u>Supplementary Figure 4.3:</u> Quantification of brain leukocytes through FACS gating.

Representative flow cytometric charts showing; **(A)** region of interest gated from all cells in the sample, **(B)** gating of only single cells, and **(C-D)** gating of $CD45^{+hi}$ events in a stained sample for the quantification of macrophages and lymphocytes. Regions in red were used for cell sorting. Total events by; 100,000 events.

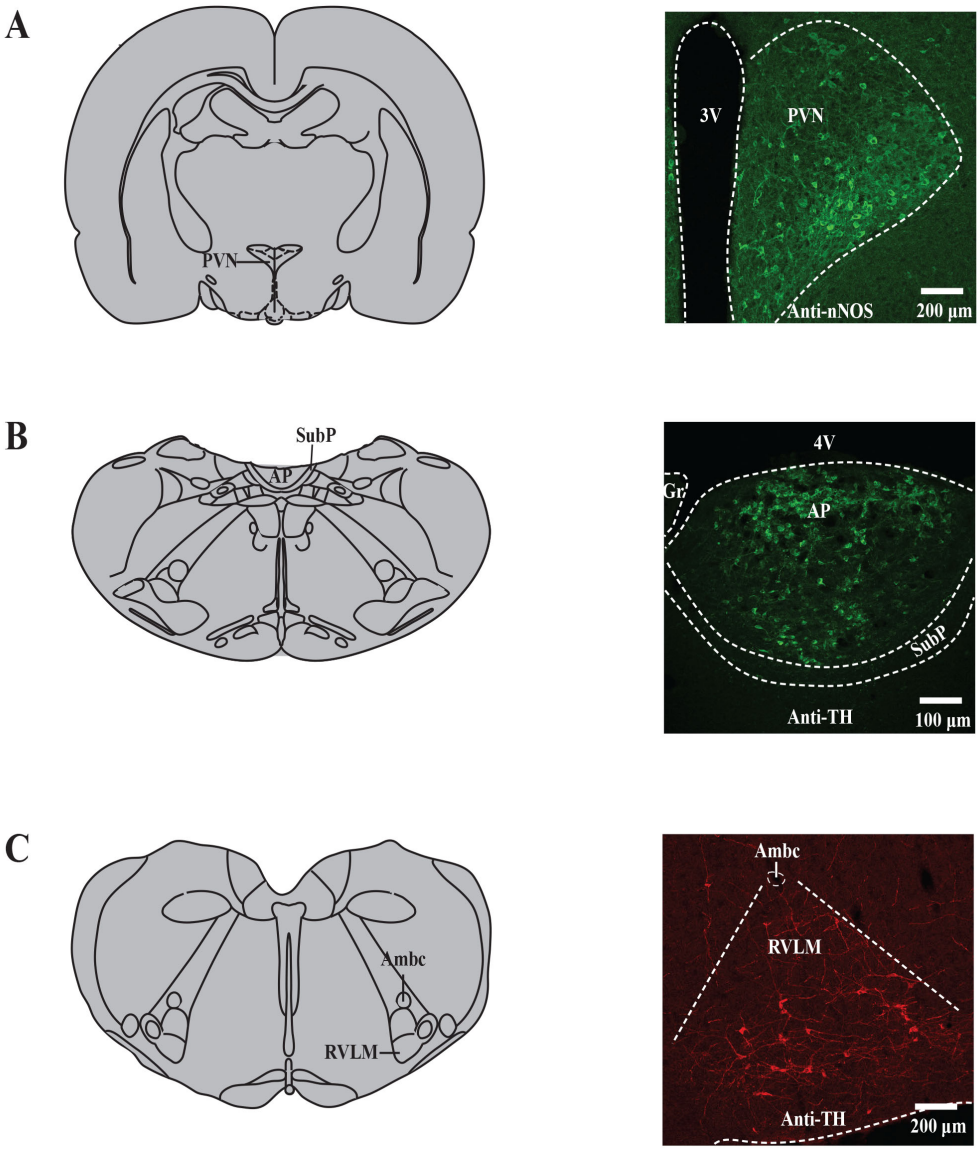


<u>Supplementary Figure 4.4:</u> Experimental protocol of the present study.

(A) Depicts the protocol utilised for the immunohistochemical analysis, while blood pressure is simultaneously recoded through telemetry transmitters. **(B)** Depicts the protocol utilised for the cohort used for the FACS analysis.



<u>Supplementary Figure 4.5:</u> Kidney and heart weights of renovascular hypertensive rats. Representative images of the right and left kidney and the heart in sham, 2K1C-Veh, and 2K1C-RS. **(B)** average heart weights and kidney weights, and **(C)** %ratio of heart weight and kidney weights to body weight. $^{**}P\leq0.01$, $^{***}P\leq0.001$, $^{****}P\leq0.0001$; two-way ANOVA of Left kidney (L) vs right kidney (R). (n=5per group).



Supplementary Figure 4.6: Identifying the different brain regions.

(A) Representative photomicrograph of the PVN labelled with nNOS, which is readily expressed by PVN neurons. Representative photomicrograph of the AP **(B)** and the RVLM **(C)** labelled with TH, which is readily expressed by AP and RVLM neurons. Abbreviations; PVN; paraventricular nucleus of the hypothalamus, 3V; third ventricle, 4V; fourth ventricle, Ambc; compact part of the nucleus ambiguus, AP; area postrema, Gr; gracilis nucleus, nNOS; neuronal nitric oxide synthase, RVLM; rostral ventrolateral medulla, SubP; subpostremal area, TH; tyrosine hydroxylase. Schematic diagrams are regenerated from (Paxinos G 2007).

5. General Discussion

5.1 Discussion

The main findings of the present thesis are that; **(1)** the chemokine CCL2 recruited macrophages to infiltrate the paraventricular nucleus (PVN) of the hypothalamus evoking increases in renal sympathetic nerve activity (RSNA) and blood pressure (BP), **(2)** recruitment of macrophages into the PVN occurred prior to the development of hypertension in renovascular hypertensive rats, and **(3)** the blockade of CCR2 receptors (cognate CCL2 receptor) in the brain prevented the development of hypertension in renovascular hypertensive rats. This thesis highlights a pivotal role for CCL2-CCR2 signalling in recruiting macrophages to the PVN, eliciting increases in SNA and BP; causing hypertension. The results here support the "neuro-immune axis" theory in hypertension (Abboud, Harwani et al. 2012, Zubcevic, Santisteban et al. 2014, Harwani 2018, Elsaafien, Korim et al. 2019), where the immune system and increased neuroinflammation drives increases in SNA and BP to cause hypertension.

Evidence has emerged in the past decade to demonstrate a role for pro-inflammatory cytokines in the brain to regulate BP in hypertension. The levels of pro-inflammatory cytokines, including TNF-α, interleukin 1 beta (IL-1β) and interleukin 6 (IL-6), are increased in the PVN of both primary and secondary rodent models of hypertension (Li, Qin et al. 2014, Song, Jia et al. 2014). Furthermore, the selective blockade of receptors for those pro-inflammatory cytokines in the PVN reduces BP in hypertensive rats (Sriramula, Cardinale et al. 2013, Song, Jia et al. 2014, Lu, Jiang et al. 2017), suggesting pivotal roles for cytokines play in mediating hypertension. This is further supported by the findings that the application of either TNF-α or IL-1β into the PVN increased SNA and BP (Shi, Gan et al. 2011). This finding raises the question of what leads to the increased levels of pro-inflammatory cytokines in the PVN of hypertensive rats. The resident macrophages of the brain, microglia, are linked to pro-inflammatory cytokine production in the PVN of hypertensive rats (Shi, Diez-Freire et al. 2010, Sharma, Yang et al. 2019). In the PVN of an angiotensin II-induced model of

hypertension, microglia exhibit a pro-inflammatory phenotype (activated), where the levels of TNF-α or IL-1β, and IL-6 are elevated (Shi, Diez-Freire et al. 2010). Interestingly, preventing the activation of microglia in the PVN reduces the level of pro-inflammatory cytokines and BP, and prevents the development of hypertension in the angiotensin II-induced model of hypertension (Shi, Diez-Freire et al. 2010). In the present study, we explored whether circulating immune cells are another source of pro-inflammatory cytokine production, and if these play a key role in the central regulation of SNA and BP in hypertensive rats. In hypertensive rats, it has been established that circulating immune cells increase the production and the secretion of pro-inflammatory cytokines (Ishibashi, Hiasa et al. 2004, Santisteban, Ahmari et al. 2015). Furthermore, peripheral macrophages have been shown to infiltrate the PVN of hypertensive rats (Wang, Kang et al. 2018), and the depletion of immune cells in hypertensive rats reduces inflammation in the PVN and decreases BP (Santisteban, Ahmari et al. 2015). Interestingly the chemokine CCL2, a pro-inflammatory chemokine known for activating and recruiting macrophages (Lu, Rutledge et al. 1998), is found to be elevated in the plasma of hypertensive patients (Antonelli, Fallahi et al. 2012). In spontaneously hypertensive rats (SHR), CCL2 forms a gradient from the bone marrow towards the cerebrospinal fluid (CSF), possibly suggesting that CCL2 plays a role in recruiting immune cells to the brain of hypertensive rats (Santisteban, Ahmari et al. 2015). Indeed, the levels of CCL2 are upregulated by at least 3-fold in the PVN of different rodent models of hypertension (Sriramula, Cardinale et al. 2013, Li, Qin et al. 2014, Song, Jia et al. 2014). Therefore, a primary aim of this thesis was to investigate whether CCL2 recruits immune cells into the PVN leading to increased SNA and BP in hypertension.

I found that CCL2 recruited macrophages into the PVN leading to increases in SNA and BP. There is much evidence to support a link between CCL2 and elevations in BP. For example, as previously described, plasma levels of CCL2 are positively correlated to BP levels

in hypertensive patients (Antonelli, Fallahi et al. 2012). In rodent models of hypertension CCL2 is upregulated in the plasma (Santisteban, Ahmari et al. 2015), and the PVN (Kang, Ma et al. 2009). In my studies, I found that the administration of CCL2 resulted in the recruitment of macrophages into the PVN eliciting dose-dependent increases in RSNA and BP. CCL2 is a chemokine involved in the inflammatory response, and is released to recruit macrophages (Rollins 1997). Activation of CCR2 receptors by CCL2 recruits and activates macrophages to move through a chemotactic gradient towards a stimulus (Ajuebor, Flower et al. 1998, Lu, Rutledge et al. 1998). Those activated macrophages induce an inflammatory cascade in tissue by secreting pro-inflammatory cytokines (Ishibashi, Hiasa et al. 2004). In hypertensive rats the levels of CCL2 are increased in the PVN (Wang, Kang et al. 2018), promoting the recruitment of macrophages to the PVN (Bush, Maeda et al. 2000). This leads to the secretion of pro-inflammatory cytokines such as TNF-α and IL-1β in the PVN (Ishibashi, Hiasa et al. 2004, Jun, Zubcevic et al. 2012, Santisteban, Ahmari et al. 2015), that can mediate increases in SNA and BP (Shi, Gan et al. 2011, Wei, Yu et al. 2015, Korim, Elsaafien et al. 2018). In line with the evidence provided, I have demonstrated that CCL2 activates and recruits' macrophages to infiltrate into the PVN leading to increases in SNA and BP.

I showed that macrophages were recruited to the PVN prior to the development of hypertension in renovascular hypertensive rats. This finding is consistent with similar observations in hypertensive animals that show macrophages to be recruited to the PVN of hypertensive rats (Santisteban, Ahmari et al. 2015, Wang, Kang et al. 2018). However, previous studies only showed recruitment of macrophages to the PVN in established hypertension (Santisteban, Ahmari et al. 2015, Wang, Kang et al. 2018). Thus, the novelty of the findings described in this thesis is that I have demonstrated a temporal profile of the recruitment of macrophages to the PVN throughout the development and the progression of hypertension. In this study, I found the number of macrophages ($CD11b^{+}$) in the PVN to be

increased prior to BP elevation in hypertension, and their levels remained sustained through the establishment of hypertension. This is in line with the finding that cells of the innate immune system are active in the peripheral circulation of pre-hypertensive rats (Harwani, Chapleau et al. 2012). Thus, the findings present in this thesis suggest that CCL2 is important in recruiting macrophages into the PVN, mediating increases in BP and causing hypertension. This is further supported by the findings of the previous chapter, were I found the central blockade of the cognate receptors for CCL2 (CCR2 receptors) to prevent the recruitment of macrophages to the PVN, preventing the development of elevated BP in renovascular hypertensive rats. This finding is supported by previous studies that demonstrate the peripheral blockade of CCR2 receptors to reduce peripheral inflammation and BP in many rodent models of hypertension (Elmarakby, Quigley et al. 2007, Chan, Moore et al. 2012, Wang, Zhu et al. 2015). Importantly, my findings demonstrate the pivotal role that CCL2-CCR2 signalling in the brain plays in recruiting macrophages into the PVN, which is essential for increases in BP and the development of hypertension.

In the present thesis, I propose a role for CCL2-CCR2 signalling in mediating the recruitment of macrophages into the PVN evoking increases in SNA and BP. In renovascular hypertension, the level of circulating angiotensin II is upregulated (Martinez-Maldonado 1991). Peripheral CCL2 is upregulated in response to circulating angiotensin II in hypertension (Crowley, Song et al. 2010), while peripheral blockade of angiotensin II receptors in hypertension, reduces CCL2 levels (Ishibashi, Hiasa et al. 2004). Furthermore, CCL2 mRNA and CCL2 protein levels are increased upon the exogenous application of angiotensin II to primary hypothalamic neuronal culture (Santisteban, Ahmari et al. 2015). The increase in CCL2 levels stimulates CCR2 receptors expressed on immune cells facilitating their infiltration into tissue (Ajuebor, Flower et al. 1998, Lu, Rutledge et al. 1998). In hypertension CCL2 forms a chemotactic gradient guiding macrophages to infiltrate into autonomic brain regions,

including the PVN (Santisteban, Ahmari et al. 2015, Wang, Kang et al. 2018). To allow macrophage infiltration into the PVN, CCL2 mediates the internalization of tight junction proteins expressed on endothelial cells, making the blood brain barrier (BBB) more permeable (Stamatovic, Keep et al. 2009, Roberts, Eugenin et al. 2012). Once activated, macrophages gain access to the PVN, release cytokines and initiating an inflammatory cascade (Ishibashi, Hiasa et al. 2004, Jun, Zubcevic et al. 2012, Santisteban, Ahmari et al. 2015), leading to sustained increases in SNA and BP (Shi, Gan et al. 2011). The results described in this thesis demonstrate that CCL2-CCR2 signalling is important for the infiltration of macrophages into the PVN, ultimately leading to increases in SNA and BP, which mediate the development of hypertension. Thus, the blockade of CCR2 receptors in the brain prevented the recruitment of macrophages to the PVN, resulting in a reduced inflammatory response, that attenuated the development of BP elevations in hypertensive animals.

5.2 Caveats and Future Directions

The present thesis focused on the role CCL2-CCR2 signalling within the PVN and how this mechanism might be important in immune cell recruitment, leading to increases in SNA and BP. However, the role CCL2-CCR2 signalling may not be limited to the PVN. The brain contains many regions that are capable of regulating SNA and BP. This includes the area postrema (AP) (Joy and Lowe 1970, Blessing, Hedger et al. 1987, Dampney, Czachurski et al. 1987, Fink, Bruner et al. 1987), the rostral ventrolateral medulla (RVLM) (Ross, Ruggiero et al. 1984, Dampney, Czachurski et al. 1987, Strack, Sawyer et al. 1989), and many other specialised brain regions. Previous studies have demonstrated an increase in the levels of CCL2 in many other brain regions in hypertension. For example, CCL2 levels are increased by 3-fold in the RVLM of renovascular hypertensive rats (Li, Qin et al. 2014). Thus, future studies are warranted to examine whether increased CCL2-CCR2 signalling in other autonomic brain

regions, such as the AP or the RVLM, would result in similar cardiovascular effects to those I demonstrated in the PVN.

While I proposed that recruitment of immune cells into the PVN would increase the expression of pro-inflammatory cytokine production, this was not definitively examined in this thesis. In the studies described in this thesis, I focused on the effects of recruiting immune cells into the PVN in increasing SNA and BP. The hypothesis was that increased infiltration of immune cells would increase the production of pro-inflammatory cytokines leading to increases in SNA and BP. Previous studies have demonstrated that the activation of immune cells leads to the production of pro-inflammatory cytokines (Ishibashi, Hiasa et al. 2004). Further studies have also demonstrated a link between peripheral immune cells, the production of pro-inflammatory cytokines and BP in hypertension (Ishibashi, Hiasa et al. 2004, Jun, Zubcevic et al. 2012, Santisteban, Ahmari et al. 2015). However, it was not known, whether those activated immune cells can infiltrate into the PVN and increase SNA and BP. Thus, I focused on investigating whether CCL2-CCR2 signalling in the PVN leads to the recruitment of immune cells into the PVN and increase BP. Therefore, future studies are needed to determine whether increased CCL2-CCR2 signalling, which leads to infiltration of immune cells into the PVN, leads to the production or the increased levels of pro-inflammatory cytokines. This would provide additional insights in the mechanisms by which immune cells activate neurons in the PVN; leading to increases in SNA and BP.

5.3 Novelty and Clinical Significance

The causes of elevated blood pressure (hypertension) are not known in the vast majority of cases. While current therapies can effectively manage the hypertension, there are a growing number of hypertensive patients in whom standard therapies are not effective (Calhoun, Jones et al. 2008). According to the World Health Organisation about 1 billion people globally have

uncontrolled hypertension. In Australia alone, 32% of adult Australians suffer from hypertension (Heart Foundation, 2016), and the expenditure for the treatment of hypertension is estimated to be $7.6 billion per year, where hypertension is described as “the highest expenditure of any disease group in Australia” (Australian Institute of Health and Welfare, 2014). The key issue is that the causes of hypertension are not known, although it has long been recognised that the brain plays a critical role (Strack, Sawyer et al. 1989, Strack, Sawyer et al. 1989, Schramm, Strack et al. 1993). It is this knowledge gap that I wanted to address in my studies. The findings described in this thesis highlight a specific interaction between the nervous system and the immune system in the regulation of sympathetic nerve activity and blood pressure. By identifying CCL2 and the recruitment of immune cells into key cardiovascular brain regions as important mediators, I have discovered a key mechanism that causes increased sympathetic nerve activity and hypertension.

5.4 Conclusion

The present thesis identified CCL2-CCR2 signalling in the paraventricular nucleus of the hypothalamus as a pivotal mediator in the recruitment of macrophages into the PVN, eliciting increases in sympathetic nerve activity and arterial blood pressure in hypertension. These findings indicate that increased CCL2-CCR2 signalling in the brain may be a novel target for the development of new therapies for the treatment of hypertension.

6. Bibliography

(Australian Institute of Health and Welfare, 2014). "Health care expenditure on cardiovascular diseases 2008-09." 61.

(Food and Drug Administration and the Department of Health and Human Services, 2011). "Guidance for Industry on Hypertension Indication: Drug Labeling for Cardiovascular Outcome Claims; Availability." Retrieved from http://www.fda.gov/downloads/Drugs/.../Guidances/ucm075072.pdf. Acessed on 3//1/2018.

(Heart Foundation, 2016). "Blood Pressure." Retrieved from http://www.heartfoundation.org.au/your-heart/know-your-risks/blood-pressure. Accessed on 12/07/2016.

(Heart Foundation, 2016). "High blood pressure statistics." Retrieved from http://heartfoundation.org.au/about-us/what-we-do/heart-disease-in-australia/high-blood-pressure-statistics. Accessed on 12/07/2016.

Abboud, F. M., S. C. Harwani and M. W. Chapleau (2012). "Autonomic neural regulation of the immune system: implications for hypertension and cardiovascular disease." Hypertension **59**(4): 755-762.

Aguilera, G., A. Kiss and X. Luo (1995). "Increased expression of type 1 angiotensin II receptors in the hypothalamic paraventricular nucleus following stress and glucocorticoid administration." Journal of neuroendocrinology **7**(10): 775-783.

Ahmari, N., M. M. Santisteban, D. R. Miller, N. M. Geis, R. M. Larkin, T. L. Redler, H. Denson, H. Khoshbouei, D. M. Baekey and M. K. Raizada (2019). "Elevated bone marrow sympathetic drive precedes systemic inflammation in angiotensin II hypertension." American Journal of Physiology-Heart and Circulatory Physiology.

Aiyar, N., R. A. Daines, J. Disa, P. A. Chambers, C. F. Sauermelch, M. Quiniou, N. Khandoudi, B. Gout, S. A. Douglas and R. N. Willette (2001). "Pharmacology of SB-273779, a nonpeptide calcitonin gene-related peptide 1 receptor antagonist." J Pharmacol Exp Ther **296**(3): 768-775.

Aiyar, N., J. Disa, J. M. Stadel and P. G. Lysko (1999). "Calcitonin gene-related peptide receptor independently stimulates 3',5'-cyclic adenosine monophosphate and Ca2+ signaling pathways." Mol Cell Biochem **197**(1-2): 179-185.

Ajami, B., J. L. Bennett, C. Krieger, K. M. McNagny and F. M. Rossi (2011). "Infiltrating monocytes trigger EAE progression, but do not contribute to the resident microglia pool." Nature neuroscience **14**(9): 1142-1149.

Ajuebor, M. N., R. J. Flower, R. Hannon, M. Christie, K. Bowers, A. Verity and M. Perretti (1998). "Endogenous monocyte chemoattractant protein-1 recruits monocytes in the zymosan peritonitis model." Journal of leukocyte biology **63**(1): 108-116.

Antonelli, A., P. Fallahi, S. Ferrari, L. Ghiadoni, A. Virdis, C. Mancusi, M. Centannp, S. Taddei and E. Ferrannini (2012). "High serum levels of CXC (CXCL10) and CC (CCL2) chemokines in untreated essential hypertension." International journal of immunopathology and pharmacology **25**(2): 387-395.

Arnoux, I. and E. Audinat (2015). "Fractalkine Signaling and Microglia Functions in the Developing Brain." Neural plasticity **2015**.

Ataka, K., A. Asakawa, K. Nagaishi, K. Kaimoto, A. Sawada, Y. Hayakawa, R. Tatezawa, A. Inui and M. Fujimiya (2013). "Bone marrow-derived microglia infiltrate into the paraventricular nucleus of chronic psychological stress-loaded mice." PLoS One **8**(11): e81744.

Baamonde, A., A. Hidalgo and L. Menendez (2011). "Involvement of glutamate NMDA and AMPA receptors, glial cells and IL-1 beta in the spinal hyperalgesia evoked by the chemokine CCL2 in mice." Neuroscience Letters **502**(3): 178-181.

Bachelard, H., S. M. Gardiner and T. Bennett (1990). "Cardiovascular responses elicited by chemical stimulation of the rostral ventrolateral medulla in conscious, unrestrained rats." Journal of the autonomic nervous system **31**(3): 185-190.

Badoer, E. (2001). "Hypothalamic paraventricular nucleus and cardiovascular regulation." Clinical and Experimental Pharmacology and Physiology **28**(1-2): 95-99.

Badoer, E., C.-W. Ng and R. De Matteo (2003). "Glutamatergic input in the PVN is important in renal nerve response to elevations in osmolality." American Journal of Physiology-Renal Physiology **285**(4): F640-F650.

Bailey, T. W., Y.-H. Jin, M. W. Doyle, S. M. Smith and M. C. Andresen (2006). "Vasopressin inhibits glutamate release via two distinct modes in the brainstem." Journal of Neuroscience **26**(23): 6131-6142.

Banisadr, G., R. D. Gosselin, P. Mechighel, P. Kitabgi, W. Rosene and S. P. M. Parsadaniantz (2005). "Highly regionalized neuronal expression of monocyte chemoattractant protein-1 (MCP-1/CCL2) in rat brain: Evidence for its colocalization with neurotransmitters and neuropeptides." Journal of Comparative Neurology **489**(3): 275-292.

Banisadr, G., R. D. Gosselin, P. Mechighel, W. Rostene, P. Kitabgi and S. M. Parsadaniantz (2005). "Constitutive neuronal expression of CCR2 chemokine receptor and its colocalization with neurotransmitters in normal rat brain: Functional effect of MCP-1/CCL2 on calcium mobilization in primary cultured neurons." Journal of Comparative Neurology **492**(2): 178-192.

Barker, J. L. and B. R. Ransom (1978). "Pentobarbitone pharmacology of mammalian central neurones grown in tissue culture." J Physiol **280**: 355-372.

Barna, B. P., J. Pettay, G. H. Barnett, P. Zhou, K. Iwasaki and M. L. Estes (1994). "Regulation of monocyte chemoattractant protein-1 expression in adult human non-neoplastic astrocytes is sensitive to tumor necrosis factor (TNF) or antibody to the 55-kDa TNF receptor." Journal of neuroimmunology **50**(1): 101-107.

Barnes, K. L., D. M. DeWeese and M. C. Andresen (2003). "Angiotensin potentiates excitatory sensory synaptic transmission to medial solitary tract nucleus neurons." American Journal of Physiology-Regulatory, Integrative and Comparative Physiology **284**(5): R1340-R1353.

Barretto, A. C., A. C. Santos, R. Munhoz, M. U. Rondon, F. G. Franco, I. C. Trombetta, F. Roveda, L. N. de Matos, A. M. Braga and H. R. Middlekauff (2009). "Increased muscle sympathetic nerve activity predicts mortality in heart failure patients." International journal of cardiology **135**(3): 302-307.

Bartoli, C., M. Civatte, J. Pellissier and D. Figarella-Branger (2001). "CCR2A and CCR2B, the two isoforms of the monocyte chemoattractant protein-1 receptor are up-regulated and expressed by different cell subsets in idiopathic inflammatory myopathies." Acta neuropathologica **102**(4): 385-392.

Biancardi, V. C., S. J. Son, S. Ahmadi, J. A. Filosa and J. E. Stern (2013). "Circulating angiotensin II gains access to the hypothalamus and brain stem during hypertension via breakdown of the blood–brain barrier." Hypertension **63**: 572-579.

Blessing, W., S. Hedger, T. Joh and J. Willoughby (1987). "Neurons in the area postrema are the only catecholamine-synthesizing cells in the medulla or pons with projections to the rostral ventrolateral medulla (C 1-area) in the rabbit." Brain research **419**(1): 336-340.

Bonham, A. and I. Jeske (1989). "Cardiorespiratory effects of DL-homocysteic acid in caudal ventrolateral medulla." American Journal of Physiology-Heart and Circulatory Physiology **256**(3): H688-H696.

Bose, S. and J. Cho (2013). "Role of chemokine CCL2 and its receptor CCR2 in neurodegenerative diseases." Arch Pharm Res **36**(9): 1039-1050.

Bowman, B. R., N. N. Kumar, S. F. Hassan, S. McMullan and A. K. Goodchild (2013). "Brain sources of inhibitory input to the rat rostral ventrolateral medulla." Journal of Comparative Neurology **521**(1): 213-232.

Bradbury, M. W. (1979). "The concept of a blood-brain barrier."

Braga, V. A., I. A. Medeiros, T. P. Ribeiro, M. S. Franca-Silva, M. S. Botelho-Ono and D. D. Guimaraes (2011). "Angiotensin-II-induced reactive oxygen species along the SFO-PVN-RVLM pathway: implications in neurogenic hypertension." Brazilian Journal of Medical and Biological Research **44**(9): 871-876.

Brown, Z., R. M. Strieter, G. H. Neild, R. C. Thompson, S. L. Kunkel and J. Westwick (1992). "IL-1 receptor antagonist inhibits monocyte chemotactic peptide 1 generation by human mesangial cells." Kidney international **42**(1): 95-101.

Buell, G., G. Collo and F. Rassendren (1996). "P2X receptors: an emerging channel family." European Journal of Neuroscience **8**(10): 2221-2228.

Burnstock, G. (1997). "The past, present and future of purine nucleotides as signalling molecules." Neuropharmacology **36**(9): 1127-1139.

Burnstock, G. and G. E. Knight (2017). "The potential of P2X7 receptors as a therapeutic target, including inflammation and tumour progression." Purinergic Signalling: 1-18.

Bush, E., N. Maeda, W. A. Kuziel, T. C. Dawson, J. N. Wilcox, H. DeLeon and W. R. Taylor (2000). "CC chemokine receptor 2 is required for macrophage infiltration and vascular hypertrophy in angiotensin II–induced hypertension." Hypertension **36**(3): 360-363.

Busnardo, C., N. C. Ferreira-Junior, J. C. Cruz, B. H. Machado, F. Correa and L. Resstel (2013). "Cardiovascular responses to ATP microinjected into the paraventricular nucleus are mediated by nitric oxide and NMDA glutamate receptors in awake rats." Experimental physiology **98**(10): 1411-1421.

Calhoun, D. A., D. Jones, S. Textor, D. C. Goff, T. P. Murphy, R. D. Toto, A. White, W. C. Cushman, W. White and D. Sica (2008). "Resistant hypertension: diagnosis, evaluation, and treatment." Circulation **117**(25): e510-e526.

Callewaere, C., G. Banisadr, M. G. Desarmenien, P. Mechighel, P. Kitabgi, W. H. Rostene and S. Melik Parsadaniantz (2006). "The chemokine SDF-1/CXCL12 modulates the firing pattern of vasopressin neurons and counteracts induced vasopressin release through CXCR4." Proc Natl Acad Sci U S A **103**(21): 8221-8226.

Carillo, B. A., E. B. Oliveira-Sales, M. Andersen, S. Tufik, D. Hipolide, A. A. Santos, P. J. Tucci, C. T. Bergamaschi and R. R. Campos (2012). "Changes in GABAergic inputs in the paraventricular nucleus maintain sympathetic vasomotor tone in chronic heart failure." Autonomic Neuroscience-Basic & Clinical **171**(1-2): 41-48.

Cédile, O., A. Wlodarczyk and T. Owens (2017). "CCL2 recruits T cells into the brain in a CCR2-independent manner." APMIS.

Cham, J. L., N. C. Owens, J. Barden, A. J. Lawrence and E. Badoer (2006). "P2X purinoceptor subtypes on paraventricular nucleus neurones projecting to the rostral ventrolateral medulla in the rat." Experimental physiology **91**(2): 403-411.

Chan, C. T., J. P. Moore, K. Budzyn, E. Guida, H. Diep, A. Vinh, E. S. Jones, R. E. Widdop, J. A. Armitage and S. Sakkal (2012). "Reversal of vascular macrophage accumulation and hypertension by a CCR2 antagonist in deoxycorticosterone/salt-treated mice." Hypertension **60**(5): 1207-1212.

Chang, A. Y., F. C. Li, C.-W. Huang, J. C. Wu, K.-Y. Dai, C.-H. Chen, S.-H. Li, C.-H. Su and R.-W. Wu (2014). "Interplay between brain stem angiotensins and monocyte chemoattractant protein-1 as a novel mechanism for pressor response after ischemic stroke." Neurobiology of disease **71**: 292-304.

Chen, Q. H., J. R. Haywood and G. M. Toney (2003). "Sympathoexcitation by PVN-injected bicuculline requires activation of excitatory amino acid receptors." Hypertension **42**(4): 725-731.

Chensue, S. W., K. S. Warmington, N. W. Lukacs, P. M. Lincoln, M. D. Burdick, R. M. Strieter and S. L. Kunkel (1995). "Monocyte chemotactic protein expression during schistosome egg granuloma formation. Sequence of production, localization, contribution, and regulation." The American journal of pathology **146**(1): 130.

Coffman, T. M. (2011). "Under pressure: the search for the essential mechanisms of hypertension." Nature medicine **17**(11): 1402-1409.

Coughlan, C., C. McManus, M. Sharron, Z.-Y. Gao, D. Murphy, S. Jaffer, W. Choe, W. Chen, J. Hesselgesser and H. Gaylord (2000). "Expression of multiple functional chemokine receptors and monocyte chemoattractant protein-1 in human neurons." Neuroscience **97**(3): 591-600.

Cowley Jr, A. W. (1992). "Long-term control of arterial blood pressure." Physiological reviews **72**(1): 231-300.

Crestani, C. C., F. H. Alves, C. Busnardo, L. B. Resstel and F. M. Correa (2010). "N-methyl-D-aspartate glutamate receptors in the hypothalamic paraventricular nucleus modulate cardiac component of the baroreflex in unanesthetized rats." Neurosci Res **67**(4): 317-326.

Crowley, S. D., S. B. Gurley, M. J. Herrera, P. Ruiz, R. Griffiths, A. P. Kumar, H.-S. Kim, O. Smithies, T. H. Le and T. M. Coffman (2006). "Angiotensin II causes hypertension and cardiac hypertrophy through its receptors in the kidney." Proceedings of the National Academy of Sciences **103**(47): 17985-17990.

Crowley, S. D., S. B. Gurley, M. I. Oliverio, A. K. Pazmino, R. Griffiths, P. J. Flannery, R. F. Spurney, H.-S. Kim, O. Smithies and T. H. Le (2005). "Distinct roles for the kidney and systemic tissues in blood pressure regulation by the renin-angiotensin system." Journal of Clinical Investigation **115**(4): 1092.

Crowley, S. D., Y.-S. Song, G. Sprung, R. Griffiths, M. Sparks, M. Yan, J. L. Burchette, D. N. Howell, E. E. Lin and B. Okeiyi (2010). "A role for angiotensin II type 1 receptors on bone marrow-derived cells in the pathogenesis of angiotensin II–dependent hypertension." Hypertension **55**(1): 99-108.

Cruz, J. C., L. G. Bonagamba and B. H. Machado (2010). "Modulation of arterial pressure by P2 purinoceptors in the paraventricular nucleus of the hypothalamus of awake rats." Autonomic Neuroscience **158**(1): 79-85.

Cruz, J. C. and B. H. Machado (2009). "GABA and nitric oxide in the PVN are involved in arterial pressure control but not in the chemoreflex responses in rats." Autonomic Neuroscience **146**(1): 47-55.

Cushing, S. D., J. A. Berliner, A. J. Valente, M. C. Territo, M. Navab, F. Parhami, R. Gerrity, C. J. Schwartz and A. M. Fogelman (1990). "Minimally modified low density lipoprotein

induces monocyte chemotactic protein 1 in human endothelial cells and smooth muscle cells." Proceedings of the National Academy of Sciences **87**(13): 5134-5138.

Dampney, R., M. Coleman, M. Fontes, Y. Hirooka, J. Horiuchi, Y. W. Li, J. Polson, P. Potts and T. Tagawa (2002). "Central mechanisms underlying short-and long-term regulation of the cardiovascular system." Clinical and Experimental Pharmacology and Physiology **29**(4): 261-268.

Dampney, R., J. Czachurski, K. Dembowsky, A. Goodchild and H. Seller (1987). "Afferent connections and spinal projections of the pressor region in the rostral ventrolateral medulla of the cat." Journal of the autonomic nervous system **20**(1): 73-86.

Dampney, R., A. Goodchild and E. Tan (1985). "Vasopressor neurons in the rostral ventrolateral medulla of the rabbit." Journal of the autonomic nervous system **14**(3): 239-254.

Dampney, R. A. (1994). "Functional organization of central pathways regulating the cardiovascular system." Physiol Rev **74**(2): 323-364.

Dampney, R. A., J. Czachurski, K. Dembowsky, A. K. Goodchild and H. Seller (1987). "Afferent connections and spinal projections of the pressor region in the rostral ventrolateral medulla of the cat." J Auton Nerv Syst **20**(1): 73-86.

de Kloet, A. D., E. G. Krause, P. D. Shi, J. Zubcevic, M. K. Raizada and C. Sumners (2013). "Neuroimmune communication in hypertension and obesity: a new therapeutic angle?" Pharmacol Ther **138**(3): 428-440.

DeFelipe, J. (1993). "Neocortical neuronal diversity: chemical heterogeneity revealed by colocalization studies of classic neurotransmitters, neuropeptides, calcium-binding proteins, and cell surface molecules." Cerebral cortex **3**(4): 273-289.

Deshmane, S. L., S. Kremlev, S. Amini and B. E. Sawaya (2009). "Monocyte Chemoattractant Protein-1 (MCP-1): An Overview." Journal of Interferon and Cytokine Research **29**(6): 313-326.

Deuchars, S. A., L. Atkinson, R. E. Brooke, H. Musa, C. J. Milligan, T. F. Batten, N. J. Buckley, S. H. Parson and J. Deuchars (2001). "Neuronal P2X7 receptors are targeted to presynaptic terminals in the central and peripheral nervous systems." Journal of Neuroscience **21**(18): 7143-7152.

Dissing-Olesen, L., J. M. LeDue, R. L. Rungta, J. K. Hefendehl, H. B. Choi and B. A. MacVicar (2014). "Activation of neuronal NMDA receptors triggers transient ATP-mediated microglial process outgrowth." The Journal of Neuroscience **34**(32): 10511-10527.

Dragunow, M. and R. Faull (1989). "The use of c-fos as a metabolic marker in neuronal pathway tracing." Journal of neuroscience methods **29**(3): 261-265.

Du, D., M. Jiang, M. Liu, J. Wang, C. Xia, R. Guan, L. Shen, Y. Ji and D. Zhu (2015). "Microglial P2X 7 receptor in the hypothalamic paraventricular nuclei contributes to sympathoexcitatory responses in acute myocardial infarction rat." Neuroscience Letters **587**: 22-28.

Edwards, F. A., A. J. Gibb and D. Colquhoun (1992). "ATP receptor-mediated synaptic currents in the central nervous system." Nature **359**(6391): 144-147.

Ehrlich, P. (1885). "Das Sauerstoff-Bedürfnis des Organismus. Eine farbenanalytische Studie.[On the oxygen consumption of the body. A study using intravital dyes.]." Verlag von August Hirschwald, Berlin.

Elmarakby, A. A., J. E. Quigley, J. J. Olearczyk, A. Sridhar, A. K. Cook, E. W. Inscho, D. M. Pollock and J. D. Imig (2007). "Chemokine receptor 2b inhibition provides renal protection in angiotensin II–salt hypertension." Hypertension **50**(6): 1069-1076.

Elsaafien, K., W. S. Korim, A. Setiadi, C. N. May and S. T. Yao (2019). "Chemoattraction and Recruitment of Activated Immune cells, Central Autonomic Control and Blood Pressure Regulation." Frontiers in Physiology **10**: 984.

Esler, M., G. Jennings, J. Johns, F. Burke, P. Little and P. Leonard (1984). "Estimation of'total'renal, cardiac and splanchnic sympathetic nervous tone in essential hypertension from measurements of noradrenaline release." Journal of hypertension. Supplement: official journal of the International Society of Hypertension **2**(3): S123-125.

Ettrup, K. S., J. C. Sorensen and C. R. Bjarkam (2010). "The anatomy of the Gottingen minipig hypothalamus." Journal of Chemical Neuroanatomy **39**(3): 151-165.

Evans, R. J., V. Derkach and A. Surprenant (1992). "ATP mediates fast synaptic transmission in mammalian neurons." Nature **357**(6378): 503-505.

Feldberg, W. and P. Guertzenstein (1976). "Vasodepressor effects obtained by drugs acting on the ventral surface of the brain stem." The Journal of physiology **258**(2): 337-355.

Ferrario, C. M., K. L. Barnes, D. I. Diz, C. H. Block and D. B. Averill (1987). "Role of area postrema pressor mechanisms in the regulation of arterial pressure." Canadian journal of physiology and pharmacology **65**(8): 1591-1597.

Ferreira-Neto, H., S. Yao and V. R. Antunes (2013). "Purinergic and glutamatergic interactions in the hypothalamic paraventricular nucleus modulate sympathetic outflow." Purinergic signalling **9**(3): 337-349.

Fink, G. D., C. A. Bruner and M. L. Mangiapane (1987). "Area postrema is critical for angiotensin-induced hypertension in rats." Hypertension **9**(4): 355-361.

Francis, G. S., S. R. Goldsmith, T. B. Levine, M. T. Olivari and J. N. Cohn (1984). "The neurohumoral axis in congestive heart failure." Annals of internal medicine **101**(3): 370-377.

Francis, J., Z.-H. Zhang, R. M. Weiss and R. B. Felder (2004). "Neural regulation of the proinflammatory cytokine response to acute myocardial infarction." American Journal of Physiology-Heart and Circulatory Physiology **287**(2): H791-H797.

Freeman, J. V., F. E. Dewey, D. M. Hadley, J. Myers and V. F. Froelicher (2006). "Autonomic nervous system interaction with the cardiovascular system during exercise." Progress in Cardiovascular Diseases **48**(5): 342-362.

Ganong, W. F. (2000). "Circumventricular organs: definition and role in the regulation of endocrine and autonomic function." Clinical and Experimental Pharmacology and Physiology **27**(5-6): 422-427.

Gao, H.-L., X.-J. Yu, J. Qi, Q.-Y. Yi, W.-H. Jing, W.-Y. Sun, W. Cui, J.-J. Mu, Z.-Y. Yuan and X.-F. Zhao (2016). "Oral CoQ10 attenuates high salt-induced hypertension by restoring neurotransmitters and cytokines in the hypothalamic paraventricular nucleus." Scientific Reports **6**.

Goldblatt, H., J. Lynch, R. F. Hanzal and W. W. Summerville (1934). "Studies on experimental hypertension I. The production of persistent elevation of systolic blood pressure by means of renal ischemia." The Journal of experimental medicine **59**(3): 347-379.

Goldman, E. (1909). "Die\l= a"\ussereund innere Secretion des gesunden und kranken Organismus im Lichte der" vitalen F\l= a"\rbung," Beitr. z. klin." Chir **64**(192): 78.

Gordon, G. R., D. V. Baimoukhametova, S. A. Hewitt, W. K. J. Rajapaksha, T. E. Fisher and J. S. Bains (2005). "Norepinephrine triggers release of glial ATP to increase postsynaptic efficacy." Nature neuroscience **8**(8): 1078-1086.

Gordon, G. R., K. J. Iremonger, S. Kantevari, G. C. Ellis-Davies, B. A. MacVicar and J. S. Bains (2009). "Astrocyte-mediated distributed plasticity at hypothalamic glutamate synapses." Neuron **64**(3): 391-403.

Gosselin, R. D., C. Varela, G. Banisadr, P. Mechighel, W. Rostene, P. Kitabgi and S. Melik-Parsadaniantz (2005). "Constitutive expression of CCR2 chemokine receptor and inhibition by MCP-1/CCL2 of GABA-induced currents in spinal cord neurones." Journal of Neurochemistry **95**(4): 1023-1034.

Grassi, G. (2004). "Counteracting the sympathetic nervous system in essential hypertension." Current opinion in nephrology and hypertension **13**(5): 513-519.

Grassi, G. (2004). "Sympathetic and baroreflex function in hypertension: implications for current and new drugs." Current pharmaceutical design **10**(29): 3579-3589.

Guertzenstein, P. and A. Silver (1974). "Fall in blood pressure produced from discrete regions of the ventral surface of the medulla by glycine and lesions." The Journal of Physiology **242**(2): 489-503.

Guyenet, P. G., J. R. Haselton and M.-K. Sun (1988). "Sympathoexcitatory neurons of the rostroventrolateral medulla and the origin of the sympathetic vasomotor tone." Progress in brain research **81**: 105-116.

Guyon, A., G. Banisadr, C. Rovere, A. Cervantes, P. Kitabgi, S. Melik-Parsadaniantz and J. L. Nahon (2005). "Complex effects of stromal cell-derived factor-1 alpha on melanin-concentrating hormone neuron excitability." Eur J Neurosci **21**(3): 701-710.

Guyton, A. C. (1991). "Blood pressure control--special role of the kidneys and body fluids." Science **252**(5014): 1813-1816.

Guzik, T. J., N. E. Hoch, K. A. Brown, L. A. McCann, A. Rahman, S. Dikalov, J. Goronzy, C. Weyand and D. G. Harrison (2007). "Role of the T cell in the genesis of angiotensin II–induced hypertension and vascular dysfunction." The Journal of experimental medicine **204**(10): 2449-2460.

Hallbeck, M., D. Larhammar and A. Blomqvist (2001). "Neuropeptide expression in rat paraventricular hypothalamic neurons that project to the spinal cord." Journal of Comparative Neurology **433**(2): 222-238.

Handel, T. M. and P. J. Domaille (1996). "Heteronuclear (1H, 13C, 15N) NMR assignments and solution structure of the monocyte chemoattractant protein-1 (MCP-1) dimer." Biochemistry **35**(21): 6569-6584.

Hardy, S. G. (2001). "Hypothalamic projections to cardiovascular centers of the medulla." Brain Res **894**(2): 233-240.

Hart, E. C., G. A. Head, J. R. Carter, B. G. Wallin, C. N. May, S. M. Hamza, J. E. Hall, N. Charkoudian and J. W. Osborn (2017). "Recording sympathetic nerve activity in conscious humans and other mammals: guidelines and the road to standardization." American Journal of Physiology-Heart and Circulatory Physiology **312**(5): H1031-H1051.

Harwani, S. C. (2018). "Macrophages under pressure: the role of macrophage polarization in hypertension." Translational Research **191**: 45-63.

Harwani, S. C., M. W. Chapleau, K. L. Legge, Z. K. Ballas and F. M. Abboud (2012). "Neurohormonal modulation of the innate immune system is pro-inflammatory in the pre-hypertensive spontaneously hypertensive rat, a genetic model of essential hypertension." Circulation research **111**: 1190-1197.

Hatten, M. E. and C. A. Mason (1990). "Mechanisms of glial-guided neuronal migration in vitro and in vivo." Experientia **46**(9): 907-916.

Hilgers, K. F., A. Hartner, M. Porst, M. Mai, M. Wittmann, C. Hugo, D. Ganten, H. Geiger, R. Veelken and J. F. Mann (2000). "Monocyte chemoattractant protein-1 and macrophage infiltration in hypertensive kidney injury." Kidney international **58**(6): 2408-2419.

Hinojosa, A. E., B. Garcia-Bueno, J. C. Leza and J. L. Madrigal (2011). "Regulation of CCL2/MCP-1 production in astrocytes by desipramine and atomoxetine: involvement of alpha2 adrenergic receptors." Brain Res Bull **86**(5-6): 326-333.

Hokfelt, T., R. Elde, K. Fuxe, O. Johansson, A. Ljungdahl, M. Goldstein, R. Luft, S. Efendic, G. Nilsson, L. Terenius, D. Ganten, S. L. Jeffcoate, J. Rehfeld, S. Said, M. Perez de la Mora, L. Possani, R. Tapia, L. Teran and R. Palacios (1978). "Aminergic and peptidergic pathways in the nervous system with special reference to the hypothalamus." Res Publ Assoc Res Nerv Ment Dis **56**: 69-135.

Inoue, K., K. Nakazawa, M. Ohara-Imaizumi, T. Obama, K. Fujimori and A. Takanaka (1991). "Selective and competitive antagonism by suramin of ATP-stimulated catecholamine-secretion from PC12 phaeochromocytoma cells." British journal of pharmacology **102**(3): 581-584.

Ishibashi, M., K.-i. Hiasa, Q. Zhao, S. Inoue, K. Ohtani, S. Kitamoto, M. Tsuchihashi, T. Sugaya, I. F. Charo and S. Kura (2004). "Critical role of monocyte chemoattractant protein-1 receptor CCR2 on monocytes in hypertension-induced vascular inflammation and remodeling." Circulation research **94**(9): 1203-1210.

Jia, L. L., Y. M. Kang, F. X. Wang, H. B. Li, Y. Zhang, X. J. Yu, J. Qi, Y. P. Suo, Z. J. Tian, Z. M. Zhu, G. Q. Zhu and D. N. Qin (2014). "Exercise Training Attenuates Hypertension and Cardiac Hypertrophy by Modulating Neurotransmitters and Cytokines in Hypothalamic Paraventricular Nucleus." Plos One **9**(1).

Joy, M. and R. Lowe (1970). "Evidence that the area postrema mediates the central cardiovascular response to angiotensin II." Nature **228**(5278): 1303-1304.

Jun, J. Y., J. Zubcevic, Y. Qi, A. Afzal, J. M. Carvajal, J. S. Thinschmidt, M. B. Grant, J. Mocco and M. K. Raizada (2012). "Brain-Mediated Dysregulation of the Bone Marrow Activity in Angiotensin II–Induced Hypertension." Hypertension **60**: 1316-1323.

Kang, Y.-M., Y. Ma, J.-P. Zheng, C. Elks, S. Sriramula, Z.-M. Yang and J. Francis (2009). "Brain nuclear factor-kappa B activation contributes to neurohumoral excitation in angiotensin II-induced hypertension." Cardiovascular Research **82**(3): 503-512.

Kang, Y.-M., D.-M. Zhang, X.-J. Yu, Q. Yang, J. Qi, Q. Su, Y.-P. Suo, L.-Y. Yue, G.-Q. Zhu and D.-N. Qin (2014). "Chronic infusion of enalaprilat into hypothalamic paraventricular nucleus attenuates angiotensin II-induced hypertension and cardiac hypertrophy by restoring neurotransmitters and cytokines." Toxicology and applied pharmacology **274**(3): 436-444.

Katzman, R. and H. M. Pappius (1973). Brain electrolytes and fluid metabolism, Williams & Wilkins.

Kc, P., K. V. Balan, S. S. Tjoe, R. J. Martin, J. C. LaManna, M. A. Haxhiu and T. E. Dick (2010). "Increased vasopressin transmission from the paraventricular nucleus to the rostral medulla augments cardiorespiratory outflow in chronic intermittent hypoxia-conditioned rats." The Journal of physiology **588**(4): 725-740.

Korim, W. S., K. Elsaafien, J. R. Basser, A. Setiadi, C. N. May and S. T. Yao (2018). "In renovascular hypertension, TNF-α type-1 receptors in the area postrema mediate increases in cardiac and renal sympathetic nerve activity and blood pressure." Cardiovascular Research.

Lawrence, A. J. and B. Jarrott (1994). "L-Glutamate as a Neurotransmitter at Baroreceptor Afferents - Evidence from in-Vivo Microdialysis." Neuroscience **58**(3): 585-591.

Lee, S. K., P. D. Ryu and S. Y. Lee (2013). "Differential distributions of neuropeptides in hypothalamic paraventricular nucleus neurons projecting to the rostral ventrolateral medulla in the rat." Neuroscience letters **556**: 160-165.

Lewandowsky, M. (1900). "Zur lehre von der cerebrospinalflussigkeit." Z klin Med **40**(480): 19.

Li, H.-B., X. Li, C.-J. Huo, Q. Su, J. Guo, Z.-Y. Yuan, G.-Q. Zhu, X.-L. Shi, J.-J. Liu and Y.-M. Kang (2016). "TLR4/MyD88/NF-κB signaling and PPAR-γ within the paraventricular nucleus are involved in the effects of telmisartan in hypertension." Toxicology and Applied Pharmacology.

Li, H.-B., D.-N. Qin, L. Ma, Y.-W. Miao, D.-M. Zhang, Y. Lu, X.-A. Song, G.-Q. Zhu and Y.-M. Kang (2014). "Chronic infusion of lisinopril into hypothalamic paraventricular nucleus modulates cytokines and attenuates oxidative stress in rostral ventrolateral medulla in hypertension." Toxicology and applied pharmacology **279**(2): 141-149.

Li, Y. F., K. L. Jackson, J. E. Stern, B. Rabeler and K. P. Patel (2006). "Interaction between glutamate and GABA systems in the integration of sympathetic outflow by the paraventricular nucleus of the hypothalamus." Am J Physiol Heart Circ Physiol **291**(6): H2847-2856.

Lu, B., B. J. Rutledge, L. Gu, J. Fiorillo, N. W. Lukacs, S. L. Kunkel, R. North, C. Gerard and B. J. Rollins (1998). "Abnormalities in monocyte recruitment and cytokine expression in monocyte chemoattractant protein 1–deficient mice." Journal of Experimental Medicine **187**(4): 601-608.

Lu, P., S.-j. Jiang, H. Pan, A.-l. Xu, G.-h. Wang, C.-l. Ma and Z. Shi (2017). "Short hairpin RNA interference targeting interleukin 1 receptor type I in the paraventricular nucleus attenuates hypertension in rats." Pflügers Archiv-European Journal of Physiology: 1-10.

Machnik, A., W. Neuhofer, J. Jantsch, A. Dahlmann, T. Tammela, K. Machura, J.-K. Park, F.-X. Beck, D. N. Müller and W. Derer (2009). "Macrophages regulate salt-dependent volume and blood pressure by a vascular endothelial growth factor-C–dependent buffering mechanism." Nature medicine **15**(5): 545-552.

Madrigal, J. L. M., B. Garcia-Bueno, A. E. Hinojosa, P. Polak, D. L. Feinstein and J. C. Leza (2010). "Regulation of MCP-1 production in brain by stress and noradrenaline-modulating drugs." Journal of Neurochemistry **113**(2): 543-551.

Mancia, G. and G. Grassi (2014). "The autonomic nervous system and hypertension." Circulation research **114**(11): 1804-1814.

Marina, N., F. Tang, M. Figueiredo, S. Mastitskaya, V. Kasimov, V. Mohamed-Ali, E. Roloff, A. G. Teschemacher, A. V. Gourine and S. Kasparov (2013). "Purinergic signalling in the rostral ventro-lateral medulla controls sympathetic drive and contributes to the progression of

heart failure following myocardial infarction in rats." Basic research in cardiology **108**(1): 1-10.

Martin, D. L. and R. W. Olsen (2000). GABA in the nervous system: the view at fifty years, Lippincott Williams and Wilkins.

Martinez-Maldonado, M. (1991). "Pathophysiology of renovascular hypertension." Hypertension **17**(5): 707-719.

Marvar, P. J., S. R. Thabet, T. J. Guzik, H. E. Lob, L. A. McCann, C. Weyand, F. J. Gordon and D. G. Harrison (2010). "Central and peripheral mechanisms of T-lymphocyte activation and vascular inflammation produced by angiotensin II–induced hypertension." Circulation research **107**(2): 263-270.

Matsuda, S., S. Umemoto, K. Yoshimura, S. Itoh, T. Murata, T. Fukai and M. Matsuzaki (2015). "Angiotensin II Activates MCP-1 and Induces Cardiac Hypertrophy and Dysfunction via Toll-like Receptor 4." Journal of atherosclerosis and thrombosis **22**(8): 833-844.

Matsumoto, J., S. Dohgu, F. Takata, T. Machida, F. F. B. Hatip, I. Hatip-Al-Khatib, A. Yamauchi and Y. Kataoka (2018). "TNF-α-sensitive brain pericytes activate microglia by releasing IL-6 through cooperation between IκB-NFκB and JAK-STAT3 pathways." Brain Research **1692**: 34-44.

McAllen, R. (1986). "Action and specificity of ventral medullary vasopressor neurones in the cat." Neuroscience **18**(1): 51-59.

McAllen, R. and R. Dampney (1989). "The selectivity of descending vasomotor control by subretrofacial neurons." Progress in brain research **81**: 233-242.

Meneton, P., X. Jeunemaitre, H. E. de Wardener and G. A. Macgregor (2005). "Links between dietary salt intake, renal salt handling, blood pressure, and cardiovascular diseases." Physiological reviews **85**(2): 679-715.

Meng, S. Z., A. Oka and S. Takashima (1999). "Developmental expression of monocyte chemoattractant protein-1 in the human cerebellum and brainstem." Brain and Development **21**(1): 30-35.

Michelini, L. C. (2007). "DIFFERENTIAL EFFECTS OF VASOPRESSINERGIC AND OXYTOCINERGIC PRE-AUTONOMIC NEURONS ON CIRCULATORY CONTROL: REFLEX MECHANISMS AND CHANGES DURING EXERCISE." Clinical and Experimental Pharmacology and Physiology **34**(4): 369-376.

Michelini, L. C. and M. Morris (1999). "Endogenous vasopressin modulates the cardiovascular responses to exercise." Annals of the New York Academy of Sciences **897**(1): 198-211.

Michelini, L. C. and J. E. Stern (2009). "Exercise-induced neuronal plasticity in central autonomic networks: role in cardiovascular control." Experimental physiology **94**(9): 947-960.

Morioka, N., M. Tokuhara, S. Harano, Y. Nakamura, K. Hisaoka-Nakashima and Y. Nakata (2013). "The activation of P2Y6 receptor in cultured spinal microglia induces the production of CCL2 through the MAP kinases-NF-kappaB pathway." Neuropharmacology **75**: 116-125.

Morrison, H. W. and J. A. Filosa (2013). "A quantitative spatiotemporal analysis of microglia morphology during ischemic stroke and reperfusion." Journal of neuroinflammation **10**(1): 782.

Müller, R., H. Steffen, R. Brunner, J. Saric, M. Pollok, C. Baldamus and W. Kaufmann (1991). "Changes in the alpha adrenergic system and increase in blood pressure with recombinant

human erythropoietin (rHuEpo) therapy for renal anemia." Clinical and investigative medicine. Medecine clinique et experimentale **14**(6): 614-622.

Nunes, F. C. and V. A. Braga (2011). "Chronic angiotensin II infusion modulates angiotensin II type I receptor expression in the subfornical organ and the rostral ventrolateral medulla in hypertensive rats." Journal of the Renin-Angiotensin-Aldosterone System **12**(4): 440-445.

Oliveira-Sales, E. B., M. A. Toward, R. R. Campos and J. F. Paton (2014). "Revealing the role of the autonomic nervous system in the development and maintenance of Goldblatt hypertension in rats." Autonomic Neuroscience **183**: 23-29.

Oliveira-Sales, E. B., E. Colombari, A. P. Abdala, R. R. Campos and J. F. Paton (2016). "Sympathetic overactivity occurs before hypertension in the two-kidney, one-clip model." Experimental physiology **101**(1): 67-80.

Pascual, O., S. B. Achour, P. Rostaing, A. Triller and A. Bessis (2012). "Microglia activation triggers astrocyte-mediated modulation of excitatory neurotransmission." Proceedings of the National Academy of Sciences **109**(4): E197-E205.

Paxinos G, W. C. (2007). The Rat Brain in Stereotaxic Coordinates, San Diego: Academic Press.

Persell, S. D. (2011). "Prevalence of resistant hypertension in the United States, 2003–2008." Hypertension **57**(6): 1076-1080.

Petroff, O. A. (2002). "Book review: GABA and glutamate in the human brain." The Neuroscientist **8**(6): 562-573.

Pilowsky, P. M. and A. K. Goodchild (2002). "Baroreceptor reflex pathways and neurotransmitters: 10 years on." J Hypertens **20**(9): 1675-1688.

Pösel, C., K. Möller, J. Boltze, D.-C. Wagner and G. Weise (2016). "Isolation and Flow Cytometric Analysis of Immune Cells from the Ischemic Mouse Brain." Journal of visualized experiments: JoVE(108).

Potts, P., Y. Hirooka and R. Dampney (1999). "Activation of brain neurons by circulating angiotensin II. Direct effects and baroreceptor-mediated secondary effects." Neuroscience **90**(2): 581-594.

Pyner, S. and J. H. Coote (2000). "Identification of branching paraventricular neurons of the hypothalamus that project to the rostroventrolateral medulla and spinal cord." Neuroscience **100**(3): 549-556.

Rahn, K. H., M. Barenbrock and M. Hausberg (1999). "The sympathetic nervous system in the pathogenesis of hypertension." J Hypertens Suppl **17**(3): S11-14.

Ramchandra, R., S. G. Hood, R. Frithiof, M. J. McKinley and C. N. May (2013). "The role of the paraventricular nucleus of the hypothalamus in the regulation of cardiac and renal sympathetic nerve activity in conscious normal and heart failure sheep." The Journal of physiology **591**(1): 93-107.

Rana, I., M. Stebbing, A. Kompa, D. J. Kelly, H. Krum and E. Badoer (2010). "Microglia activation in the hypothalamic PVN following myocardial infarction." Brain research **1326**: 96-104.

Rapoport, S. I. (1976). Blood-brain barrier in physiology and medicine, Raven Press.

Reyes, T. M., J. R. Walker, C. DeCino, J. B. Hogenesch and P. E. Sawchenko (2003). "Categorically distinct acute stressors elicit dissimilar transcriptional profiles in the paraventricular nucleus of the hypothalamus." J Neurosci **23**(13): 5607-5616.

Roberts, T. K., E. A. Eugenin, L. Lopez, I. A. Romero, B. B. Weksler, P.-O. Couraud and J. W. Berman (2012). "CCL2 disrupts the adherens junction: implications for neuroinflammation." Laboratory investigation **92**(8): 1213.

Rollins, B. J. (1997). "Chemokines." Blood **90**(3): 909-928.

Ross, C. A., D. A. Ruggiero, T. H. Joh, D. H. Park and D. J. Reis (1984). "Rostral ventrolateral medulla: selective projections to the thoracic autonomic cell column from the region containing C1 adrenaline neurons." Journal of Comparative Neurology **228**(2): 168-185.

Ross, C. A., D. A. Ruggiero, D. H. Park, T. H. Joh, A. F. Sved, J. Fernandez-Pardal, J. M. Saavedra and D. J. Reis (1984). "Tonic vasomotor control by the rostral ventrolateral medulla: effect of electrical or chemical stimulation of the area containing C1 adrenaline neurons on arterial pressure, heart rate, and plasma catecholamines and vasopressin." The Journal of neuroscience **4**(2): 474-494.

Rostene, W., P. Kitabgi and S. Melik-Parsadaniantz (2007). "Opinion - Chemokines: a new class of neuromodulator?" Nature Reviews Neuroscience **8**(11): 895-904.

Ruchaya, P. J., V. R. Antunes, J. F. R. Paton, D. Murphy and S. T. Yao (2014). "The cardiovascular actions of fractalkine/CX3CL1 in the hypothalamic paraventricular nucleus are attenuated in rats with heart failure." Experimental Physiology **99**(1): 111-122.

Santisteban, M. M., N. Ahmari, J. M. Carvajal, M. B. Zingler, Y. Qi, S. Kim, J. Joseph, F. Garcia-Pereira, R. D. Johnson and V. Shenoy (2015). "Involvement of bone marrow cells and neuroinflammation in hypertension." Circulation research **117**(2): 178-191.

Schramm, L. P., A. M. Strack, K. B. Platt and A. D. Loewy (1993). "Peripheral and central pathways regulating the kidney: a study using pseudorabies virus." Brain Res **616**(1-2): 251-262.

Scislo, T. J. and D. S. O'Leary (2000). "Differential role of ionotropic glutamatergic mechanisms in responses to NTS P2x and A2a receptor stimulation." American Journal of Physiology-Heart and Circulatory Physiology **278**(6): 2057-2068.

Shafton, A. D., A. Ryan and E. Badoer (1998). "Neurons in the hypothalamic paraventricular nucleus send collaterals to the spinal cord and to the rostral ventrolateral medulla in the rat." Brain Res **801**(1-2): 239-243.

Shapiro, R. E. and R. R. Miselis (1985). "The central neural connections of the area postrema of the rat." Journal of Comparative Neurology **234**(3): 344-364.

Sharma, R. K., T. Yang, A. C. Oliveira, G. O. Lobaton, V. Aquino, S. Kim, E. M. Richards, C. J. Pepine, C. Sumners and M. K. Raizada (2019). "Microglial Cells Impact Gut Microbiota and Gut Pathology in Angiotensin II-Induced Hypertension." Circulation research.

Shen, X. Z., Y. Li, L. Li, K. H. Shah, K. E. Bernstein, P. Lyden and P. Shi (2015). "Microglia Participate in Neurogenic Regulation of Hypertension." Hypertension **66**(2): 309-316.

Shi, P., C. Diez-Freire, J. Y. Jun, Y. Qi, M. J. Katovich, Q. Li, S. Sriramula, J. Francis, C. Sumners and M. K. Raizada (2010). "Brain microglial cytokines in neurogenic hypertension." Hypertension **56**(2): 297-303.

Shi, P., M. K. Raizada and C. Sumners (2010). "Brain cytokines as neuromodulators in cardiovascular control." Clinical and Experimental Pharmacology and Physiology **37**(2): e52-e57.

Shi, Z., X. B. Gan, Z. D. Fan, F. Zhang, Y. B. Zhou, X. Y. Gao, W. De and G. Q. Zhu (2011). "Inflammatory cytokines in paraventricular nucleus modulate sympathetic activity and cardiac sympathetic afferent reflex in rats." Acta physiologica **203**(2): 289-297.

Sim, J. J., S. K. Bhandari, J. Shi, I. L. A. Liu, D. A. Calhoun, E. A. McGlynn, K. Kalantar-Zadeh and S. J. Jacobsen (2013). Characteristics of resistant hypertension in a large, ethnically diverse hypertension population of an integrated health system. Mayo Clinic proceedings, Elsevier.

Simms, A., J. Paton, A. Allen and A. Pickering (2008). Amplified respiratory-sympathetic coupling in neonatal and juvenile spontaneously hypertensive rats. Proceedings of The Physiological Society, The Physiological Society.

Smith, P. A., L. N. Graham, A. F. Mackintosh, J. B. Stoker and D. A. Mary (2002). "Sympathetic neural mechanisms in white-coat hypertension." Journal of the American College of Cardiology **40**(1): 126-132.

Smith, P. A., L. N. Graham, A. F. Mackintosh, J. B. Stoker and D. A. Mary (2004). "Relationship between central sympathetic activity and stages of human hypertension." American journal of hypertension **17**(3): 217-222.

Smith, R. E. and M. Ashiya (2007). "Antihypertensive therapies." Nature Reviews Drug Discovery **6**(8): 597-598.

Soares, D. M., D. Ott, M. C. Melo, G. E. Souza and J. Roth (2013). "Chemokine ligand (CCL)-3 promotes an integrated febrile response when injected within pre-optic area (POA) of rats and induces calcium signaling in cells of POA microcultures but not TNF-alpha or IL-6 synthesis." Brain Behav Immun **34**: 120-129.

Song, X.-A., L.-L. Jia, W. Cui, M. Zhang, W. Chen, Z.-Y. Yuan, J. Guo, H.-H. Li, G.-Q. Zhu and H. Liu (2014). "Inhibition of TNF-α in hypothalamic paraventricular nucleus attenuates hypertension and cardiac hypertrophy by inhibiting neurohormonal excitation in spontaneously hypertensive rats." Toxicology and applied pharmacology **281**(1): 101-108.

Sperlágh, B., A. Köfalvi, J. Deuchars, L. Atkinson, C. J Milligan, N. J. Buckley and E. S. Vizi (2002). "Involvement of P2X7 receptors in the regulation of neurotransmitter release in the rat hippocampus." Journal of neurochemistry **81**(6): 1196-1211.

Sriramula, S., J. P. Cardinale and J. Francis (2013). "Inhibition of TNF in the brain reverses alterations in RAS components and attenuates angiotensin II-induced hypertension." PloS one **8**(5): e63847.

Stamatovic, S. M., R. F. Keep, M. M. Wang, I. Jankovic and A. V. Andjelkovic (2009). "Caveolae-mediated internalization of occludin and claudin-5 during CCL2-induced tight junction remodeling in brain endothelial cells." Journal of Biological Chemistry: jbc-M109.

Standiford, T. J., S. Kunkel, S. Phan, B. Rollins and R. Strieter (1991). "Alveolar macrophage-derived cytokines induce monocyte chemoattractant protein-1 expression from human pulmonary type II-like epithelial cells." Journal of Biological Chemistry **266**(15): 9912-9918.

Stern, J. E. (2004). "Nitric oxide and homeostatic control: an intercellular signalling molecule contributing to autonomic and neuroendocrine integration?" Prog Biophys Mol Biol **84**(2-3): 197-215.

Stern, J. E., P. M. Sonner, S. J. Son, F. C. Silva, K. Jackson and L. C. Michelini (2012). "Exercise training normalizes an increased neuronal excitability of NTS-projecting neurons of the hypothalamic paraventricular nucleus in hypertensive rats." Journal of neurophysiology **107**(10): 2912-2921.

Strack, A., W. Sawyer, J. Hughes, K. Platt and A. Loewy (1989). "A general pattern of CNS innervation of the sympathetic outflow demonstrated by transneuronal pseudorabies viral infections." Brain research **491**(1): 156-162.

Strack, A. M., W. B. Sawyer, J. H. Hughes, K. B. Platt and A. D. Loewy (1989). "A general pattern of CNS innervation of the sympathetic outflow demonstrated by transneuronal pseudorabies viral infections." Brain Res **491**(1): 156-162.

Strack, A. M., W. B. Sawyer, K. B. Platt and A. D. Loewy (1989). "CNS cell groups regulating the sympathetic outflow to adrenal gland as revealed by transneuronal cell body labeling with pseudorabies virus." Brain Res **491**(2): 274-296.

Su, Q., D.-N. Qin, F.-X. Wang, J. Ren, H.-B. Li, M. Zhang, Q. Yang, Y.-W. Miao, X.-J. Yu and J. Qi (2014). "Inhibition of reactive oxygen species in hypothalamic paraventricular nucleus attenuates the renin–angiotensin system and proinflammatory cytokines in hypertension." Toxicology and applied pharmacology **276**(2): 115-120.

Suga, M., S. Kurihara, Y. Iino and A. Terashi (1996). "Acute effects of human recombinant erythropoietin on cardiovascular dynamics and vasoactive substances." Nihon Jinzo Gakkai shi **38**(12): 634-639.

Talman, W. T., M. H. Perrone and D. J. Reis (1980). "Evidence for L-glutamate as the neurotransmitter of baroreceptor afferent nerve fibers." Science **209**(4458): 813-815.

Tavares, E. and F. J. Minano (2004). "Differential sensitivities of pyrogenic chemokine fevers to CC chemokine receptor 5 antibodies." Fundam Clin Pharmacol **18**(2): 163-169.

Todd, P. A. and E. M. Sorkin (1988). "Diclofenac sodium." Drugs **35**(3): 244-285.

Tomassoni, D., R. Avola, M. A. Di Tullio, M. Sabbatini, L. Vitaioli and F. Amenta (2004). "Increased expression of glial fibrillary acidic protein in the brain of spontaneously hypertensive rats." Clinical and Experimental hypertension **26**(4): 335-350.

Ullian, E. M., S. K. Sapperstein, K. S. Christopherson and B. A. Barres (2001). "Control of synapse number by glia." Science **291**(5504): 657-661.

Undesser, K. P., E. M. Hasser, J. R. Haywood, A. K. Johnson and V. S. Bishop (1985). "Interactions of vasopressin with the area postrema in arterial baroreflex function in conscious rabbits." Circulation Research **56**(3): 410-417.

Vaccari, C., S. J. Lolait and N. L. Ostrowski (1998). "Comparative Distribution of Vasopressin V1b and Oxytocin Receptor Messenger Ribonucleic Acids in Brain** Portions of the OTR mRNA distribution data were presented at the Wenner-Gren Conference, Stockholm, Sweden, 1996. This work was funded by the NIMH, NIH and by grant no. MH-01050 to CS Carter that provided partial support to C. Vaccari and E. Gournelos, who were also recipients of Howard Hughes Undergraduate Fellowships from the University of Maryland, College Park." Endocrinology **139**(12): 5015-5033.

Van Coillie, E., J. Van Damme and G. Opdenakker (1999). "The MCP eotaxin subfamily of CC chemokines." Cytokine & Growth Factor Reviews **10**(1): 61-86.

van der Kooy, D. and L. Y. Koda (1983). "Organization of the projections of a circumventricular organ: the area postrema in the rat." Journal of Comparative Neurology **219**(3): 328-338.

van Gassen, K. L., J. G. Netzeband, P. N. de Graan and D. L. Gruol (2005). "The chemokine CCL2 modulates Ca2+ dynamics and electrophysiological properties of cultured cerebellar Purkinje neurons." Eur J Neurosci **21**(11): 2949-2957.

Walz, D. A., V. Y. Wu, R. D. Lamo, H. Dene and L. E. Mccoy (1977). "Primary Structure of Human Platelet Factor-4." Thrombosis Research **11**(6): 893-898.

Walz, W. (1989). "Role of glial cells in the regulation of the brain ion microenvironment." Prog Neurobiol **33**(4): 309-333.

Wang, M.-L., Y.-M. Kang, X.-G. Li, Q. Su, H.-B. Li, K.-L. Liu, L.-Y. Fu, R. O. Saahene, Y. Li and H. Tan (2018). "Central blockade of NLRP3 reduces blood pressure via regulating inflammation microenvironment and neurohormonal excitation in salt-induced prehypertensive rats." Journal of neuroinflammation **15**(1): 95.

Wang, M.-L., X.-J. Yu, X.-G. Li, D.-Z. Pang, Q. Su, R. O. Saahene, H.-B. Li, X.-Y. Mao, K.-L. Liu and L.-Y. Fu (2018). "Blockade of TLR4 within the Paraventricular Nucleus Attenuates Blood Pressure by Regulating ROS and Inflammatory Cytokines in Prehypertensive Rats." American journal of hypertension: hpy074.

Wang, Y., M. Zhu, H. Xu, L. Cui, W. Liu, X. Wang, S. Shen and D. H. Wang (2015). "Role of the monocyte chemoattractant protein-1/CC chemokine receptor 2 signaling pathway in transient receptor potential vanilloid type 1 ablation-induced renal injury in salt-sensitive hypertension." Experimental Biology and Medicine: 1535370214565970.

Wei, S.-G., Y. Yu and R. B. Felder (2017). "Blood-borne Interleukin-1β Acts upon the Subfornical Organ to Upregulate the Sympathoexcitatory Milieu of the Hypothalamic Paraventricular Nucleus." American Journal of Physiology-Regulatory, Integrative and Comparative Physiology **314**: R447-R458.

Wei, S.-G., Y. Yu, Z.-H. Zhang and R. B. Felder (2015). "Proinflammatory cytokines upregulate sympathoexcitatory mechanisms in the subfornical organ of the rat." Hypertension **65**(5): 1126-1133.

Weindl, A. (1973). "Neuroendocrine aspects of circumventricular organs." Frontiers in neuroendocrinology **3**: 3-32.

Whelton, P. K., R. M. Carey, W. S. Aronow, D. E. Casey, K. J. Collins, C. D. Himmelfarb, S. M. DePalma, S. Gidding, K. A. Jamerson and D. W. Jones (2018). "2017 ACC/AHA/AAPA/ABC/ACPM/AGS/APhA/ASH/ASPC/NMA/PCNA guideline for the prevention, detection, evaluation, and management of high blood pressure in adults: a report of the American College of Cardiology/American Heart Association Task Force on Clinical Practice Guidelines." Journal of the American College of Cardiology **71**(19): e127-e248.

Wittendorp, M. C., H. W. G. M. Boddeke and K. Biber (2004). "Adenosine A(3) receptor-induced CCL2 synthesis in cultured mouse astrocytes." Glia **46**(4): 410-418.

Wu, Q., H. Xu, L. Hao, G. Ma, J. Sun, X. Song, F. Ding and N. Wang (2017). "P2X7 receptor regulates sympathoexcitatory response in myocardial infarction rats via NF-κB and MAPK pathways." American journal of translational research **9**(11): 4954.

Xie, Q.-y., M. Sun, T.-l. Yang and Z.-L. Sun (2006). "Losartan reduces monocyte chemoattractant protein-1 expression in aortic tissues of 2K1C hypertensive rats." International journal of cardiology **110**(1): 60-66.

Yamaguchi, N., S. Okada, D. Usui and K. Yokotani (2009). "Nitric oxide synthase isozymes in spinally projecting PVN neurons are involved in CRF-induced sympathetic activation." Autonomic Neuroscience **148**(1-2): 83-89.

Yang, Z. and J. H. Coote (1998). "Influence of the hypothalamic paraventricular nucleus on cardiovascular neurones in the rostral ventrolateral medulla of the rat." J Physiol **513 (Pt 2)**: 521-530.

Yang, Z., M. Wheatley and J. H. Coote (2002). "Neuropeptides, amines and amino acids as mediators of the sympathetic effects of paraventricular nucleus activation in the rat." Experimental Physiology **87**(6): 663-674.

Yao, S., J. Barden and A. Lawrence (2001). "On the immunohistochemical distribution of ionotropic P2X receptors in the nucleus tractus solitarius of the rat." Neuroscience **108**(4): 673-685.

Yao, S., A. Gourine, K. Spyer, J. Barden and A. Lawrence (2003). "Localisation of P2X 2 receptor subunit immunoreactivity on nitric oxide synthase expressing neurones in the brain stem and hypothalamus of the rat: a fluorescence immunohistochemical study." Neuroscience **121**(2): 411-419.

Yao, S. T., J. A. Barden, D. I. Finkelstein, M. R. Bennett and A. J. Lawrence (2000). "Comparative study on the distribution patterns of P2X1–P2X6 receptor immunoreactivity in the brainstem of the rat and the common marmoset (Callithrix jacchus): association with catecholamine cell groups." Journal of Comparative Neurology **427**(4): 485-507.

Yoshimura, T., E. Robinson, S. Tanaka, E. Appella and E. Leonard (1989). "Purification and amino acid analysis of two human monocyte chemoattractants produced by phytohemagglutinin-stimulated human blood mononuclear leukocytes." The Journal of Immunology **142**(6): 1956-1962.

Yoshimura, T., N. Yuhki, S. K. Moore, E. Appella, M. I. Lerman and E. J. Leonard (1989). "Human monocyte chemoattractant protein-1 (MCP-1) full-length cDNA cloning, expression in mitogen-stimulated blood mononuclear leukocytes, and sequence similarity to mouse competence gene JE." FEBS letters **244**(2): 487-493.

Yu, X.-J., D.-M. Zhang, L.-L. Jia, J. Qi, X.-A. Song, H. Tan, W. Cui, W. Chen, G.-Q. Zhu and D.-N. Qin (2015). "Inhibition of NF-κB activity in the hypothalamic paraventricular nucleus attenuates hypertension and cardiac hypertrophy by modulating cytokines and attenuating oxidative stress." Toxicology and applied pharmacology **284**(3): 315-322.

Yu, Y., S.-G. Wei, R. M. Weiss and R. B. Felder (2017). "TNF-α receptor 1 knockdown in subfornical organ ameliorates sympathetic excitation and cardiac hemodynamics in heart failure rats." American Journal of Physiology-Heart and Circulatory Physiology: ajpheart. 00280.02017.

Zimmerman, M. C., E. Lazartigues, R. V. Sharma and R. L. Davisson (2004). "Hypertension caused by angiotensin II infusion involves increased superoxide production in the central nervous system." Circulation research **95**(2): 210-216.

Zlotnik, A. and O. Yoshie (2012). "The chemokine superfamily revisited." Immunity **36**(5): 705-716.

Zoccal, D. B., A. E. Simms, L. G. Bonagamba, V. A. Braga, A. E. Pickering, J. F. Paton and B. H. Machado (2008). "Increased sympathetic outflow in juvenile rats submitted to chronic intermittent hypoxia correlates with enhanced expiratory activity." The Journal of physiology **586**(13): 3253-3265.

Zubcevic, J., J. Y. Jun, S. Kim, P. D. Perez, A. Afzal, Z. Shan, W. Li, M. M. Santisteban, W. Yuan and M. Febo (2013). "Altered inflammatory response is associated with an impaired autonomic input to the bone marrow in the spontaneously hypertensive rat." Hypertension **63**: 542-550.

Zubcevic, J., M. M. Santisteban, P. D. Perez, R. Arocha, H. Hiller, W. L. Malphurs, L. M. Colon-Perez, R. K. Sharma, A. De Kloet and E. G. Krause (2017). "A Single Angiotensin II

Hypertensive Stimulus Is Associated with Prolonged Neuronal and Immune System Activation in Wistar-Kyoto Rats." Frontiers in Physiology **8**: 592.

Zubcevic, J., M. M. Santisteban, T. Pitts, D. M. Baekey, P. D. Perez, D. C. Bolser, M. Febo and M. K. Raizada (2014). "Functional neural–bone marrow pathways: implications in hypertension and cardiovascular disease." Hypertension **63**(6): 129-139.

Zucker, I. H., H. D. Schultz, Y. F. Li, Y. Wang, W. Wang and K. P. Patel (2004). "The origin of sympathetic outflow in heart failure: the roles of angiotensin II and nitric oxide." Prog Biophys Mol Biol **84**(2-3): 217-232.

7. Appendices

Remark: The following section contains publications which I have contributed to, during my PhD.

The Role of the Blood Brain Barrier in Hypertension

Remark: The following article was published by *Experimental Physiology* on October 2017.

Exp Physiol 103.3 (2018) pp 337–342

Experimental Physiology

Symposium Report

The role of the blood–brain barrier in hypertension

Anthony Setiadi[1], Willian S. Korim[1], Khalid Elsaafien[1] and Song T. Yao[1,2]

[1]*Florey Institute of Neuroscience and Mental Health, University of Melbourne, Victoria, Australia*
[2]*Florey Department of Neuroscience and Mental Health, University of Melbourne, Victoria, Australia*

Edited by: Carolyn Barrett

New Findings

- **What is the topic of this review?**
  This review highlights the importance of the blood–brain barrier in the context of diseases involving autonomic dysfunction, such as hypertension and heart failure.
- **What advances does it highlight?**
  It highlights the potential role of pro-inflammatory cytokines, leucocytes and angiotensin II in disrupting the blood–brain barrier in cardiovascular diseases. Advances are highlighted in our understanding of neurovascular unit cells, astrocytes and microglia, with a specific emphasis on their pathogenic roles within the brain.

The blood–brain barrier (BBB) is a crucial barrier that provides both metabolic and physical protection to an immune-privileged CNS. The BBB has been shown to be disrupted in hypertension. This review addresses the importance of the BBB in maintaining homeostasis in the context of diseases related to autonomic dysfunction, such as hypertension. We highlight the potentially important roles of the immune system and neurovascular unit in the maintenance of the BBB, whereby dysregulation may lead to autonomic dysfunction in diseases such as heart failure and hypertension. Circulating leucocytes and factors such as angiotensin II and pro-inflammatory cytokines are thought ultimately to downregulate endothelial tight junction proteins that are a crucial component of the BBB. The specific mechanisms underlying BBB disruption and their role in contributing to autonomic dysfunction are not yet fully understood but are a growing area of interest. A greater understanding of these systems and advances in our knowledge of the molecular mechanisms causing BBB disruption will allow for the development of future therapeutic interventions in the treatment of autonomic imbalance associated with diseases such as heart failure and hypertension.

(Received 6 August 2017; accepted after revision 5 October 2017; first published online 6 October 2017)
Corresponding author S. T. Yao: Florey Department of Neuroscience and Mental Health, Howard Florey Laboratories, University of Melbourne, VIC 3010, Australia. Email: song.yao@florey.edu.au

Introduction

The blood–brain barrier (BBB) is crucial in the regulation of central homeostasis because it is the primary barrier separating the peripheral circulation from the CNS (reviewed by Abbott *et al.* 2010). Endothelial cells that express tight junction proteins form the main component of the BBB. These proteins limit paracellular movement of substrates across the cerebral vasculature. These tight junctions are specialized protein complexes consisting of claudins, occludins and junctional adhesion molecules (Begley & Brightman, 2003). The on-going regulation of the BBB also involves astrocytes, pericytes and microglia, which collectively form part of the neurovascular unit (Obermeier *et al.* 2013). Astrocytic end-feet processes extend and contact endothelial cells to form the glia limitans, a membrane barrier that further

© 2017 The Authors. Experimental Physiology © 2017 The Physiological Society

DOI: 10.1113/EP086434

limits movement across the BBB (Sofroniew & Vinters, 2010). This highly regulated system is essential to CNS homeostasis, allowing only minimal movement of small, lipid-soluble molecules into the CNS. However, the BBB can become compromised in neurological diseases, such as Alzheimer's (Kook *et al.* 2013), Parkinson's (Chung *et al.* 2013) and multiple sclerosis (Johnson *et al.* 2014). These neurological diseases lead to both widespread and sparse BBB disruption. Interestingly, the BBB has also been shown to be disrupted in cardiovascular diseases, such as neurogenic hypertension (Biancardi *et al.* 2014).

Although the pathogenesis of hypertension involves dysfunction of the cardiovascular system, the autonomic nervous system and renin–angiotensin systems are also major contributors to the disease. The pathogenesis of hypertension has been widely linked to the actions of the renin–angiotensin system, both within the periphery and in the brain. Infusion of angiotensin II (Ang II), a potent vasoactive peptide, elevates blood pressure and increases sympathetic output (reviewed by Young & Davisson, 2015). Moreover, Ang II induces oxidative stress and inflammation, which can further disease progression (Braga *et al.* 2011). Although the central actions of Ang II on autonomic function have long been realized (Scholkens *et al.* 1982), the downstream effects, including oxidative stress, neuroinflammation and BBB disruption, have only been uncovered recently.

In this report, we highlight the growing body of evidence that supports the hypothesis that BBB integrity is important for central autonomic control. We discuss the potential role of the immune system and its effects on BBB integrity and consider the role of the BBB and its constituent parts as potential therapeutic targets for the treatment of diseases that are, in part, mediated or exacerbated by autonomic dysfunction.

Blood–brain barrier disruption in hypertension

Angiotensin II and the blood–brain barrier. Given the important role of Ang II in the pathogenesis of hypertension, our group previously showed that disruption of the BBB via hyperosmotic mannitol allowed the entry of peripherally injected Ang II into the rostral ventrolateral medulla (RVLM), which activated tyrosine hydroxylase-expressing neurons involved in central cardiovascular regulation (Yao & May, 2013). Moreover, administration of losartan, an angiotensin II type 1 receptor (AT_1R) antagonist, in part, prevented the activation of RVLM neurons.

Recent studies have furthered these findings in a disease context using animal models of hypertension. These studies found that the BBB was disrupted in spontaneously and renovascular hypertensive rats (Biancardi *et al.* 2014). Importantly, they found that leakage of the 10 kDa fluorescent dextran was localized to central autonomic nuclei, including the nucleus of the solitary tract (NTS), paraventricular nucleus of the hypothalamus (PVN) and the RVLM, but not in the amygdala or somatosensory cortex. Furthermore, they showed that peripherally infused Ang II tagged with a fluorescent marker could enter these regions and gain access to neurons and microglia. This suggests that peripherally circulating factors can enter a leaky BBB and influence CNS signalling. Administration of losartan was found to prevent this disruption in the BBB and restore, in part, blood pressure homeostasis. However, administration of hydralazine, a direct vasodilator, failed to restore BBB integrity, thus suggesting that BBB disruption, via an Ang II–AT_1R mechanism, might precede and contribute to the hypertension.

Other studies have also shown that the BBB is disrupted in the hippocampus and corpus callosum of Dahl salt-sensitive hypertensive rats, which resulted in cognitive deficits, whereas AT_1R blockade using olmesartan was also found to restore the BBB and improve cognitive function (Pelisch *et al.* 2011). Angiotensin II is thought to elicit these effects by acting on the AT_1R on endothelial cells to increase BBB permeability. However, although BBB disruption is commonly associated with a decrease in tight junction protein expression, the levels of claudin-5 and occludin were not decreased by administration of Ang II *in vitro* (Fleegal-DeMotta *et al.* 2009). This is contrast with *in vivo* studies on hypertensive rats that have reported decreased levels of occludin and zonula occludens-1 alongside disturbances in the ultrastructure of tight junctions, as determined by electron microscopy (Fan *et al.* 2015). Given these findings, it is still unclear whether BBB disruption occurs before or is a result of hypertension. The mechanisms involved in allowing Ang II into the brain are still unclear, and therefore, further studies are warranted to determine whether there is a causal relationship between BBB disruption and hypertension via an Ang II-mediated process.

Immune system and the blood–brain barrier. A number of studies suggest that a chronic, low-grade inflammation is evident in hypertension (Coffman, 2011; Zubcevic *et al.* 2011). In response to this low-grade inflammation, the adaptive immune system is activated, causing an increase in circulating levels of inflammatory cells and mediators. Guzik and colleagues (2007) showed that mice lacking both T and B cells have a blunted hypertensive response, which supports a role of inflammation in hypertension. Circulating inflammatory molecules, such as tumour necrosis factor-α (TNF-α), C-reactive protein, interleukin (IL)-6, monocyte chemoattractant protein-1 (MCP-1; also known as chemokine ligand 2 or CCL2) and IL-1β, have all been found to be upregulated in both hypertensive patients and hypertensive animal models (Coffman, 2011). More recently, these pro-inflammatory markers have been found

© 2017 The Authors. Experimental Physiology © 2017 The Physiological Society

to be upregulated within the brain, suggesting a role of neuroinflammation in this disease (Winklewski *et al.* 2015).

In the periphery, T cells and other lymphocytes release pro-inflammatory molecules, which elicit cytotoxic effects on peripheral tissues, leading to end-organ damage (Rudemiller & Crowley, 2017). However, whether these cells can enter the CNS is less clear. Although the CNS is immune privileged, given that the BBB is compromised in hypertension (Biancardi *et al.* 2014), it is plausible that leucocytes or inflammatory mediators might extravasate into the CNS. Indeed, there is evidence that circulating leucocytes can infiltrate the CNS. In one study, Ang II-induced hypertension resulted in the accumulation of $CD3^+$ T cells into the cerebral artery wall, suggesting that the vasculature was deleteriously affected (Meissner *et al.* 2017). A more conclusive study showed that spontaneously hypertensive rats with reconstituted bone marrow from normotensive Wistar–Kyoto rats had decreased blood pressure and inflammation (Santisteban *et al.* 2015). Furthermore, these bone marrow labelled cells were found within the PVN of naive Sprague–Dawley rats when challenged with a continuous infusion of Ang II. Interestingly, these bone marrow-derived cells were positive for the microglial marker, Iba1, suggesting the differentiation of these monocytes into functional macrophages or microglia, which could ultimately lead to the upregulation of a pro-inflammatory state within the brain. Although this study did not conclusively determine the mechanism by which these leucocytes entered the CNS, it is clear that these cells were able to enter from the circulation and into autonomic nuclei, such as the PVN.

Although these studies provide further evidence that the BBB is a crucial interface and that its disruption may lead to altered brain function, autonomic imbalance and disease progression or exacerbation, the mechanisms remain unclear. A potential explanation for these findings can be attributed to the effects of circulating pro-inflammatory cytokines on the luminal side of the BBB. Pro-inflammatory cytokines are known to modulate BBB permeability. For example, administration of the chemokine MCP-1, *in vitro*, was shown to decrease transendothelial electrical resistance, a surrogate marker for BBB disruption (Stamatovic *et al.* 2005). Furthermore, Stamatovic and colleagues (2005) showed that MCP-1 caused a rearrangement of the actin cytoskeleton, including reorganization of tight junction proteins, possibly via a Rho/Rho kinase pathway. However, MCP-1 is not the only pro-inflammatory mediator that can influence BBB permeability, because both TNF-α and IL-6 contribute to BBB disruption via generation of reactive oxygen species (Rochfort *et al.* 2014). These studies demonstrated that the structural integrity of the tight junction complex can be affected by inflammatory mediators, which ultimately increased the permeability. Given the upregulation of pro-inflammatory cytokines and leucocyte generation during autonomic dysfunction in hypertension (Guzik *et al.* 2007; Santisteban *et al.* 2015) and heart failure (Mann, 2015), it is likely that these factors may mediate the initial dysfunction within the BBB, working alongside Ang II to disrupt the BBB and exacerbate the disease state, although further evidence is still required (Fig. 1). These findings will be important to uncover new pathways for circulating factors to enter the CNS, other than through the circumventricular organs, which lack a functional BBB. Importantly, uncovering these pathways could reveal novel therapeutic targets to treat these autonomic system-related cardiovascular diseases.

Neurovascular unit and the blood–brain barrier. There is clear emerging evidence that circulating inflammatory factors and inflammatory cells can enter the CNS. However, another major source of inflammatory molecules is thought to arise from within the brain itself; specifically, from the glial components of the neurovascular unit, namely astrocytes and microglia (Heneka *et al.* 2014; Sofroniew, 2015). Microglia are the brain's innate immune cells, and their role in hypertension has increasingly been realized. For example, microglial inhibition with minocycline in hypertensive rats leads to a decrease in blood pressure (Shi *et al.* 2010). Furthermore, ablation of microglia in transgenic mice has been found to reduce blood pressure and decrease levels of TNF-α and IL-1β in the PVN of Ang II-induced hypertensive mice (Shen *et al.* 2015). Interestingly, adoptive transfer of activated microglia into naive mice did not itself increase blood pressure; however, stimulation with Ang II resulted in a sustained pressor response when compared with sham controls. Collectively, these findings suggest a role of microglia in the maintenance of sustained hypertension; however, their role in the initiation of autonomic dysfunction still requires further investigation.

Astrocytes have also been shown to work in concert with microglia, as both cells release a myriad of pro-inflammatory mediators upon pathogen-induced activation. Once they have assumed a pro-inflammatory phenotype, astrocytes can release a host of chemokines and cytokines, such as TNF-α, IL-1β, MCP-1 and IL-6, amongst many others (Sofroniew, 2015). Cumulatively, these factors are involved in the recruitment of leucocytes, monocytes and macrophages to the target site of injury. Interestingly, astrocytes also release vascular endothelial growth factors, which have been shown to disrupt the BBB and increase leucocyte extravasation (Argaw *et al.* 2012). In the spontaneously hypertensive rat, anatomical changes to the intermediate insular cortex, a cardiovascular system-related region, was recently demonstrated (Marins *et al.* 2017). Increased density of

© 2017 The Authors. Experimental Physiology © 2017 The Physiological Society

the NMDA receptor, angiogenesis, glial fibrillary acidic protein immunoreactivity and microglial activation were found to increase within this region, further supporting the theory that the neurovascular unit appears has a role in autonomic signalling in hypertension.

Furthermore, it was recently shown that astrocytes are involved in the signalling cascade of the sympathoexcitatory effects of Ang II in the PVN (Stern *et al.* 2016). Here, they showed that astrocytic glutamate transporters were predominantly responsible for maintaining glutamate homeostasis and thus had a crucial influence on neuronal activity. Injections of Ang II were found to inhibit glutamate transporter activity on astrocytes within the PVN, therefore indirectly increasing neuronal activity and sympathetic outflow. In addition, our group has also recently found that pharmacological inhibition of astrocytes using sodium fluoroacetate causes an increase in blood pressure in normotensive animals, which was coupled with a decrease in BBB permeability within the PVN (Setiadi *et al.* 2017), which further highlights the importance of this glial subtype in autonomic regulation.

Although the role of astrocytes and microglia and their effects on the BBB have been realized in neurodegenerative and neurological diseases, their role on the abluminal (brain) side of the BBB in hypertension is gaining significant interest. Given the diverse roles these glial cells play in maintaining homeostasis and the need for these cells and their effectors to operate in a fine-tuned balance of both pro- and anti-inflammatory responses,

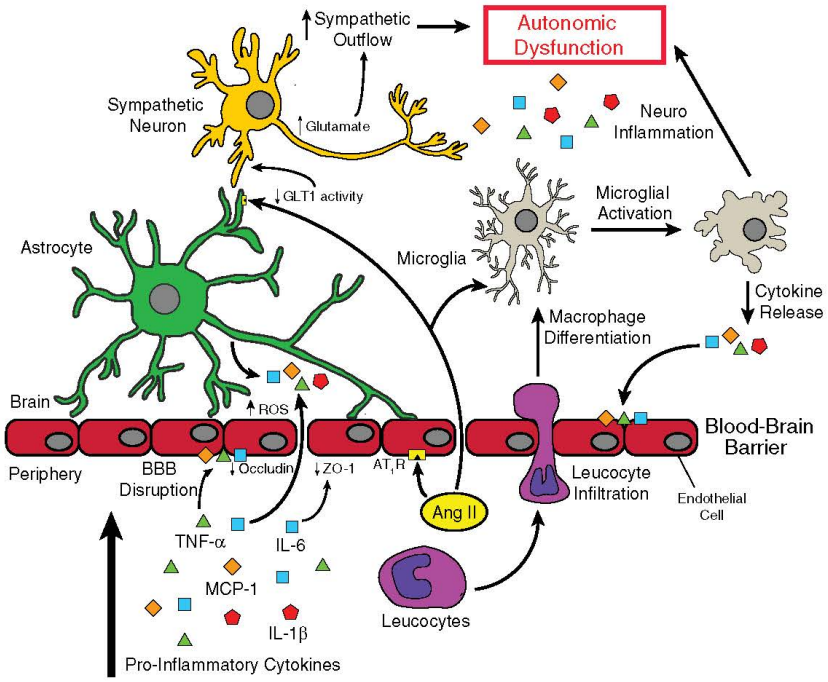


Figure 1. Proposed mechanism whereby the blood–brain barrier (BBB) is disrupted leading to autonomic dysfunction
Circulating pro-inflammatory cytokines and Ang II from the periphery act on the AT_1R on the BBB endothelium, which causes disruption in TJ proteins, occludin and ZO-1. Circulating leucocytes gain access to the brain and differentiate into functional microglia. These release pro-inflammatory cytokines and cause neuroinflammation. Angiotensin II can act directly on astrocytes to inhibit GLT1 activity to increase glutamate that activates sympathetic neurons and autonomic dysfunction. The BBB is further disrupted owing to release of pro-inflammatory cytokines from astrocytes and microglia. Abbreviations: Ang II, angiotensin II; AT_1R, angiotensin II type 1 receptor; GLT1, glutamate transporter 1; IL, interleukin; MCP-1, monocyte chemoattractant protein-1; ROS, reactive oxygen species; TJ, tight junction; TNF-α, tumour necrosis factor-α; and ZO-1, zonula occludens-1.

© 2017 The Authors. Experimental Physiology © 2017 The Physiological Society

their effect on the BBB needs further detailed investigation. This growing area of investigation is exciting, because the BBB is a prime target for therapeutic intervention. Given that the BBB is an important interface between the brain and circulation, it plays a crucial role in preserving central homeostasis and, as such, is an important target for new therapeutic agents. Further investigation of the downstream molecular mechanisms will be crucial in uncovering the importance of BBB integrity and allowing for targeted interventions, which could ultimately treat or limit the progression of autonomic diseases, such as hypertension and heart failure.

References

Abbott NJ, Patabendige AA, Dolman DE, Yusof SR & Begley DJ (2010). Structure and function of the blood–brain barrier. *Neurobiol Dis* **37**, 13–25.

Argaw AT, Asp L, Zhang J, Navrazhina K, Pham T, Mariani JN, Mahase S, Dutta DJ, Seto J, Kramer EG, Ferrara N, Sofroniew MV & John GR (2012). Astrocyte-derived VEGF-A drives blood-brain barrier disruption in CNS inflammatory disease. *J Clin Invest* **122**, 2454–2468.

Begley D & Brightman M (2003). Structural and functional aspects of the blood-brain barrier. In *Peptide Transport and Delivery into the Central Nervous System*, ed. Prokai L & Prokai-Tatrai K, pp. 39–78. Birkhäuser Basel, Basel.

Biancardi VC, Son SJ, Ahmadi S, Filosa JA & Stern JE (2014). Circulating angiotensin II gains access to the hypothalamus and brain stem during hypertension via breakdown of the blood–brain barrier. *Hypertension* **63**, 572–579.

Braga VA, Medeiros IA, Ribeiro TP, França-Silva MS, Botelho-Ono MS & Guimarães DD (2011). Angiotensin-II-induced reactive oxygen species along the SFO-PVN-RVLM pathway: implications in neurogenic hypertension. *Braz J Med Biol Res* **44**, 871–876.

Chung YC, Kim Y-S, Bok E, Yune TY, Maeng S & Jin BK (2013). MMP-3 contributes to nigrostriatal dopaminergic neuronal loss, BBB damage, and neuroinflammation in an MPTP mouse model of Parkinson's disease. *Mediators Inflamm* **2013**, 370526.

Coffman TM (2011). Under pressure: the search for the essential mechanisms of hypertension. *Nat Med* **17**, 1402–1409.

Fan Y, Yang X, Tao Y, Lan L, Zheng L & Sun J (2015). Tight junction disruption of blood–brain barrier in white matter lesions in chronic hypertensive rats. *Neuroreport* **26**, 1039–1043.

Fleegal-DeMotta MA, Doghu S & Banks WA (2009). Angiotensin II modulates BBB permeability via activation of the AT_1 receptor in brain endothelial cells. *J Cereb Blood Flow Metab* **29**, 640–647.

Guzik TJ, Hoch NE, Brown KA, McCann LA, Rahman A, Dikalov S, Goronzy J, Weyand C & Harrison DG (2007). Role of the T cell in the genesis of angiotensin II induced hypertension and vascular dysfunction. *J Exp Med* **204**, 2449–2460.

Heneka MT, Kummer MP & Latz E (2014). Innate immune activation in neurodegenerative disease. *Nat Rev Immunol* **14**, 463–477.

Johnson HL, Willenbring RC, Jin F, Manhart WA, LaFrance SJ, Pirko I & Johnson AJ (2014). Perforin competent CD8 T cells are sufficient to cause immune-mediated blood-brain barrier disruption. *PLoS One* **9**, e111401.

Kook S-Y, Seok Hong H, Moon M & Mook-Jung I (2013). Disruption of blood-brain barrier in Alzheimer disease pathogenesis. *Tissue Barriers* **1**, e23993.

Mann DL (2015). Innate immunity and the failing heart: the cytokine hypothesis revisited. *Circulation Research* **116**, 1254–1268.

Marins FR, Iddings JA, Fontes MAP & Filosa JA (2017). Evidence that remodeling of insular cortex neurovascular unit contributes to hypertension-related sympathoexcitation. *Physiol Rep* **5**, e13156.

Meissner A, Minnerup J, Soria G & Planas AM (2017). Structural and functional brain alterations in a murine model of angiotensin II-induced hypertension. *J Neurochem* **140**, 509–521.

Obermeier B, Daneman R & Ransohoff RM (2013). Development, maintenance and disruption of the blood-brain barrier. *Nat Med* **19**, 1584–1596.

Pelisch N, Hosomi N, Ueno M, Nakano D, Hitomi H, Mogi M, Shimada K, Kobori H, Horiuchi M, Sakamoto H, Matsumoto M, Kohno M & Nishiyama A (2011). Blockade of AT1 receptors protects the blood–brain barrier and improves cognition in Dahl salt-sensitive hypertensive rats. *Am J Hypertens* **24**, 362–368.

Rochfort KD, Collins LE, Murphy RP & Cummins PM (2014). Downregulation of blood-brain barrier phenotype by proinflammatory cytokines involves NADPH oxidase-dependent ROS generation: consequences for interendothelial adherens and tight junctions. *PLoS One* **9**, e101815.

Rudemiller NP & Crowley SD (2017). The role of chemokines in hypertension and consequent target organ damage. *Pharmacol Res* **119**, 404–411.

Santisteban MM, Ahmari N, Carvajal JM, Zingler MB, Qi Y, Kim S, Joseph J, Garcia-Pereira F, Johnson RD, Shenoy V, Raizada MK & Zubcevic J (2015). Involvement of bone marrow cells and neuroinflammation in hypertension. *Circ Res* **117**, 178–191.

Scholkens BA, Jung W, Rascher W, Dietz R & Ganten D (1982). Intracerebroventricular angiotensin II increases arterial pressure in rhesus monkeys by stimulation of pituitary hormones and the sympathetic nervous system. *Experimentia* **38**, 469–470.

Setiadi A, May CN & Yao ST (2017). Ablation of astrocytes in the paraventricular nucleus disrupts the blood-brain barrier and increases blood pressure in rats. *FASEB J* **31**(Suppl 1), 1010.5.

Shen XZ, Li Y, Li L, Shah KH, Bernstein KE, Lyden P & Shi P (2015). Microglia participate in neurogenic regulation of hypertension. *Hypertension* **66**, 309–316.

Shi P, Raizada MK & Sumners C (2010). Brain cytokines as neuromodulators in cardiovascular control. *Clin Exp Pharmacol Physiol* **37**, e52–e57.

Sofroniew MV (2015). Astrocyte barriers to neurotoxic inflammation. *Nat Rev Neurosci* **16**, 249–263.

© 2017 The Authors. Experimental Physiology © 2017 The Physiological Society

Sofroniew MV & Vinters HV (2010). Astrocytes: biology and pathology. *Acta Neuropathol* **119**, 7–35.
Stamatovic SM, Shakui P, Keep RF, Moore BB, Kunkel SL, Van Rooijen N & Andjelkovic AV (2005). Monocyte chemoattractant protein-1 regulation of blood–brain barrier permeability. *J Cereb Blood Flow Metab* **25**, 593–606.
Stern JE, Son S, Biancardi VC, Zheng H, Sharma N & Patel KP (2016). Astrocytes contribute to angiotensin II stimulation of hypothalamic neuronal activity and sympathetic outflow. *Hypertension* **68**, 1483–1493.
Winklewski PJ, Radkowski M, Wszedybyl-Winklewska M & Demkow U (2015). Brain inflammation and hypertension: the chicken or the egg? *J Neuroinflammation* **12**, 85.
Yao ST & May CN (2013). Intra-carotid angiotensin II activates tyrosine hydroxylase-expressing rostral ventrolateral medulla neurons following blood–brain barrier disruption in rats. *Neuroscience* **245**, 148–156.
Young CN & Davisson RL (2015). Angiotensin-II, the brain, and hypertension: an update. *Hypertension* **66**, 920–926.
Zubcevic J, Waki H, Raizada MK & Paton JFR (2011). Autonomic-immune-vascular interaction: an emerging concept for neurogenic hypertension. *Hypertension* **57**, 1026–1033.

Additional information

Competing interests

None declared.

Author contributions

All authors conceived and discussed the content of the manuscript. A.S. drafted the manuscript and figure. W.S.K., K.E. and S.T.Y. critically revised the intellectual content. All authors approved the final version of the manuscript and agree to be accountable for all aspects of the work in ensuring that questions related to the accuracy or integrity of any part of the work are appropriately investigated and resolved. All persons designated as authors qualify for authorship, and all those who qualify for authorship are listed.

Acknowledgements

We thank Dr Lindsea C. Booth for helpful comments. This work was supported by the National Health and Medical Research Council of Australia (GNT 1079680 to S.T.Y.), the High Blood Pressure Research Council of Australia and the Rebecca L. Cooper Medical Foundation (to W.S.K.). K.E. and A.S. are supported by Australian Government Research Training Program Scholarships. S.T.Y. is supported by an Australian Research Council Future Fellowship (FT170100363).

© 2017 The Authors. Experimental Physiology © 2017 The Physiological Society

In Renovascular Hypertension, TNF-a type-1 Receptors in the Area Postrema Mediate Increases in Cardiac and Renal Sympathetic Nerve Activity and Blood Pressure

Remark: The following article was published by *Cardiovascular Research* on October 2018.

ESC European Society of Cardiology
Cardiovascular Research
doi:10.1093/cvr/cvy268

In renovascular hypertension, TNF-α type-1 receptors in the area postrema mediate increases in cardiac and renal sympathetic nerve activity and blood pressure

Willian S. Korim[1,2*†], Khalid Elsaafien[1†], Jeremy R. Basser[1], Anthony Setiadi[1], Clive N. May[1], and Song T. Yao[1,3]

[1]Florey Institute of Neuroscience and Mental Health, University of Melbourne, Parkville, VIC 3052, Australia; [2]Wade Institute of Entrepreneurship, University of Melbourne, Parkville, VIC 3052, Australia; and [3]Florey Department of Neuroscience and Mental Health, University of Melbourne, Parkville, VIC 3052, Australia

Received 10 April 2018; revised 2 October 2018; editorial decision 19 October 2018; accepted 24 October 2018

Time for primary review: 34 days

Aims Neuroinflammation is a common feature in renovascular, obesity-related, and angiotensin II mediated hypertension. There is evidence that increased release of the pro-inflammatory cytokine tumour necrosis factor-α (TNF-α) contributes to the development of the hypertension, but the underlying neural mechanisms are unclear. Here, we investigated whether TNF-α stimulates neurons in the area postrema (AP), a circumventricular organ, to elicit sympathetic excitation, and increases in blood pressure (BP).

Methods and results In rats with renovascular hypertension, AP neurons that expressed TNF-α type-1 receptor (TNFR1) remained constantly activated (expressed c-Fos) and injection of TNFR1 neutralizing antibody into the AP returned BP (systolic: ~151 mmHg) to normotensive levels (systolic: ~108 mmHg). Nanoinjection of TNF-α (100 pg/50 nL) into the AP of anaesthetized normotensive rats increased BP (~16 mmHg) and sympathetic nerve activity, predominantly to the heart (~53%), but also to the kidneys (~35%). These responses were abolished by prior injection of a TNFR1 neutralizing antibody (1 ng/50 nL) within the same site. TNFR1 were expressed in the somata of neurons activated by TNF-α that were retrogradely labelled from the rostral ventrolateral medulla (RVLM).

Conclusion These findings indicate that in renovascular hypertension, blocking TNFR1 receptors in the AP significantly reduces BP, while activation of TNFR1 expressing neurons in the AP by TNF-α increases BP in normotensive rats. This is mediated, in part, by projections to the RVLM and an increase in both cardiac and renal sympathetic nerve activity. These findings support the notion that proinflammatory cytokines and neuroinflammation are important pathological mechanisms in the development and maintenance of hypertension.

Keywords Brain inflammation • Sympathetic system • Cytokine • Renovascular hypertension

1. Introduction

Neuroinflammation is a common feature in hypertension,[1] and the underlying molecular pathways largely involve pro-inflammatory cytokines.[2] Tumour necrosis factor-α (TNF-α) is a key pro-inflammatory cytokine that mediates overnutrition-related,[2] angiotensin II-induced,[3] and in renovascular (2 kidney-1 Clip; 2K1C)[4] hypertension; presumably through excitation of the sympathetic nervous system.[5] Sympathetic control of the cardiovascular system depends on precise coordination between neurons in central autonomic nuclei including the nucleus of the solitary tract (NTS), the first relay of the baroreceptor reflex,[6] and the rostral ventrolateral medulla (RVLM), the main generator of sympathetic tone.[7] Hence, because circulating TNF-α is increased in the plasma of 2K1C hypertensive rats[4] direct or indirect changes in the activity of NTS and RVLM neurons induced by TNF-α may result in changes in sympathetic outflow. Located immediately dorsal to the NTS, the area

* Corresponding author. Tel: +61 3 83440182, E-mail: willian.korim@unimelb.edu.au
†The first two authors served as equal first authors.

Published on behalf of the European Society of Cardiology. All rights reserved. © The Author(s) 2018. For permissions, please email: journals.permissions@oup.com.

Downloaded from https://academic.oup.com/cardiovascres/advance-article-abstract/doi/10.1093/cvr/cvy268/5144672 by University of Melbourne user on 14 December 2018

postrema (AP) is also an important autonomic structure that communicates with both the NTS and RVLM.[8] The lack of a blood–brain barrier and high permeability of blood vessels in the AP allows free transit of circulating TNF-α into this nucleus, permitting the direct activation of these neurons.[9,10] Furthermore, activation of microglia, which occurs in hypertension, leads to increased expression of TNF-α in the brain.[1] The normal activity of neurons depends on the physiological state of the surrounding microglia,[11] which is disrupted by overexpression of pro-inflammatory cytokines.[12] Whilst there is a growing body of evidence to show a key role for inflammation in hypertension and cardiovascular disorders, particularly in neurogenic hypertension,[1] the brain mechanisms by which central TNF-α alters sympathetic tone and blood pressure (BP) are unclear.

In this study, we investigated whether TNF-α acts on neurons expressing TNF-α type-1 receptor (TNFR1) in the AP to increase sympathetic nerve activity to the heart and kidneys and if this increases BP and heart rate (HR). We then examined whether these neurons project to the RVLM and activate sympathetic premotor neurons. To determine the importance of this system in hypertension, we tested if neurons containing TNFR1 are activated in a rat model of renovascular hypertension and if inhibition of TNF-α in the AP decreased BP.

2. Methods

All protocols were approved by the Animal Ethics Committee of the Florey Institute of Neuroscience and Mental Health. All experiments were performed in accordance with the Prevention of Cruelty to Animals Act (1986) under the guidelines set out by the Australian National Health and Medical Research Council 'Code of Practice for the Care and Use of Animals for Experimental Purposes in Australia' and according to Directive 2010/63/EU of the European Parliament on the protection of animals used for scientific purposes.

2.1 General procedures

Studies examining the responses to nanoinjections into the AP were completed in anaesthetized (pentobarbitone, 60 mg kg^{-1} i.v.), paralysed (pancuronium bromide, 1 mg kg^{-1} i.v.), and artificially ventilated adult male Sprague-Dawley rats (250–350 g; $N = 36$) maintained at ~37.5°C, prepared as previously described.[13] Additionally, pulse-modulation was observed in sympathetic activity to the heart and kidney (Supplementary material online, *Figure S2*). The right femoral vein and artery were cannulated for drug administration and arterial BP recordings, respectively. HR and systolic blood pressure (SBP) were derived from the BP channel. HR variability was calculated in the frequency domain. Power spectra were determined by a fast Fourier transformation (size: 4096) extracted from the interbeat interval interpolation of 5-min periods. The cut-offs for low- and high-frequency bands were 0.38–0.45 Hz and 1.04–1.13 Hz, respectively.[14]

2.2 Renovascular hypertension

Renovascular hypertension was induced in adult male Sprague-Dawley rats by clipping the left renal artery (2 kidney-1 Clip model; 2K1C) as previously described.[15] Animals that underwent SHAM surgery (where the animals underwent exactly the same surgery as the 2K1C group; however, the renal artery was not clipped) were used as controls. Development of hypertension was confirmed by measurement of BP with telemetric transmitters (PA-C40, Data Sciences International, MN, USA). Briefly, animals were anaesthetized with 2% isoflurane, the left renal artery was isolated and clipped to allow partial kidney perfusion, and a BP cannula connected to a telemetry device was implanted in the descending aorta. BP recordings were performed two to three times per week until renovascular hypertension was established in the third and fourth weeks.

2.3 Sympathetic nerve recordings

The left renal and cardiac sympathetic nerves were prepared for recording as described previously.[16,17] Briefly, recordings of renal (RSNA) and cardiac (CSNA) sympathetic nerve activity were made using bipolar silver hook electrodes. The signals were amplified (×10 000; Neurolog, Digitimer, Hertfordshire, UK) and filtered (50–1000 Hz). Signals were sampled at 10 000 Hz, and digitized using a Power1401 (Cambridge Electronic Design, Cambridge, UK), using Spike2 v7.02 software. Neurograms were quantified by rectifying and time-averaging the signal using a 1 s constant, followed by subtraction of the noise level (0%) after nerve crush, and normalization adopting 100% as baseline. Under resting conditions, CSNA and RSNA displayed pulse-synchronous baroreceptor modulation and the activity in both nerves was momentarily inhibited by baroreceptor loading with phenylephrine (10 μg/kg, i.v.; Supplementary material online, *Figure S2*), indicating that these recordings were derived from sympathetic nerves.

2.4 Nanoinjections and histology

A volume of 10 nL was used for retrograde tracer injections. The skull was positioned horizontally and the RVLM (~4.0 mm caudal and 1.8 mm lateral from Lambda, and 9.2 mm ventral from the dorsal surface) was functionally located by identifying the site with the highest increase in BP in response to local glutamate nanoinjection (50 mM/50 nL). Compounds were diluted in phosphate buffered saline (pH 7.4), which was used as a vehicle and a control for any cardiovascular change due to mechanical stimulation of AP cells.

For injections into the AP [0.5 mm rostral and 0.0 mm lateral (midline) from the *calamus scriptorius*, and 0.3 mm ventral from the dorsal surface], the skull was positioned at 45°. Multibarreled glass micropipettes were loaded with TNF-α (1 pg to 1 ng, PeproTech, Rocky Hill, NJ, USA), anti-TNFR1 antibody (1 ng, ab19139, Abcam, Cambridge, UK), and 2% pontamine sky blue (Sigma-Aldrich) or 2% fluorescent latex microbeads (LumaFluor Inc., USA). Injections where performed in both 2K1C and SHAM-operated control groups. Controls also included groups where vehicle was injected into the AP. All nanoinjections of drugs into the AP were 50 nL in volume.

At the end of the experiments, the rats received a nanoinjection of 2% pontamine sky blue or fluorescent latex beads to identify the centre of injection (*Figure 1C*). Animals were transcardially perfused with phosphate-buffered saline (pH 7.4) followed by 4% paraformaldehyde in 0.1 M phosphate buffer, pH 7.4. Brains were removed and processed for histology or immunohistochemistry. Nanoinjection sites were identified histologically as described previously.[18]

2.5 Immunohistochemistry

Coronal sections (30 μm) containing the AP were first washed and incubated in PBS-0.3% Triton-X 100 on a shaker for 15 min at room temperature, to facilitate antibody penetration. Sections were then incubated with the following primary antibodies (i) goat anti-CTB (1:10 000; Sigma Aldrich, MO, USA), (ii) mouse anti-CD11b at (1:5000; Bio-Rad Laboratories, USA), (iii) rabbit anti-TNFR1 (1:2000; Abcam, Cambridge, UK), (iv) rabbit anti-c-fos (1:5000; Synaptic Systems, Germany), and (v)

Downloaded from https://academic.oup.com/cardiovascres/advance-article-abstract/doi/10.1093/cvr/cvy268/5144672 by University of Melbourne user on 14 December 2018

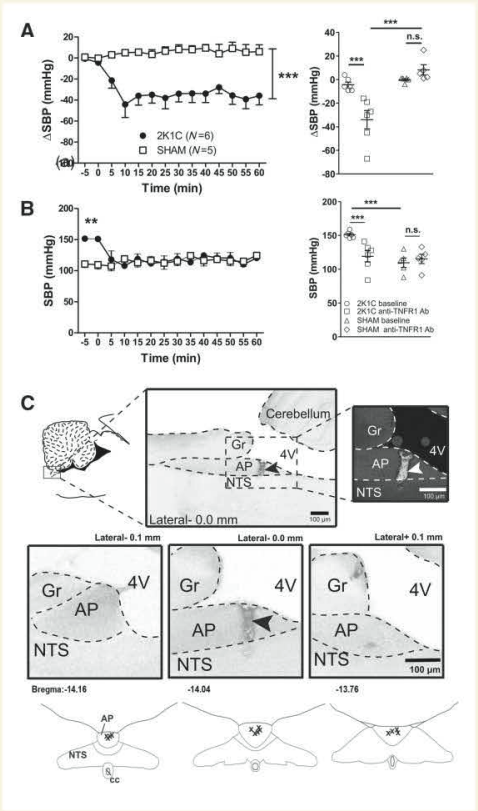


Figure 1 Haemodynamic changes to inactivation of TNFR1 in the AP of renovascular hypertensive rats. (*A*) Grouped data showing the decrease in systolic blood pressure (ΔSBP) following nanoinjection of anti-TNFR1 antibody (TNFR1 Ab, 1 ng/100 nL) into the AP of 2K1C rats ($N = 6$) at time 0, compared with no effect in the SHAM control group ($N = 5$). (*B*) Changes in SBP to nanoinjection of anti-TNFR1 into the AP in absolute values. (*C*) Histology confirming the site of nanoinjections into the AP. The sagittal view shows that 50 nL injections containing fluorescent beads (arrowhead) were restricted to the AP. Coronal drawings show the centre of injections—indicated by 'x'. cc, centre canal; 4V, fourth ventricle; Gr, Gracile nucleus; ns, non-significant; NTS, nucleus of the solitary tract. Scale bars 100 µm. $^{**}P < 0.01$, $^{***}P < 0.001$; two-way ANOVA Bonferroni correction.

mouse anti-tyrosine hydroxylase (TH) (1:1000; Merck Millipore, USA), for 1 h on the shaker at room temperature. Sections were then transferred to a refrigerator (4°C) for 24 h. On the following day, sections were washed (0.1 M PBS; 3 × 5 min) on a shaker at room temperature then incubated with the following secondary antibodies (i) biotinylated donkey anti-rabbit, (ii) biotinylated donkey anti-mouse, and (iii) biotinylated donkey anti-goat all at 1:500 dilution (Jackson ImmunoResearch Laboratories, Inc., USA), for 1 h on a shaker at room temperature. Sections were washed (0.1 M PBS; 3 × 5 min) then incubated in streptavidin conjugated with fluorophores (AlexaFluor-488, 594 680) at 1:500 dilution (Jackson ImmunoResearch laboratories, Inc., USA) for 1 h on a shaker at room temperature. Finally, sections were washed in 0.1 M PBS three more times (3 × 5 min) and mounted on gel-coated microscope slides (76 × 26 mm; Menzel-Glaser, 50 slides, Lomb). After drying (10–15 min) they were cover-slipped using anti-fade mountant (FluoroShield™ mountant containing DAPI; Sigma-Aldrich, MO, USA).

2.6 Tyramide signal amplification

For immunohistochemistry using antibodies raised in the same species, a tyramide signal amplification (TSA) protocol was used. Firstly, sections were incubated in 0.01% hydrogen peroxide (H_2O_2, 500 mL, Selby Scientific Limited, Victoria, Australia), for 15 min on a shaker at room temperature. Sections were washed (0.1 M PBS; 2 × 10 min) then incubated with the primary antibody (raised in the same species as another primary antibody) at a ×10 lower concentration than normally used. After 24 h (at 4°C), the sections were washed in 0.1 M PBS for 10 min and in TNT for another 10 min. Sections were then blocked with TNB blocking buffer for 30–45 min. Sections were then incubated with a HRP-conjugated secondary antibody at 1:500, for 30 min on a shaker at room temperature followed by two rinses in TNT, each time for 20 min. Sections were then incubated in fluorophore tyramide diluted in amplification diluent (TSA™-Plus Fluorescein System, PerkinElmer) at 1:100 for a maximum of 10 min at room temperature. After washes with TNT (2 × 20 min) and in 0.1 M PBS (2 × 20 min), sections were then ready to begin standard immunohistochemistry (with the other antibody raised in the same species) as described above.

2.7 Immunohistochemistry quantification and analysis

We used two different quantification methods to determine microglial activation, both of which have previously described and validated.[1,19,20] The first method involves manual assessment and quantification of activated microglia based on morphology as previously described.[1,19] Microglia were defined as resting/quiescent based on their non-inflammatory morphology of having longer branched processes and a smaller cell body; whereas, activated/ramified microglia were defined as having shorter retracted processes with larger cell bodies, giving it an amoeboid appearance (*Figure 2B*). The percentage of activated microglia was calculated by dividing the number of activated microglia over the total number of microglia quantified in a given section. The second method was based on a FIJI (NIH, MD, USA) skeleton analysis script, described by.[20] Briefly, the image was firstly converted into an 8-bit binary image and then a threshold contrast applied, removing low intensity pixels (i.e. removing background non-specific reactivity). The image was then skeletonised, converting all microglia to a skeletonised vector. Finally, an automated analysis function was used to analyse individual skeletons, giving the total number of branches and the average processes length. The automated analysis then averages all parameters in a specified region of interest; where the output represents the average number of processes per skeleton and the average process length. Generally, this automated method complements manual counting of activated microglia, as it gives a general indication of whether or not microglia are activated in a specific region (Supplementary material online, *Figures S3 and S4*).

A similar automated method in FIJI was used to quantify c-fos expression in the AP. Briefly, the image was firstly converted into an 8-bit binary image and then a threshold applied to remove low intensity pixels and non-circular labelling. An analyse particle function was then used to

Downloaded from https://academic.oup.com/cardiovascres/advance-article-abstract/doi/10.1093/cvr/cvy268/5144672 by University of Melbourne user on 14 December 2018

quantify the number of c-fos positive nuclei in a specific region of interest. To confirm the specificity of c-fos labelling, only nuclei that express c-fos and colocalised with DAPI (a specific nuclear stain) were identified as a c-fos positive nuclei.

2.8 Photomicroscopy and figure preparation

Photomicrographs were taken with a confocal laser-scanning microscope (Leica TCS SP8^{TM}; Leica GmbH, Wetzlar, Germany) to obtain high resolution images of the AP labelled for cholera toxin-B (CTB), c-Fos, CD11b, TNFR1, and the RVLM labelled for c-Fos and TH with the Leica Application Suite Advanced Fluorescence software (LSAF AF version 3.0, Leica GmbH, Wetzlar, Germany). Images were saved as Leica Image files (.lif) then converted into JPEG using FIJI open source image analysis software (NIH, USA). All confocal images were taken at constant settings for each image to allow for post-image capture analysis. All images were post-processed with Adobe Photoshop CS6 (Adobe Systems, Mountain View, CA, USA) to merge the separate fluorescent channels. Other analyses such as cell counting, skeletal analysis, and the addition of scale bars were performed using the image analysis tools/scripts available in ImageJ or FIJI (NIH, USA).

2.9 Statistics

The D'Agostino and Pearson omnibus test was performed to confirm normal distribution of the data within samples. Parametric statistical analysis was performed using Student's *t*-test, one-way, or two-way ANOVA repeated measures followed by the Bonferroni correction. All statistical tests for *in vivo* data were performed using GraphPad Prism 6.0. Data are presented as mean ± standard error of the mean. Statistical significance was determined when $P < 0.05$.

3. Results

3.1 Activation of TNFR1-expressing neurons and microglia in the area postrema of renovascular hypertensive rats

To investigate the role of the AP in the development of renovascular hypertension, we determined the effects of blockade of TNFR1 in the AP of 2K1C rats. We also quantified the number of activated neurons and microglial cells in the AP of 2K1C hypertensive rats. Three weeks following the clipping of the left renal artery, 2K1C rats showed significantly increased BP (SBP: 151 ± 2 mmHg; $N = 6$) in comparison with the SHAM (SBP: 111 ± 9 mmHg; $N = 5$) control group ($F(1,9) = 17.55$, $P = 0.0023$). The induced increase in SBP in 2K1C animals was significantly reduced ($F(1,9) = 20.65$, $P = 0.0014$) by nanoinjection (*Figure 1C*) of the anti-TNFR1 antibody (1 ng/100 nL) into the AP (*Figure 1A and B*). Nanoinjections of the anti-TNFR1 antibody into the AP of SHAM-operated control rats did not elicit any cardiovascular changes.

A functional neuroanatomic study was conducted in a different cohort ($N = 5$/group) of animals. Three weeks after the left renal artery was clipped the rats became hypertensive (Supplementary material online, *Figure S1*). This increase in BP was accompanied by a greater than three-fold increase in the number of c-Fos positive neurons in the AP of 2K1C rats in comparison with SHAM operated, normotensive animals (62 ± 4 vs. 15 ± 2, respectively; $t(8) = 11.01$, $P < 0.0001$, $N = 5$; *Figure 2C*). Additionally, we observed a greater numbers of c-Fos and TNFR1 co-labelled neurons in the AP of the hypertensive 2K1C rats compared with normotensive SHAM controls (15 ± 1 vs. 4 ± 1 respectively; $t(8) = 6.777$, $P < 0.0001$, $N = 5$; *Figure 2C*). We also observed an increase in activated microglia in the AP of the 2K1C hypertensive rats in comparison with SHAM controls (28 ± 5 vs. 12 ± 1, $t(8) = 3.052$, $P = 0.0079$, $N = 5$; *Figure 2E*)—using the microglia biomarker CD11b. In addition, we used FIJI to confirm the quantification of activated microglia. In comparison with SHAM normotensive controls, renovascular 2K1C rats showed decreased number of branches per skeletonised microglia (64 ± 6 vs. 99 ± 6, $t(8) = 3.919$, $P = 0.0044$, $N = 5$) and decreased average branch length (9.8 ± 0.4 vs. 12.3 ± 0.4 µm, $t(8) = 4.156$, $P = 0.0016$, $N = 5$)—representative of the morphological changes observed in activated microglia.

3.2 Effects of nanoinjection of TNF-α in the area postrema on arterial blood pressure

In order to understand the mechanisms underpinning the central role of TNF-α in the development of hypertension, we directly nanoinjected TNF-α into the AP of normotensive rats. Nanoinjection of TNF-α into the AP produced increases in BP (*Figure 3A*) that were dose dependent (1 pg to 1 ng; *Figure 3B*), whilst nanoinjection of the vehicle did not produce any cardiovascular changes (*Figure 3C–E*). TNF-α (100 pg/50 nL) injected into the AP elicited a rise (+22 ± 3 mmHg) in SBP. This increase was blocked by a prior (~5 to 10 min) nanoinjection of the anti-TNFR1 antibody (1 ng/50 nL) into the same site (ΔSBP: +1 ± 2 mmHg, $t(16) = 5.997$, $P = 0.0002$, $N = 9$; *Figure 3C*). In addition, TNFR1 blockade abolished the increase in HR produced by injection of TNF-α into the AP (ΔHR: +35 ± 6 vs. -8 ± 6 b.p.m., $t(20) = 4.762$, $P = 0.0001$, $N = 11$; *Figure 3D*). Finally, nanoinjection of the TNFR1 antibody into the AP significantly reduced the increase in the spectral low frequency/high frequency (LF/HF) ratio elicited by TNF-α (8.3 ± 0.8 vs. 3.4 ± 0.5, $t(12) = 5.066$, $P = 0.0102$, $N = 7$; *Figure 3E*). Finally, control nanoinjections of TNF-α (100 pg/50 nL; *Figure 3H*) into the fourth ventricle, immediately dorsal of the AP did not change SBP when compared to injections made directly into the AP (95 ± 2 vs. 140 ± 5 mmHg, $t(8) = 8.688$, $P < 0.001$, $N = 5$; *Figure 3F and G*).

3.3 Cardiac and renal sympathetic responses to nanoinjection of TNF-α into the area postrema

In order to determine whether the TNF-α induced changes to SBP were mediated by the sympathetic nervous system, we recorded the changes in sympathetic nerve activities to the heart and kidney in normotensive rats. Nanoinjection of TNF-α (100 pg/50 nL) into the AP significantly increased CSNA (100 ± 1% vs. 153 ± 12%, $t(4) = 4.104$, $P = 0.007$, $N = 5$) and RSNA (100 ± 2% vs. 135 ± 7%, $t(4) = 4.521$, $P = 0.005$, $N = 5$; *Figure 4*) in normotensive rats—in comparison to baseline. The increases in sympathetic discharge were accompanied by rises in MBP (88 ± 5 vs. 97 ± 8 mmHg, $t(4) = 11.2$, $P = 0.015$, $N = 5$). The rises in BP were positively correlated (Supplementary material online, *Figure S2*) with increases in CSNA ($P < 0.0001$, $r^2 = 0.921$) and RSNA ($P < 0.0001$, $r^2 = 0.945$). Similarly, changes in HR were correlated with levels of CSNA ($P < 0.0001$, $r^2 = 0.955$) and RSNA ($P < 0.0001$, $r^2 = 0.950$). Nanoinjection of the antibody against TNFR1 (1 ng/50 nL) into the same site in the AP, 10 min prior to TNF-α nanoinjection (100 pg/50 nL), prevented the increase in CSNA in response to TNF-α (153 ± 12 vs. 99 ± 8%, $F(2, 12) = 13.43$, $P = 0.001$, $N = 5$, *Figure 4D and E*). Cardiovascular-related activity in both sympathetic nerves was confirmed by inhibition in response to an increase in BP elicited by

Downloaded from https://academic.oup.com/cardiovascres/advance-article-abstract/doi/10.1093/cvr/cvy268/5144672 by University of Melbourne user on 14 December 2018

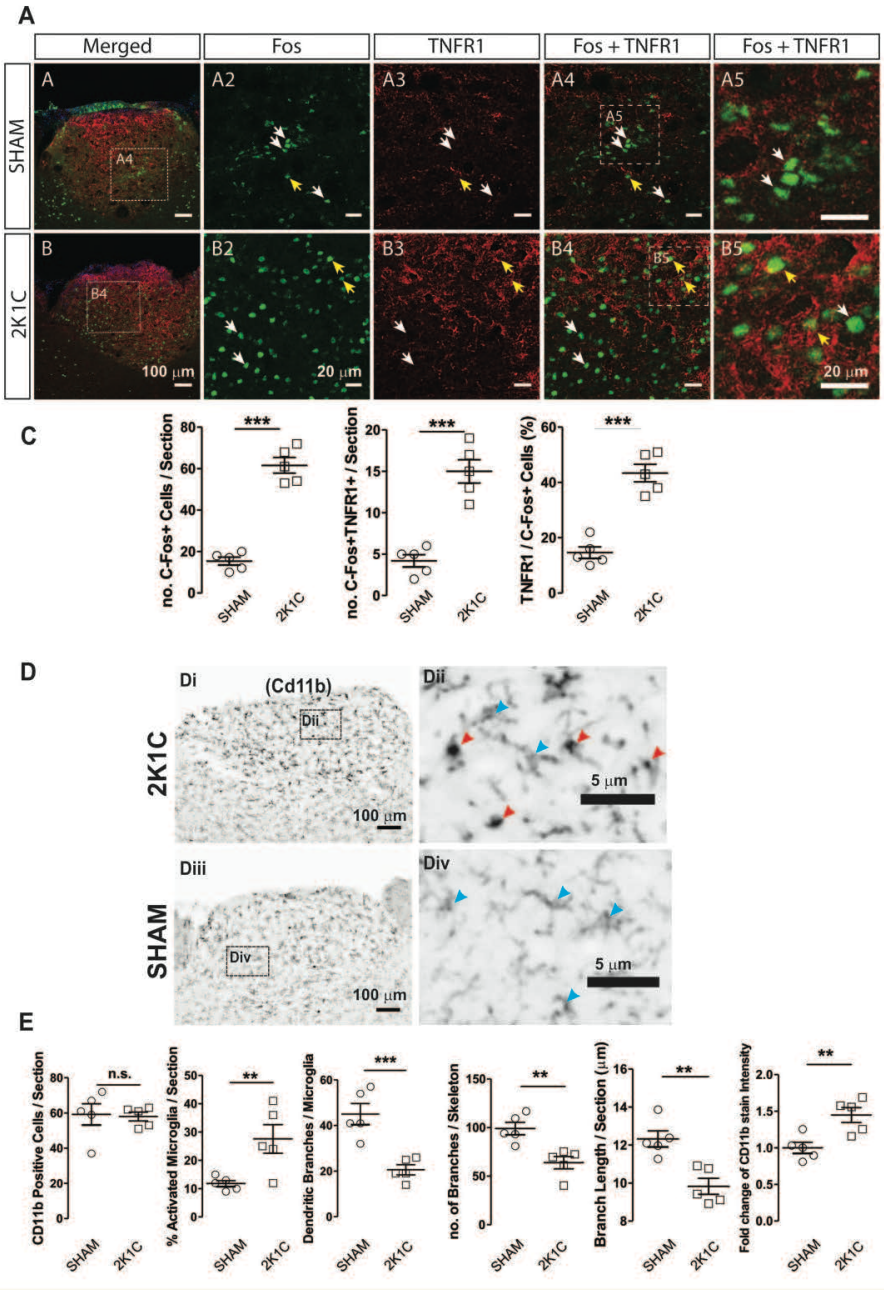


Figure 2 Cell activation in the AP of renovascular hypertensive rats. (*A* and *B*) Expression of c-Fos^{+} (white arrowheads) and TNFR1 in the AP and NTS of 2K1C renovascular hypertensive rats ($N = 5$) or SHAM control ($N = 5$). Yellow arrowheads indicate neurons that co-expressed c-Fos and TNFR1. (*C*) Group data showing number of activated neurons, and activated neurons that expressed TNFR1 in the AP of 2K1C rats. (*D*) Bi-Bii non-activated (blue arrowheads) and activated (red arrowheads) microglial cells in the AP of 2K1C ($N = 5$) or SHAM ($N = 5$) rats, labelled with CD11b. (*E*) 2K1C hypertensive rats displayed a higher proportion of activated microglia. Morphological analysis was performed manually, whereas skeletal analysis was automated using a FIJI script. ns, non-significant. $^{*}P \leq 0.05$, $^{**}P < 0.01$, $^{***}P < 0.001$ to control; Student's *t*-test. Data are expressed as mean ± standard error of the mean.

Downloaded from https://academic.oup.com/cardiovascres/advance-article-abstract/doi/10.1093/cvr/cvy268/5144672 by University of Melbourne user on 14 December 2018

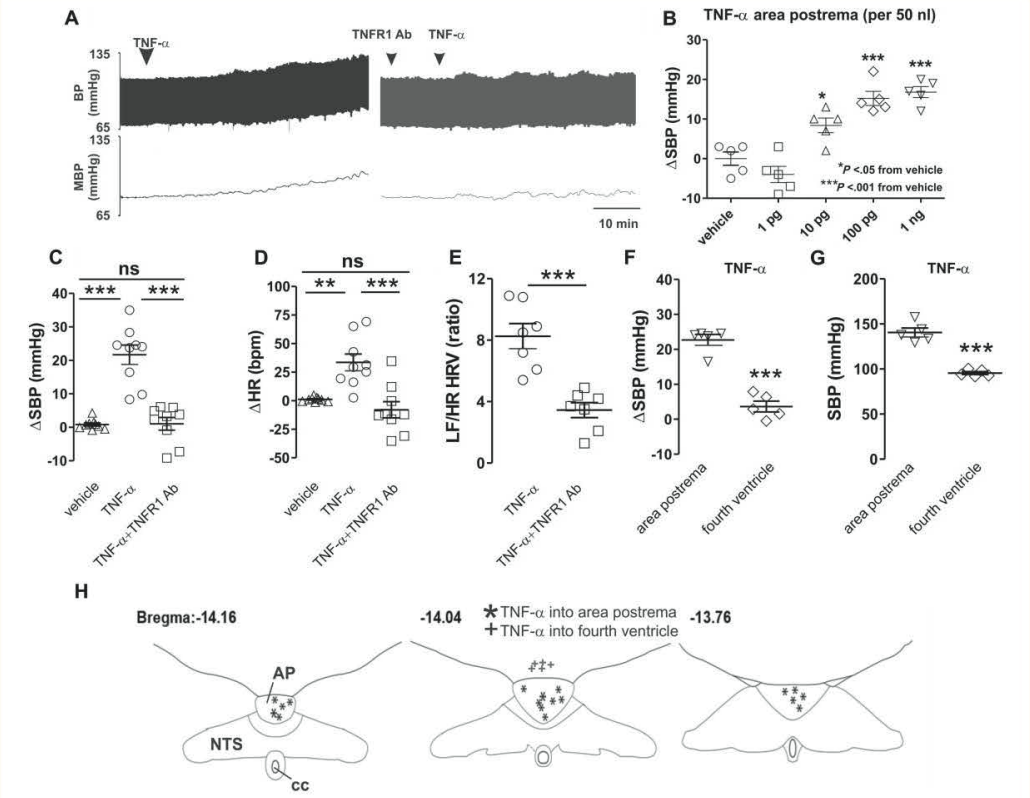


Figure 3 Cardiovascular effects in response to injection of TNF-α into the AP. (*A*) Changes in BP in response to TNF-α (100 pg/50 nL) into the AP, and in response to TNF-α into the AP following prior blockade of TNFR1 receptors with the anti-TNFR1 antibody (1 ng/50 nL). Scale bar: 10 min. (*B*) Nanoinjection of TNF-α in the AP produced a dose-dependent increase in SBP (1 pg^{-1} ng; $N = 5$). $^{*}P < 0.05$, $^{***}P < 0.001$; one-way ANOVA with Bonferroni correction. (*C*) Changes in systolic blood pressure (ΔSBP) responses to TNF-α nanoinjection into the AP. Blockade of TNFR1 abolished the increases in *C*. SBP ($N = 9$) and *D*. HR ($N = 11$) changes in response to TNF-α into the AP. (*E*) TNFR1 nanoinjection into the AP decreased the elevated LF/HF ratio HR variability (HRV) ratio produced by TNF-α ($N = 7$). (*F* and *G*) Negative controls: nanoinjection of TNF-α (100 pg/50 nL) into the fourth ventricle did not change blood pressure. (*H*) Coronal drawings show the centre of injections are indicated by '*', whilst fourth ventricle injections are indicated by '+'. AP, area postrema; cc, centre canal; ns, non-significant; NTS, nucleus of the solitary tract. $^{**}P$, 0.01, $^{***}P < 0.001$ to TNF-α; Student's *t*-test. Data are expressed as mean ± standard error of the mean.

phenylephrine treatment and by the pulse modulated nature of the activity (*Figure 4A* and Supplementary material online, *Figure S2*).

3.4 TNF-α activates RVLM-projecting neurons in the area postrema

To understand the connectome and the neural pathways involved in the increase in SBP in response to TNF-α into the AP, RVLM-projecting neurons in the AP that expressed TNFR1 were activated by nanoinjection of TNF-α. The retrograde tracer CTB was nanoinjected into the RVLM and, after 7 days recovery, TNF-α or vehicle (phosphate buffered saline; pH 7.4) was nanoinjected into the AP (100 pg/50 nL) of normotensive, anaesthetized rats. The animals were allowed to rest for 90 min to achieve maximal c-Fos expression. Nanoinjection of TNF-α into the AP activated more neurons (c-fos positive; *Figure 5A*) than vehicle injected animals (80 ± 3 vs. 14 ± 3 respectively; $t(8) = 16.67$; $P < 0.0001$, $N = 5$). Moreover, the number of neurons activated that project to the RVLM was also greater in the TNF-α vs. vehicle injected rats (25 ± 2 vs. 5 ± 1, respectively; $t(8) = 7.846$; $P < 0.0001$, $N = 5$; *Figure 5A*). We found that a proportion (26%) of TNFR1 positive neurons in the AP that projected to the ipsilateral RVLM (i.e. immunoreactive for CTB) were activated (expressed c-Fos) by TNF-α (*Figure 5A*). In the same animals ($N = 5$), nanoinjection of TNF-α into the AP (100 pg/50 nL) also elicited greater c-Fos expression in RVLM neurons compared with vehicle injected

Downloaded from https://academic.oup.com/cardiovascres/advance-article-abstract/doi/10.1093/cvr/cvy268/5144672 by University of Melbourne user on 14 December 2018

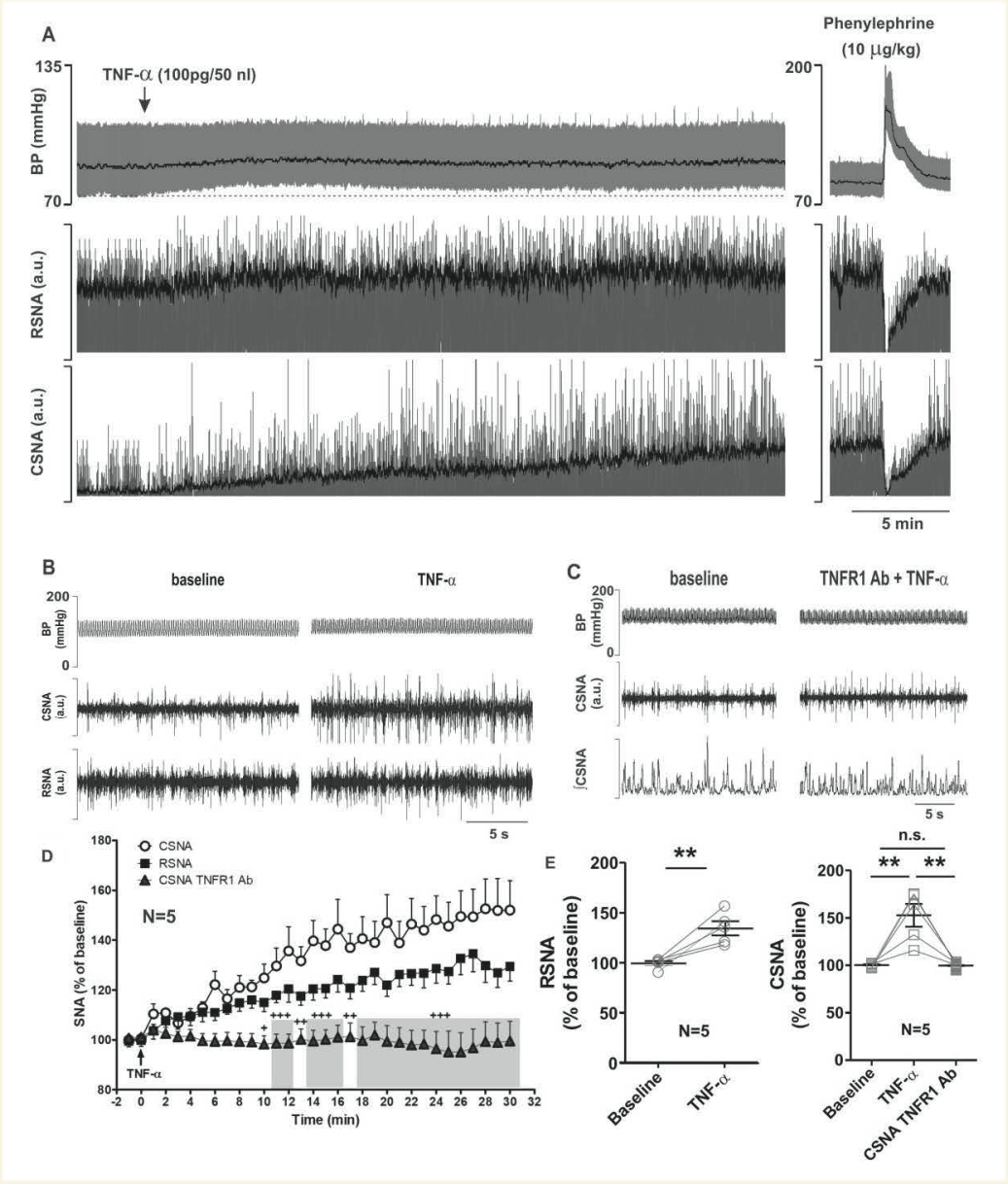


Figure 4 Effects of injection of TNF-α into the AP on cardiac and renal sympathetic nerve activity. (*A*) Blood pressure (BP), and rectified (grey) and averaged (black) traces of cardiac (CSNA) and renal (RSNA) sympathetic nerve activities in response to nanoinjection of TNF-α (100 pg/50 nL) into the AP. Scale bar: 5 min. (*B*) Raw traces showing rises in CSNA and RSNA following nanoinjection of TNF-α into the AP. Scale bar: 5 s. (*C*) TNFR1 blockade with the anti-TNFR1 antibody (1 ng/50 nL) blocked the CSNA increase to nanoinjection of TNF-α into the AP. Scale bar: 5 s. (*D*) Averaged ($N = 5$) time-course of changes in CSNA and RSNA in response to TNF-α into the AP, and following the blockade of TNFR1. (*D*) Group data ($N = 5$) showing maximum increases in BP, HR, CSNA, and RSNA. $^{**}P < 0.01$ to TNF-α; $^{+}P < 0.05$, $^{++}P < 0.01$, $^{+++}P < 0.001$ to CSNA control; Student's *t*-test or two-way ANOVA with Bonferroni correction. n.s., non-significant. Data are expressed as mean ± standard error of the mean.

Downloaded from https://academic.oup.com/cardiovascres/advance-article-abstract/doi/10.1093/cvr/cvy268/5144672 by University of Melbourne user on 14 December 2018

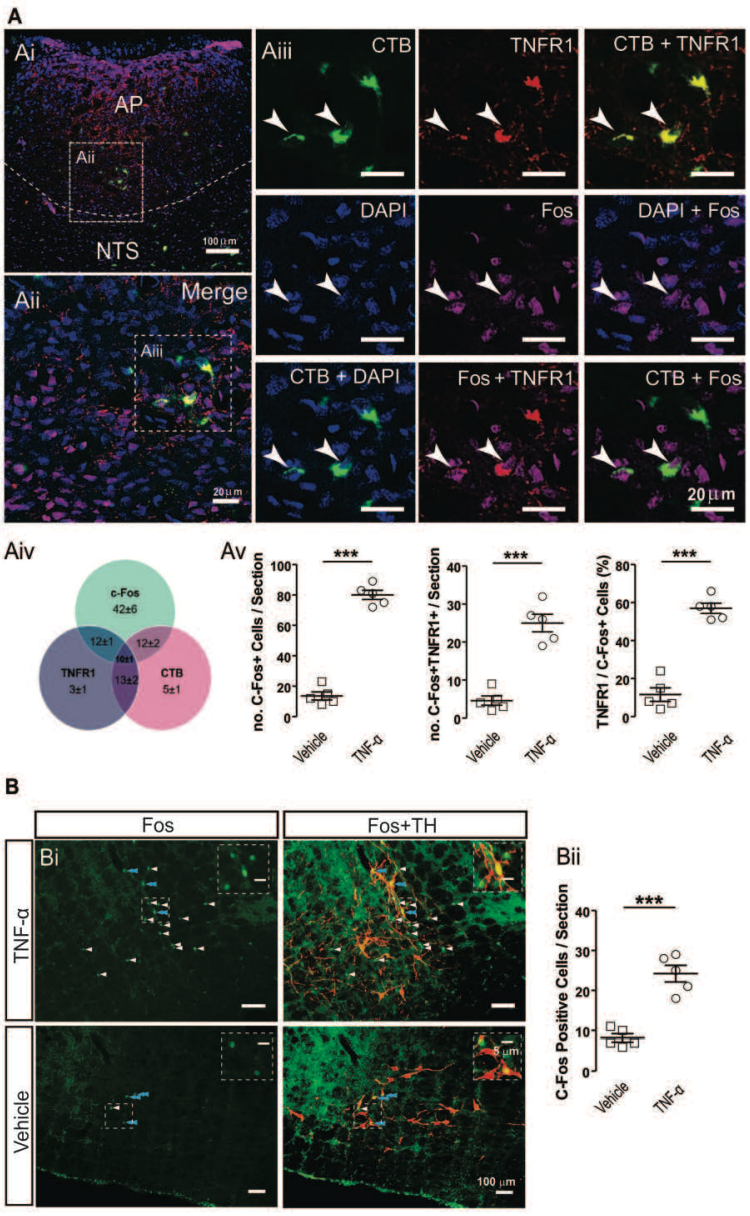


Figure 5 RVLM-projecting TNFR1 positive neurons in the AP are activated by TNF-α. (*A*) Ai–Aiii, co-expression (arrowheads) in AP neurons of CTB, retrogradely transported from the RVLM, TNFR1, and c-Fos expression induced by TNF-α (100 pg/50 nL) into the AP. Scale bar Ai: 100 µm; Aii: 20 µm. (Aiv) Venn diagram showing the distribution of neuron subsets in the AP immunoreactive to CTB, c-Fos, and TNFR1 ($N = 3$). (Av) Group data showing larger number of activated neurons and activated neurons that expressed TNF-α in the AP following nanoinjection of TNF-α into the AP, compared with vehicle. (*B*) Bi RVLM C1 (tyrosine hydroxylase, TH^+; blue double arrowheads) and non-C1 (TH^-; white arrowheads) neurons activated by TNF-α into the AP. Scale bar: low magnification: 100 µm; high-magnification: 50 µm. (Bii) Group data ($N = 5$) showing quantification of all activated cells in the RVLM in response to TNF-α or vehicle into the AP. ***$P < 0.001$, Student's *t*-test; Data are expressed as mean ± standard error of the mean.

Downloaded from https://academic.oup.com/cardiovascres/advance-article-abstract/doi/10.1093/cvr/cvy268/5144672 by University of Melbourne user on 14 December 2018

animals (24 ± 2 vs. 8 ± 1, respectively; $t(8) = 6.963$; $P < 0.0001$, $N = 5$; *Figure 5B*), a hallmark of sympathetic excitation. TNF-α nanoinjections in the AP activated both C1 and non-C1 RVLM neurons that were TH positive and negative, respectively.

4. Discussion

Although there is evidence that neuroinflammation is associated with hypertension,[1,11] the mechanisms and neural pathways underlying the actions of inflammatory mediators remain to be elucidated. In a renovascular model of hypertension, we identified activated neurons in the AP that expressed TNFR1. We also demonstrated that renovascular hypertension depends on activation of microglia and TNFR1-expressing neurons in the AP. Our results show that exogenous TNF-α can activate TNFR1 on neurons in the AP, leading to increases in BP by stimulation of CSNA and RSNA, a common feature seen in hypertension. We demonstrated that a proportion of TNFR1 positive neurons in the AP that project to the RVLM are activated by TNF-α, which activates both C1 and non-C1 RVLM neurons. The activation of TH-positive neurons can increase sympathetic outflow to the heart and kidney either directly (e.g. spinal-projections)[21] or indirectly (e.g. arousal-related hypothalamic relay)[22] by stimulating the sympathetic preganglionic neurons. Thus, these findings reveal a potentially important signalling mechanism and neural pathway by which neuroinflammation can promote the development of hypertension.

In the first series of studies, the role of TNF-α in determining renovascular hypertension was investigated in 2K1C rats.[15,23] By the third or fourth weeks after renal artery clipping, when hypertension had developed, there was a three-fold greater activation of neurons in the AP of 2K1C rats compared with SHAM control rats. Significantly more of these activated neurons expressed the TNFR1 in the hypertensive 2K1C rats compared with SHAM control normotensive rats. Importantly, we demonstrated that blocking TNFR1 in the AP reduced BP to a greater degree in 2K1C rats compared with normotensive control rats. Our findings are in line with previous reports showing that kidney hypoperfusion in 2K1C rats increased expression and circulating levels of the pro-inflammatory cytokines TNF-α, IL-6, and TGF-β1.[24] This might explain why we see a difference in the number of activated neurons that expresses the TNFR1 receptor in 2K-1C hypertensive rats compared with their normotensive, SHAM control, counterparts. Indeed, in chronic experimental renal artery stenosis there are increased levels of cytokines in the renal vein of the ischaemic kidney, which has been used as an index of renal parenchymal inflammation.[25] Thus, since the AP is a circumventricular organ and lacks a blood–brain barrier, the increased circulating levels of TNF-α, and possibly other cytokines such as IL-6, and TGF-β1, likely stimulate neurons in the AP. Our findings suggest that in renovascular hypertension, activation of these neurons in the AP, which have excitatory projections to sympathetic premotor neurons in the RVLM, increases sympathetic outflow and arterial BP.

In addition to the action of increased plasma levels of TNF-α on circumventricular organs in renovascular hypertension,[26] it is possible that degradation of the blood–brain barrier by high levels of circulating angiotensin II[27] allows passage of TNF-α into the brain. Additionally, in the renovascular hypertensive model, there is enhanced endogenous production of angiotensin II in the RVLM.[28] Angiotensin II can stimulate the release of neurotrophic factors via activation of microglia that leads to local production of inflammatory cytokines, including TNF-α, in the AP.[11,29] Indeed, we observed increased activated microglia in the AP of hypertensive 2K1C rats, which may lead to production of TNF-α in the AP. A further mechanism by which the levels of pro-inflammatory cytokines within the brain can be increased is via an action of TNF-α on its receptor to activate an intracellular signalling pathway. This pathway involves up-regulation of the Nuclear Transcription factor-κB,[5] which further increases the expression of pro-inflammatory cytokines within the brain.[30]

In this study, the effects of TNF-α were also assessed in normotensive rats, because hypertension up-regulates several pro-inflammatory cytokines that could confound interpretation of the data. Pharmacological activation of AP neurons with TNF-α predominantly stimulated CSNA, with lesser increases in RSNA. The finding that these increases in SNA were inhibited by selective blockade of TNFR1, which also prevented the accompanying increases in MBP and HR, suggests that these cardiovascular changes were dependent on the increases in SNA. The ability of TNF-α to alter autonomic control of the heart was also indicated by increased LF/HF HR variability,[31] which was attenuated by blockade of TNFR1 in the AP. These findings indicate that TNF-α can act on TNFR1 expressing neurons in the AP to increase SNA. Since the AP is a circumventricular organ, neuroinflammation induced by increased circulating TNF-α, as occurs in cardiovascular disease,[26,32] may contribute to the increased levels of SNA and the development of hypertension.

The neural pathway by which stimulation of neurons in the AP by TNF-α results in increases in SNA were also investigated. We demonstrated that the retrograde tracer CTB injected into the RVLM, labelled neurons in the AP that contain TNFR1. This anatomical evidence suggests that direct projections from the AP might be responsible for activating cardiovascular sympathetic premotor neurons in the RVLM. This is supported by the finding that activation of TNFR1 in the AP elicited c-Fos expression in C1 (TH-positive) and non-C1 (TH-negative) RVLM neurons. Cardiovascular sympathetic premotor neurons in the RVLM[21] are part of the C1 catecholaminergic neuronal group,[33,34] responsible for the genesis of sympathetic tone and the maintenance of BP at homeostatic levels.[7] Hence, the increases in cardiac and renal SNA and BP in response to TNF-α may result from activation of neurons in the AP expressing TNFR1, which have a direct excitatory projections to cardiovascular sympathetic premotor neurons in the RVLM.[21]

There is increasing interest in the pathological role that inflammation plays in the development of cardiovascular disease. There is little evidence that systemic anti-inflammatory drugs have a beneficial effect in hypertension, and it is likely that effective treatments will require inhibition of specific inflammatory pathways at targeted sites. In this study, we have demonstrated that, in renovascular hypertension, neuroinflammation plays an important role in mediating sympathoexcitation and in maintaining the hypertension. We propose that a prolonged action of TNF-α on neurons in the AP, via a pathway that includes activation of RVLM neurons, results in a sustained increase in cardiac and renal sympathetic tone that is an essential component in the development of renovascular hypertension. Neuroinflammation and overexpression of pro-inflammatory cytokines in the brain are also observed in other experimental models of hypertension, including spontaneously hypertensive rats,[35] obesity-induced hypertension,[36] and deoxycorticosterone-induced[37,38] hypertension. Understanding the central signalling mechanisms of individual pro-inflammatory cytokines, such as TNF-α, might facilitate the identification of new therapeutic targets for translational studies to treat hypertension.

Supplementary material

Supplementary material is available at *Cardiovascular Research* online.

Downloaded from https://academic.oup.com/cardiovascres/advance-article-abstract/doi/10.1093/cvr/cvy268/5144672 by University of Melbourne user on 14 December 2018

Acknowledgements

The authors would like to thank Prof. Robin McAllen, Dr David Farmer, and Dr Natasha Pracejus for providing their knowledge for the recording of cardiac sympathetic nerve activity, and Mr David Trevaks for helping with equipment setup. The authors would also like to acknowledge the support of the Advanced Microscopy Facility at the Florey Institute of Neuroscience and Mental Health for training, advice and assistance in using the microscopes at the facility.

Conflict of interest: none declared.

Funding

This work was supported by the National Health and Medical Research Council of Australia (GNT 1079680 to S.T.Y.), the High Blood Pressure Research Council of Australia, the Rebecca L Cooper Medical Foundation, the Wade Institute and Ormond College—University of Melbourne (to W.S.K.) and the Victorian Government through the Operational Infrastructure Scheme. K.E. and A.S. are supported by the Australian Government Research Training Program Scholarships. S.T.Y. is supported by an Australian Research Council Future Fellowship (FT170100363).

References

1. Shi P, Diez-Freire C, Jun JY, Qi Y, Katovich MJ, Li Q, Sriramula S, Francis J, Sumners C, Raizada MK. Brain microglial cytokines in neurogenic hypertension. *Hypertension* 2010;**56**:297–303.
2. Cai D. Neuroinflammation and neurodegeneration in overnutrition-induced diseases. *Trends Endocrinol Metab* 2013;**24**:40–47.
3. Sriramula S, Francis J. Tumor necrosis factor-alpha is essential for angiotensin II-induced ventricular remodeling: role for oxidative stress. *PLoS One* 2015;**10**: e0138372.
4. Bivol LM, Berge RK, Iversen BM. Tetradecylthioacetic acid prevents the inflammatory response in two-kidney, one-clip hypertension. *Am J Physiol Regul Integr Comp Physiol* 2008;**294**:R438–R447.
5. Purkayastha S, Zhang G, Cai D. Uncoupling the mechanisms of obesity and hypertension by targeting hypothalamic IKK-β and NF-κB. *Nat Med* 2011;**17**:883–887.
6. Chan RK, Sawchenko PE. Organization and transmitter specificity of medullary neurons activated by sustained hypertension: implications for understanding baroreceptor reflex circuitry. *J Neurosci* 1998;**18**:371–387.
7. Guertzenstein PG, Silver A. Fall in blood pressure produced from discrete regions of the ventral surface of the medulla by glycine and lesions. *J Physiol* 1974;**242**:489–503.
8. Shapiro RE, Miselis RR. The central neural connections of the area postrema of the rat. *J Comp Neurol* 1985;**234**:344–364.
9. Nadeau S, Rivest S. Effects of circulating tumor necrosis factor on the neuronal activity and expression of the genes encoding the tumor necrosis factor receptors (p55 and p75) in the rat brain: a view from the blood-brain barrier. *Neuroscience* 1999;**93**: 1449–1464.
10. Hermann G, Holmes G, Rogers R. TNF(alpha) modulation of visceral and spinal sensory processing. *Curr Pharm Des* **11**:1391–1409.
11. Shen XZ, Li Y, Li L, Shah KH, Bernstein KE, Lyden P, Shi P. Microglia participate in neurogenic regulation of hypertension. *Hypertension* 2015;**66**:309–316.
12. Santisteban MM, Ahmari N, Carvajal JM, Zingler MB, Qi Y, Kim S, Joseph J, Garcia-Pereira F, Johnson RD, Shenoy V, Raizada MK, Zubcevic J. Involvement of bone marrow cells and neuroinflammation in hypertension. *Circ Res* 2015;**117**:178–191.
13. Korim WS, Egwuenu E, Fong AY, McMullan S, Cravo SL, Pilowsky PM. Noxious somatic stimuli diminish respiratory-sympathetic coupling by selective resetting of the respiratory rhythm in anaesthetized rats. *Exp Physiol* 2012;**97**:1093–1104.
14. Cerutti C, Gustin MP, Paultre CZ, Lo M, Julien C, Vincent M, Sassard J. Autonomic nervous system and cardiovascular variability in rats: a spectral analysis approach. *Am J Physiol Heart Circ Physiol* 1991;**261**:H1292–H1299.
15. Kuwajima I, Kardon MB, Pegram BL, Sesoko S, Frohlich ED. Regression of left ventricular hypertrophy in two-kidney, one clip Goldblatt hypertension. *Hypertension* 1982; **4**:113–118.
16. Yao Y, Hildreth CM, Farnham MM, Saha M, Sun QJ, Pilowsky PM, Phillips JK. The effect of losartan on differential reflex control of sympathetic nerve activity in chronic kidney disease. *J Hypertens* 2015;**33**:1249–1260.
17. Pracejus NH, Farmer DG, McAllen RM. Segmental origins of cardiac sympathetic nerve activity in rats. *Auton Neurosci* 2015;**187**:45–49.
18. Korim WS, Bou-Farah L, McMullan S, Verberne AJ. Orexinergic activation of medullary premotor neurons modulates the adrenal sympathoexcitation to hypothalamic glucoprivation. *Diabetes* 2014;**63**:1895–1906.
19. Rana I, Stebbing M, Kompa A, Kelly DJ, Krum H, Badoer E. Microglia activation in the hypothalamic PVN following myocardial infarction. *Brain Res* 2010;**1326**: 96–104.
20. Morrison HW, Filosa JA. A quantitative spatiotemporal analysis of microglia morphology during ischemic stroke and reperfusion. *J Neuroinflammation* 2013;**10**:782.
21. Brown DL, Guyenet PG. Electrophysiological study of cardiovascular neurons in the rostral ventrolateral medulla in rats. *Circ Res* 1985;**56**:359–369.
22. Bochorishvili G, Nguyen T, Coates MB, Viar KE, Stornetta RL, Guyenet PG. The orexinergic neurons receive synaptic input from C1 cells in rats. *J Comp Neurol* 2014; **522**:3834–3846.
23. Oliveira-Sales EB, Colombari DS, Davisson RL, Kasparov S, Hirata AE, Campos RR, Paton JF. Kidney-induced hypertension depends on superoxide signaling in the rostral ventrolateral medulla. *Hypertension* 2010;**56**:290–296.
24. Matavelli LC, Huang J, Siragy HM. Angiotensin AT(2) receptor stimulation inhibits early renal inflammation in renovascular hypertension. *Hypertension* 2011;**57**: 308–313.
25. Eirin A, Zhang X, Zhu XY, Tang H, Jordan KL, Grande JP, Dietz AB, Lerman A, Textor SC, Lerman LO. Renal vein cytokine release as an index of renal parenchymal inflammation in chronic experimental renal artery stenosis. *Nephrol Dial Transplant* 2014;**29**:274–282.
26. Moubarak M, Jabbour H, Smayra V, Chouery E, Saliba Y, Jebara V, Fares N. Cardiorenal syndrome in hypertensive rats: microalbuminuria, inflammation and ventricular hypertrophy. *Physiol Res* 2012;**61**:13–24.
27. Biancardi VC, Stern JE. Compromised blood-brain barrier permeability: novel mechanism by which circulating angiotensin II signals to sympathoexcitatory centres during hypertension. *J Physiol* 2016;**594**:1591–1600.
28. Li P, Sun HJ, Cui BP, Zhou YB, Han Y. Angiotensin-(1-7) in the rostral ventrolateral medulla modulates enhanced cardiac sympathetic afferent reflex and sympathetic activation in renovascular hypertensive rats. *Hypertension* 2013;**61**: 820–827.
29. Harden LM, Rummel C, Luheshi GN, Poole S, Gerstberger R, Roth J. Interleukin-10 modulates the synthesis of inflammatory mediators in the sensory circumventricular organs: implications for the regulation of fever and sickness behaviors. *J Neuroinflammation* 2013;**10**:22.
30. Kawai T, Akira S. Signaling to NF-κB by Toll-like receptors. *Trends Mol Med* 2007;**13**: 460–469.
31. Montano N, Ruscone TG, Porta A, Lombardi F, Pagani M, Malliani A. Power spectrum analysis of heart rate variability to assess the changes in sympathovagal balance during graded orthostatic tilt. *Circulation* 1994;**90**:1826–1831.
32. Wei SG, Zhang ZH, Beltz TG, Yu Y, Johnson AK, Felder RB. Subfornical organ mediates sympathetic and hemodynamic responses to blood-borne proinflammatory cytokines. *Hypertension* 2013;**62**:118–125.
33. Ross CA, Ruggiero DA, Park DH, Joh TH, Sved AF, Fernandez-Pardal J, Saavedra JM, Reis DJ. Tonic vasomotor control by the rostral ventrolateral medulla: effect of electrical or chemical stimulation of the area containing C1 adrenaline neurons on arterial pressure, heart rate, and plasma catecholamines and vasopressin. *J Neurosci* 1984; **4**:474–494.
34. Schreihofer AM, Guyenet PG. Identification of C1 presympathetic neurons in rat rostral ventrolateral medulla by juxtacellular labeling *in vivo*. *J Comp Neurol* 1997;**387**: 524–536.
35. Tan X, Jiao PL, Wang YK, Wu ZT, Zeng XR, Li ML, Wang WZ. The phosphoinositide-3 kinase signaling is involved in neuroinflammation in hypertensive rats. *CNS Neurosci Ther* 2017;**23**:350–359.
36. de Kloet AD, Pioquinto DJ, Nguyen D, Wang L, Smith JA, Hiller H, Sumners C. Obesity induces neuroinflammation mediated by altered expression of the renin-angiotensin system in mouse forebrain nuclei. *Physiol Behav* 2014;**136**:31–38.
37. Dai SY, Peng W, Zhang YP, Li JD, Shen Y, Sun XF. Brain endogenous angiotensin II receptor type 2 (AT2-R) protects against DOCA/salt-induced hypertension in female rats. *J Neuroinflammation* 2015;**12**:47.
38. Sriramula S, Xia H, Xu P, Lazartigues E. Brain-targeted angiotensin-converting enzyme 2 overexpression attenuates neurogenic hypertension by inhibiting cyclooxygenase-mediated inflammation. *Hypertension* 2015;**65**:577–586.

Downloaded from https://academic.oup.com/cardiovascres/advance-article-abstract/doi/10.1093/cvr/cvy268/5144672 by University of Melbourne user on 14 December 2018